

DEVELOPMENT OF A NON-FUSION SCOLIOSIS CORRECTION DEVICE

DESIGNING AND TESTING

DEVELOPMENT OF A NON-FUSION SCOLIOSIS CORRECTION DEVICE

Martijn Wessels

DEVELOPMENT OF A NON-FUSION SCOLIOSIS CORRECTION DEVICE

DESIGNING AND TESTING



This research is supported by the Dutch Technology Foundation STW, which is part of the Netherlands Organisation for Scientific Research (NWO) and partly funded by the Ministry of Economic Affairs, Agriculture and Innovation (project number 07618)

DEVELOPMENT OF A NON-FUSION SCOLIOSIS CORRECTION DEVICE

DESIGNING AND TESTING

PROEFSCHRIFT

ter verkrijging van
de graad van doctor aan de universiteit Twente,
op gezag van de rector magnificus,
prof.dr. H. Brinksma,
volgens besluit van het College voor Promoties
in het openbaar te verdedigen
op donderdag 13 september 2012 om 16:45 uur

door
Martijn Wessels
geboren op 30 juni 1974
te Vriezenveen

De promotor prof.dr.ir. G.J. Verkerke en de assistent-promotor dr.ir. J.J. Homminga hebben dit proefschrift goedgekeurd

Copyright © 2012 by M. Wessels, Vriezenveen, The Netherlands

All rights reserved

ISBN: 978-90-365-3377-5

Ter herinnering aan

Mart Wessels

4 april 2012

5 april 2012

CONTENTS

CHAPTER 1. GENERAL INTRODUCTION.....	11
1.1. INTRODUCTION.....	11
1.2. SPINAL ANATOMY.....	11
1.3. ADOLESCENT IDIOPATHIC SCOLIOSIS (AIS).....	17
1.4. NON-SURGICAL TREATMENT.....	21
1.5. SURGICAL TREATMENT.....	22
1.6. PROBLEM ANALYSIS.....	29
1.7. REFERENCES.....	31
CHAPTER 2. FRAMEWORK.....	41
2.1. INTRODUCTION.....	41
2.2. DESIGN STRATEGY.....	41
2.3. SPINE MODELS FOR RESEARCH.....	46
2.4. CONCLUSIONS.....	48
2.5. REFERENCES.....	48
CHAPTER 3. DESIGN PROCEDURES.....	53
3.1. INTRODUCTION.....	53
3.2. STAKEHOLDERS.....	53
3.3. REQUIREMENTS.....	54
3.4. DESIRES.....	59
3.5. TECHNICAL SPECIFICATIONS.....	60
3.6. SYSTEM FUNCTIONS.....	60
3.7. CONCLUSION.....	63
3.8. REFERENCES.....	64
CHAPTER 4. STRUCTURAL DESIGN.....	69
4.1. INTRODUCTION.....	69
4.2. SOLUTIONS FOR SCOLIOSIS CORRECTION.....	69
4.3. GENERATION OF GENERAL CONCEPT.....	72
4.4. FINAL DESIGN (XS LATOR).....	79
4.5. MANUFACTURING PROCEDURES.....	87
4.6. SURGICAL INSTRUMENTS.....	87
4.7. STERILISATION PROCEDURES.....	91
4.8. IMPLANTATION PROCEDURES.....	91
4.9. FUNCTIONAL PROTOTYPES.....	91
4.10. REFERENCES.....	96
CHAPTER 5. A NOVEL ANCHORING SYSTEM FOR THE NON-FUSION SCOLIOSIS CORRECTION DEVICE.....	99
5.1. ABSTRACT.....	99
5.2. INTRODUCTION.....	100
5.1. MATERIALS AND METHODS.....	100
5.2. RESULTS.....	104
5.3. DISCUSSION.....	107
5.4. ACKNOWLEDGEMENTS.....	110
5.5. REFERENCES.....	110

CHAPTER 6. MECHANICAL BEHAVIOUR OF THE NON-FUSION SCOLIOSIS CORRECTION DEVICE	115
6.1. ABSTRACT.....	115
6.2. INTRODUCTION.....	117
6.3. MATERIALS AND METHODS	117
6.4. RESULTS.....	122
6.5. DISCUSSION	126
6.6. CONCLUSION.....	128
6.7. REFERENCES.....	128
CHAPTER 7. BENDING FATIGUE OF PSEUDO-ELASTIC NITI ROD IMPLANTS.....	133
7.1. ABSTRACT.....	133
7.2. INTRODUCTION.....	135
7.3. MATERIALS AND METHODS	136
7.4. RESULTS.....	140
7.5. DISCUSSION	145
7.6. CONCLUSIONS	148
7.7. REFERENCES.....	148
CHAPTER 8. NON-FUSION SCOLIOSIS INDUCTION IN AN <i>IN VIVO</i> PORCINE MODEL	155
8.1. ABSTRACT.....	155
8.2. INTRODUCTION.....	157
8.3. MATERIALS AND METHODS.....	158
8.4. RESULTS.....	165
8.5. DISCUSSION	172
8.6. CONCLUSION.....	176
8.7. ACKNOWLEDGEMENTS	177
8.8. REFERENCES.....	177
CHAPTER 9. GENERAL DISCUSSION	183
9.1. INTRODUCTION.....	183
9.2. FEEDBACK TO THE REQUIREMENTS.....	184
9.3. FAILURE MODE EFFECT ANALYSIS (FMEA).....	193
9.4. RECOMMENDATIONS	198
9.5. CONCLUSIONS	201
9.6. REFERENCES.....	202
SUMMARY	205
SAMENVATTING.....	207
DANKWOORD	209
APPENDIX.....	214
I. IMPLANTATION SYSTEM FOR TREATMENT OF A DEFECTIVE CURVATURE OF THE SPINAL COLUMN	214
INDEX.....	242

Chapter 1



GENERAL INTRODUCTION

CONTENTS

- CHAPTER 1. GENERAL INTRODUCTION..... 11**
- 1.1. INTRODUCTION..... 11
- 1.2. SPINAL ANATOMY..... 11
 - 1.2.a. *Definitions* 11
 - 1.2.b. *The human spine* 12
 - 1.2.a. *Intervertebral discs*..... 13
 - 1.2.b. *Vertebral structure* 13
 - 1.2.a. *Ligaments, muscles and joints*..... 14
- 1.3. ADOLESCENT IDIOPATHIC SCOLIOSIS (AIS)..... 17
 - 1.3.a. *Definitions* 17
 - 1.3.b. *Epidemiology and natural history* 18
 - 1.3.c. *Classification of curves* 18
 - 1.3.d. *Typical curvatures* 18
- 1.4. NON-SURGICAL TREATMENT..... 21
- 1.5. SURGICAL TREATMENT 22
 - 1.5.a. *Correction strategies* 22
 - 1.5.b. *Conventional surgery*..... 23
 - 1.5.c. *Posterior systems* 23
 - 1.5.d. *Anterior systems*..... 24
 - 1.5.e. *Anchoring to the spine* 24
 - 1.5.f. *Non-fusion surgery* 26
- 1.6. PROBLEM ANALYSIS 29
 - 1.6.a. *Problem definition*..... 29
 - 1.6.b. *Objectives*..... 30
- 1.7. REFERENCES..... 31

CHAPTER 1. GENERAL INTRODUCTION

1.1. INTRODUCTION

From a biomechanical point of view, the human spine is a highly sophisticated assembly, able to flex and rotate in different directions. One of its tasks is to support the trunk, head and upper extremities. While the spine has to be able to transfer loads, flexibility of must be preserved. Flexibility is provided by means of accumulative segmental motion. Although the spine is a highly functional and stable construction, problems concerning stability occasionally occur. If, for example, for some reason spinal development during adolescence malfunctions, a deformity such as scoliosis may develop. Scoliosis, characterised by a twisted and sideways curved spine, must be treated if the deformity is progressive and expected to cause pulmonary problems. In addition, treatment may be indicated on cosmetic grounds. Treatment includes surgical and non-surgical intervention. Current treatment of scoliosis is unsatisfactory which has raised a demand for improved methods. This thesis reports the development of a new implant system that delivers a revolutionary surgical solution to a problem classified as 'adolescent idiopathic scoliosis' (AIS).

This report is organized following the advice by Van Hee and Van Overveld who formulated criteria for writing a professional report on designing new technologies.¹ This chapter first discusses the spinal anatomy. Subsequently, 'adolescent idiopathic scoliosis' and the state of the art in current treatment techniques are considered and a problem definition is determined. Finally, objectives of this study in terms of a design assignment are formulated.

1.2. SPINAL ANATOMY

Biomechanical knowledge and definitions of spinal anatomy are required for proper understanding of scoliosis and its treatment. Therefore, background information is presented before formulating objectives concerning the development of a novel scoliosis correction system.

1.2.a. Definitions

In (biomedical) science, internationally standardised terms are used for references to anatomy. Basically, three orthogonal planes are included, consisting of a frontal (or coronal) plane, a sagittal plane, and a transverse plane (Figure 1.1). The frontal plane can be defined as an imaginary plane dividing the body in a front and a rear section. A sagittal plane divides the body into a right and a left section; a transversal plane divides the body into an inferior and a superior section.

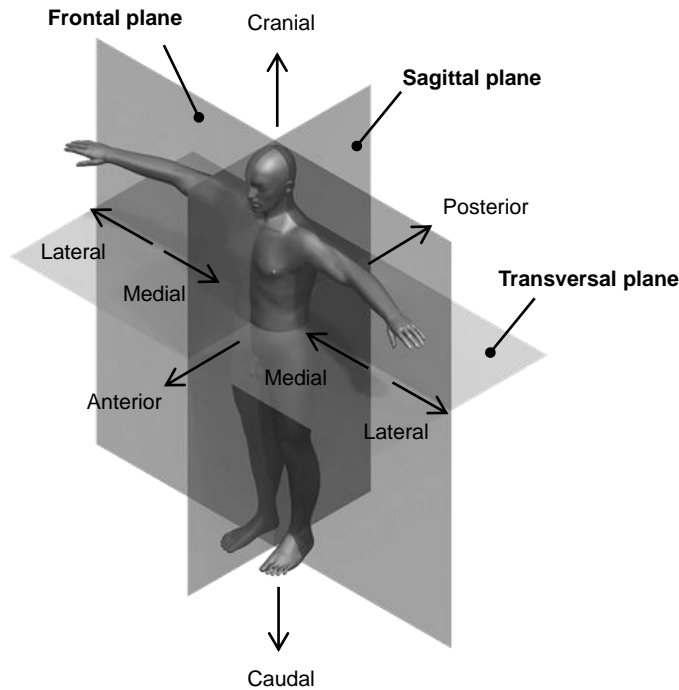


Figure 1.1: Anatomical planes and directions

Three basic planes are used for intersection and projection to provide anatomical information. Anatomical directions are defined orthogonal to the planes.

Along the planes, different anatomical directions can be identified (Figure 1.1). Forward bending of the spine is defined as flexion, backward bending as extension. Sideways bending is called lateral flexion. An overview of anatomical terms is given in Table 1.

1.2.b. The human spine

The human spine, also known as vertebral column, consists of vertebrae that are connected through joints, intervertebral discs, and soft tissue structures like muscles and ligaments to form a flexible, curved assembly (Figure 1.2). The sacrum and tailbone are located most caudally and contain nine vertebrae that become fused during adolescence. The remaining vertebrae can be sorted into three categories: cervical, thoracic, and lumbar vertebrae. The seven cervical vertebrae form the neck; twelve thoracic vertebrae (T1-T12) outline the area where the thorax is attached to the spine. The five remaining vertebrae form the lumbar region (L1-L5).

In lateral view, cervical and lumbar vertebrae show a concave curvature, also known as lordosis, whereas the thoracic spine shows a convex curvature (kyphosis). In anterior or posterior view, the total spine does not show any significant curvatures (Figure 1.2).

<i>Class</i>	<i>Anatomical term</i>	<i>Description</i>
Directions	Anterior	Toward the front
	Posterior	Toward the back
	Caudal	Toward the feet
	Cranial	Toward the head
	Medial	Toward the midline
	Lateral	Away from the midline
Locations	Inferior	Below
	Superior	Above
Rotations	Flexion	Forward bending
	Extension	Backward bending
	Axial torsion	Longitudinal twisting
	Lateral flexion	Sideways bending

Table 1.1: Anatomical terms

This table shows an overview of the anatomical terms that are used in this thesis.

Typical vertebral bony structures and soft tissue arrangements allow explicit relative motions of the vertebrae, which limits strain on spinal cord providing maximal protection. Focus in this dissertation will be on the thoracic and lumbar spinal regions.

1.2.a. Intervertebral discs

The intervertebral discs are located between, attached to the vertebral bodies, and deliver the main contribution to the flexibility of the spine. Each disc consists of a nucleus pulposus, a fibrous gelatinous core, and a surrounding annulus fibrosus, which includes multiple fibro-cartilage layers. The nucleus pulposus absorbs shocks to relieve spinal loads while keeping the vertebrae separated.

1.2.b. Vertebral structure

Although geometries differ considerably from one vertebra to another, each vertebra has a principle structure in which an anterior part (vertebral body), and a posterior part (vertebral arch) can be distinguished. The vertebral body is the part that transfers the weight bearing loads. Traveling from cranial to caudal, the vertebrae increase in size, the most caudal vertebrae being the largest, as they must bear the largest weight. Each vertebral body contains a large mass of spongy (trabecular) bone and an outer shell of

compact (cortical) bone with two endplates forming the boundaries between intervertebral discs and vertebra. The posterior part consists of seven processes, interconnected by two laminae creating the arch, and the vertebral body (Figure 1.3). Four articular processes (two superior, two inferior) form pairs with processes of adjacent vertebrae, creating facet joints that are held together by ligaments (Figure 1.4). Facet joints guide vertebral movements to limit spinal cord strain. Two laterally directed transverse processes and one posterior spinous process provide attachments of ligaments and muscles. Thoracic vertebrae are connected to ribs via costotransverse joints. Vertebral arches of consecutive vertebrae create the spinal canal, in which the spinal cord is situated.

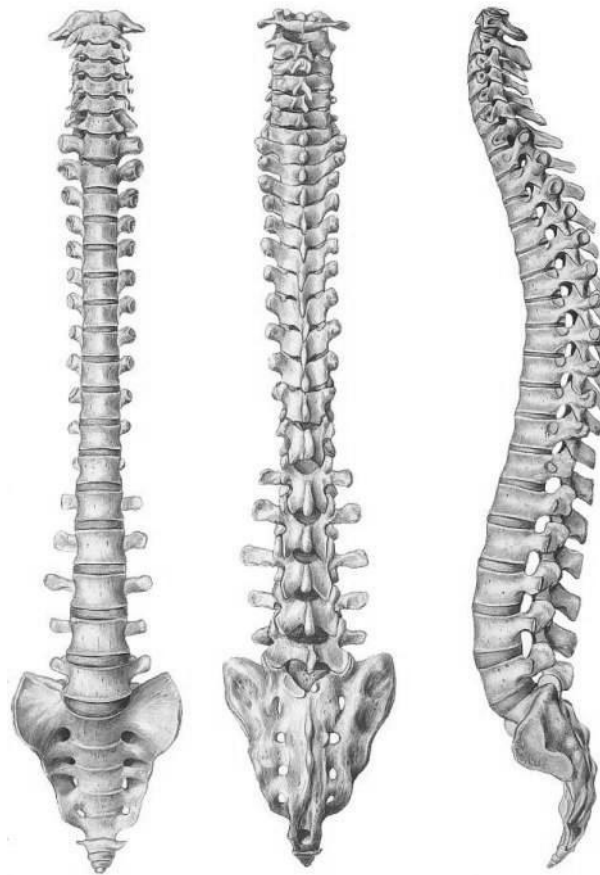


Figure 1.2: Anterior, posterior, and lateral views of the spine

The spine, consisting of vertebrae and intervertebral discs, shows multiple curves in lateral view and no distinct curves in anterior/posterior views. Picture taken from: Sobotta.²

1.2.a. Ligaments, muscles and joints

A structure of numerous ligaments combines the vertebrae, creating a strong connection and providing structural stability. Ligaments, consisting of fibrous connective tissue, can be categorised in intersegmental and intrasegmental systems. Intrasegmental ligaments,

such as the intertransverse ligament and the ligament flavum, combine individual vertebrae. Intersegmental ligaments, which include the anterior and posterior longitudinal ligaments, extend across multiple vertebral levels. The complexity of the ligament orientation is illustrated in Figure 1.4.

Facet joints guide vertebral movements limiting spinal cord strain. Each articular process forms a facet joint with an articular process of the linked vertebra. In a facet joint, a superior articular process and an inferior articular process are tied together with a capsular ligament (Figure 1.5).

Muscle structures control spinal motions within the geometrical boundaries created by intervertebral discs, ligaments, and facet joints. Spinal muscles participate in a complex motion system to balance the spine, keeping it upright and providing motions like twisting and bending in different directions. Three different types of spinal muscles can be defined including flexor, extensor and oblique muscles. Flexor muscles, which are attached to the anterior of the cervical spine, enable the spine to flex (bending forward). Flexion of the lumbar and thoracic spine is provided by abdominal muscles. Extensor muscles are attached posteriorly and enable extension (bending backward), while the oblique muscles enable axial rotation. Together, these structures collaborate to facilitate posture and motion.

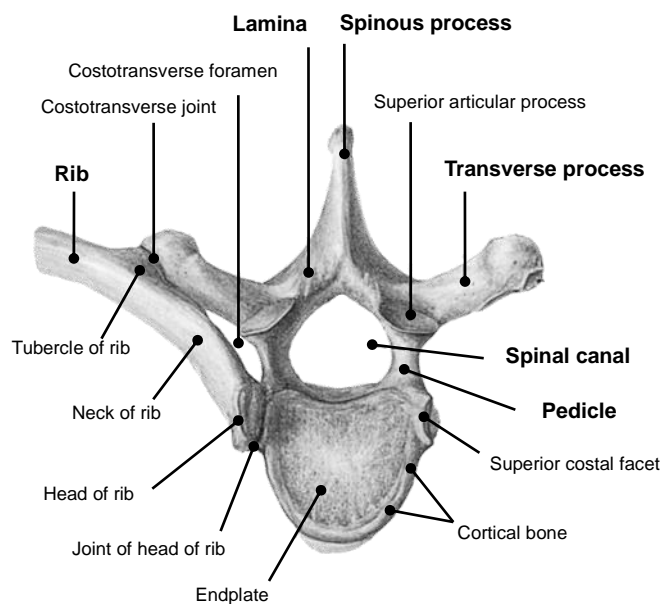


Figure 1.3: Characteristics of a thoracic vertebra

Thoracic vertebrae each have two ribs attached. A thoracic vertebra with one rib is shown above. The posterior part of the vertebra includes a vertebral arch consisting of laminae, spinous process, transverse processes and pedicles. Picture taken from: Sobotta.²

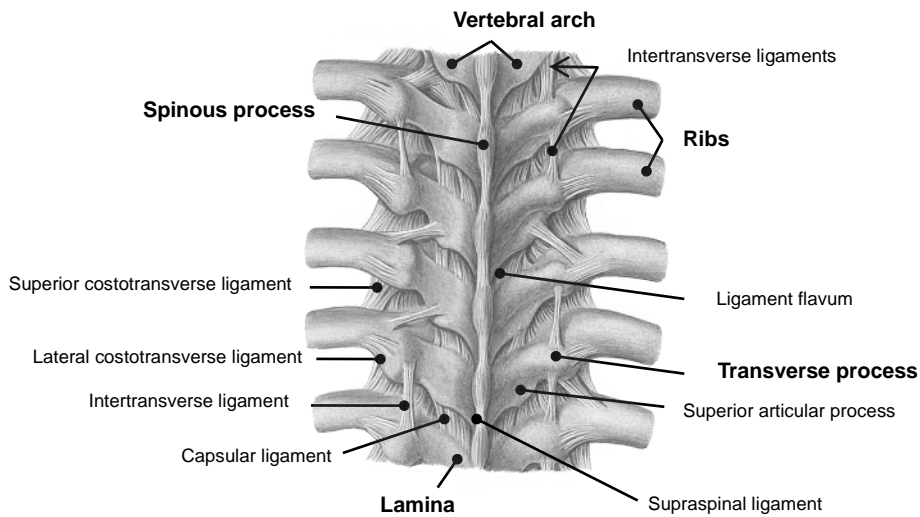


Figure 1.4: Posterior ligaments of the thoracic spine

A complex ligament structure provides a solid connection between vertebrae and provides structural stability. Picture taken from: Sobotta.²

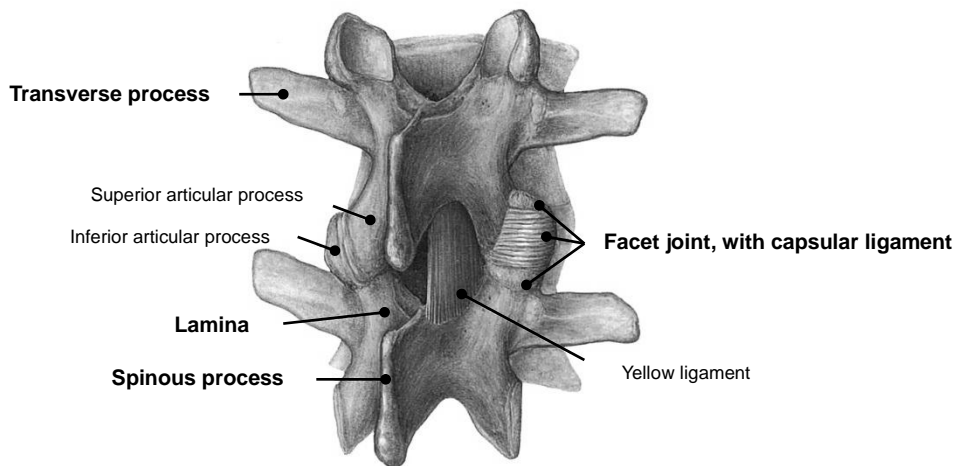


Figure 1.5: Facet joints of lumbar vertebrae

Yellow and capsular ligament are removed from left side. The superior articular process forms a facet joint with the inferior articular process of the adjacent superior vertebra. Picture taken from: Sobotta.²

1.3. ADOLESCENT IDIOPATHIC SCOLIOSIS (AIS)

1.3.a. Definitions

Scoliosis is a classification used for describing a spinal disorder in which, in frontal view, the spine shows a significant permanent curve (lateral deviation). Scoliosis that develops during growth with unknown cause is usually described as 'idiopathic'. Focus in this study is on adolescent idiopathic scoliosis (AIS) in which the idiopathic scoliosis develops during adolescence. AIS is a complex three dimensional (3D) deformity in which the lateral deviation is usually accompanied by an axial rotation and a sagittal deformation (Figure 1.6). Axial rotation is characterised by a phenomenon in which the vertebral bodies are rotated towards the convexity and consequently vertebral arches are rotated into the concavity of the curve. Depending on the deformed levels, sagittal curves may decrease or increase. In most cases, AIS is limited to the thoracic and/or lumbar region(s). Typical structural changes in spinal architecture in idiopathic scoliosis are concave-side shortening of soft tissues, abnormalities in vertebral shape and thoracic deformities.

The degree of deformity in (adolescent idiopathic) scoliosis is generally determined by the 'Cobb-angle' which classifies the deformity in the frontal plane. The Cobb-angle can be defined as the angle between two lines drawn parallel to the endplates of the most tilted vertebrae (MTV), viewed in the frontal plane (Figure 1.6b). In scoliosis, the most laterally deviated (and occasionally most axially rotated) vertebra is known as the 'apex'.

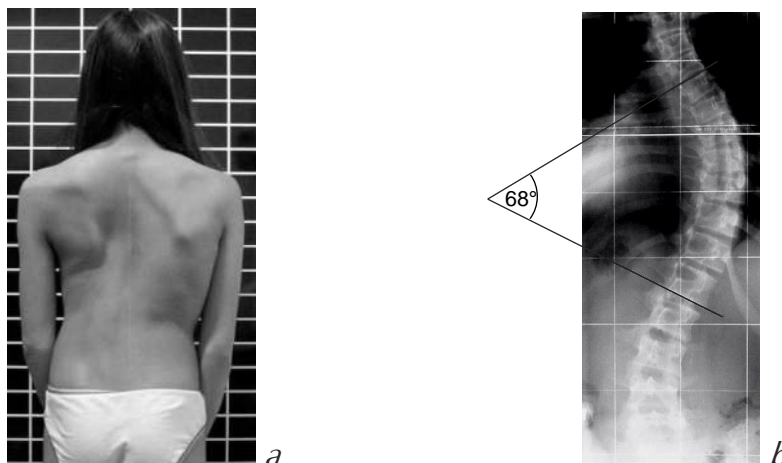


Figure 1.6: Adolescent female with idiopathic scoliosis

(a) An adolescent female diagnosed with idiopathic scoliosis. (b) From a radiograph, the Cobb-angle is determined in the frontal view by drawing lines parallel to the most tilted vertebra and measuring the angle between the lines. Lateral bending is accompanied with axial rotation, in which the vertebral arch is rotated into the concavity. Pictures taken from: Weiss.³

1.3.b. Epidemiology and natural history

Adolescent idiopathic scoliosis, determined for curves with Cobb-angles exceeding 10° , occurs in about 3% of all adolescents and occurs more often in girls than in boys.⁴⁻⁹ Scoliosis with Cobb-angles larger than 21° occurs 6 times more in girls than in boys.⁵ When cosmetic deformation and asymmetry become apparent, problems of psychosocial nature can develop. These problems can be significant for boys and girls. Adolescent scoliosis patients consider themselves as unhealthier than non-scoliosis patients and have more difficulties with physical activities.¹⁰ In mild and moderate scoliosis, some cardiopulmonary restrictions may occur during exercises.¹¹ In addition, back pain can develop during maturity. In severe scoliosis, respiratory failure and even premature death may occur.¹² During the second growth spurt, which takes place during adolescence and generally lasts for several years, there is a serious risk that scoliosis becomes progressive.⁷ After skeletal maturity, the deformity usually will not progress if the Cobb-angle is less than 30° .¹³

1.3.c. Classification of curves

Protocols for scoliosis treatment are based on classification systems describing the deformity. Determination is generally achieved from radiographs, which are two dimensional (2D) images. To date, many classifications are used to characterise spinal curvatures. Despite the fact that AIS is a 3D deformity, the majority of classification methods is based on a frontal plane projection of the curve.¹⁴⁻¹⁷ Although the Lenke Classification system, which uses the sagittal plane for supplementary reference, proved to be reproducible¹⁵⁻¹⁷ and is considered to be reliable,¹⁸ this classification has proven not to be appropriate for use in non-surgical treatments.¹⁹ Accurate treatment of AIS should use a genuine 3D classification system. Several attempts have been made to introduce 3D classification systems,^{20,21} however they have not been used in practice because determination of axial rotation of vertebra from 2D images is difficult and usually not very accurate. Although use of 3D CT (Computed Tomography) images is proposed,²² due to high radiation exposure this technique is being avoided.²³ Innovative systems using low radiation such as the EOS system are able to generate 3D digital models from two 2D images.²⁴ However, these systems are still expensive, so often measurements are still performed using 2D X-ray images.

1.3.d. Typical curvatures

Although deformity in AIS is different for each patient, lateral deviation is almost always associated with axial rotation, in which the posterior parts are usually rotated into the concavity of the spine. Deformities in AIS can be progressive when remaining untreated. Besides with large Cobb-angles, progression of scoliosis is correlated with large axial rotation.^{14,17,25-28} Therefore, it seems important that a non-fusion scoliosis correction implant should focus, apart from decreasing lateral deviation, on axial derotation. In

contrast, current systems are unable to apply enough torque to successfully derotate spine segments.²⁹

From literature it can be concluded that a (lateral) deformity in idiopathic scoliosis generally consist of one or two primary curves, resulting in a C- or S-shaped curve.³⁰ In 99% of AIS, deformities are C- or S-shaped, when viewed from a frontal plane projection.²⁶ In more complicated deformities, these primary curves are most prominent. Secondary curves can be considered supplementary.³¹ Therefore, in this project, lateral correction is primarily focused on C- and S-shaped curves. Using this strategy, correction of a primary curve is expected to correct the secondary curves.³¹ In addition, the S-shaped curve will be considered as a double C-shaped (single) curve.

An overview of typical progressive scoliotic curves is given in Table 1.2. Cobb-angles and axial rotation angles, both characteristic for moderate AIS, are presented together with the ranges of vertebrae that are associated with them.

C-shaped curves

Deformities of single curves can be divided into two categories: thoracic scoliosis and thoracolumbar scoliosis. The non-fusion implant (being developed in this project) will be designed to correct a small to moderate scoliosis in the thoracic or thoracolumbar region. Generally, a Cobb-angle of a single curved (mild/moderate) scoliosis is in the range between 20° and 45°; axial rotation is generally in the range between 15° and 35°. A typical thoracic curvature runs from the third thoracic vertebra (T3) to the twelfth thoracic vertebra (T12), with T8 as apex.³² A typical moderate thoracolumbar scoliosis runs from T6 to L4 with T12 as apex (Figure 1.7).

<i>Curve</i>	<i>Apex</i>	<i>Range</i>	<i>Cobb[°]</i>	<i>Ax rot [°]</i>	<i>Apex</i>	<i>Range</i>	<i>Cobb</i>	<i>Ax rot [°]</i>
C	T8	T3-T12	40	30	x	x	0	0
C	T12	T6-L4	40	30	x	x	0	0
S	T8	T6-T12	45	40	T4	T1-T6	30	30
S	L2	T11-L5	45	40	T9	T6-T11	30	30

Table 1.2: Typical scoliotic curves

An overview of progressive curves shows characteristic Cobb-angles and axial rotations.

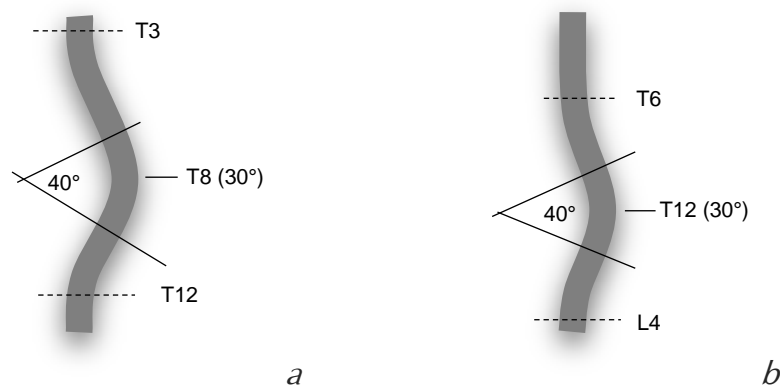


Figure 1.7: Typical C-shaped curves

(a) A typical thoracic single curve roughly runs from T3 to T12 with apex at T8. Cobb-angle is 40° and axial rotation of T8 is 30° . (b) In a typical thoracolumbar single curve, Cobb-angle is 40° and axial rotation of T12 is 30° . The curvature runs from T6 to L4, with T12 as apex.

Most tilted vertebrae (MTV) generally are somewhere between apex and most cranial and most caudal vertebrae of the deformed regions. In thoracolumbar scoliosis this would mean most tilted vertebrae at T9 and L2. MTV at T5 and T10 are typical for a thoracic scoliosis.

S-shaped curves

Double major curves (S-shaped) consist of two apparent arches and apices. A typical double thoracic scoliosis is located between T1 and T12, with T4 and T8 forming the apices. Curves of a typical thoracolumbar scoliosis are located between T6 and L5. Apices of a typical double thoracolumbar curve are T9 and L2 (Figure 1.8).

Correlation of lateral deviation and axial rotation

Although one would expect that the apices in axial rotation and lateral deviation will always coincide, data used in the thesis by Nijenbanning³³ and in a related study of Veldhuizen *et al*³⁴ showed that the laterally most deviated vertebra (apex) is often not the most axially rotated vertebra. Figure 1.9 shows an example of the deformity of a girl with adolescent idiopathic scoliosis. Obviously, the two most laterally deviated vertebrae are T8 and T9 whereas T7 is the most axially rotated vertebra. This phenomenon emphasises the complexity of three dimensional nature of idiopathic scoliosis.

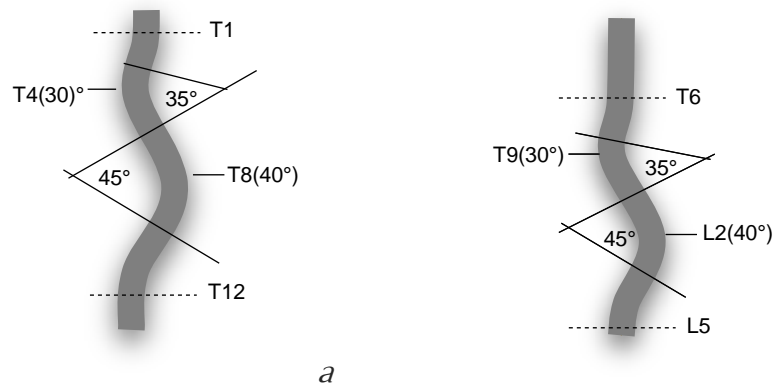


Figure 1.8: Typical S-shaped curves

(a) A double thoracic curve runs from T1 to T12 with apices at T4 and T8. Cobb-angles are 35° and 45° and axial rotations are 30° and 40°. (b) In a double thoracolumbar curve. Cobb-angles are 35° and 45°, axial rotations are 30° and 40°. The curvature runs from T6 to L4, with T12 as apex.

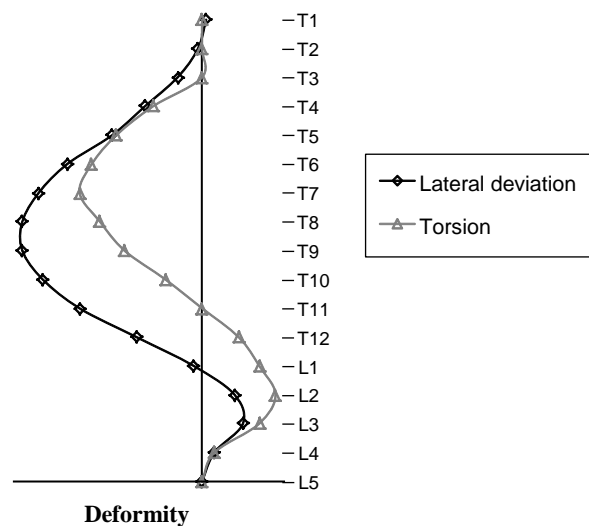


Figure 1.9: Correlation lateral deviation and axial rotation

Although correlation between lateral deviation and axial rotation is clear, the apex (T8/T9) is not the most axially rotated vertebra (T7). Data used in: Nijebanning.³³

1.4. NON-SURGICAL TREATMENT

Treatment of AIS generally is considered when Cobb-angles of lateral curves exceed 20°, especially if curves are progressive.³⁵ Non-surgical treatment of adolescent idiopathic scoliosis is executed by physiotherapy or bracing for curves less than 40° Cobb-angle.³⁶ In physiotherapy, the patient is guided in improving coordination and stimulated in motor development. Focus in postural improvement is on spinal balance. Often, physiotherapy is used in combination with bracing. The variety of braces used in treatment is very high.³⁷ Braces are designed to push on pelvis and thorax and/or distract

the spine in order to stabilise the deformity. Examples are the Chêneau type and TriaC™ braces, as shown in Figure 1.10. Although no surgery is performed, wearing braces can be psychologically and mentally burdening.^{38,39} For maximal results, braces should be worn 23 hours a day, which is very challenging.⁴⁰ Curve progression is likely to resume after the end of brace treatment, especially during adolescence.⁴¹ However, patients wearing braces are able to continue growing and fusion of the spine is prevented. Despite of this, if curves are still progressive after reaching maturity, surgical treatment usually will be performed.³⁶

Non-surgical treatment is usually unsuccessful in spinal curve correction.^{44,45} Moreover, results for non-surgical treatments are very unpredictable.⁴⁵ Therefore, the main objective for non-surgical treatment is to maintain spinal shape and prevent progression until maturity.

1.5. SURGICAL TREATMENT

Surgical treatment is much more effective than non-surgical treatment in correcting deformity in the frontal and the sagittal plane and is considered the only clinical treatment that holds a permanent solution for treatment of a progressive adolescent idiopathic scoliosis. Spine surgery is generally performed after skeletal maturity for curves larger than 35° (Cobb-angle).

1.5.a. Correction strategies

Regarding scoliosis correction, different strategies have been used to reduce the deformity. Surgery is generally carried out by performing spondylodesis, a surgical technique that invokes fusion of the vertebrae, either posterior or anterior⁴⁶ by immobilization of vertebrae, which is achieved by implanting rod constructs that are securely anchored by hooks or screws. Together with addition of bone graft, which is added to activate bone growth,⁴⁷ this procedure results in fused spine segments. Rationale for spondylodesis is to generate long-term stabilisation and to reduce high peak loads on anchors. Spinal fusion surgery preferably preformed at skeletal maturity.^{48,49} A wide range of different fusion implant systems is available. While spondylodesis focuses on instant mechanical correction, other strategies in surgical treatment of AIS try to gradually achieve correction of the deformity. These non-fusion techniques attempt to avoid/postpone fusion or to control growth, and are based on allowing a significant amount of vertebral motion. Moreover, in non-fusion surgery less invasive surgical procedures are used in order to avoid heterotopic ossification. This excessive bone formation is a typical biological reaction to periosteal (the periosteum being a membrane that lies on the outer surface a bone) damage occurring during standard spine surgery procedures.

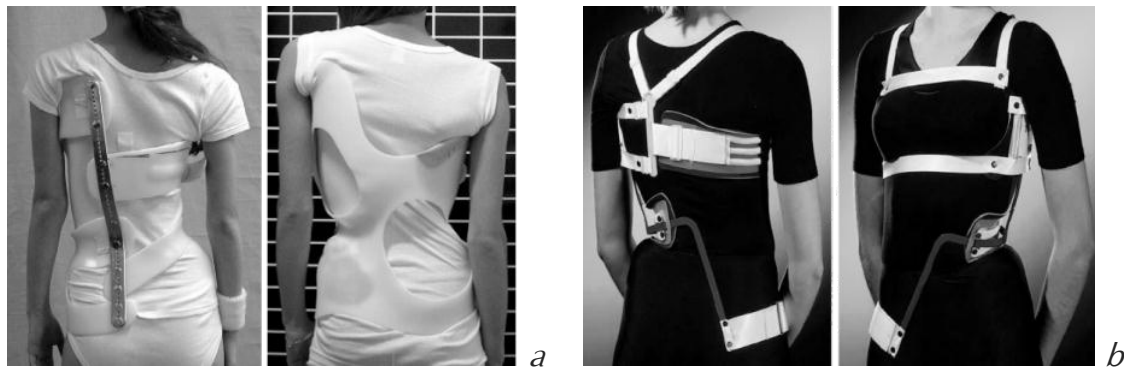


Figure 1.10: Braces

Braces should be worn 23 hours a day which can be mentally challenging. (a) Girl with Chêneau type braces. (b) Girl with TriaC™ brace. Pictures taken from: (a) Weiss³, Weiss et al⁴² and (b) Wynne.⁴³

1.5.b. Conventional surgery

Conventional methods used in spine surgery are based on mechanical correction in combination with vertebral fusion. The majority of surgical systems are based on implanting posterior instrumentation which applies high forces or moments to different parts of the spine in order to generate instant curve transformation. Paul Harrington was the first to successfully carry out spondylodesis.⁵⁰ His method, known as the Harrington procedure, is still a practiced procedure for surgical treatment. In this procedure, the surgeon uses a stainless steel distraction rod, attached to and extending from the most cranial to the most caudal vertebra of the curve, applying axial forces. Although the Harrington procedure is (to some extent) successful in straightening the spine, sagittal and rotational imbalance remains untreated. Besides correcting the lateral curve, straightening the spine reduces sagittal curvature. For that reason, improved Harrington procedures have been performed by contouring the implant in the sagittal plane and applying a configuration to prevent the rod from twisting.⁵¹

1.5.c. Posterior systems

The Harrington method is an example of implementation of a posterior implant system. Currently, the most commonly used posterior implant procedure is the implementation of a segmental spinal construct. In this procedure, the rods are attached to the spine at various vertebral levels using a multitude of anchors forcing the spine into the desired curvature.⁵² The posterior segmental spinal instrumentation proved to be more corrective with respect to sagittal balance,^{53,54} however the instrumentation merely focuses on correction in frontal and sagittal plane. To correct the axial rotation, a technique called Direct Vertebral Rotation (DVR) is applied. This procedure in which two cross-linked rods are applied, creating a stiff assembly in torsion, involves a derotation manoeuvre using a DVR device.⁵⁵ Screws transfer the generated torque to the

spine. This technique, which aims for 3D correction applies an amount of torque that is higher than conventional techniques do. Generated torsion moments however are small and derotation is hardly achieved.^{51,56} Although the instrumentation is considered successful in spinal correction surgery, clinical complications remain considerable.⁵⁷ Most recent developments in posterior spinal fusion surgery are the implementation of multiple segmental and hybrid constructs using a combination of screws, wires and hooks (Figure 1.11a, b).

1.5.d. Anterior systems

Typical anterior systems consist of rod or plate constructs, in which the instrumentation is fixed by screws (Figure 1.11c). Anterior instrumentation surgery is being performed in lumbar and thoracolumbar scoliosis while posterior systems usually are applied in thoracic scoliosis. No scientific basis however for preference of either system has been found.^{58,59}

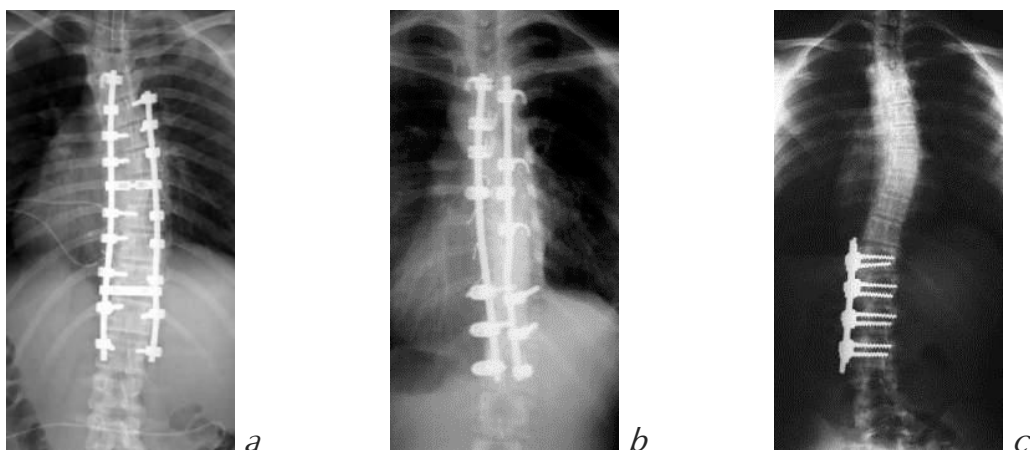


Figure 1.11: Radiographs of posterior and anterior constructs

(a) A posterior hybrid construct. (b) A segmental construct. (c) An anterior system. Pictures taken from: Maruyama.⁴⁸

1.5.e. Anchoring to the spine

The first Harrington rod systems exclusively used hooks for anchoring the construction to the spine. Modern scoliosis correction systems use wires, screws and hooks for anchoring. Many different configurations, optimised for application in particular vertebral regions and applications, are available. Often, combinations of several anchor types are used. Pedicle screws used in posterior systems are inserted into the pedicles and extend into the vertebral bodies. The surgical rods are attached to the heads of the screws by locking nuts or set screws (Figure 1.12a). To facilitate rod insertion, poly-axial pedicle screws, which include pivoting heads, can be used. Mono-axial screws, without the pivoting heads, can also be used. Pedicle screws can provide a very solid fixation, but have a serious risk of spinal cord damage. Despite this risk, pedicle screws are

increasingly used. Advanced screw insertion procedures, with or without assistance of 3D imaging techniques, will limit this risk significantly.

Hooks used in posterior systems are secured to the laminae or transverse processes and are available in many sizes and geometries (Figure 1.12c). Often, hooks are part of a claw construction to create a solid clamp construction. Posterior instrumentation techniques can also include wires for tying surgical rods to the vertebral arches. Pioneered by Resina,⁵⁴ Luque applied the wiring technique successfully for segmental spinal instrumentation,^{53,54} in which the implant is firmly tied to all vertebrae along the rods (Figure 1.13a). Although mainly stainless steel wires are used, modern systems may use different wiring techniques and materials. One example is the Universal Clamp® by Zimmer Spine (Figure 1.13c).

Anterior systems (generally plate or rod constructions) are anchored by screws (Figure 1.12b). These screws are inserted laterally into the vertebral bodies of the spine. Like in all systems, size and shape of these screws highly depend on the application.

Choice of anchors used in surgical systems may depend on several factors, such as the applied system, the instrumented vertebral level and personal preference of the surgeon.



Figure 1.12: Example of different anchor systems

Hooks and screws in different sizes and geometries are used. (a) Screws in a posterior rod system, (b) screws in an anterior plate system and (c) hooks used in a posterior system. Figures copyright: (a) Elite Surgical Supplies,⁶⁰ (b) Aesculap Implant Systems⁶¹ and (c) TST Tıbbi Aletler San. Ve Tic. Ltd.Şti.⁶²

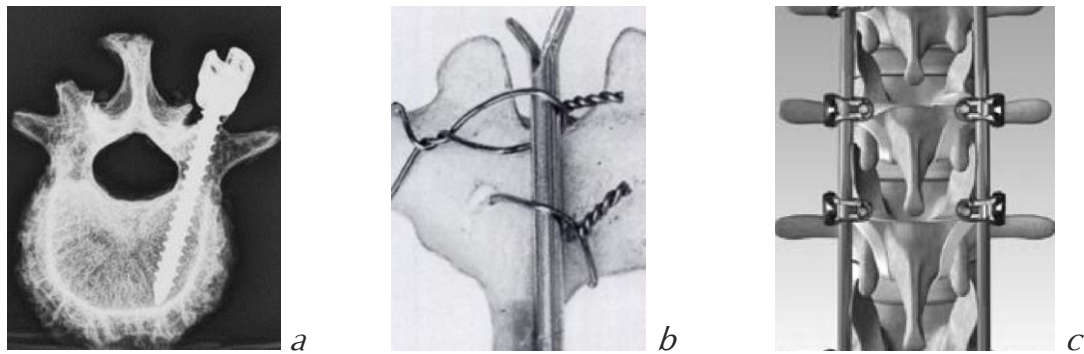


Figure 1.13: Vertebral fixation methods

(a) Radiograph of an inserted poly-axial pedicle screw. (b) Attachment of a rod through wires around a transverse process and through the spinous process. (c) Rods fixed to the spine using Universal Clamps[®]. Taken from: (a) Santoni,⁶³ (b) Kiely.⁶⁴ Copyright: (c) Zimmer Spine.⁶⁵

1.5.f. Non-fusion surgery

In growing children, fusion is likely to result in vertebral growth arrest, which can cause serious pulmonary deficiencies. In addition, vertebral fusion will result in decreased spinal flexibility with obvious consequences. Therefore, researchers have been attempting to develop scoliosis correction systems that eliminate the need for fusion.

State of the art

One method of performing non-fusion surgery is epiphysiodesis; a type of growth control surgery in which the growth plate of one or more vertebral bodies is removed from the convex side of the scoliotic curve. Growth at the convex side is thereby arrested, allowing only the concave side to grow. Although study showed that epiphysiodesis in congenital scoliosis is not very promising,⁶⁶ growth control by means of stapling the convex side of vertebral bodies in adolescent idiopathic scoliosis showed some good results.^{67,68} However, growth control is challenging because accurate estimation of future growth is required. For that, solid criteria must still be formulated.

Systems with non-rigid fixations and flexible systems, with or without self-growing constructs are currently explored by different researchers.⁶⁹⁻⁷¹ One example is the use of single or double 'growing' rods. These correction rods are periodically expanded in subsequent surgical procedures.^{48,64,72} Figure 1.15c shows the Vertical Expandable Prosthetic Titanium Rib (VEPTR[™]). Most recent development is the application of a construct that requires just a single surgical procedure wherein the self-lengthening instrumentation is capable of continuous adjustment to growth (Figure 1.15a).^{48,73} Although these systems are able to postpone fusion, spinal growth will still be arrested and fusion will occur.

Another example of an approach that is able to postpone fusion is the implantation of the NiTi memory metal device that was developed by the University of Twente and

UMC Groningen.^{74,75} In fact, with this device, postponement of fusion is intended instead of prevention of fusion. The device, which uses the typical physical properties of memory metal, was tested in a porcine model. A spinal curve of about 40° Cobb-angle was induced.⁷⁶ Generated lateral bending moment was between 7.5 Nm and 12 Nm and the generated torque was estimated between 2 Nm and 5 Nm. The system is able to allow some amount of vertebral motion while forces are sustained for a longer period of time.

In addition, a similar system was recently implanted by Newton *et al.*⁷¹ They examined the effects of single *versus* dual memory metal rod systems. The instrumentation was able to generate a considerable curve in mature mini-pigs.⁷¹ The spine fused as intended at the instrumented level. The single rod construction generated a significant curve which progressed in a week. Interestingly, contrary to the expectations, the dual rod system did not perform better than single rod construct, even though it applied a larger bending moment (Figure 1.14a, b). These results suggest that higher initial force will not necessary result in larger curve change.

Kim *et al* indicated that a non-rigid implant fixation can prevent fusion.⁶⁹ The implant they used was the Orthobiom™, which itself is not a flexible implant but mainly consists of two stainless steel rods. However its non-rigid fixation allows a small range of motion for the vertebrae, by means of sliding and pivoting joints (mobile connectors). Clinical research confirmed that this small amount of relative vertebral motion is enough to prevent facet joints and intervertebral discs from fusing.^{69,77} Figure 1.15b shows a radiogram of an implanted Orthobiom™ system.

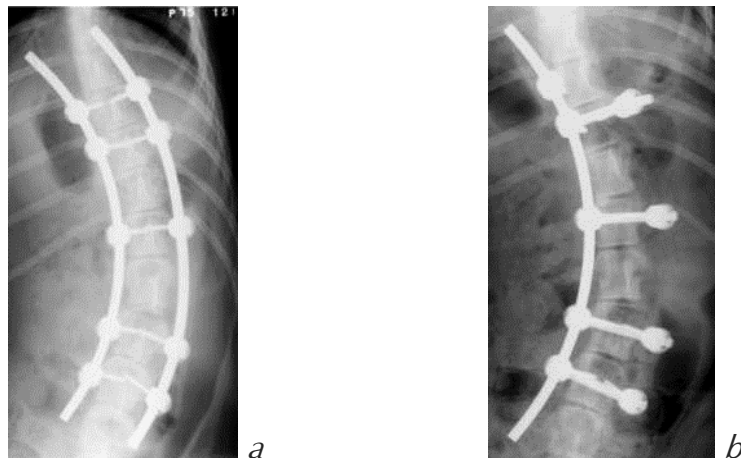


Figure 1.14: NiTi shape memory implants

(a) Dual NiTi rod system implanted in a mini-pig generates a significant lateral bending thereby creating a scoliosis. (b) Single rod system implanted likewise creates similar deformity in a mini-pig. Pictures taken from: Newton.⁷¹

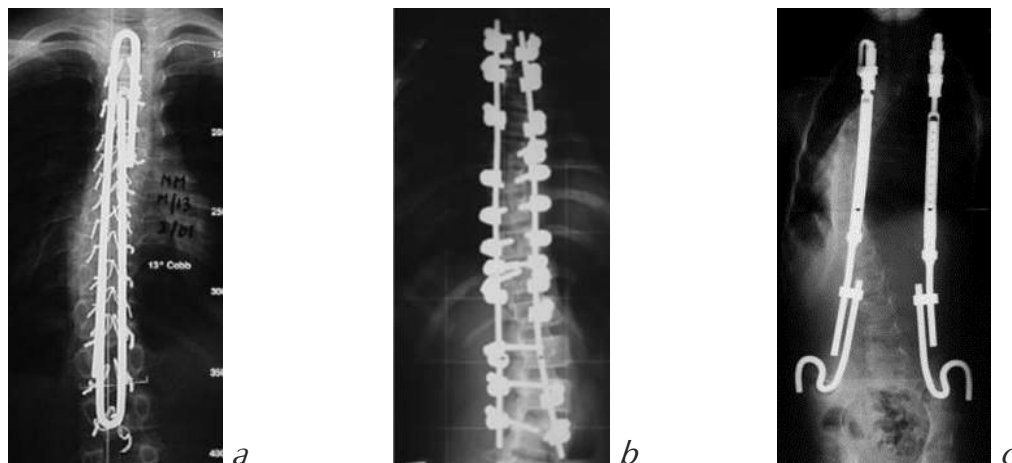


Figure 1.15: Radiographs of novel approaches in non-fusion surgery

(a) A rigid Luque trolley system provides a solid segmental fixation while allowing spinal growth. (b) The Orthobiom™ system with non-rigid fixation. (c) Vertical Expandable Prosthetic Titanium Ribs™ are periodically extended. Pictures taken from: (a) Kiely,⁶⁴ (b) Newton,⁷¹ (c) Samdani.⁷⁸

In vivo pilot study

In a pilot study performed by Van der Kuij (1996), a non-rigid implant comprising a NiTi shape memory rod was implanted in a porcine model. The unpublished results with the axially extendable implant showed considerable lateral deformation. The posterior implant was used to induce scoliosis in healthy (straight) porcine spine. An initial lateral bending moment of approximately 2.4 Nm was applied. After fixation, the applied bending moment reduced to 1.7 Nm resulting in equilibrium as deduced from radiographs. 13 Weeks post-surgery, estimated lateral bending moment had reduced to 1.4 Nm (Table 1.3). Figure 1.16 shows a radiograph of a porcine model in which a scoliosis of 24° was induced. The experiment indicated that a small and rather constant bending moment is able to generate a considerable curve change. However, posterior bone growth (fusion) may have contributed to the resulting deformity.

The pilot study included some limitations. The implant only applied lateral forces. Torque was not applied and thus torsion was not invoked. Although the extendable implant was able to sustain a bending moment even after induction of significant sagittal curvature (contrary to materials such as stainless steel and titanium), the bending moment decreased due to growth of the system.

<i>Instant</i>	<i>Bending moment [Nm]</i>
Initial	2.4
Balanced per op	1.7
13 Weeks post op	1.4

Table 1.3: Applied bending moments of NiTi implant

Estimation of applied bending moments of the axially expandable NiTi implant by Van der Kuij.

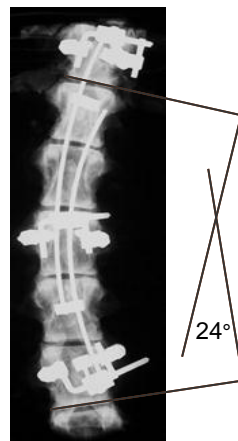


Figure 1.16: *In vivo* experiment with an implant generating a scoliosis

A low stiffness NiTi shape memory implant was tested in vivo in immature pigs. Although small moments were applied, generated scoliosis was considerable.

1.6. PROBLEM ANALYSIS

Problems concerning different approaches lead to new objectives for surgical procedures. These objectives form the basis for a design assignment to develop an innovative non-fusion scoliosis correction device.

1.6.a. Problem definition

Treatment should be considered especially when deformity is progressive. Treatment will cause additional problems which makes it difficult to find a proper solution for the patient. A summary of problems regarding scoliosis and current treatments is presented in Table 1.4.

Spondylodesis is the most common and effective surgical technique used in scoliosis treatment and is performed on scoliotic curves with Cobb-angles of at least 35°. Although curve correction can be considerable, fusion of vertebrae usually arrests spinal growth. In adolescent idiopathic scoliosis where considerable growth still remains, fusion of vertebrae can result in short stature and serious pulmonary deficits. Due to

increased mobility of vertebrae adjacent to the fused levels, degeneration of intervertebral discs and vertebral bodies may occur. A tethering mechanism induced by high stiffness implants can generate a phenomenon known as crankshafting,⁷⁹ which causes progression of the deformity. In addition, high peak loads generated during daily activities increase the risk of bone fracture and implant failure.

Due to the increased risk of complications in adolescents, spondylodesis surgery is usually delayed until after reaching maturity. Pending that moment, it is attempted to arrest curve progression with braces, which is often not very effective. Nevertheless, surgical procedures are still being carried out. Although various techniques are explored to postpone fusion, in general fusion will occur eventually. Current spinal fusion systems aim at instantaneous correction of the lateral curve. Maximal correction is achieved during surgery. After surgery, correctional forces drop dramatically, preventing further correction.

1.6.b. Objectives

Although some surgical non-fusion systems are being explored by researchers, these alternatives have not proven to provide long-term stability and correction without fusion of vertebral levels. Consequently, a demand for a surgical scoliosis correction system that applies long-term corrective forces, but does not induce spinal fusion, still exists.

The non-fusion scoliosis correction system should limit the problems summarised in Table 1.4. Main objective of the system is to correct adolescent idiopathic scoliosis when it is still in an early stage, while allowing continued growth. A full correction of spinal anatomy is thereby aimed for, which means that lateral deviation and associated axial rotation should be fully corrected. Full curve correction will reduce the patient's problems regarding idiopathic scoliosis itself. The correction system has to prevent the vertebrae from fusing in order to maintain full range of motion. Prevention of fusion will restore and preserve all spinal functionalities and makes it possible to remove the implant after correction. At the same time, the growth potential of the spine must not be limited by the device. Allowing spinal growth will resolve the problems associated with conventional surgical treatment such as crankshafting and degeneration of vertebrae.

Problems associated with		
Idiopathic scoliosis	Surgical treatments	Non-surgical treatments
Back pain	Decreased flexibility	Deprivation of correction
Psychosocial difficulties	Degeneration of vertebrae	Psychologically challenging
Pulmonary deficit	Inhibition of growth	Physically inconvenient
Physical activities	Crankshafting	Obviously perceptible
Death	Implant irremovable	

Table 1.4: Problem analysis

This table shows an overview of the main problems associated with AIS and its treatment. Available treatment is still not satisfying.

1.7. REFERENCES

1. Van Hee, K. & Van overveld, K. Criteria for assessing a technological design. http://www.3tu.nl/fileadmin/sai/Assessment_criteria/Criteria_Design_Assignments.pdf (2010).
2. Sobotta. *Atlas of human anatomy*, (Bohn Stafleu van Loghum, Houten/Zaventum, 1994).
3. Weiss, H.R. Is there a body of evidence for the treatment of patients with Adolescent Idiopathic Scoliosis (AIS)? *Scoliosis* **2**, 19 (2007).
4. Bunnell, W.P. The natural history of idiopathic scoliosis. *Clin Orthop Relat Res* **229**, 20-25 (1988).
5. Rogala, E.J., Drummond, D.S. & Gurr, J. Scoliosis: incidence and natural history. A prospective epidemiological study. *J Bone Joint Surg Am* **60**, 173-176 (1978).
6. Al-Arjani, A.A.M., Al-Sebai, M.M.W., Al-Khawashki, H.H.M. & Saadeddin, M.M.F. Epidemiological patterns of scoliosis in a spinal center in Saudi Arabia. *Saudi medical journal* **21**, 554 (2000).
7. Dickson, R.R.A. Scoliosis in the community. *British medical journal* **286**, 615 (1983).
8. Soucacos, P.N., Soucacos, P.K., Zacharis, K.C., Beris, A.E. & Xenakis, T.A. School-screening for scoliosis. a prospective epidemiological study in northwestern and central Greece. *J Bone Joint Surg Am* **79**, 1498-1503 (1997).
9. Brooks, H.L., Azen, S.P., Gerberg, E., Brooks, R. & Chan, L. Scoliosis: a prospective epidemiological study. *J Bone Joint Surg Am* **57**, 968-972 (1975).

10. Payne, W.K., 3rd, *et al.* Does scoliosis have a psychological impact and does gender make a difference? *Spine* **22**, 1380-1384 (1976).
11. Barrios, C., Perez-Encinas, C., Maruenda, J.I. & Laguia, M. Significant ventilatory functional restriction in adolescents with mild or moderate scoliosis during maximal exercise tolerance test. *Spine* **30**, 1610-1615 (1976).
12. Libby, D.M., Briscoe, W.A., Boyce, B. & Smith, J.P. Acute respiratory failure in scoliosis or kyphosis: prolonged survival and treatment. *Am J Med* **73**, 532-538 (1982).
13. Bjerkreim, I. & Hassan, I. Progression in untreated idiopathic scoliosis after end of growth. *Acta Orthopaedica* **53**, 897-900 (1982).
14. King, H.A., Moe, J.H., Bradford, D.S. & Winter, R.B. The selection of fusion levels in thoracic idiopathic scoliosis. *J Bone Joint Surg Am* **65**, 1302-1313 (1983).
15. Lenke, L., *et al.* Adolescent idiopathic scoliosis: a new classification to determine extend of spinal arthrodesis. *The Journal of Bone and Joint Surgery American* **83**, 1169 - 1181 (2001).
16. Lenke, L., Edwards, C. & Bridwell, K. The Lenke classification of adolescent idiopathic scoliosis: how it organizes curve patterns as a template to perform selective fusions of the spine. *Spine* **28**, S199 - 207 (2003).
17. Lenke, L.G., *et al.* Intraobserver and interobserver reliability of the classification of thoracic adolescent idiopathic scoliosis. *J Bone Joint Surg Am* **80**, 1097-1106 (1998).
18. Ogon, M., *et al.* Interobserver and intraobserver reliability of Lenke's new scoliosis classification system. *Spine* **27**, 858 - 862 (2002).
19. Rigo, M. Intra-observer reliability of a new classification correlating with brace treatment. *Pediatric Rehabilitation* **7**, 63 (2004).
20. Negrini, S., Negrini, A., Atanasio, S. & Santambrogio, G. Three-dimensional easy morphological (3-DEMO) classification of scoliosis, part I. *Scoliosis* **1**, 1-16 (2006).
21. Sangole, A.P., *et al.* Three-dimensional classification of thoracic scoliotic curves. *Spine* **34**, 91-99 (2009).
22. Boisvert, J., Cheriet, F., Pennec, X., Ayache, N. & Labelle, H. A novel framework for the 3D analysis of spine deformation modes. *Stud Health Technol Inform* **123**, 176-181 (2006).
23. Vrtovec, T., Pernuš, F. & Likar, B. A review of methods for quantitative evaluation of axial vertebral rotation. *European Spine Journal* **18**, 1079-1090 (2009).

24. Dubousset, J., *et al.* A new 2D and 3D imaging approach to musculoskeletal physiology and pathology with low-dose radiation and the standing position: the EOS system. *Bull Acad Natl Med* **189**, 287-297 (2005).
25. Cruickshank, J.L., Koike, M. & Dickson, R.A. Curve patterns in idiopathic scoliosis. a clinical and radiographic study. *J Bone Joint Surg Br* **71-B**, 259-263 (1989).
26. Qiu, G.M.D., *et al.* A new operative classification of idiopathic scoliosis: a Peking Union Medical College method. *Spine June* **30**, 1419-1426 (2005).
27. Coonrad, R.W.M.D., Murrell, G.A.C.M.D., Motley, G.M.D., Lytle, E.B.S. & Hey, L.A.M.D.M.S. A logical coronal pattern classification of 2,000 consecutive idiopathic scoliosis cases based on the Scoliosis Research Society-defined apical vertebra. *Spine* **23**, 1380-1391 (1998).
28. Lonstein, J.E. & Carlson, J.M. The prediction of curve progression in untreated idiopathic scoliosis during growth. *J Bone Joint Surg Am* **66**, 1061-1071 (1984).
29. Lee, S.M. Direct vertebral rotation: a new technique of three-dimensional deformity correction with segmental pedicle screw fixation in adolescent idiopathic scoliosis. *Spine (Philadelphia, Pa. 1976)* **29**, 343 (2004).
30. Lehnert-Schroth, C. Introduction to the three-dimensional scoliosis treatment according to Schroth. *Physiotherapy* **78**, 810-815 (1992).
31. Andriacchi, T.P., Schultz, A.B., Belytschko, T.B. & Dewald, R. Milwaukee brace correction of idiopathic scoliosis: a biomechanical analysis and a retrospective study. *J Bone Joint Surg Am* **58**, 806-815 (1976).
32. Moe, J. & Kettleson, D. Idiopathic scoliosis: analysis of curve patterns and preliminary results of Milwaukee brace treatment in one hundred sixty-nine patients. *The Journal of Bone and Joint Surgery American* **52**, 1509 - 1533 (1970).
33. Nijenbanning, G. Soliosis redress - design of a force controlled orthosis. PhD-thesis, University of Twente, Enschede. (1998).
34. Veldhuizen, A.G., Cheung, J., Bulthuis, G.J. & Nijenbanning, G. A new orthotic device in the non-operative treatment of idiopathic scoliosis. *Medical Engineering & Physics* **24**, 209-218 (2002).
35. Reamy, B.V. & Slakey, J.B. Adolescent idiopathic scoliosis: review and current concepts. *Am Fam Physician* **64**, 111-116 (2001).
36. Wiley, J.W., Thomson, J.D., Mitchell, T.M., Smith, B.G. & Banta, J.V. Effectiveness of the Boston brace in treatment of large curves in adolescent idiopathic scoliosis. *Spine* **25**, 2326-2332 (2000).

37. Negrini, S. Bracing adolescent idiopathic scoliosis today. *Disability and Rehabilitation: Assistive Technology* **3**, 107-111 (2008).
38. Climent, J.M. Impact of the type of brace on the quality of life of adolescents with spine deformities. *Spine (Philadelphia, Pa. 1976)* **24**, 1903 (1999).
39. Ugwonalu, O.F., *et al.* Effect of bracing on the quality of life of adolescents with idiopathic scoliosis. *The Spine Journal* **4**, 254-260 (2004).
40. Helfenstein, A., *et al.* The objective determination of compliance in treatment of adolescent idiopathic scoliosis with spinal orthoses. *Spine* **31**, 339-344 (2006).
41. Carr, W.A., *et al.* Treatment of idiopathic scoliosis in the Milwaukee brace: long-term results. *J Bone Joint Surg Am* **62**, 599-612 (1980).
42. Weiss, H.R., Werkmann, M. & Stephan, C. Correction effects of the ScolioLogiC® „Chêneau light" brace in patients with scoliosis. *Scoliosis* **2**, 1-6 (2007).
43. Wynne, J.H. The Boston Brace and TriaC systems. *Disability and Rehabilitation: Assistive Technology* **3**, 130-135 (2008).
44. Rinsky, L.A. & Gamble, J.G. Adolescent idiopathic scoliosis. *West J Med* **148**, 182-191 (1988).
45. Nachemson, A.L. & Peterson, L.E. Effectiveness of treatment with a brace in girls who have adolescent idiopathic scoliosis. A prospective, controlled study based on data from the Brace Study of the Scoliosis Research Society. *J Bone Joint Surg Am* **77**, 815-822 (1995).
46. Betz, R.R. & Shufflebarger, H. Anterior *versus* posterior instrumentation for the correction of thoracic idiopathic scoliosis. *Spine* **26**, 1095-1100 (2001).
47. Craig Boatright, K. & Boden, S.D. Biology of spine fusion. in *Bone Regeneration and Repair* (eds. Lieberman, J.R. & Friedlaender, G.E.) 225-239 (Humana Press, 2005).
48. Maruyama, T. & Takeshita, K. Surgical treatment of scoliosis: a review of techniques currently applied. *Scoliosis* **3**, 6 (2008).
49. Bridwell, K.H. Spinal instrumentation in the management of adolescent scoliosis. *Clin Orthop Relat Res* **335**, 64-72 (1997).
50. Harrington, P.R. Treatment of scoliosis: correction and internal fixation by spine instrumentation. *J Bone Joint Surg Am* **44**, 591-634 (1962).
51. Webb, J.K., Burwell, R.G., Cole, A.A. & Lieberman, I. Posterior instrumentation in scoliosis. *European Spine Journal* **4**, 2 (1995).

52. Cotrel, Y., Dubousset, J. & Guillaumat, M. New universal instrumentation in spinal surgery. *Clin Orthop Relat Res* **227**, 10-23 (1988).
53. Luque, E.R. Segmental spinal instrumentation for correction of scoliosis. *Clin Orthop Relat Res* **163**, 192-198 (1982).
54. Resina, J. & Alves, A.F. A technique of correction and internal fixation for scoliosis. *J Bone Joint Surg Br* **59-B**, 159-165 (1977).
55. Chang, M.S. & Lenke, L.G. Vertebral derotation in adolescent idiopathic scoliosis. *Operative Techniques in Orthopaedics* **19**, 19-23 (2009).
56. Remes, V., *et al.* Cotrel-Dubousset (CD) or Universal Spine System (USS) instrumentation in adolescent idiopathic scoliosis (AIS): comparison of midterm clinical, functional, and radiologic outcomes. *Spine* **29**, 2024-2030 (2004).
57. Helenius, I., *et al.* Harrington and Cotrel-Dubousset instrumentation in adolescent idiopathic scoliosis - long-term functional and radiographic outcomes. *J Bone Joint Surg Am* **85**, 2303-2309 (2003).
58. Potter, B., Kuklo, T. & Lenke, L. Radiographic outcomes of anterior spinal fusion *versus* posterior spinal fusion with thoracic pedicle screws for treatment of Lenke type I adolescent idiopathic scoliosis curves. *Spine* **30**, 1859 - 1866 (2005).
59. Hee, H., Yu, Z. & Wong, H. Comparison of segmental pedicle screw instrumentation *versus* anterior instrumentation in adolescent idiopathic thoracolumbar and lumbar spine. *Spine* **32**, 1533 - 1542 (2007).
60. <http://functions.safeshop.co.za/View.asp?ID=111776>, accessed 1/7/2011, Elite Surgical Supplies, (2011).
61. http://www.aesculapimplantsystems.com/assets/base/image/ais/Spine/Anterior_Cervical/ABC2_Dynamic_Anterior_Cervical_Plating_System/ABC2_large.jpg, accessed 5/7/2011, Aesculap Implant Systems, (2011).
62. http://www.ttsan.com/resimler/alt_kategori/o_LeftRightAngled_LaminarHook.jpg, accessed 5/7/2011, TST Tibbi Aletler San. Ve Tic. Ltd.Şti, (2011).
63. Santoni, B.G., *et al.* Cortical bone trajectory for lumbar pedicle screws. *The Spine Journal* **9**, 366-373 (2009).
64. Kiely, P.J. & Grevitt, M.P. Recent developments in scoliosis surgery. *Current Orthopaedics* **22**, 42-47 (2008).

65. http://www.zimmer.com/web/enUS/pdf/Spine_Universal_Clamp_Surgical_Technique.pdf, accessed 1/9/2011, Zimmer Spine, (2008).
66. Marks, D.S., Sayampanathan, S.R.E., Thompson, A.G. & Piggott, H. Long-term results of convex epiphysiodesis for congenital scoliosis. *European Spine Journal* **4**, 296-301 (1995).
67. Trobisch, P.D., Samdani, A., Cahill, P. & Betz, R.R. Vertebral body stapling as an alternative in the treatment of idiopathic scoliosis. *Operative Orthopädie und Traumatologie*, 1-5 (2011).
68. Betz, R.R., *et al.* Vertebral body stapling: a fusionless treatment option for a growing child with moderate idiopathic scoliosis. *Spine* **35**, 169-176 (2010).
69. Kim, W.J., *et al.* The influence of fixation rigidity on intervertebral joints: an experimental comparison between a rigid and a flexible system. *J Korean Neurosurg Soc* **37**, 364-369 (2005).
70. Rohlmann, A., Zander, T., Burra, N.K. & Bergmann, G. Flexible non-fusion scoliosis correction systems reduce intervertebral rotation less than rigid implants and allow growth of the spine: a finite element analysis of different features of orthobiom. *Eur Spine J* **17**, 217-223 (2008).
71. Newton, P.O., *et al.* Dual and single memory rod construct comparison in an animal study. *Spine* **36**, E904-E913 (2011).
72. Campbell, R., *et al.* The effect of opening wedge thoracostomy on thoracic insufficiency syndrome associated with fused ribs and congenital scoliosis. *J Bone Joint Surg Am* **86**, 1659 - 1674 (2004).
73. Ouellet, M.J. & FRCSC. Surgical technique: modern Luqué trolley, a self-growing rod technique. *Clin Orthop Relat Res* **469**, 1356-1367 (2011).
74. Veldhuizen, A.G., Sanders, M.M. & Cool, J.C. A scoliosis correction device based on memory metal. *Medical Engineering & Physics* **19**, 171-179 (1997).
75. Sanders, M.M. A memory metal based scoliosis correction system. PhD-thesis, University of Twente, Enschede. (1993).
76. Wever, D.J., Elstrodt, J.A., Veldhuizen, A.G. & v Horn, J.R. Scoliosis correction with shape-memory metal: results of an experimental study. *Eur Spine J* **11**, 100-106 (2002).
77. Geiger, F. & Rauschmann, M. Dynamische Verfahren bei der juvenilen Skoliose. *Der Orthopäde* **38**, 122-130 (2009).

78. Samdani, A.F., *et al.* Bilateral use of the vertical expandable prosthetic titanium rib attached to the pelvis: a novel treatment for scoliosis in the growing spine. *J Neurosurg Spine* **10**, 287-292 (2009).
79. Kesling, K.L. The crankshaft phenomenon after posterior spinal arthrodesis for congenital scoliosis: a review of 54 patients. *Spine (Philadelphia, Pa. 1976)* **28**, 267 (2003).

Chapter 2



FRAMEWORK

CONTENTS

- CHAPTER 2. FRAMEWORK 41**
- 2.1. INTRODUCTION..... 41
- 2.2. DESIGN STRATEGY 41
 - 2.2.a. *Mechanical correction* 42
 - 2.2.b. *Design boundaries*..... 42
 - 2.2.c. *Patient group*..... 43
 - 2.2.d. *Correction based on visco-elasticity* 44
 - 2.2.e. *Application of NiTi*..... 46
- 2.3. SPINE MODELS FOR RESEARCH 46
 - 2.3.a. *The porcine model*..... 47
 - 2.3.b. *Finite Element modelling*..... 48
- 2.4. CONCLUSIONS 48
- 2.5. REFERENCES..... 48

CHAPTER 2. FRAMEWORK

2.1. INTRODUCTION

The study, described in this thesis is part of a project that is committed to the development of an innovative non-fusion scoliosis correction device. In this project, which is labelled as 'a non-fusion scoliosis correction device', three PhD students were assigned to cover the various aspects of the design process. In collaboration with UMC Groningen, VU University Medical Centre in Amsterdam and University of Twente, the activities were split into three elements. One of performing *in vitro* measurements on porcine and human spine models and providing clinical input to the project, one of developing a Finite Element (FE) model of a typical human adolescent human spine and one of designing and testing the non-fusion scoliosis correction implant. Measurements from the human *in vitro* models are used for generation of the FE model. Data from the porcine, the human, and FE models will be used in the design process, which is described in this thesis.

The design process of a new system requires a clearly defined framework to focus on specific areas without getting lost in infinity. Therefore, in the following sections, a design strategy is defined as part of a systematic approach to generate a high quality design.

2.2. DESIGN STRATEGY

Most obvious task of the non-fusion scoliosis correction system is to correct the lateral deformation and axial rotation that are present in adolescent idiopathic scoliosis. Correction will be obtained by 'pushing' the spine into its desired shape by means of forces and moments. Prevention of spinal fusion however, requires preservation of spinal flexibility. Therefore, an optimal surgical correction system should include three main functions. The system must be able to correct the deformed curvature, to allow spinal growth and to allow a considerable amount of vertebral motion.

The development of a novel implant system in which an overall prevention of spinal fusion, achieved by maintaining high spinal flexibility and minimizing surgical invasiveness is aimed for, can be considered revolutionary. Within the design, flexion/extension, lateral flexion, and axial rotation will be allowed as much as feasible. In addition, prevention of fusion will be realised to allow growth of the spine in order to maintain natural (healthy) spine dynamics.

2.2.a. Mechanical correction

The strategy that is used in our 'non-fusion' approach is based upon a mechanical correction of the scoliosis. The system will consist of an implant that is anchored to the spine. In order to maintain flexibility of the spine, magnitude of applied forces and moments will be limited. After implantation, functionality and properties of the spine will be comparable with those of a healthy person's spine.

2.2.b. Design boundaries

The system to be developed is intended for C-type scoliosis only. In case of an S-type scoliosis, two systems should be applied. The system aims to treat patients aged between 10 years and 17 years, who have been diagnosed with AIS with Cobb-angle between 15° and 45°.

Counteraction of the lateral deviation will be achieved by applying lateral forces and/or moments at several fixation points. It is important to distinguish two different approaches for fixation. In the first approach, the implant will be fixed posteriorly to the spine, wherein the vertebral arches are rotated towards the concavity of the curve, assuming that the centre of rotation is in the spinal canal. Lateral forces will apply torsion to the spine resulting in an additional axial rotation (Figure 2.1c). Consequently, apart from the originally required scoliosis derotation torque, axial torque must be raised to counteract the torque generated by the posterior lateral forces. The second approach is an anteriorly applied correction force since, from an anterior view; the vertebral bodies are rotated towards the convexity of the curve. In this case, lateral correction forces will (partly) correct axial rotation because the consequent direction of torsion is similar to the required direction for correction (Figure 2.1a). Additional derotation will be achieved by applying supplementary torsion to the spine. In both approaches, sagittal correction is assumed to occur simultaneously with the lateral correction and axial derotation.

Technical feasibility of an anterior approach appeared low due to difficulties regarding the required surgical techniques. For example, the presence of major (anterior) blood vessels increases the risks of complications in an anterior approach. Therefore, despite mechanical advantages of an anterior approach, in this project the posterior approach is employed.

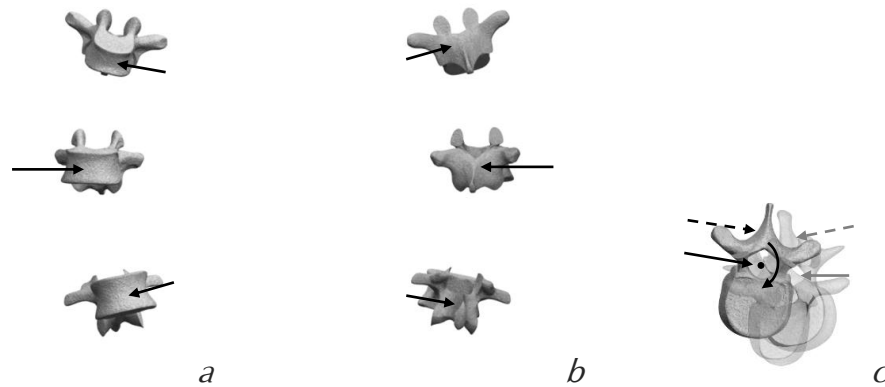


Figure 2.1: Application of lateral forces

(a) Lateral forces applied anteriorly to a typical scoliotic spine. (b) Lateral forces applied posteriorly to same scoliotic spine. (c) Posterior applied force (dashed arrow) can be resolved to a force and torsion moment (black arrows) on the centre of a vertebra (spinal canal). Consequently, for correction in a posterior approach with lateral forces, additional correction moments in opposite directions are required.

2.2.c. Patient group

The key group of patients that should be treated with the new system cannot be determined easily. Although the target group should be as large as possible, it would not be wise to include all scoliosis patients, because some patients must be submitted to fusion of the spine due to the severity of the curve. The target group is restricted to persons who meet the following criteria.

The scoliotic deformity is a C- or S-shaped curve.

The patient is not obese or underweight. To minimise health risks, only patients with Body Mass Index (BMI) within the age-related boundaries will be treated.¹⁻³

The Cobb-angle is between 15° and 45° . Patients with such curves are usually treated with non-surgical solutions such as braces.

The age of the patient is between 10 years and 17 years.

The patient has a minimal length of 128 cm, which is the P2 length of a 10-year-old (European) child.^{2,3}

The patient has a maximal length of 196 cm, which is the P98 length of a 17-year-old adolescent.²

The patient has a minimal weight of 14 kg and a maximal weight (BMI = 24.5) is 90 kg.³

Approximately 0.5% of children develop scoliosis with Cobb-angles exceeding 20° .⁴ Total birth rate in Western Europe and United States is 6.1 million per year.⁵ The number of patients requiring non-fusion surgery would be 30,500 each year. Assuming a 20% market interest, the system will be implanted in approximately 6,000 adolescents per year.

2.2.d. Correction based on visco-elasticity

Full correction without overloading the joints should consist of applying small forces of constant magnitudes, which thus will be attained by making use of the short- and long-term viscosity of the spine including spinal growth. The approach to obtain full correction is based upon using force control in a period of several months/years following surgery.

In vitro and *in vivo* studies confirm time-dependent deformation of spine segments under stress.^{6,7} In these studies, short-term viscosity, with intervals of several minutes to hours, was examined. Nachemson examined intermediate-term (several days/weeks) relaxation of axial forces in Harrington rod implants,⁸ and showed that axial forces in the implant reduced to one third of the initial forces after 12 days (Figure 2.2).⁸ Nevertheless, little is known about intermediate-term and long-term (months/years) spinal viscosity. To date, long-term viscosity of spinal structures, both *in vitro* and *in vivo*, has not been studied properly.

In general, soft tissues such as muscles, tendons, ligaments and fascia, exhibit creep and relaxation.^{9,10} It may therefore be expected that soft tissues in spinal structures will behave in a similar fashion. Ligaments show unusual visco-elastic behaviour. Creep in ligaments will not necessarily occur at high stresses only. In fact, medial collateral ligaments (MCL) in rats show a creep rate that is higher at smaller stresses (Figure 2.3).¹¹ Thornton *et al.*¹² examined creep rate of MCL in rabbits and showed that total creep strain is virtually independent of stresses below 14 MPa.

Previous reports presented results of *in vitro* creep experiments in rats and rabbits. No results however of creep and relaxation in living human tissues have been reported. An indication for the mechanisms of creep in living tissues may be found in orthodontics. In orthodontics, braces are used to move teeth slowly to their desired position. Forces of fairly constant magnitude are applied to induce bone remodelling. Stresses of low magnitude appeared to contribute to (considerable) tooth movement with less unwanted movements than with high force levels.¹³ In addition, the role of ligaments in bone remodelling, which can be considered as a long-term visco-elastic response, appeared to be significant.¹⁴ These results may be generalised to wider areas, such as spinal tissues, that consist of similar soft tissue structures. Although not supported by evidence, application of small sustained moments on a scoliotic spine may induce a slow (long-term) visco-elastic response in which curvature slowly deforms to the desired shape.

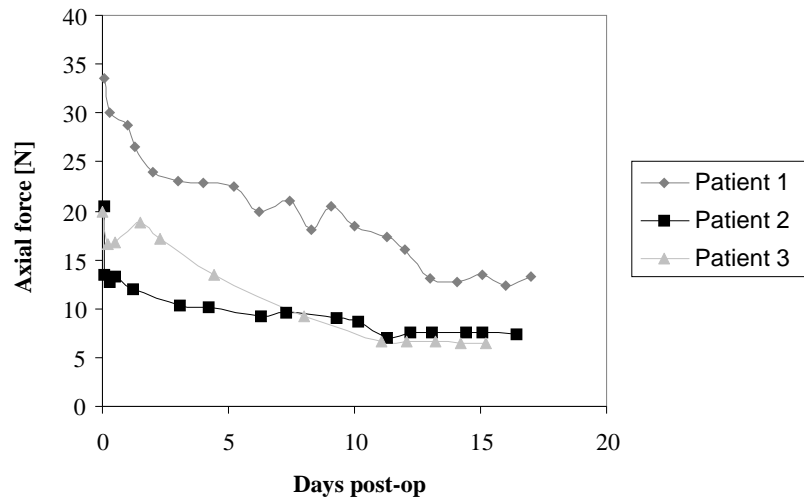


Figure 2.2: Force relaxation in Harrington rods

Measurements in Harrington rods showed reduction of forces with more than 65% in two weeks. Data taken from: Nachemson, 1971.⁸

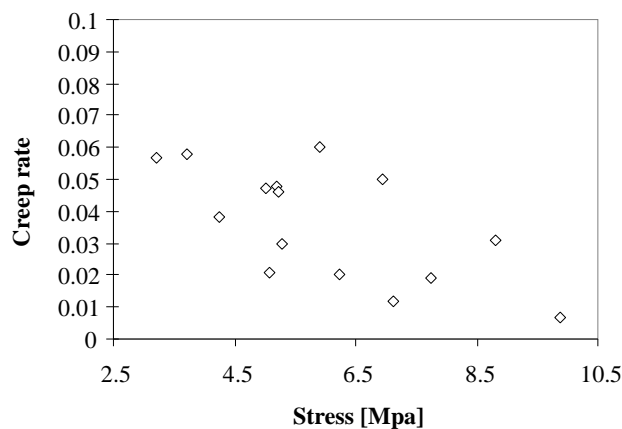


Figure 2.3: Creep in ligaments

Non-linear creep in medial collateral ligaments in rats. Creep rate is dimensionless and was obtained from curve fitting with a power law t^n with time represented as t and creep rate represented as n . Data taken from: Provenzano.¹¹

2.2.e. Application of NiTi

Regarding scoliosis correction, the strategy followed in this non-fusion project consists of mechanical correction based on force control. Force control preferably requires materials demonstrating a low modulus of elasticity in combination with a large elastic response. Polymers, typically showing a low modulus of elasticity, are not suitable because the long-term elastic response is small due to creep and relaxation.

A biocompatible material that answers previous requirements is NiTi, an alloy of nickel and titanium with two stable solid-state phases. NiTi shows shape memory behaviour when heated above a transition temperature. The high-temperature austenitic phase shows pseudo-elastic behaviour. Pseudo-elasticity is characterised by a reversible stress induced crystal phase transformation from austenite to martensite (low-temperature phase). The phase transformation enables NiTi to undergo a high amount of elastic strain (6-8%).

The application of NiTi was introduced by Schmerling *et al.* who showed advantages of NiTi in Harrington rod constructs.¹⁵ Recently, the application of NiTi rods was examined. They found that gradual (short-term) correction can be achieved by applying sustained forces using NiTi.¹⁶⁻¹⁸ Although non-fusion is generally not aimed for, use of pseudo-elastic NiTi seems promising for use in non-fusion systems because of the specific material properties.

Use of the shape memory effect of NiTi is employed by researchers not only for permanent implants, but also for temporary implants during surgery. For example, Wang *et al.* reported on a pre-contoured NiTi rod that was cooled and effortlessly bent in a scoliotic shape followed by posterior pedicle screw anchoring. The rod was warmed up to generate correction force and induce shape correction. The pseudo-elastic NiTi rod was then replaced by two rigid rods. Fusion of vertebrae was invoked by adding bone graft.¹⁹

2.3. SPINE MODELS FOR RESEARCH

Every newly developed system must be subjected to several testing procedures. For example, physical models, which are composed of artificial materials, are used for evaluation of new devices when actual tissue properties are not yet significant.²⁰ Although these models are very helpful during the design process, often kinematics and physical properties of bone and soft tissue must be modelled. *In vitro* and *in vivo* models can be used; however, testing the internal stresses and strains is challenging and often impossible. In that case, computer models can be helpful. Models, such as Finite Element (FE) models, can be used for specific applications to study the effects of *e.g.* trauma and surgery.²⁰ Despite this, *in vitro* and *in vivo* studies still have to be performed for validation of such applications. Due to limited availability of adolescent human cadaver material, *in vitro* studies are commonly performed on animal models. In

addition, *in vivo* experiments, which are essential for researching impacts of surgical techniques and instrumentations, are performed using animal models prior to *in vivo* testing in humans. Large implants are generally tested on large animal models, such as goats, sheep, pigs, and dogs.²¹ As a model though, not all animals are equally suitable.

2.3.a. The porcine model

For proper testing of spinal implants, animal spines with comparable mechanical and geometrical properties must be used. Busscher *et al.* studied the anatomy of human and porcine spine segments and concluded that porcine spine models are representative for researching human spine anatomy.²² Busscher *et al.* also found that the biomechanical behaviour of the human lumbar spine is comparable with the low thoracic and lumbar porcine spine, which implies that the porcine model can be used as a valid model for investigation.²³ Figure 2.4 shows geometries of lumbar and thoracic human and porcine spine models. However, pigs do not have scoliosis. Testing will be performed in an 'inverse' way, *i.e.* inducing scoliosis, assuming that a system that successfully induces scoliosis in pigs is able to correct scoliosis in humans. For evaluation of the novel non-fusion scoliosis correction device, *in vitro* and *in vivo* porcine models will be used, in accordance with the advice of Busscher *et al.*²³

Avoidance of fusion is essential to maintain spinal functionality. Prevention of bone formation in the instrumented area is a prerequisite to avoid fusion. Spine surgery, usually accompanied with periosteal damage, is an osteoinductive treatment. Osteoinduction (induction of bone formation) must be avoided by using (minimal invasive) procedures in which periosteum and soft tissue damage is minimised.

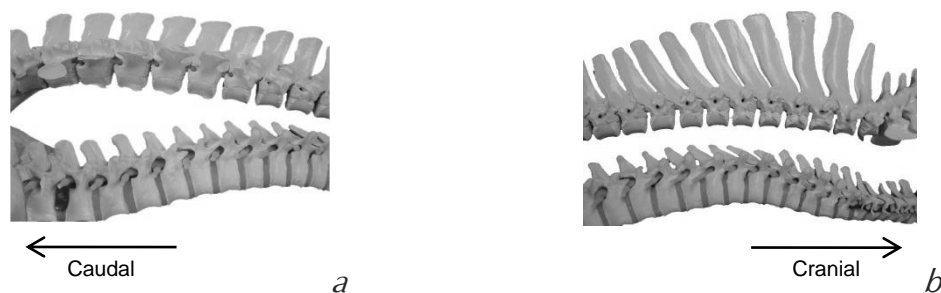


Figure 2.4: Porcine and human spines

(a) The porcine (top) and human (bottom) lumbar spine show comparable dimensions of pedicles and vertebral bodies and comparable behaviour. (b) Porcine (top) and human (bottom) thoracic spines show less similarity. Pictures taken from: Menhusen.²⁴

2.3.b. Finite Element modelling

Induction of scoliosis in a spine model is the first stage of testing the non-fusion scoliosis correction device. Prediction of scoliosis correction can however be quite difficult and cannot be based entirely upon data from the porcine models. Therefore, an FE model was generated to make a translation from scoliosis induction to scoliosis correction.

Meijer developed an FE model of an adolescent (10-year-old) spine in which the developed implant was tested. Meijer proposed that scoliosis induction could be dissimilar to scoliosis correction. The FE model can be used for prediction of the implant's effect of the implant on a human adolescent spine. She demonstrated that long-term correction of a mild scoliosis using a small torque of 1.5 Nm is feasible.²⁵

2.4. CONCLUSIONS

This project describes the design of an implant that is capable of correcting scoliosis by generating a small but significant lateral bending moment and an axial torque on a single C-shaped curve. The applied bending moment/torque will be maintained during a period of months/years. To avoid fusion, vertebral motion will be preserved and spinal growth will be allowed. The philosophy of exploiting creep and perhaps growth control does not essentially imply the generation of a considerable amount of instantaneous correction. Instead, it is intended that small moments and/or forces will generate a gradual shape change, as observed in orthodontic braces. In addition, the allowed range of vertebral motion will be as large as possible.

In vitro and *in vivo* models will be used to test the implant in several areas. *In vitro* porcine models will be used to test surgical procedures and proper geometric characteristics. In addition, prototypes of the implant will be tested *in vivo* in porcine models for long-term effects and particularly for non-fusion characteristics. To avoid osteoinductivity, surgery will be performed using minimal invasive techniques. The effect of the implant on a human adolescent will be tested using a FE model created by Meijer.

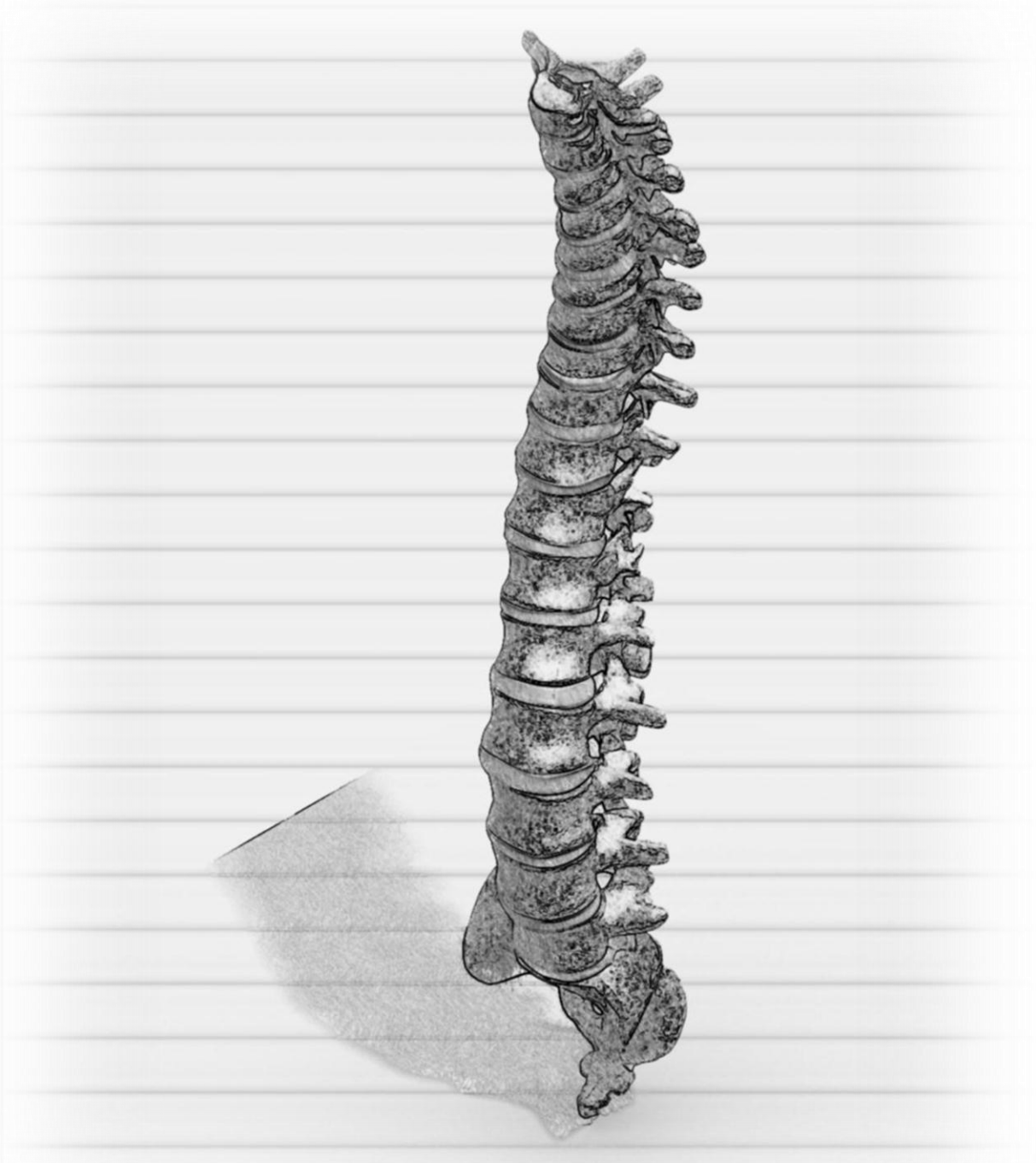
2.5. REFERENCES

1. Gallagher, D., *et al.* Healthy percentage body fat ranges: an approach for developing guidelines based on body mass index. *Am J Clin Nutr* **72**, 694-701 (2000).
2. <http://downloads.tno.nl/anonymous/kvl/NJCX1.pdf>, accessed 04-04-2011, Groeidiagram 1-21 jaar jongens NL 2010, (Netherlands Organisation for Applied Scientific Research, Delft, 2010).
3. <http://downloads.tno.nl/anonymous/kvl/NMCX1.pdf>, accessed 04-04-2010, Groeidiagram 1-21 jaar meisjes NL 2010, (Netherlands Organisation for Applied Scientific Research, Delft, 2010).

4. Bunnell, W.P. The natural history of idiopathic scoliosis. *Clin Orthop Relat Res* **229**, 20-25 (1988).
5. PRB. 2007 World population data sheet. (ed. http://prb.org/pdf07/07WPDS_Eng.pdf) (Population Reference Bureau, Washington DC, 2007).
6. Broberg, K.B. Slow deformation of intervertebral discs. *Journal of Biomechanics* **26**, 501-512.
7. McGill, S.M. & Brown, S. Creep response of the lumbar spine to prolonged full flexion. *Clinical Biomechanics* **7**, 43-46 (1992).
8. Nachemson, A.L.F. & Elfstrom, G. Intravital wireless telemetry of axial forces in Harrington distraction rods in patients with idiopathic scoliosis. *J Bone Joint Surg Am* **53**, 445-465 (1971).
9. Thornton, G.M., Oliynyk, A., Frank, C.B. & Shrive, N.G. Ligament creep cannot be predicted from stress relaxation at low stress: A biomechanical study of the rabbit medial collateral ligament. *Journal of Orthopaedic Research* **15**, 652-656 (1997).
10. Frank, C.B., Hart, D.A. & Shrive, N.G. Molecular biology and biomechanics of normal and healing ligaments—a review. *Osteoarthritis and Cartilage* **7**, 130-140 (1999).
11. Provenzano, P., Lakes, R., Keenan, T. & vanderby, R. Nonlinear ligament viscoelasticity. *Annals of Biomedical Engineering* **29**, 908-914 (2001).
12. Thornton, G.M., Shrive, N.G. & Frank, C.B. Ligament creep recruits fibres at low stresses and can lead to modulus-reducing fibre damage at higher creep stresses: a study in rabbit medial collateral ligament model. *Journal of Orthopaedic Research* **20**, 967-974 (2002).
13. Iwasaki, L.R., Haack, J.E., Nickel, J.C. & Morton, J. Human tooth movement in response to continuous stress of low magnitude. *American Journal of Orthodontics and Dentofacial Orthopedics* **117**, 175-183 (2000).
14. Middleton, J., Jones, M. & Wilson, A. The role of the periodontal ligament in bone modeling: The initial development of a time-dependent finite element model. *American Journal of Orthodontics and Dentofacial Orthopedics* **109**, 155-162 (1996).
15. Schmerling, M.A., Wilkov, M.A., Sanders, A.E. & Woosley, J.E. Using the shape recovery of nitinol in the Harrington rod treatment of scoliosis. *Journal of Biomedical Materials Research* **10**, 879-892 (1976).
16. Sanders, M.M. A memory metal based scoliosis correction system. PhD-thesis, University of Twente, Enschede. (1993).

17. Wever, D.J., Elstrodt, J.A., Veldhuizen, A.G. & v Horn, J.R. Scoliosis correction with shape-memory metal: results of an experimental study. *Eur Spine J* **11**, 100-106 (2002).
18. Newton, P.O., *et al.* Dual and single memory rod construct comparison in an animal study. *Spine* **36**, E904-E913 (2011).
19. Wang, Y., *et al.* Temporary use of shape memory spinal rod in the treatment of scoliosis. *Eur Spine J* **20**, 118-122 (2011).
20. Panjabi, M.M. Cervical spine models for biomechanical research. *Spine (Philadelphia, Pa. 1976)* **23**, 2684-2700 (1998).
21. Pearce, A.I., Richards, R.G., Milz, S., Schneider, E. & Pearce, S.G. Animal models for implant biomaterial research in bone: a review. *Eur Cell Mater* **13**, 1-10 (2007).
22. Busscher, I., Ploegmakers, J., Verkerke, G. & Veldhuizen, A. Comparative anatomical dimensions of the complete human and porcine spine. *European Spine Journal* **19**, 1104-1114 (2010).
23. Busscher, I., *et al.* In vitro biomechanical characteristics of the spine: a comparison between human and porcine spinal segments. *Spine* **35**, E35-E42 (2010).
24. Menhusen, M. Comparative human/porcine anatomy - *Sus scrofa domesticus*. in *Swine* (2002).
25. Meijer, G.J.M. Development of a non-fusion scoliosis correction device - numerical modelling of scoliosis correction. PhD-thesis, University of Twente, Enschede. (2011).

Chapter 3



DESIGN PROCEDURES

CONTENTS

- CHAPTER 3. DESIGN PROCEDURES 53**
- 3.1. INTRODUCTION..... 53
- 3.2. STAKEHOLDERS..... 53
 - 3.2.a. *Analysis*..... 53
- 3.3. REQUIREMENTS 54
 - 3.3.a. *Functional requirements* 55
 - 3.3.b. *Dimensional requirements* 55
 - 3.3.c. *Manufacturing requirements* 56
 - 3.3.d. *Materials requirements*..... 56
 - 3.3.e. *Fixation requirements* 57
 - 3.3.f. *Correctional forces/moments*..... 57
 - 3.3.g. *Surgical procedure*..... 58
 - 3.3.h. *Postoperative aspects* 58
- 3.4. DESIRES 59
- 3.5. TECHNICAL SPECIFICATIONS 60
- 3.6. SYSTEM FUNCTIONS 60
 - 3.6.a. *Main functions*..... 61
 - 3.6.b. *Sub functions* 62
- 3.7. CONCLUSION..... 63
- 3.8. REFERENCES..... 64

CHAPTER 3. DESIGN PROCEDURES

3.1. INTRODUCTION

First step in designing a new correction system is to determine functional properties of the correction system and to setup a requirements list with technical specifications and desires. This chapter describes the requirements and the main and sub functions of the system.

3.2. STAKEHOLDERS

For a designer it is important to recognise all possible individuals and groups that in some way will affect or will be affected by the development of the novel non-fusion scoliosis correction device. These stakeholders include developers, financiers, manufactures, implementers *etc.*

3.2.a. Analysis

The stakeholder analysis helps in awareness of the different interests of all parties involved. This will have some implications for the design process. It is essential in the design process to keep in mind the qualities of the stakeholders to formulate a balanced requirements and specifications list that will be used as a guide during development of the non-fusion implant. An overview of the stakeholders with their goals, essential knowledge en deficiency is presented in Table 3.1.

Although the researcher/designer has in depth mechanical knowledge and design skills, clinical knowledge is lacking. Therefore, close consultation with surgeon(s) must be carried out on, *e.g.* the state of the art of surgical techniques and feasibility of concepts. In addition, requirements regarding surgery, biocompatibility *etc.* must be determined in collaboration with the surgical staff.

As surgical intervention is mainly financed by the insurance companies, which try to keep expenses as low as possible, essential in development of new implants and surgical procedures is to present a low-priced product. Of course, patient, designer and manufacturer want to develop a high quality product, which means that a good price/quality ratio is essential. To keep the costs within boundaries, manufacturing procedures must be taken into account. The manufacturer's knowledge will be important for determining proper production techniques.

Stakeholder		Quality			
Group	Individual	Main goal	Essential knowledge	Deficiency	
Development	S1	Researcher	Testing	Functioning of implants	Clinical knowledge
	S2	Designer	Designing implant	Developing implants	Clinical knowledge
Industry	S3	Manufacturer	Production	Production methods	Functioning of implant
	S4	Distributor	Selling	Market	Functioning of implant
Finance	S5	Insurance company	Low-priced treatment	Competition	Clinical knowledge
	S6	Patient (&family)	Good price/quality ratio	Personal budget	Treatment knowledge
Diagnostics	S7	Physician	Proper diagnosis	Significance of scoliosis	Technical knowledge
	S8	Physiotherapist	Proper treatment	Posture	Clinical knowledge
Consumption	S9	Patient (&family)	Reduction of scoliosis	Comfort	Functioning of implant
Application	S10	Surgeon	Successful surgery	Surgical technique	Technical knowledge
	S11	Surgical crew	Successful surgery	Apparatus	Functioning of implant
	S12	Nursing staff	Quick recovery	Medical care	Functioning of implant
	S13	Purchaser	Purchase at low price	Competitors	Quality of implant
Regulations	S14	Regulatory affairs	Safety of the device	Biocompatibility	Functioning of implant

Table 3.1: Stakeholder analysis

The stakeholder analysis is used as a guide in the design process. S1 to S13 will be used for reference to the stakeholders involved in the formulation of requirements described in the next sections.

3.3. REQUIREMENTS

The requirements for the non-fusion correction system, directed by the stakeholder analysis, are categorized under requirements regarding functionality, dimensions, manufacturing, materials, fixation, correctional forces/moments, surgical procedures and post-operative aspects. In the following sections, the requirements are presented and numbered. In front of each requirement, the associated stakeholders, referring to Table 3.1, are listed between brackets.

3.3.a. Functional requirements

A functional requirements list describes the prerequisites regarding the actual performance of the implant system.

1. (S7, S9) Primary requirement of the non-fusion scoliosis correction device is a full correction of lateral deviation, the main characteristic of a scoliotic spine. Definition of a full correction is as follows:
2. A full lateral correction of a scoliosis is achieved if the measured Cobb-angle is equal to or less than 5° .
3. There are two distinct reasons for using a 5° Cobb-angle as a margin for full correction. First, the standard deviation in determining Cobb-angles approximately 2.5° .¹ Therefore, Cobb-angle increments of 5° or more are believed to be true changes.² Definition of a scoliosis is a curve with at least a 10° measured Cobb-angle.³
4. (S7, S9) Another main requirement of the system concerns the axial derotation. Analogues to the previous lateral correction, the definition of a full axial derotation is:
5. A full axial rotation is achieved if the axial rotation of the apex is equal to or smaller than 5° .
6. (S9) Third system requirement is the adaptation to spinal growth. Despite the fact that the system might use correctional forces to redirect spinal growth, the implant may not obstruct this spinal growth. Axial (tethering) forces generated by the implant must therefore be very low.
7. (S10) The spine must preserve some flexibility to prevent fusion.⁴ Flexibility in all directions is required. The stiffness of system must be lower than the spinal stiffness (without instrumentation). Therefore, the upper limit for flexibility is defined at $0.5 \text{ Nm}/^\circ$ in lateral and sagittal flexion and $1.1 \text{ Nm}/^\circ$ in torsion.⁵

3.3.b. Dimensional requirements

The non-fusion scoliosis correction system will have geometrical requirements, which are retrieved from the characteristics of the patient group. These requirements are essential to generate proper implant dimensions.

1. (S7, S9) The maximal length (P_{98}) of a single (C-curved) scoliosis between T5 and L5 is 440 mm for an adult (scoliotic) person.⁶ The implant length will be estimated half that size at most because it will be fixed to the most tilted vertebrae (MTV). Maximal remaining growth in the instrumented spine a 10-year-old patient is 85 mm.⁷
2. (S7, S9) Minimal implant length for the same single curved scoliosis will therefore be $220 - 85 = 135 \text{ mm}$.
3. (S9, S10) Physical system boundaries may not impede abruptly in movements in order to minimise thrust forces.
4. (S7, S9) The implant must not be visible after implantation.

5. (S9, S10) Dimensions of the system must be as small as possible considering tissues and organs such as heart and lungs.
6. (S10) The implant must not contain sharp edges that could damage surrounding tissues during spinal movements.
7. (S9, S2) Weight of the complete system is limited to a maximum of 5% of the total body mass. Minimal weight of patients is 14 kg, resulting in a maximal weight of 700 g for the complete system.

3.3.c. Manufacturing requirements

To minimize costs and to maximize quality of the implant, following requirements list is set up

1. (S3, S4) Manufacturability of all components of the system must be straightforward by applying common (or improved) techniques. Materials must be obtained from established manufacturers.
2. (S5, S6, S13) Total cost of the system may not exceed the mean cost of comparable fusion systems. Total costs comprise costs concerning material, manufacturing, surface finish and assemblage.

3.3.d. Materials requirements

The materials used in the implant must be resistive to sterilisation procedures, the body environment, and wear.

1. (S11) Materials must be able to be sterilised while maintaining material properties or remaining with a specific property after sterilisation. Common sterilisation methods are steam and dry heat sterilisation. Most frequently used method in hospitals is steam sterilisation. Due to high risk of ethylene oxide and gamma irradiation, the autoclave (steam) is preferred.^{8,9}
2. (S11) Linked to the previous requirement, materials must be heat resistive, consequently resistant to a temperature of 134°C during 6 minutes.
3. (S10) Materials must be water and corrosion resistant.
4. (S10) Materials must be resistant to pH levels between 6 and 8.¹⁰
5. (S10) Due to the requirement of biocompatibility, materials may not evoke thrombosis, allergic reactions such as redness and protuberances or inflammation. In addition, the system must not change blood compound or affect blood structures in any other way. Materials must not be carcinogenic or mutagenic and have no effect on composition of cells or cell growth.
6. (S1, S2) Roughness of the surface (finish) must be small ($R_a < 0.5\mu\text{m}$). Low roughness value lowers crack forming speed and accordingly has a positive effects on fatigue strength. Limit on surface roughness is dependent on the used materials.

3.3.e. Fixation requirements

An important requirement for the implant is movability of parts to provide for an adjustable system that can adapt to growth and to daily activities.

1. (S2) Static (μ_s) and kinetic (μ_k) friction coefficients between movable elements must be low to facilitate motion ($\mu_k, \mu_s < 0.2$).
2. (S2) Wear of the system must be minimised to guarantee maximal life span. Slack in joint parts must be limited.

3.3.f. Correctional forces/moments

Measurements from Busscher *et al.* showed serious deformities by applying moments of 2.0 Nm in young porcine and 4.0 Nm in aged humane models in different directions.¹¹ Consistent with this test, other experiments showed deformations with similar moments. Schmidt *et al.* used 2.5 Nm in aged human and young porcine cervical spines in all directions¹² and showed similar stiffness in flexion, extension and lateral bending. In axial rotation, human cervical spines showed higher range of motion. Goertzen *et al.* used moments and torques of 2.0 Nm in a porcine *in vitro* model.¹³ Although Busscher *et al.* found that the young porcine spines were more flexible than the aged human spines,¹¹ it would be likely that adolescent human spines and young porcine spines would have comparable stiffness because it is assumed that mature and aged spines usually are stiffer than adolescent spines due to altered material (tissue) properties and spine dimensions.¹⁴ These results imply that significant instant deformation will be generated when applying moments of 2.0 Nm (in torsion and lateral bending).

1. (S1) Because the focus is on a gradual correction using the viscoelastic properties of the spine, correctional forces need to be low. For indication of the necessary correction moment, the minimal estimated moment is a fraction (one-half to one-fourth) of the moment used for instantaneous correction. Lower limit of correction moment will therefore be set on 0.6 Nm in torsion and lateral bending.
2. (S1) After implantation of the implant, force equilibrium will occur. Depending on the stiffness of the implant, the generated force will lower than initial force generated by the implant in the original scoliotic shape. Assuming a linear implant stiffness, maximal applied moment might be twice the necessary moment of 2.0 Nm resulting in an upper limit of 4.0 Nm in lateral bending and torsion.
3. (S10) After fixation of the system, resulting forces and moment must be high enough to counteract progression that is dependent on the amount of lateral deviation and axial rotation. Progression could be fed by a combination of postural amplification (a result from gravity and tethering of ligaments and muscles) and scoliosis initiation. Therefore, forces should be sustained after fixation of the implant.
4. (S1) Correction must be obtained through a force-controlled mechanism. Force controlled correction means that a (more or less) constant force, applied over a long

period, achieves a gradual correction. A force-controlled system is more efficient in deforming visco-elastic structures than a position-controlled system.¹⁵⁻¹⁷

5. (S2) The system must apply some kind of correction control that controls the magnitude of correction forces required for optimal correction.

3.3.g. Surgical procedure

During surgery, the amount of tissue damage and the risks regarding the patient's health must be minimised. Following requirements must be fulfilled.

1. (S10) Fixation must be possible at vertebrae ranging from T1 to L5, also on wedged vertebrae.
2. (S10, S11, S12) Generally, surgery time in posterior spine surgery varies between 2.5 hours and 6 hours.^{18,19} To minimise infections and promote quick recovery, surgery time must be limited as much as possible. Therefore, implantation of the system must not exceed a 4 hours' time limit.
3. (S10, S11) Necessary muscle power for surgeons and assistants must be kept low. Every physically healthy person should be able to handle the system.
4. (S9) Damage to ligaments, muscles, and surrounding tissues must be minimised to preserve functionality of the spinal structure.
5. (S9) Damage to the periosteum must be avoided to prevent heterotopic bone growth that could lead to spinal fusion.
6. (S9, S10, S14) The risk of damaging peripheral nerves must be as small as possible. Risk of neurological damage must therefore be smaller than 0.3 %.²⁰
7. (S10) Blood loss in the patient during operation must be minimized and hence not exceed the blood loss during standard spinal surgery procedures. An upper limit of 100 ml per operation is acceptable.²¹
8. (S9, S14) The surgery must not be life threatening to the patient. Mortality risk for patients in common spine surgery is 0.1 %.²²
9. (S10, S11) Surgical actions should be performed through structured and normalised procedures.

3.3.h. Postoperative aspects

After surgery, the implant will be in the body for several years. Therefore, the following aspects must be taken into consideration:

1. (S10, S2) The implant must be operational at least until reaching spinal maturity (age of 19 years). Therefore, assuming patients' maximal implantation age of 17 years, the lower limit for life span of the implant is 2 years. Assuming the implant will be removed after reaching maturity; maximum life span is 10 years.
2. (S2, S9, S14) Risk of system failure, such as implant breakage and migration of fasteners, must be minimised. Acceptable lower limit for risk of failure is 1 %.²³⁻²⁵

3. *(S10, S9, S12)* In case of system failure, health risks for patients must be minimised.²⁶ Mortality risk due to system failure must be as small as possible (smaller than 0.1%).
4. *(S2, S1)* The system must function under different loading conditions, including lifting of heavy weights such as a person (maximum 100 kg). During sports, such as running, cycling, and swimming, the system must not fail.
5. *(S10)* Considering degeneration of proteins, the maximal allowed temperature of the device is 45°C, since denaturation of cells is first detectable at referenced temperature.²⁷
6. *(S10)* During the implantation period, the implant must not coalesce with spinal tissues. Additionally, fusion of vertebrae must be prevented. Experiments may reveal the degree of motion that is needed to prevent fusion.
7. *(S9)* The system must function in a temperature range from 35°C to 41°C during a long period.
8. *(S9, S12)* The Patient's life after operation must be of superior quality compared to preoperational life.
9. *(S7, S8, S9, S12)* Discomfort from the non-fusion implant must be less than from a fusion implant or an orthopaedic brace. Back pain must be avoided.
10. *(S7)* The system must not generate forces that exceed forces generated during normal activities when placed in a 3 Tesla magnetic field.²⁸
11. *(S7)* When placed in a magnetic field of 3 Tesla, the implant must not generate heat that results in temperature above 45°C.²⁷
12. *(S10)* It must be possible to remove the system. After reaching maturity and/or when correction is completed, or if complications occur, the implant will be removed.

3.4. DESIRES

In addition to the requirements, a number of desires could be extracted in order to obtain full efficiency.

1. *(S9, S5)* It is desirable to obtain a universal system that can be implanted in patients with any type/form of scoliosis and any age.
2. *(S2)* To obtain an easy construction and hence a lower risk of implant failure, the system must consist of a minimal number of parts.
3. *(S9, S10, S11)* The risk for surgeon, assistants, and patients during surgical procedures must be minimised.
4. *(S2)* It is advantageous to use form-closed connections in the implant because these are reliable over a long period. Force-closed connections however use frictional forces and are dependent on tension, which can reduce over time due to relaxation. Relaxation of forces can result in loosening of connections after a long implantation period.
5. *(S10)* Fixation of the system should be possible by means of common techniques and current surgical skills.

6. (*S10, S11*) The number of surgical actions should be minimised to reduce operation time.
7. (*S10*) The spinal fixation procedure must be as simple and non-invasive as possible. Consequently, the amount of fixations must be kept as low as possible.
8. (*S10, S2*) Surgical procedures should be as simple as possible to avoid errors and complications.
9. (*S9*) After the procedure, the visibility of scoliosis surgery should be minimised.
10. (*S10, S2*) Proportion of torsion, lateral and possibly sagittal correction forces should be adjustable. This way the system can be customised to individual patients, since each scoliotic curve has a different shape.
11. (*S10*) Surgeons should be able to use a standard system to avoid making too many choices before and during surgery.
12. (*S9*) Patients with Cobb-angles over 45° should also be qualified for surgery.
13. (*S9, S2*) There should be a possibility for fast intervention in case of system failure.
14. (*S7, S9*) Besides spinal correction, a full correction of the thorax should be accomplished. An assumption is a spontaneous correction of the thorax when full correction of the (thoracic spine) is achieved.^{29,30}
15. (*S10, S2*) Relative micro-motion of vertebrae should be possible, which will be enough to prevent fusion.⁴ Despite that, forces should be kept as low as possible to prevent the vertebrae from fusing.
16. (*S2, S9*) It would be desirable to make different combinations or connections at different locations of the spine to assemble a patient-specific correction system.

3.5. TECHNICAL SPECIFICATIONS

The technical specifications are extracted from the requirements list. A summary of the most significant specifications is presented in Table 3.2.

3.6. SYSTEM FUNCTIONS

The system will consist of an implant that corrects an idiopathic scoliosis. The implant will be connected to the spine. During the correction phase, fusion of vertebrae will be prevented by allowing spinal motion. The system will achieve a gradual but full correction through a mechanical transfer. Correction strategy aims primarily for reduction of lateral deviation and axial rotation.

Constraint	Min	Max
Growth (T1-L4)	x	85 mm
Implant length	20 mm	260 mm
Life span	10 years	x
Fabrication costs	x	1000 Euro
Weight	x	900 g
Environmental temperature	0°C	134°C
Generated temperature	35°C	45°C
Blood loss	x	1000 ml
Surgery time	x	4 hours
Lateral flexion stiffness	x	0.5 Nm/°
Torsion stiffness	x	1.1 Nm/°
Lateral correctional moment	0.6 Nm	4 Nm
Axial torsion moment	0.6 Nm	4 Nm
Axial translation posterior	-10%	18%
Implant failure risk	x	1%
Surface roughness implant	x	0.5 µm
Risk of neurological injury	x	0.30%
Mortality risk	x	0.10%

Table 3.2: Technical specifications

An overview of important constraints with the upper and lower limits. An 'x' means no limit is required.

3.6.a. Main functions

Because surgery is usually performed on patients that show accelerated growth, the system must allow significant spinal growth. In view of that, the following three main functions are subtracted.

Full lateral correction

A full correction of the lateral deviation will be accomplished by applying a bending moment to the spine. The bending moment will be generated by coupling of counteracting forces in a non-linear fashion.

Full axial derotation

An axial moment (torque) must be applied to correct the axial rotation.

Growth adaptation

Growth of the spine must be allowed by adaptation to the spinal growth. The system must axially be extendable without generation of (major) forces.

3.6.b. Sub functions

The three main functions are divided into various sub functions. These sub functions of the system are specified to gain insight in issues concerning design course. Subsequently solutions can be provided from a series of possibilities. Following this scheme, a structural design configuration will be supplied to achieve a whole package of solutions.

Sub functions of the system concerning lateral correction and axial derotation are similar. The application of correctional forces and fixation to the spine is valid in both cases. Additionally, flexibility must be preserved in the direction of correction. Lateral forces must act on the spine at the fixation points while allowing lateral flexion of the spine. Consequently, correctional forces must be low. Another sub function of the system is to control correction. Correctional forces must act on the spine when correction is still incomplete but must diminish after full correction (in order to avoid overcorrection). In Figure 3.1 an overview of the sub functions is presented.

Generation of forces must be supplied by one or more energy sources. Energy from the source must be transformed into mechanical energy, finally resulting in shape correction. The system will be anchored to the spine and will transfer the exerted forces to the spine through the fixation points. Fusion of the vertebrae must be prevented by preserving spinal flexibility to some degree. Flexion, extension, lateral flexion and axial rotation must be allowed for preservation of functionality and flexibility. Despite this, significant correctional forces must still be applied to the spine. These forces influence the stiffness behaviour of the instrumented spine. Therefore, a compromise must be made.

Due to remaining growth in most (adolescent) patients, it is essential for the system to adapt to length growth. Vertebral growth will attempt to impose a displacement on the fixation joints. For preservation of growth, the system must be lengthened or adjusted at fixation joints while absorbing only a minor amount of energy to avoid growth obstruction. Therefore, the stiffness of the system must be minimised in axial direction while the functionality of the implant is preserved.

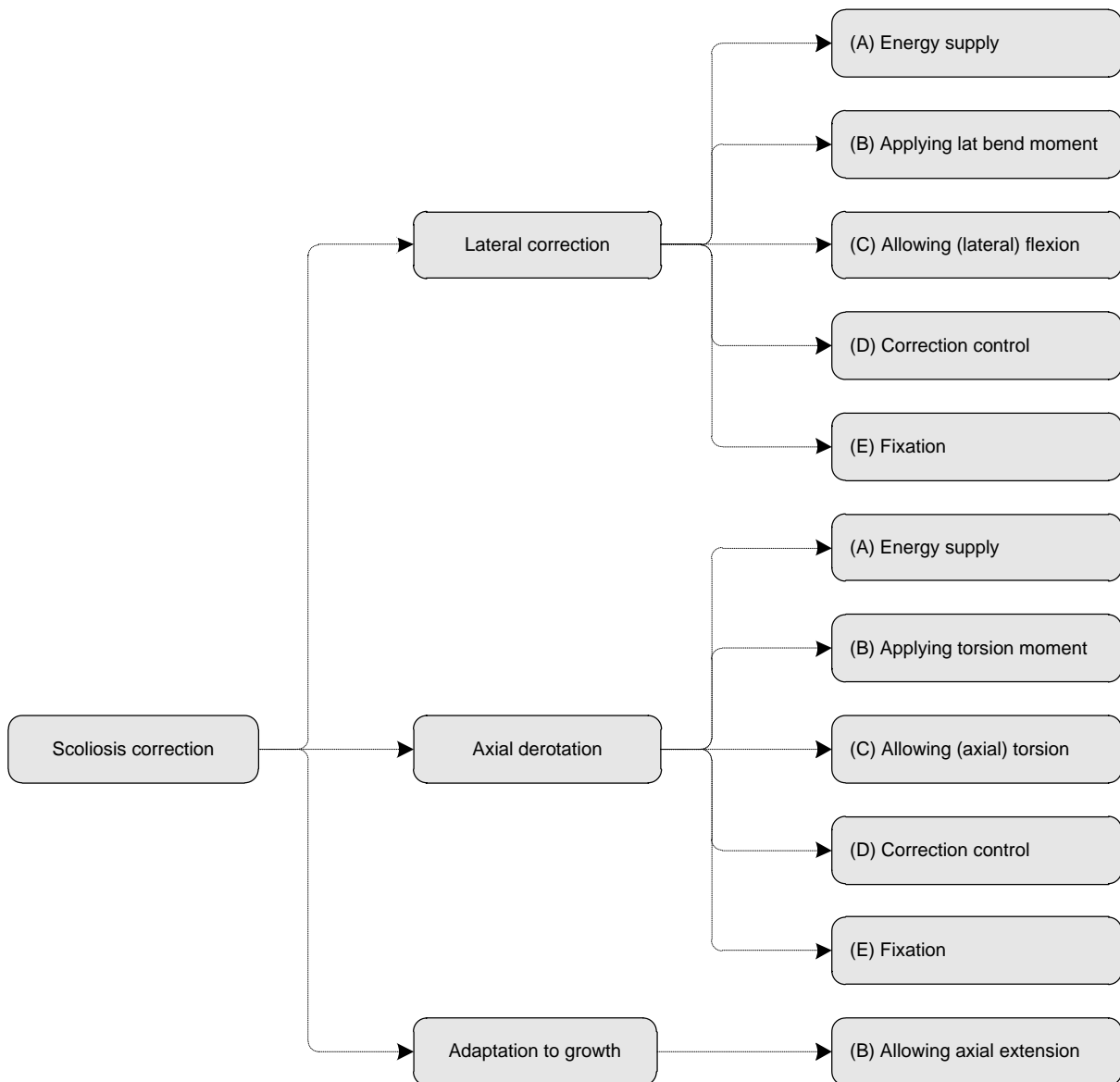


Figure 3.1: Hierarchical function model

The hierarchical function model shows the main and sub functions of the non-fusion scoliosis correction device.

3.7. CONCLUSION

In this chapter, a stakeholder analysis was performed. This resulted in an extensive requirements list that is used for designing of the non-fusion scoliosis correction system. Together with the identified main and sub functions, all boundaries for proper implementation of a methodological design are set. Within these boundaries, multiple solutions will be generated for each individual (sub) function. The next chapter describes the following steps in the design process.

3.8. REFERENCES

1. Pruijs, J.E.H., Hageman, M.A.P.E., Keessen, W., Meer, R. & Wieringen, J.C. Variation in Cobb angle measurements in scoliosis. *Skeletal Radiology* **23**, 517 (1994).
2. Lenke, L.G., *et al.* Intraobserver and interobserver reliability of the classification of thoracic adolescent idiopathic scoliosis. *J Bone Joint Surg Am* **80**, 1097-1106 (1998).
3. Bunnell, W.P. The natural history of idiopathic scoliosis. *Clin Orthop Relat Res* **229**, 20-25 (1988).
4. Kim, W.J., *et al.* The influence of fixation rigidity on intervertebral joints: an experimental comparison between a rigid and a flexible system. *J Korean Neurosurg Soc* **37**, 364-369 (2005).
5. Wilke, H.-J., Geppert, J. & Kienle, A. Biomechanical *in vitro* evaluation of the complete porcine spine in comparison with data of the human spine. *European Spine Journal* **20**, 1859-1868 (2011).
6. Stokes, I.A.F. & Windisch, L. Vertebral height growth predominates over intervertebral disc height growth in adolescents with scoliosis. *Spine* **31**, 1600-1604 (2006).
7. Wever, D.J., Tonseth, K.A., Veldhuizen, A.G., Cool, J.C. & van Horn, J.R. Curve progression and spinal growth in brace treated idiopathic scoliosis. *Clin Orthop Relat Res* **377**, 169-179 (2000).
8. Matthews, I.P., Gibson, C. & Samuel, A.H. Sterilisation of implantable devices. *Clinical Materials* **15**, 191-215 (1994).
9. Ayliffe, G.A.J. The use of ethylene oxide and low temperature steam/formaldehyde in hospitals. *Infection* **17**, 109-110 (1989).
10. Juel, C. Muscle pH regulation: role of training. *Acta Physiologica Scandinavica* **162**, 359-366 (1998).
11. Busscher, I., *et al.* *In vitro* biomechanical characteristics of the spine: a comparison between human and porcine spinal segments. *Spine* **35**, E35-42 (2010).
12. Schmidt, R., Richter, M., Claes, L., Puhl, W. & Wilke, H.-J. Limitations of the cervical porcine spine in evaluating spinal implants in comparison with human cervical spinal segments: a biomechanical *in vitro* comparison of porcine and human cervical spine specimens with different instrumentation techniques. *Spine* **30**, 1275-1282 (2005).
13. Goertzen, D.J., Lane, C. & Oxland, T.R. Neutral zone and range of motion in the spine are greater with stepwise loading than with a continuous loading protocol. An *in vitro* porcine investigation. *Journal of Biomechanics* **37**, 257-261 (2004).

14. Meijer, G.J.M., Homminga, J., Hekman, E.E.G., Veldhuizen, A.G. & Verkerke, G.J. The effect of three-dimensional geometrical changes during adolescent growth on the biomechanics of a spinal motion segment. *Journal of Biomechanics* **43**, 1590-1597 (2010).
15. Iwasaki, L.R., Haack, J.E., Nickel, J.C. & Morton, J. Human tooth movement in response to continuous stress of low magnitude. *American Journal of Orthodontics and Dentofacial Orthopedics* **117**, 175-183 (2000).
16. Veldhuizen, A.G., Sanders, M.M. & Cool, J.C. A scoliosis correction device based on memory metal. *Medical Engineering & Physics* **19**, 171-179 (1997).
17. Veldhuizen, A.G., Cheung, J., Bulthuis, G.J. & Nijenbanning, G. A new orthotic device in the non-operative treatment of idiopathic scoliosis. *Medical Engineering & Physics* **24**, 209-218 (2002).
18. Holt, R.T., Majd, M.E., Vadhva, M. & Castro, F.P. The efficacy of anterior spine exposure by an orthopedic surgeon. *Journal of Spinal Disorders & Techniques* **16**, 477-486 (2003).
19. Biscevic, M., *et al.* The posterior corrective spondylodesis - method of choice of surgical scoliosis treatment. *Med Arh* **65**, 149-152 (2011).
20. Winter, R.B. Neurologic safety in spinal deformity surgery. *Spine* **22**, 1527-1533 (1997).
21. Marks, M.P.T., *et al.* Outcomes of surgical treatment in male versus female adolescent idiopathic scoliosis patients. *Spine* **32**, 544-549 (2007).
22. Shapiro, S.A. & Snyder, W. Spinal instrumentation with a low complication rate. *Surgical Neurology* **48**, 566 (1997).
23. Betz, R.R., *et al.* Comparison of anterior and posterior instrumentation for correction of adolescent thoracic idiopathic scoliosis. *Spine* **24**, 225-239 (1999).
24. Moe, J.H., Purcell, G.A. & Bradford, D.S. Zielke instrumentation (VDS) for the correction of spinal curvature: analysis of results in 66 patients. *Clin Orthop Relat Res* **180**, 133-153 (1983).
25. McMaster, M.J. Luque rod instrumentation in the treatment of adolescent idiopathic scoliosis. a comparative study with Harrington instrumentation. *J Bone Joint Surg Br* **73-B**, 982-989 (1991).
26. Bagchi, K., Mohaideen, A., Thomson, J. & Foley, C. Hardware complications in scoliosis surgery. *Pediatric Radiology* **32**, 465-475 (2002).

27. Lepock, J.R. Measurement of protein stability and protein denaturation in cells using differential scanning calorimetry. *Methods* **35**, 117 (2005).
28. Shellock, F.G. Biomedical implants and devices: assessment of magnetic field interactions with a 3.0-Tesla MR system. *Journal of Magnetic Resonance Imaging* **16**, 721-732 (2002).
29. Kaneda, K., Shono, Y., Satoh, S. & Abumi, K. Anterior correction of thoracic scoliosis with Kaneda anterior spinal system: a preliminary report. *Spine June* **22**, 1358-1368 (1997).
30. Wood, K.B., Schendel, M.J., Dekutoski, M.B., Boachie-Adjei, O. & Heithoff, K.H. Thoracic volume changes in scoliosis surgery. *Spine* **21**, 718-723 (1996).

Chapter 4



STRUCTURAL DESIGN

CONTENTS

CHAPTER 4. STRUCTURAL DESIGN.....	69
4.1. INTRODUCTION.....	69
4.2. SOLUTIONS FOR SCOLIOSIS CORRECTION.....	69
4.2.a. <i>Energy supply</i>	69
4.2.b. <i>Applying moment</i>	70
4.2.a. <i>Allowing motion</i>	70
4.2.b. <i>Correction control</i>	72
4.2.c. <i>Fixation</i>	72
4.2.d. <i>Growth adaptation</i>	72
4.3. GENERATION OF GENERAL CONCEPT.....	72
4.4. FINAL DESIGN (XS LATOR)	79
4.4.a. <i>General description</i>	79
4.4.b. <i>The XS TOR torsion system</i>	81
4.4.c. <i>The XS LAT lateral bending system</i>	83
4.4.d. <i>Fixation</i>	85
4.5. MANUFACTURING PROCEDURES.....	87
4.6. SURGICAL INSTRUMENTS	87
4.6.a. <i>Bridge bender iXS BEN</i>	87
4.6.a. <i>Torque generator iXS SET</i>	88
4.6.b. <i>Bridge-angle measuring device iXS ANG</i>	88
4.7. STERILISATION PROCEDURES.....	91
4.8. IMPLANTATION PROCEDURES.....	91
4.9. FUNCTIONAL PROTOTYPES.....	91
4.9.a. <i>The in vivo experiment</i>	91
4.9.b. <i>Design modifications</i>	92
4.9.c. <i>Fixation to the porcine spine</i>	94
4.9.d. <i>Additionally designed instruments</i>	95
4.10. REFERENCES.....	96

CHAPTER 4. STRUCTURAL DESIGN

4.1. INTRODUCTION

In Chapter 1, we presented an extensive list of requirements and a hierarchical function model. Following a systematic approach regarding the design process, main and sub functions of the non-fusion implant are imbedded in a morphological chart which is used to generate solution principles. Guided by these solution principles, different concepts for the novel non-fusion scoliosis correction device were formulated. Illustration of all different concepts however reaches beyond the purpose of this thesis. This chapter presents the general concept by defining the most feasible solutions after consideration of the requirements list, and the final design. Additionally, surgical instruments, which have been designed to assist implantation, are presented. Functional prototypes were generated to test the final design *in vitro* and *in vivo*. These will also be presented in this chapter.

4.2. SOLUTIONS FOR SCOLIOSIS CORRECTION

Scoliosis correction using a mechanical approach is achieved by application of lateral forces that generate a lateral bending moment and by application of force couples that generate an axial torsion moment (torque). The morphologic chart in Table 4.2 gives an overview of possible solutions found for the (sub) functions identified in the previous chapter. This section describes the potential solutions. References to the sub functions categorised in Table 4.2. are presented between brackets.

4.2.a. Energy supply

(A) Generation of forces must be supplied by one or more energy sources. Practical solutions suitable in spine surgery include magnetic, thermal, electric and mechanical energy sources. Using a mechanical approach, energy from the source must be transformed into mechanical energy (Table 4.1). Energy transformation can be provided by *e.g.* an electromotor or a magnet. In addition, transformation of thermal energy into mechanical energy can be accomplished by using the body heat to generate a crystal phase change in a shape memory metal which results in a shape change (of the memory metal). In case the energy source is not thermal but mechanical, direct application of mechanical energy is possible. Another possible solution is to use the axial motion from growth to adapt the system in a way that a higher bending moment is generated. A (cork-) screw mechanism with a large lead, for example, is able to convert linear (axial) motion into rotational motion (torsion).

<i>Source</i>	<i>Energy</i>	<i>Transformation (mechanical)</i>
Electrical	Voltage · current · time	Electromotor
Magnetic	Force · displacement	Magnet (attraction force)
Mechanical	Force · displacement (torque · rotation)	xxx
Thermal	Temperature · heat conductivity · time	Shape change

Table 4.1: Energy sources

Main energy sources with potential for use in the non-fusion correction device. The supplied energy must be transformed to mechanical energy to generate required correction moment. Direct application of mechanical energy avoids the use of a transformation device.

4.2.b. Applying moment

(B) To correct the C-shaped (lateral) curve over time, a significant bending moment must be applied continuously. Possible solutions for generation of bending moments are ‘three-point’ and ‘four-point’ application of forces. In addition, the application of distraction forces, a distributed load and direct application of a bending moment are possible.

Different solutions offer different bending moment characteristics. Direct application of a bending moment, for example, results in a moment that is constant between the locations of application. A ‘three-point’ force application results in a bending moment that linearly increases from outer fixation points to the middle fixation point. Distraction forces also result in a bending moment, however to maintain moment, these forces must increase considerably when deformation becomes smaller.

4.2.a. Allowing motion

(C) Lateral and sagittal flexion of the spine must be allowed by the system. One solution is the use of a bending spring that is integrated in the implant and able to bend along with the spine in sagittal and lateral flexion. Use of one or more unidirectional springs, such as tension or compression springs, is another solution to provide the necessary flexibility between fixation points. Other solutions include the use of joints between rigid parts, allowing vertebral motion around different axes. For example, a hinge joint permits rotation around a fixed axis, whereas a plane joint allows sliding along the plane of the connected surfaces.

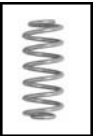




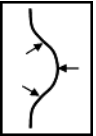




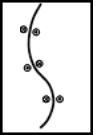


































Category			Solution						
Energy	A	Supply							
Applying moment	B1	Lateral bending							
	B2	Axial rotation							
Allowing motion	C1	Lateral flexion							
	C2	Sagittal flexion							
	C3	Axial rotation							
Control	D	Correction							
Fixation	E1	Spine							
	E2	Implant							
Growth	F	Adaptation							

Table 4.2: Morphologic chart

The morphologic chart shows an overview of the solutions found for each function in the different categories. Chosen solutions in the final concept are marked with frames. For some functions, multiple solutions were selected. In addition, it appeared that several solutions cover multiple functions.

4.2.b. Correction control

(D) The correction system must apply a bending moment that will remain until final correction is achieved. Control of correction can be accomplished by a control system that adjusts the applied moment to the amount of deformation. An example is a spring, which can be either active or passive. Active control requires an additional energy source. Another solution is the use of a control that switches off the applied correction forces after correction is achieved. Manual control is possible by interaction of for example the surgeon who inactivates the implant.

4.2.c. Fixation

(E) Fixation of the implant will be accomplished by using an interface between the functional part of the implant and the spine. Therefore, the interface must connect to the spine and the implant. A large range of fixation possibilities can be considered, such as screws, clamps, ties and rivets, and other systems such as bolt/nut anchors or glue. Generally, in spine surgery, pedicle screws, lamina hooks, transverse process hooks, and sublaminar wires are used in various combinations and configurations. Additionally, growth of bone tissue surrounding selective parts of the implant can be employed to secure anchoring of the interface to the spine.

4.2.d. Growth adaptation

(F) Adaptation to growth must be facilitated by the system in such way that the spine is able to continue growing in axial direction. Application of a flexible spring system that is able to adjust to the lengthening of the spine is one option. Another option is the use of a telescopic system that adjusts to the axial extension of the spine. An example of a more sophisticated system, which is able to expand without losing its functionality, is a pantograph. A completely different solution would be the implementation of living tissue that can grow along with the spinal growth.

4.3. GENERATION OF GENERAL CONCEPT

The number of offered solutions was narrowed down to a final concept. For each category, the best options were selected and combined. Although different solutions were explored and several concepts were generated, the final concept is presented in this section. Table 4.3 gives an overview of the selected solutions with their characteristics and the associated sub functions. In addition, most important considerations are reported. Energy supply

Use of an electrical or a magnetic source is an option; however, the accompanying energy transformation devices, such as an electromotor and a magnet, are space consuming. Considering the dimensional requirements, the system must be as small as possible. An elegant solution would be the direct application of stored mechanical

energy, which can be delivered instantly by a mechanical accumulator. Therefore, a mechanical accumulator, which is basically a pre-stressed spring, was selected for energy supply. This concept of using a mechanical accumulator can be applied for the generation of either a lateral bending moment or a torsion moment. In addition, a spring manufactured from shape memory metal can use body heat as a thermal energy source to generate the required pre-stress after fixation. Therefore, in lateral bending, a shape memory that is mouldable at room temperature and elastic at body temperature was selected for spring material. Using a spring system with a specific geometrical construction, explained in the final design, the lengthening of the system is used to adjust delivered bending moment. In torsion, a similar approach is used. A torsion spring offers a simple solution for the generation of mechanical energy. Because a large diameter is an adverse consequence from use of memory metal in the torsion spring, due to lower strength, another flexible but high strength material (Ti6Al4V) was selected.

Applying moments

C-shaped lateral curves can be best corrected using the application of a three-point bending mechanism that applies lateral forces at the apex and at the two most tilted vertebrae of the curve.¹ To reduce peak loads on the vertebrae, the generated bending moment and torque must be transferred preferably at multiple locations per vertebra. For transferring appropriate torque, at least two force couples must act on the spine. Therefore, forces will be delivered at two locations at a least three different vertebrae. Similarly, for transferring a bending moment using forces, the implant will be anchored to three different vertebrae, preferably at two locations per vertebra.

Fixation

Fixation of the implant to the spine is achieved by an interface consisting of transverse bridges that will be attached to the spine using screws or cables. Fixation of implants to the spine is commonly achieved by use of pedicle screws, hooks or wires, which have proven to be useful in spine surgery. Although pedicle screws provide for the most solid fixation, use must be avoided in the thoracic region since the facet joints are likely to be damaged during insertion of the screws,² resulting in degeneration of the joints and fusion of the adjacent vertebra. Wires damage the periosteum, leading to osteoinduction, and hooks have a risk of slipping off the laminae and transverse processes because of the vertebral motion in the flexible system. These solutions are therefore not appropriate in the use of a non-fusion scoliosis correction system. In the thoracic region, a fixation, which uses a cable that ties the implant to the transverse processes of the vertebrae, was selected as the best solution (See Chapter 5). In the lumbar and low thoracic region, pedicle screws will not obstruct facet joint motion or damage the joints during insertion. Therefore screws can and will be used in these areas.

<i>Solution</i>	<i>Characteristics</i>	<i>Sub functions</i>			
Bending spring	Pre-stressed	(A) Energy supply	(B1) Applying bending moment	(C1,2) Allowing (lateral) flexion	(C3) Allowing axial rotation
	Flexible Moment adapts to growth				
Torsion spring	Pre-stressed	(A) Energy supply	(B2) Applying torsion moment	(C3) Allowing axial rotation	(C1,2) Allowing (lateral) flexion
	Flexible Torque adapts to growth				
Bearing system	Allowing rotations in 3 directions	(F) Growth adaptation	(C1,2) Allowing (lateral) flexion	(C3) Allowing axial rotation	
	Allowing axial motion				
Bridge system	Bridges	(E1) Fixation to the spine	(E2) Fixation to implant	(2C) Applying torsion moment	(1C) Applying bending moment
	Couple creating dual fixation				
Explantation	Removal after correction	(D) Correction control			

Table 4.3: Main solutions for different sub functions

Four elements hold the solutions for all sub functions. Basically, two spring assemblies that are attached to transverse bridges using bearing systems generate corrective forces. The bridge system transfers the forces to the spine at different vertebral levels.

Allowing motion and growth adaptation

To allow spinal growth, the anchored vertebrae must be able to make relative translations in axial direction. Therefore, when anchoring the implant to three vertebrae, at least two sliding anchors must be applied. However, to secure the implant in its position, one anchor must prevent the implant from sliding axially. Application of sliding anchors at both ends of the implant and a fixed anchor at the centre vertebrae will keep the implant best in position.

The implant must be able to transfer a torque to correct the axial rotation but also to keep the implant positioned. A bent spring can apply a maximal bending moment only if it is prevented from rotating axially. A system with a non-circular cross-section is able to expand axially and deliver a torque at the same time. For example, a rod with a square cross-section is able to transfer a torque; however, the high pressure on the edges of the rod will result in a very high friction, obstructing axial translation. To reduce friction, a force couple with a large moment arm is preferred. A rod with circular cross-section that is bent into a U-shape resolves the problem. It offers a non-circular cross-section as a whole and is able to generate a torsion moment.

High implant flexibility is required to allow spinal motion. In addition to the selection of flexible materials, the use of springs that are compliant in bending and in torsion will attribute to the required spinal motion. The posterior implant cannot be placed at the natural axes of rotation of the vertebrae (in bending or torsion), which intersect in the spinal canal. Therefore, the system must have an additional flexibility in axial direction. The U-shaped springs, which deliver the bending moment and torque needed for correction, are not flexible in axial extension. A bearing system is introduced to offer a translational degree of freedom *i.e.* axial translation to enable flexion/extension. The two sliding anchors applied for allowing spinal growth, can be used for that purpose.

Since the spine is able to bend and twist in different directions, many different spinal configurations are possible. Therefore, the applied bearing systems must not only supply for motion in axial direction but also in other directions. Bearings with three rotational degrees of freedom (DOF) and one translational degree of freedom offer a solution to the wide range of motion of the vertebrae.

However, because U-shaped springs are used, axial rotation cannot be provided by (just) the bearing system. This problem is partly solved by the springs itself (including the torsion spring and the lateral bending spring), which are very flexible in torsion, and partly by allowing a relative axial rotation of the legs of the U-shaped springs.

Most straightforward solution for a bearing system with three rotational degrees of freedom is offered by ball bearings. By application of two ball bearings containing holes for the legs of the U-shaped rod that travel through the centre of two balls, a fourth degree of freedom is created. The result is however an over-constrained support design (Figure 4.1a) in which parts of the system must undergo elastic deformation to provide for motion in the bearing system. The result of that is additional friction. To diminish friction, a mailbox bearing is introduced (Figure 4.1b).

The U-shape of the springs can be used for an additional purpose, namely the adjustment of torque/bending moment during extension of the system. Using a straightforward bending/torsion spring, the increasing distance between the fixations as a result of for example axial spinal growth, will increase the flexibility of the spring. Simple mechanics show that deflection of a straight cantilever beam (at distance l from a fixed support) as a result from a force P (Figure 4.2a) increases when the lever arm l (distance between P and the fixed support) increases. Although initially more flexible than the simple straight cantilever beam construction, an U-shaped rod construction, with a force P acting on the right leg (Figure 4.2b), becomes stiffer when the lever arm l (distance between P and fixed support) increases. A more complex (closed) U-shaped rod system is shown in Figure 4.2c.

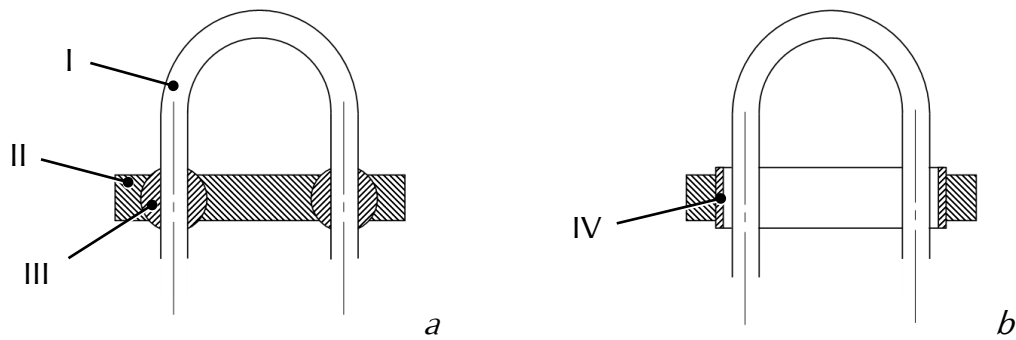


Figure 4.1: Bearing systems

(a) A U-shaped rod (I) passes two ball bearings (III), which are both fixed in a bearing house (II). Although the ball bearings themselves have 4 degrees of freedom (3 rotations and 1 axial translation), this double ball bearing system is over-constrained. (b) Introducing an extra DOF in the total system using one slide bearing (IV) diminishes friction.

The deflection mechanism of the U-shaped rod (Figure 4.2b) is illustrated in Figure 4.3a. When a constant force, acting on the U-shaped rod, travels upwards, starting from the end of the right leg, the deviation at the point of force application becomes smaller. In Figure 4.3b, a similar mechanism is demonstrated for a force couple.

For all three spring mechanisms illustrated in Figure 4.2, the bending characteristics are presented in Figure 4.4. The (lateral) deviations at distance l caused by force P (acting at distance l) are shown in Figure 4.4a. For normalised length in the range between 0.7 and 1.0, increase in deflection (with increasing normalised length) is smallest for the closed U-shape rod. When keeping the deflection at a constant value, the decrease in bending moment as a result of increasing distance l (in the same range) is least for the closed U-shaped rod construction (Figure 4.4b). Therefore, the system shown in Figure 4.2c, which compromises between the two constructions, is selected as optimal solution for the design of the non-fusion scoliosis correction system. In the application of torsion, a similar approach is used. The result is a (to growth) adjusted bending/torsion moment facilitated by this specific geometrical construction.

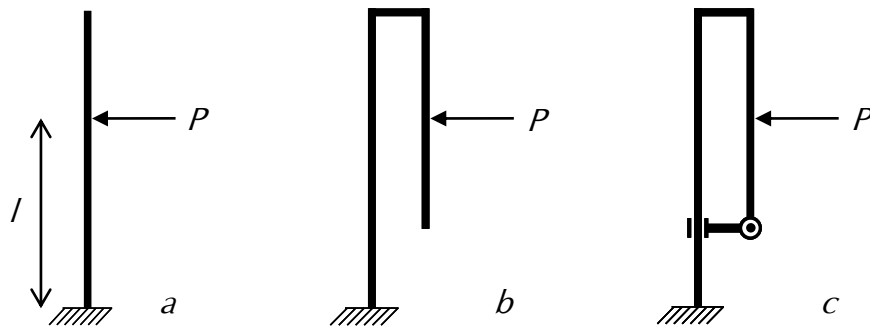


Figure 4.2: Different bending spring systems

(a) Deflection of a straight cantilever beam at distance l from fixed support as a result from a force P increases when the lever arm (l) increases, indicating that the bending spring becomes more flexible. (b) Although more flexible than the simple cantilever beam construction, deflection of a U-shaped rod at distance l as a result of force P acting on the right leg, becomes less when the lever arm increases. (c) A compromise between (a) and (b), a closed U-shaped rod, results in optimal solution.

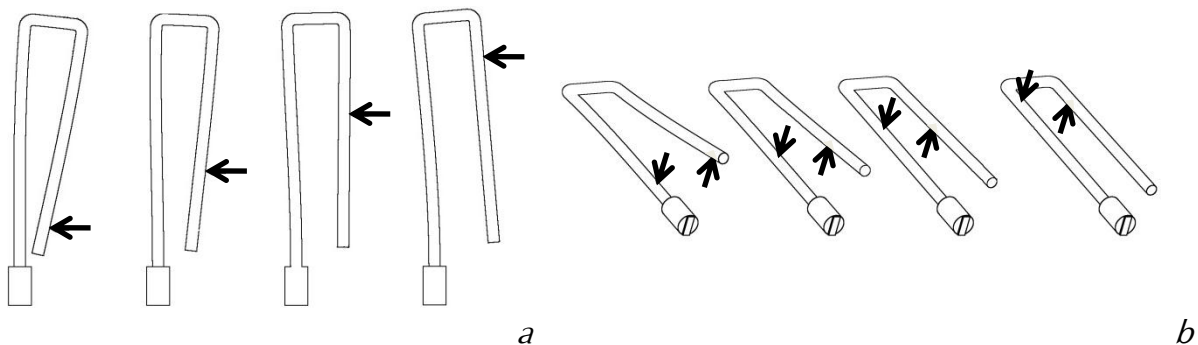


Figure 4.3: Demonstration of spring deformation mechanisms

(a) When a constant force travels upwards starting from the end of the right leg, deviation at the point of force application becomes smaller. (b) Similar mechanism applies when a force couple travels along the U-loop. In this case, the torsion (at the location of the force couple) becomes smaller.

Correction control

The implant system must be removed after full correction, which is one of the system requirements. Correction control is automatically achieved by removal of the system; therefore, an additional control system is not necessary.

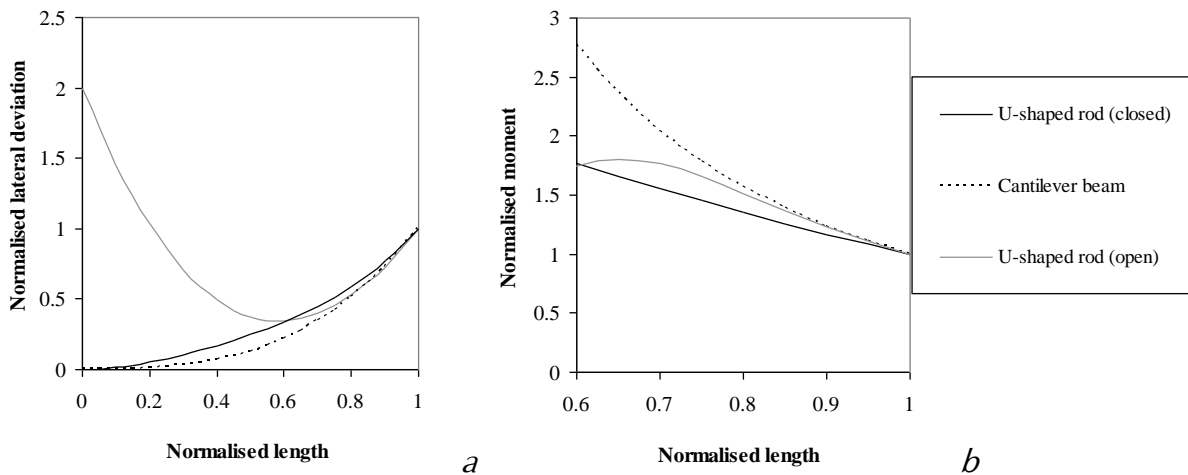


Figure 4.4: Bending characteristics of various rod configurations

(a) Three spring configurations show different deflection characteristics at distance l (normalised length) as a result of force P (at distance l). An open U-shaped rod shows a large deflection at small distance l . (b) In the range between 0.7 and 1.0 (normalised length), both open and closed U-rods perform better than a straight cantilever beam in maintaining bending moment when deflection is kept at a constant value.

Materials

Since all system parts will be implanted, biocompatible materials that are well established in orthopaedics are chosen. The most prominent material used is Ti6Al4V (grade 23) because of its extreme low tissue response, its high strength and its flexibility. Because of its extremely low friction coefficient when sliding over metal surfaces, UHMWPE is chosen for use in the plain bearings, facilitating the axial sliding over the U-shaped springs. UHMWPE is a polymer, which has successfully been used as a biomaterial in (spinal) implants over the past decades. However, creep in UHMWPE does make the material inappropriate in high stress applications. PEEK (polyetheretherketone) is a creep resistant polymer with excellent mechanical properties, such as high young's modulus and tensile strength. The centre bearing in a three-point system is loaded with high stresses and must allow small motion. At the same time, the bending spring must not be damaged. Therefore, despite the much higher friction coefficient, PEEK is used in this centre bearing system, thereby combining high strength with low wear.

NiTi is chosen as material for the (three-point) lateral bending spring since it is highly biocompatible and it has additional advantages such as pseudo-elastic properties at body temperature, resulting in low stiffness at high stress levels.

Outline

Application of the bending moment is executed by a (pre-stressed) flexible bending spring that is aligned with the spine, thus offering solutions for several functions. The spring assembly supplies energy, after pre-stressing it, and generates a bending moment by application of forces at different locations. In addition, the flexible spring assembly allows (lateral) flexion and axial rotation. To generate a bending moment, three forces will be applied at three vertebral levels.

The similar application of a torsion spring resolves multiple solutions regarding energy supply, applying torsion and allowing motion.

A bearing system with multiple degrees of freedom facilitates a large range of vertebral motion offering flexion of the spine in different directions and allowing axial growth of the spine.

Finally, each implant is connected to the spine by means of three transverse bridges. Each implant can use its own set of bridges or the implants can share one or more bridges. Each bridge is anchored at two locations per vertebra to facilitate the application of force couples and the distribution of forces at the desired levels.

4.4. FINAL DESIGN (**XSLATOR**)

4.4.a. General description

In the final design, the system referred to as **XSLATOR** comprises two implants, splitting up the system in two functional elements. The first implant, the **XSTOR**, is a torsion-generating element that applies mainly a torque on the spine to generate torsion. The second part, the **XSLAT** is a lateral bending implant that mainly applies a bending moment to generate lateral bending. Unlike current fusion systems,³ the system is highly flexible. The method of fixation, materials, and geometry provide for the flexibility of the system. The forces on the spine are limited but remain present within a large range of motion (ROM). Because the imposed corrective forces and torque are small and the system is flexible, fusion of the vertebrae is avoided. The functionality of the spine remains thereby preserved. After a certain period of implantation, when shape correction has occurred, the system will be removed without permanent functional damage to the spine.

By intervening during the growing period, not only can the surgery be performed timely, but also use can be made of the spinal growth. Growth of the system, accompanied with geometrical changes, is used for compensation of the loss of bending moment and torque, which commonly occurs in current implants. This loss of moment/torque is a logical result from accomplished correction and progressing length of the system. The **XSTOR** and the **XSLAT** are placed on the posterior side of the spine and attached to

anchor systems at three vertebrae (Figure 4.5). The implants are attached in a stress-free state, after which these can be stressed to generate the required bending moment or torque. The implants facilitate axial expansion of the system in order to adapt to growth and daily movements. Each implant is capable of allowing 35% axial spinal growth and daily motion.



Figure 4.5: Dual implant system XS LATOR

The dual implant system consists of two implants that are attached on the left and right sides of the vertebrae to anchor systems at three different vertebrae. A scoliotic spine with a lateral bending to the right and an axial rotation to the left (into the concavity) is instrumented on the right side with an XS LAT lateral system and on the left side with a XS TOR torsion system.

4.4.b. The **XS TOR** torsion system

First element, the **XS TOR**, is an implant that generates the torque needed for correction of the axial rotation (Figure 4.6a). In a scoliosis with a lateral curve (and apex) to the right, the **XS TOR** is placed laterally on the left (concave) side of the spine. The **XS TOR** is attached to three different vertebrae spanning a vertebral region of six or seven vertebrae. Main contribution to the functionality of the system is delivered by two torsion springs integrated in the system. The springs generate a significant torque but at the same time have a low bending stiffness so that during bending of the spine (and thus also bending of the implant) only a slight bending moment occurs. The two titanium grade 23 (Ti6Al4V) coil springs with low stiffness and high yield strength coil springs, are interconnected by a multifaceted part (Figure 4.7) and fitted with a U-part (titanium grade 23) at each end. Each U-part transfers the torque via sliding anchors to a transverse bridge system (Figure 4.6). The U-parts contribute to the flexibility of the implant. The sliding anchors, which both exist basically of a bearing house containing a UHMWPE (Ultra High Molecular Weight Polyethylene) bushing that slides over the U-part, is able to adjust to the spinal movement and growth (Figure 4.6b). The bearing houses which are each secured to a bridge (titanium grade 23) form the two outer fixation elements (cranially and caudally) of the implant. A third fixation element is formed by a middle part that is secured to a third bridge. Each transverse bridge is anchored to the spine in two fixing points per vertebra. After (unloaded) anchoring, the **XS TOR** is preloaded using a torque-generating instrument. The instrument creates an axial rotation of the multifaceted middle part after which the multifaceted part is shifted into the box-shaped part containing a square hole (Figure 4.7a, b). Thus, torsion is created in the springs. This preloading is secured by a setscrew. Because the tension-free shape of the implant is not reached after implantation, the implant is able to generate a torque that remains significant during the implantation period. The construction as a whole is a torsion generator in which four spring elements (two springs and two U-parts) are placed in series. The fraction of the U-part that is loaded in torsion depends on the distance between the anchors. The increase of the stiffness caused by extension (growth) counteracts the decrease in spinal torsion (correction) because of the applied torque, which results in a torque-controlled system.

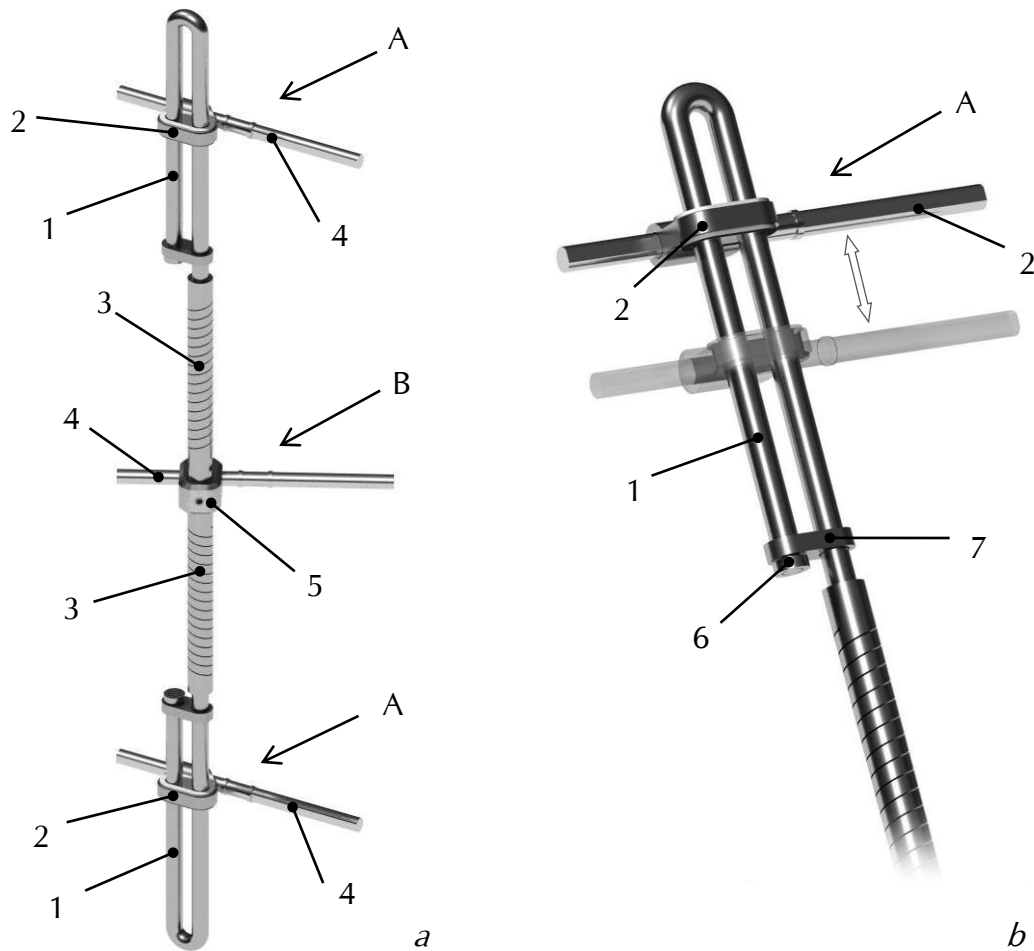


Figure 4.6: The XS TOR torsion system

(a) The XS TOR is an implant comprising two coil springs (3) that are fixed under tension, generating a torque. As a result, the middle fixation element (B), including box-shaped part (5) and bridge (4), is axially rotated relative to the outer fixation elements (A), when unstressed. The three transverse bridges (4) are fixed to the spine at three vertebral levels. The two outer fixation elements (A) are able to slide via sliding anchors (2) over the U-parts (1) to adjust to spinal movement and growth (b) The fixation element (A) with bridge (4) and bearing system (2) is able to translate axially by sliding over the U-part (1). The U-part is closed by a connector part (7) and a locking ring (6).

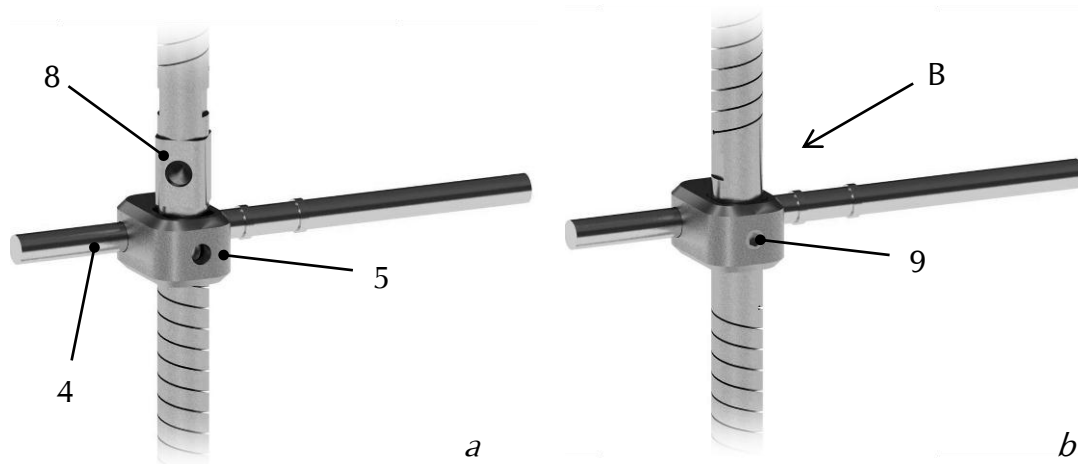


Figure 4.7: Application of torque

The torsion springs contain a multifaceted part (8). In this example, the part contains four facets. Torque is applied by creating torsion in the springs (and the multifaceted part) followed by shifting the implant into a box-shaped middle part (5) that contains a square hole and which is fixed to a transverse bridge (4). (b) The fixation element (B) is secured with a small setscrew (9).

4.4.c. The **XS LAT** lateral bending system

The second element is the **XS LAT**, an implant that generates the bending moment needed for correction of the lateral deformation (Figure 4.8). The functionality of the **XS LAT** is partly based on the properties of NiTi (memory metal), a material with low stiffness and high yield strength. The bending moment is delivered by a pre-bent NiTi (55.8wt% Ni, Ti balanced) rod that is in full austenitic crystal phase at a temperature of 37°C (A_f finish temperature). The 4 mm NiTi rod is anchored posteriorly to the spine, creating a highly flexible system that will induce a sufficient lateral bending moment. The implant is able to retain the full range of motion of the spine (ROM). Like the **XS TOR**, the **XS LAT** is attached to the spine by three transverse bridges to three different vertebrae spanning a vertebral region of six to seven vertebrae. In a scoliosis with a lateral curve to the right, the **XS TOR** is placed at the right of the spinous processes. The **XS LAT** is pre-stressed, so a significant force is transmitted continuously. The NiTi rod contains two U-parts that will keep the rod in proper orientation. The U-parts are interconnected with one leg each creating two closed U-loops. The outer two anchors, which are fixed cranially and caudally, are attached to the U-parts each by a sliding bearing system consisting of a titanium grade 23 bearing house and a UHMWPE bushing, similar to the **XS TOR** anchors. The anchor in the middle of the implant contains a bearing house with a PEEK (polyetheretherketone) element. The middle anchor locks the implant so that the implant itself will not move in axial direction. Another PEEK element closes the loop of the rod.

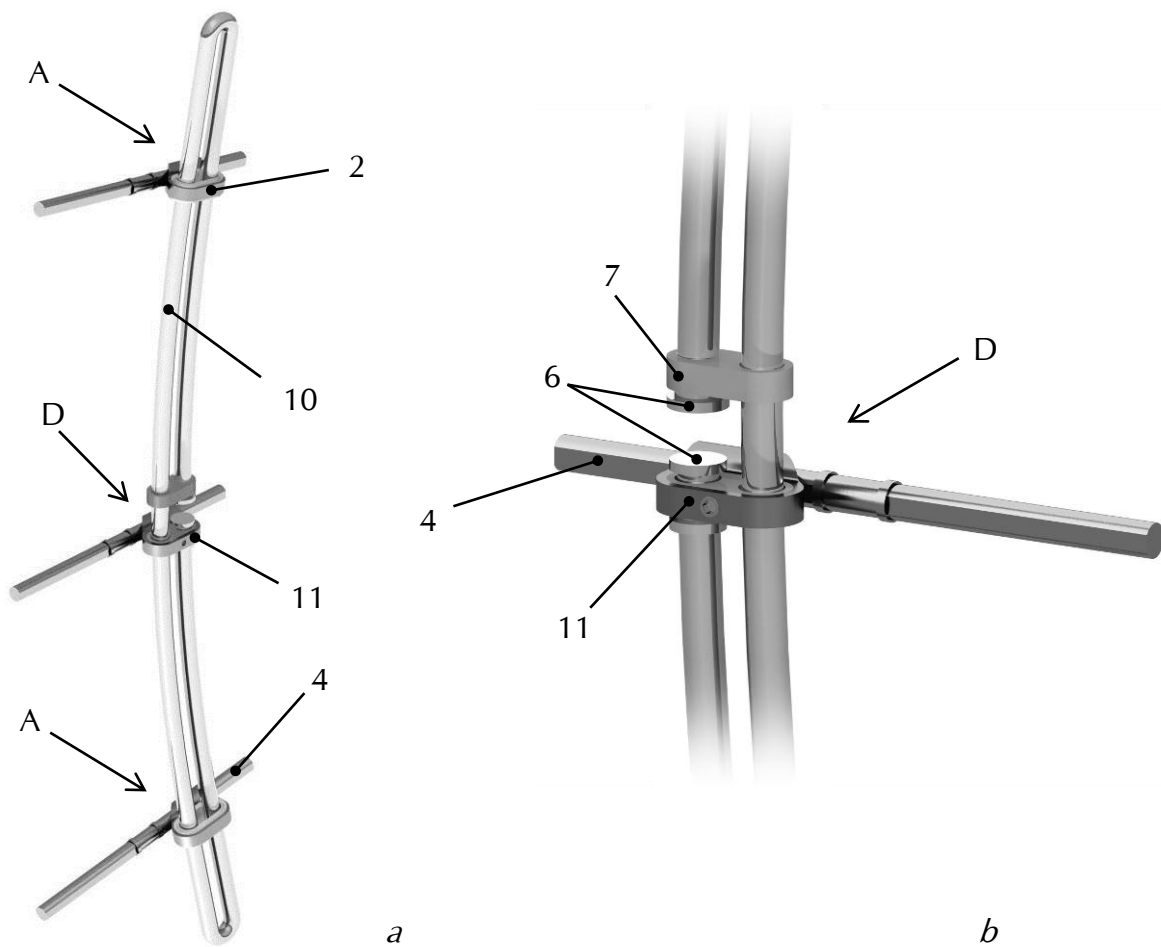


Figure 4.8: The XS LAT lateral system

(a) The XS LAT is an implant comprising a 4 mm NiTi rod (10) with a stress-free curvature at body temperature of 37°C that is dissimilar to the scoliotic curve. After anchoring the system to the spine via three fixation elements (A, D), it generates a bending moment that will induce shape change of the scoliotic spine. Sliding bearings (2) connect the NiTi rod to bridges (4) creating the two outer fixation elements (A). The sliding bearings (2) each consist of a bearing house and a UHMWPE bushing. (b) In the middle fixation element (D), the bearing system (11) locks the system axially preventing shifting of the rod. The U-shape is closed by a PEEK part (7) and two locking rings (6).

The NiTi rod is in a malleable (martensitic) crystal phase at room temperature. Before anchoring, the rod can be manoeuvred into the deformed scoliotic shape, in order to facilitate stress-free insertion. After anchoring, a bending moment is induced by allowing the implant to warm up to body temperature. The NiTi rod 'remembers' its original shape deformation at body temperature when anchored to the spine. The pre-bent shape, the closed U-shaped rod configuration and the pseudo-elastic properties of NiTi compensate for the decrease in lateral bending moment caused by the lateral correction

as a result of the generated bending moment, which results in a moment-controlled system. Figure 4.9 illustrates the generation of the bending moment as a result of the mounting procedure.

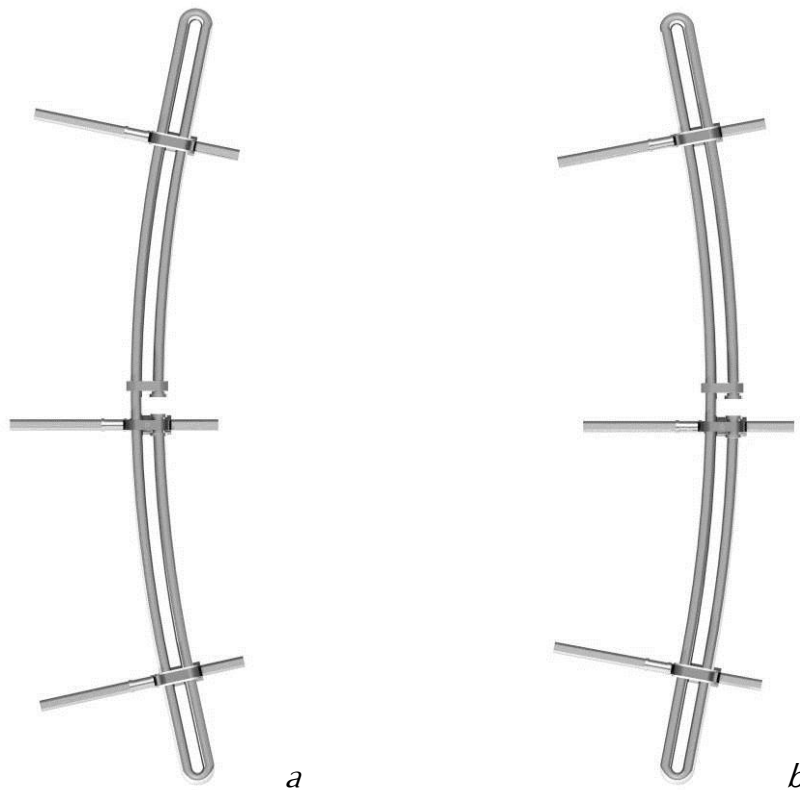


Figure 4.9: Generation of bending moment

(a) This is the original high temperature shape. In the low temperature phase, which is at room temperature, the implant is mouldable and can be bent into a deformed shape.
(b) The implant is moulded to the deformed spinal shape, which in this example is a right lateral curve. After the implant is fixed to the spine and the wound is closed, the temperature rises to 37°C and the implant ‘remembers’ its high temperature shape. Because the implant is fixed to the spine, it generates a bending moment.

4.4.d. Fixation

The anchoring of both systems and thus the transfer of forces is obtained in a similar manner. Both devices can use the same bridge-sections, if the required locations for application of torque and bending moment are similar. Each device has double U-shaped parts, which ensures that the implant maintains orientation and delivers the required torque or bending moment. At both ends, each implant runs through sliding anchors that allow longitudinal motion of the implant, which thus can ‘grow’ along with the spine. The forces in longitudinal direction will remain low during the functional movements of the spine.

The sliding anchors of the U-shaped rods limit only two degrees of freedom, namely those that provide the desired bending moment and torque. This means that the two implants allow as much movement as possible.

Both systems are fixed to the most tilted vertebrae (MTV) and the apex. In a typical thoracic scoliosis, as described in Chapter 1, fixation will be to the vertebrae T5, T8, and T10. In a typical thoracolumbar scoliosis, fixation will be to vertebrae T9, T12, and L2. The implants have dimensions that are required for fixation at these levels. In the mid and high thoracic regions (T3-T10), fixation of the bridges will be realised using the **XS FIX**, a cable system that is attached to the transverse processes of the vertebrae, which is described in Chapter 5. In the low thoracic and lumbar regions, pedicles screws will be used for fixation (Figure 4.10).

An international patent application for the total implant system, including fixation, was filed under PCT application number PCT/NL2012/050340 on 16 May, 2012. The patent specification (including claims and figures) is stored in Appendix I.

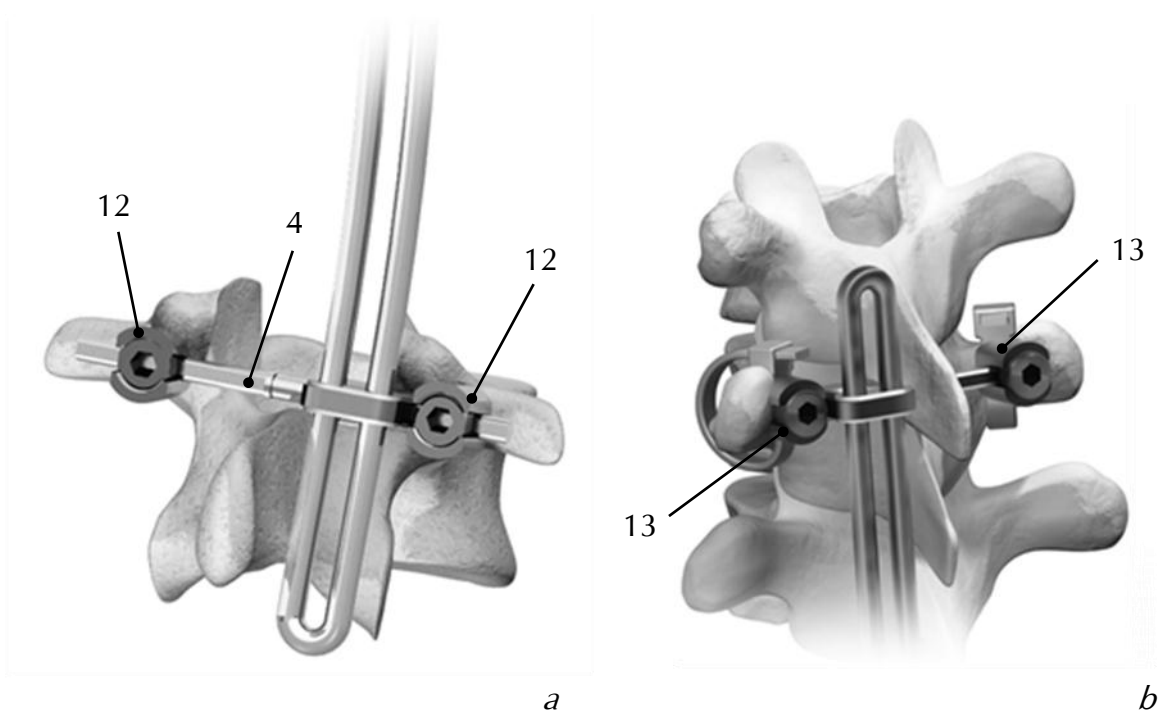


Figure 4.10: Pedicle screw fixation

*The bridges (4) are anchored by means of poly-axial pedicle screws (12) in the low thoracic and lumbar region (a) or **XS FIX** (13) in the mid and high thoracic region (b).*

4.5. MANUFACTURING PROCEDURES

The majority of the system parts are entirely manufactured using common machining techniques such as milling, drilling and turning. Some parts, such as the torsion springs and bearing houses are partly manufactured using a machining process referred to as Electric Discharge Machining (EDM).⁴

The springs, U-shaped rods, and locking rings are joined together using a Laser Beam Welding (LBW) technique, which has proven an excellent method for accurate joining of Ti6Al4V.⁵ The lateral NiTi bending rod achieves its characteristic shape memory and pseudo-elastic behaviour after a heat treatment consisting of annealing at 525°C for 60 minutes followed by a rapid cooling and an additional aging at 400°C for 20 minutes and another rapid cooling (See Chapter 1 for details).

To avoid tissue response, ion-release into the tissue will be minimised by passivation of Ti6Al4V parts. During the process, a significant oxidation layer will be obtained.⁶ Before passivation, all parts are mechanically polished minimizing friction and preventing osteoblast proliferation and consequently adhesion of bone tissue.⁷ The NiTi rod will be passivated in nitric acid, which proves to be the optimal passivation procedure for NiTi implants.⁸

4.6. SURGICAL INSTRUMENTS

In spine surgery and surgery in general, surgical tools are used for opening and closing the wound and for preparation of tissue before implantation. For the insertion of poly-axial pedicle screws, specialised tools such as pedicle probes, awls and screwdrivers, are used. Implantation of the **XS LATOR** requires some additional specialised tools. Several instruments have been designed. These instruments include a bridges bender (**iXS BEN**), a bridge-angle measuring device (**iXS ANG**), a torque generator (**iXS SET**), and a modified pedicle screwdriver. For the *in vivo* experiments, some additional instruments were designed and manufactured to meet the altered requirements. The instruments are described in the next sections.

4.6.a. Bridge bender **iXS BEN**

The bridges are attached to the pedicle screws and cross the spinous processes. To make this fixation possible, the transverse bridges may need to be bent to adjust to the posterior vertebral shape preventing bone damage. Therefore, a tool that bends the bridges (**iXS BEN**) is used. This simple tool consists of two tubes that slide over the bridge. With a simple bending movement, the bridge is bent into the required angle (Figure 4.11).



Figure 4.11: Bridge bender iXS BEN

*The **iXS BEN** bridge bender consists of two identical elements. One element mainly consists of a tube and a handle. The tubes slide over the bridge until they meet the rims in the middle of the bridge. By using the handles, the bridges are bent into the desired angle.*

4.6.a. Torque generator **iXS SET**

After fixation, the torsion system must be stressed to generate the proper torsion load. A special tool, the **iXS SET**, has been designed to make that possible. The instrument will generate torsion and a final connection between the parts. The **iXS SET** is placed over the spring assembly after which it is rotated around the longitudinal axis of the springs. The accompanied rotation of the multifaceted part allows the spring assembly to be shifted axially fitting the multifaceted part into the box-shaped part of the **XS TOR** (Figure 4.13).

4.6.b. Bridge-angle measuring device **iXS ANG**

The bridges pass the spinous processes and are fixed to the pedicles screws. Although the screws have pivoting heads that can be adjusted to fit the bridges, the angle of the bridges needs to be accurate. For that reason, the **iXS ANG**, a tool that measures the required angle for the bridges, was designed and manufactured. The **iXS ANG** is placed in the two heads of the screws of an instrumented vertebra in neutral position, and makes the same angle as required for the bridge (Figure 4.12). On top of the device, two channels were created to fit the bridge. The bridge must be bent using the bridge bender in such an angle that it fits the channels.

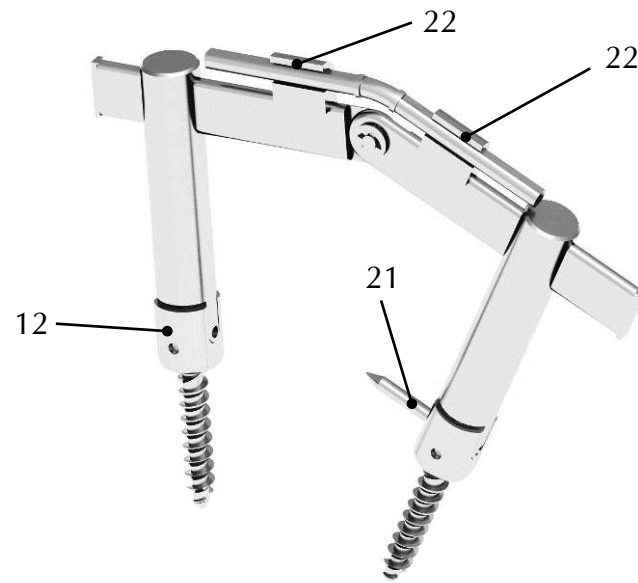


Figure 4.12: Bridge-angle measuring device iXS ANG

This measuring device can be placed onto the pivoting heads of the pedicle screws (). The bridge must be bent until it fits the channels (22) on top of the device. A pin (21) points to the place where the spinous process must be penetrated with the awl.

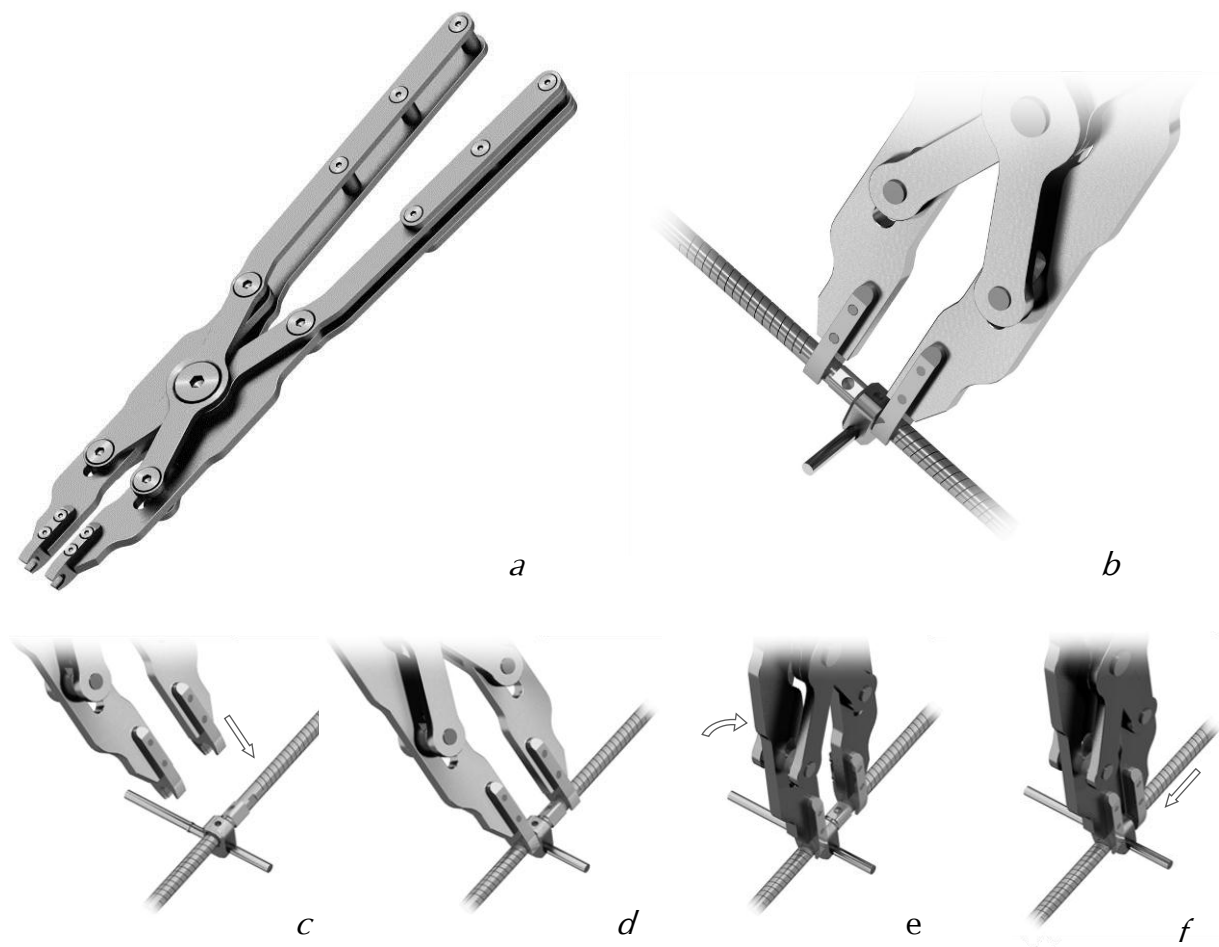


Figure 4.13: Torque generator *iXS SET*

*(a, b) The **iXS SET** is an instrument that creates the required torque in the implant. (c) The instrument will be placed over the torsion spring assembly, which contains a pair of flat sides that fits one end of the nose of the **iXS SET**. (d) The other end of the nose is able to slide axially over the springs. (e) Torque is generated by rotation of the instrument around the longitudinal axis of the springs resulting in torsion. (f) After the rotation, the spring assembly is shifted axially by a squeezing of the **iXS SET**, fitting the multifaceted part into the box-shaped part of the **XS TOR**.*

4.7. STERILISATION PROCEDURES

The designed implants including all fixations parts and surgical instruments are sterilised in an autoclave (at a temperature between 121°C and 134°C).

4.8. IMPLANTATION PROCEDURES

The implantation of the implants is analogous for both implants, with the exception of the application of pre-stress. First, the instrumented vertebrae must be identified. For a typical thoracolumbar scoliosis (as described in Chapter 2), the vertebrae T9, T12 and L2 are selected for instrumentation (MTV and apex). Implantation of an implant (to correct such typical thoracolumbar scoliosis) will be performed according the steps summarised below:

Posterior skin incision longitudinal over the spinous processes (T9-L2).

Blunt dissection of muscle tissue along the incision.

Exposing of the vertebrae T9-L2.

Insertion of screws/**iXS FIX** to the vertebrae T9, T12 and L2.

Determination of bridge-angles with **iXS ANG.**

Bending of bridges with **iXS BEN.**

Insertion of implants and middle bridge (apex, T12).

Fixation of the middle (apex) bridge to the screws.

Insertion of the cranial and caudal bridges (MTV, T9, and L2), which pass through the (distal) bearing systems.

Fixation of the distal bridges to the screws.

Pre-stressing of the torsion implant **XS TOR** with the **iXS SET.**

The lateral implant **XS LAT** is automatically pre-stressed by body temperature.

Closing of the muscle tissue and skin.

4.9. FUNCTIONAL PROTOTYPES

4.9.a. The *in vivo* experiment

In chapter 2, the strategy of using a porcine model for testing the implant was described. An ('inverse') implant that is used for scoliosis induction is different from a scoliosis correction implant. In addition, an implant used in a porcine model has altered requirements due to several differences between the human and the porcine spine. For example, spinal age is quite different. The porcine model used in the experiment between two months and three months, which is quite a contrast with the adolescent patients. Despite the differences in spine ages, geometry and in spinal mechanical behaviour, requirements for this different design are quite similar.^{4,5} Similarities in vertebral height and spinal growth result in similar requirements regarding the size of

the implant. Due to differences in other vertebral dimensions, such as the size of the vertebral bodies, spinous processes and transverse process, the fixation of the bridges to the spine of the implant is different. Therefore, certain design modifications were implemented.

4.9.b. Design modifications

One of the modifications that were carried through meeting the requirements of the *in vivo* experiment relate to the configuration of the implants. To test different configurations, two different types of the lateral and torsion implants were designed and manufactured. Two sizes, a narrow, and a wide version with according configurations of the **XS TOR** and the **XS LAT** were manufactured (Figure 4.14). The narrow versions were designed to fit between the screws as a hole and the wide versions were designed to fit partly between the screws and partly outside the screws. Although the wide version is larger, the space required between the screws is smaller. (The wide version was designed for implantation in case the small version would not fit between the screws.) The wide and narrow versions were realised using different anchoring configurations. A narrow version is placed between two pedicle screws whereas a wide version is attached laterally to the pedicle screws (Figure 4.15). The bearing systems are fixed to the bridges while able to slide axially over two U-shaped loops facilitating adaptation to growth and daily movements.



Figure 4.14: Functional prototypes

Four different prototypes were designed and manufactured for *in vivo* implantation using a porcine model. Wide and narrow versions of the **XSLAT** and the **XSTOR** were manufactured. The narrow versions (b, c) were placed between the screws and the wide versions (a, d) were partly placed between the screws and partly lateral. Narrow versions are slid onto the bridges before the bridges are mounted onto the screws. The wide versions are slid onto the extending end of the bridges after the bridges have been put into position. To stop the wide version from sliding back off the bridge, the protruding end of the bridge (see Figure 4.15) is deformed using a special pair of pliers. All implants (a, b, c, d) contained rings attached to the end of the U-shaped loops that prevented the implant from disassembly. Only the two rings of the narrow torsion system (c) are illustrated in the figure.

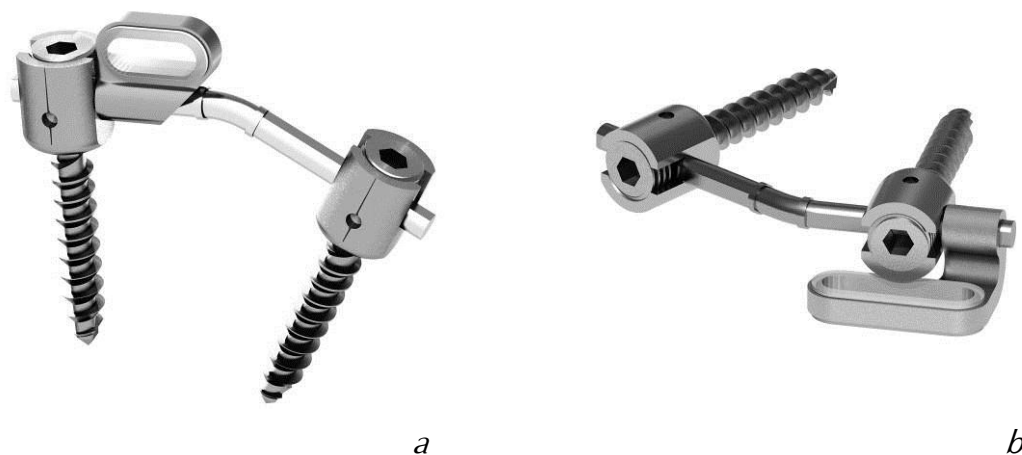


Figure 4.15: Different anchor configurations

Pedicle screws were used for fixation in the porcine model. (a) Bridges, travelling from left to right, formed the foundation of a solid fixation. (b) A wide system is placed after fixation of the bridges. The protruding end of the bridge is deformed to prevent the bearing from sliding back off the bridge.

4.9.c. Fixation to the porcine spine

Like in the original design of the scoliosis correction system described in the previous sections, three bridges are fixed to three different vertebrae in the porcine models. The **XS FIX** however cannot be used due to the small transverse processes of the porcine vertebrae. Therefore, the bridges are fixed just by using pedicles screws. For the experiment, special pedicle screws were designed. Existing screws used in humans could not be used for our purpose due to the different vertebral body and pedicle geometry of the porcine model. Original thoracic pedicle screws are large and only available for 6 mm rods. A smaller screw was designed fitting the porcine vertebrae and suited for $\varnothing 3.5$ mm bridges. In addition, the application of the bridges is different. Porcine spinous processes hinder the bridges, which are spanned from right to left. As a solution, the bridges travel through the spinous processes after creation of a small hole in the spinous processes.

Before placement of the bridge, the required hole in the spinous process must be created. To locate the place of the hole, the bridge-angle measuring device **iXS ANG** is used. The device contains a pin that points to the position where a hole must be created. After the holes are created with an awl and the bridges are bent into the proper angles, the bridges can be placed easily.

4.9.d. Additionally designed instruments

Some additional instruments were specially machined for the assistance of the surgical staff, facilitating the insertion of screw and attachment of the implants. A special screwdriver was manufactured, by means of modification of an existing one. Other examples are a tap for tapping screw thread into the bone, and special pliers for deforming the end of the bridges after fixation of the wide bearings to the bridges (Figure 4.16).

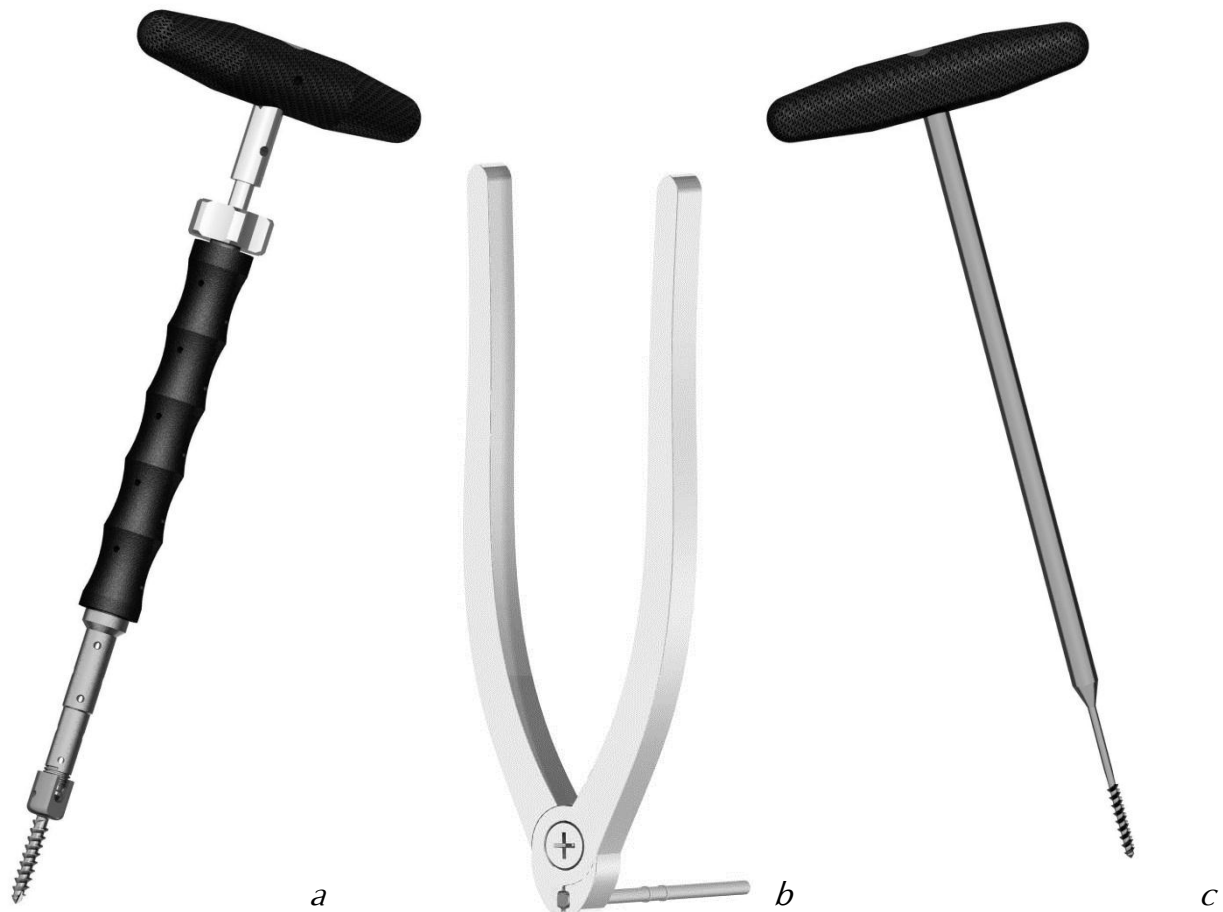


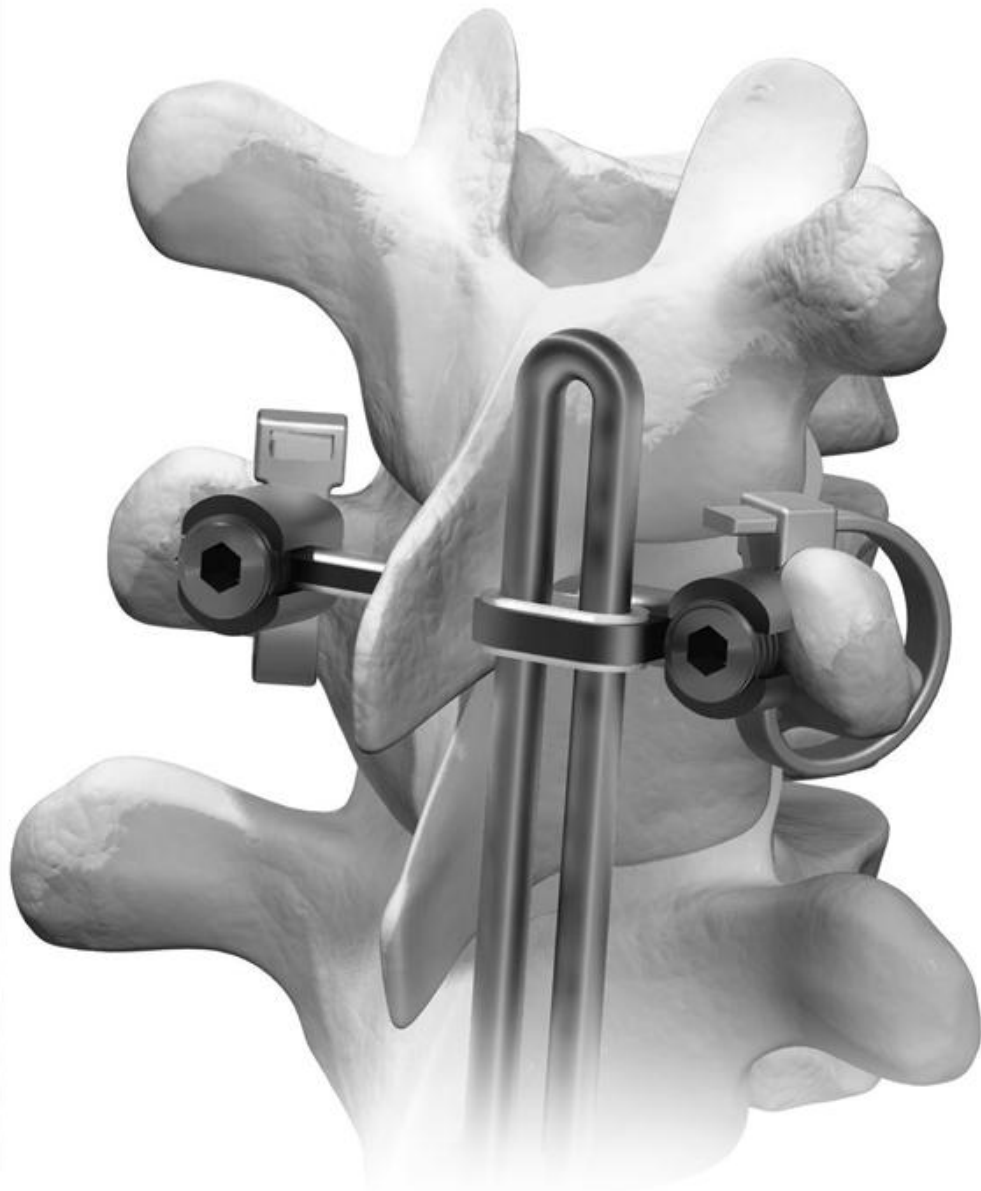
Figure 4.16: Additional instruments

(a) The pedicle screwdriver is used to lock the poly-axial screw after which the screw is firmly fixed. The screw passes the pedicle and is secured into vertebral body. (b) With special pliers the end of the bridges are deformed to lock the wide bearings to the bridges. (c) With a screw thread tap, the pedicles are prepared for screw insertion.

4.10. REFERENCES

1. Sanders, M.M. A memory metal based scoliosis correction system. PhD-thesis, University of Twente, Enschede. (1993).
2. Chung, K., Suh, S., Swapnil, K., Yang, J. & Song, H. Facet joint violation during pedicle screw insertion: a cadaveric study of the adult lumbosacral spine comparing the two pedicle screw insertion techniques. *International Orthopaedics* **31**, 653-656 (2007).
3. Maruyama, T. & Takeshita, K. Surgical treatment of scoliosis: a review of techniques currently applied. *Scoliosis* **3**, 6 (2008).
4. Ho, K.H. & Newman, S.T. State of the art electrical discharge machining (EDM). *International Journal of Machine Tools and Manufacture* **43**, 1287-1300 (2003).
5. Akman, E., Demir, A., Canel, T. & Sınmazçelik, T. Laser welding of Ti6Al4V titanium alloys. *Journal of Materials Processing Technology* **209**, 3705-3713 (2009).
6. Lee, T.M., Chang, E. & Yang, C.Y. A comparison of the surface characteristics and ion release of Ti6Al4V and heat-treated Ti6Al4V. *Journal of Biomedical Materials Research* **50**, 499-511 (2000).
7. Mustafa, K., *et al.* Determining optimal surface roughness of TiO₂ blasted titanium implant material for attachment, proliferation and differentiation of cells derived from human mandibular alveolar bone. *Clinical Oral Implants Research* **12**, 515-525 (2001).
8. O'Brien, B., Carroll, W.M. & Kelly, M.J. Passivation of nitinol wire for vascular implants - a demonstration of the benefits. *Biomaterials* **23**, 1739-1748 (2002).

Chapter 5



**A NOVEL ANCHORING SYSTEM FOR THE NON-FUSION
SCOLIOSIS CORRECTION DEVICE**

CONTENTS

CHAPTER 5. A NOVEL ANCHORING SYSTEM FOR THE NON-FUSION SCOLIOSIS CORRECTION DEVICE 99

- 5.1. ABSTRACT..... 99
- 5.2. INTRODUCTION..... 100
- 5.1. MATERIALS AND METHODS 100
- 5.2. RESULTS..... 104
 - 5.2.a. *Lateral force* 106
 - 5.2.b. *Axial rotation*..... 107
- 5.3. DISCUSSION 107
- 5.4. ACKNOWLEDGEMENTS 110
- 5.5. REFERENCES..... 110

CHAPTER 5. A NOVEL ANCHORING SYSTEM FOR THE NON-FUSION SCOLIOSIS CORRECTION DEVICE

5.1. ABSTRACT

In spine surgery, implants are commonly anchored by pedicle screws. Although a pedicle screw anchor is a very firm means of fixation, insertion of a pedicle screw in the mid and high thoracic region has a serious risk of facet joint or spinal cord violation. Since flexible implant systems such as non-fusion stabilizers require intact facet joints for maintaining spinal functionality, we developed an enhanced fixation that is less destructive to spinal structures. The **XS FIX** is a posterior fixation system that does not use screws for anchoring. Instead, it attaches to both transverse processes of a vertebra to create a strong fixation.

To test the strength of the **XS FIX**, we performed an experiment, in which the **XS FIX** was compared with a commonly used pedicle screw anchor (PSA) system. Both fixations were subjected to a lateral force and an axial torque until failure occurred.

It appeared that the lower thoracic and lumbar vertebrae can best be instrumented with pedicle screws. For the high and mid thoracic region, the **XS FIX** appeared to be a rigid fixation with strength comparable to that of the PSA. In conclusion, for fixation of flexible spinal systems in which intact facet joints are crucial, the **XS FIX** is preferred over the PSA in the thoracic region above T11.

Key terms

Fixation, transverse process, facet joint, thoracic, lumbar, screws, cables, force, torque

5.2. INTRODUCTION

Pedicle screws are commonly used for posterior anchoring of spinal implants. These implants include plates, spinal stabilizers, and rods.¹⁻³ Although pedicle screws are mostly used on the lumbar spine, screws may also be used on thoracic and cervical vertebrae.² In the thoracic region, the shape of the pedicles is inconsistent, especially in spinal deformities such as scoliosis.^{4,5} As a result of this, pedicle screw placement is very challenging in this region.⁶⁻⁹ Currently, pedicle screws are inserted by using either the free hand technique (as in the Roy-Camille procedure), the open lamina technique where a partial laminectomy is performed, or under application of an image-guidance system. In each of these techniques, required accuracy is very high.^{10,11} Even a well-placed pedicle screw may still violate the facet joint. Particularly in the thoracic region, the size and position of the screw head can result in obstruction of movements of the facet joints. Facet joint violation in pedicle screw anchoring in the thoracic region is a common occurrence in spinal surgery.¹² This process is often desirable but particularly troublesome in the recent trend toward dynamic, non-fusion systems that aim to maintain the flexibility of the spine. Consequently, a demand for an enhanced fixation, that is less destructive to spinal structures, has grown.

For these reasons a novel fixation system was developed, the **XS FIX**; a system that consists of two anchors, with a bridge in between. Each of these anchors consists of a connector that is attached to a transverse process by means of a cable (Figure 5.1). This new fixation system can be applied for non-fusion spinal implant systems that will correct spinal deformities *e.g.* scoliosis. A system, such as the **XS LATOR** is estimated to deliver a maximal lateral force of around 200 N and/or a maximal axial torque (around the local spinal longitudinal axis) of 7 Nm. These loads are smaller than the loads applied by fusion systems, because the non-fusion implant systems use the visco-elastic properties of the spine to correct the deformity.

Goal of this study is to determine whether a fixation to the transverse process is strong enough to withstand the loads applied by the non-fusion implant system and thus whether it is a suitable alternative for pedicle screw fixation.

5.1. MATERIALS AND METHODS

58 Vertebrae were isolated from four adult human cadavers (aged between 84 and 98 years) and cleaned of all soft tissues. All specimens were kept frozen until testing. Prior to the experiment, all vertebrae were DXA-scanned to determine the bone mineral density scores. All spines were identified as osteoporotic (Table 5.1); T-scores were well below -2.5.¹³

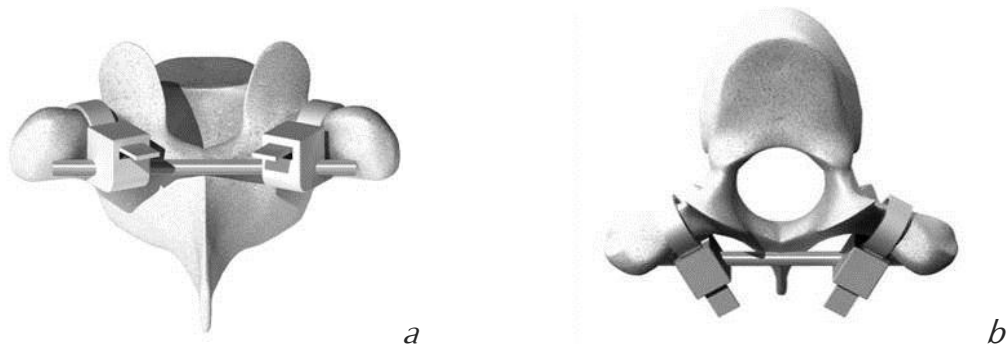


Figure 5.1: Illustration of an XS FIX prototype

A bridge is fixed to the transverse processes via two cable connectors. (a) Posterior view. (b) Top view.

<i>Spine</i>	<i>T-score</i>		<i>Gender</i>	<i>Age</i>
	T6-T12	L1-L5		
1	-4.4	-3.6	Male	80
2	-3.3	-4.1	Male	84
3	-4.8	-4.3	Male	98
4	-6.4	-5.5	Female	92

Table 5.1: T-Scores

T-scores taken from DXA scans show osteoporosis in all spines.

Each vertebra was instrumented with either a pedicle screw anchor (PSA) system or a prototype of the XS FIX system. The PSA consisted of two poly-axial pedicle screws (one in each pedicle) that were rigidly interconnected with a 5 mm diameter rod (Figure 5.2b). The XS FIX prototype consisted of two stainless steel bodies that were fixed to the left and right transverse processes of the vertebrae with cable ties, and were rigidly interconnected with a 5mm diameter rod (Figure 5.2a).

Before testing, each vertebra was embedded with PMMA bone cement in a metal housing that was rigidly clamped onto the testing setup. Each fixation system was subjected to one of two loading conditions until failure.

A lateral force (in the local coordinate system) was applied to the bridge, with a loading rate of 1.0 N/s (Figure 5.3a and Figure 5.3b).

An axial torque (in the local coordinate system) was applied to the bridge (Figure 5.3c), with a loading rate of 0.05 Nm/s. In the test setup a narrow (Figure 5.4a) or a wide (Figure 5.4b) fork construction was used to generate torque, depending on the available space.

A hydraulic tensile/compression machine (MTS, Berlin, Germany) was used to generate the appropriate loading on the bridge. Time and loads were recorded digitally with a sample rate of 2 Hz. The vertebrae from the four spines were alternately assigned to a type of fixation and to a loading condition (Table 5.2).

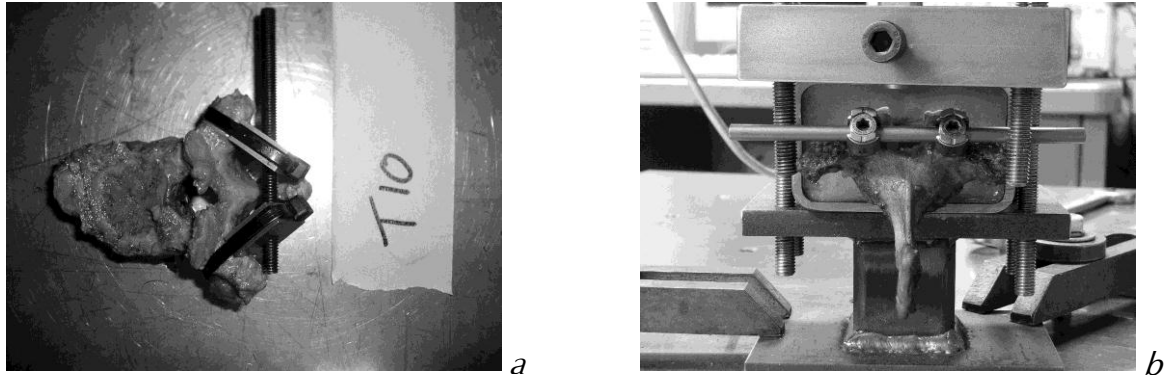


Figure 5.2: Two anchor systems

*The two different fixations were attached to the vertebrae and the vertebrae were fixed in cups with PMMA. (a) Vertebra with the **XS FIX**. (b) Vertebra with the PSA in setup.*

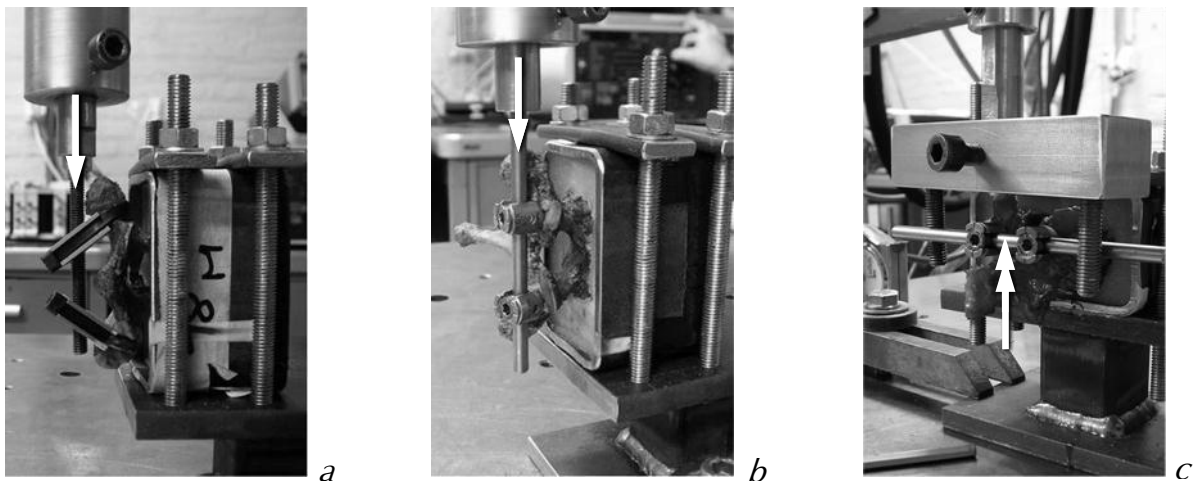


Figure 5.3: Loading of **XS FIX** and PSA

Loading with a vertical (lateral) force on XS FIX (a), PSA (b), and torque around a vertical axis on PSA (c) was performed using a hydraulic tensile/compression machine.

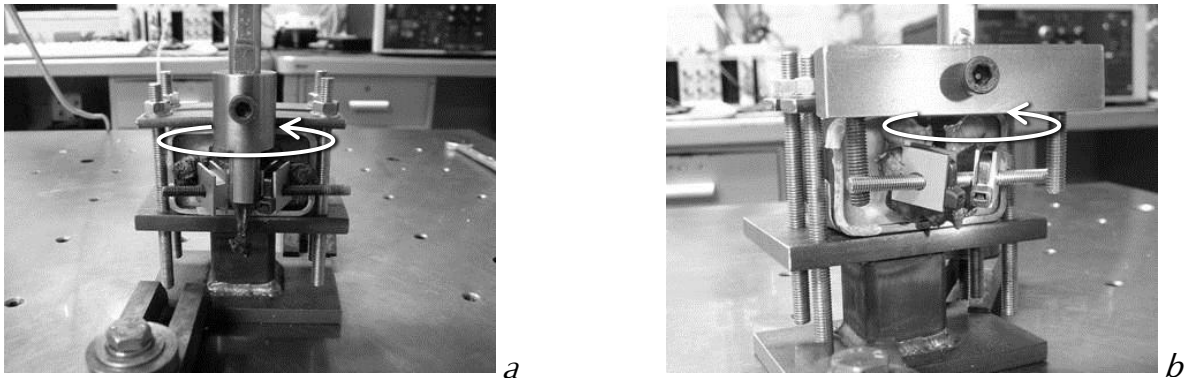


Figure 5.4: Application of torque

The cemented cups were clamped into a framework, which was clamped onto a table. Torque was applied either between the cables (a) using a narrow rotating fork or on the ends of the rod (b) using a wide rotating fork.

Failure was defined as the point at which the displacement suddenly increased (as shown by the rotation-time graphs (Figure 5.5a and Figure 5.5b)). The absolute maximal force for each construct was also measured, which represented the point of complete separation of the fixation system from the vertebra. However, as clinically relevant failure clearly started long before that point, the initiation of failure seems a more relevant strength criterion.

For statistical analysis, no difference in vertebral strength between spines was assumed. Results were analysed based on four regions: high thoracic (HT): T1-T5; mid thoracic (MT): T6-T10; low thoracic (LT): T11-T12 and lumbar (L): L1-L5. The anatomy of T11 and T12 was markedly different from the other thoracic vertebrae by poorly articulated transverse processes (which are essential for attaching the **XS FIX** system). Because of this, T11 and T12 represent a separate group. Fixation failure strengths for torque and lateral force were compared between vertebral levels and between fixation techniques using ANOVA (with significance set at $p=0.05$).

		<i>HT</i>					<i>MT</i>					<i>LT</i>		<i>L</i>				
		T1	T2	T3	T4	T5	T6	T7	T8	T9	T10	T11	T12	L1	L2	L3	L4	L5
XS FIX	S1		F		T		T	T	F			T						T
	S2			T	F		T	F			T	F			T		F	
	S3		T			F			T	T	F		T					T
	S4			F		T				F		F			T	F	F	
PSA	S1								F			T		T		F		T
	S2	F	T			F			F	T		F	T			F		T
	S3	T		T	F		F	T			T		F	T				T
	S4				T		T	F	T		F		F	T				F

Table 5.2: Overview of applied loading

Loading types ('F' for lateral force and 'T' for torque) and fixations (**XS FIX**/PSA) were altered between different spines and spinal levels. Four different spinal levels were defined for comparison: high thoracic (HT), mid thoracic (MT), low thoracic (LT), and lumbar (L).

5.2. RESULTS

The PSA typically showed slow migration of the screws until the structures ruptured completely. The **XS FIX** generally showed large deformation of the vertebral arc before actual rupture of the structures. Both fixation types typically show a point of sudden increase in rotation (or displacement), see Figure 5.5a and Figure 5.5b, indicating an early collapse of bone structures, defining the clinically relevant point of fixation failure.

No differences in fixation strength for either spinal region were found between spines loaded with lateral force ($p > 0.445$) or torsion ($p > 0.13$). General type of failure for **XS FIX** in all spines was transverse process failure in axial torsion (Figure 5.6a) and pedicle failure in lateral loading. General types of failure for PSA in all spines were pedicle screw migration and vertebral body rupture (Figure 5.6b). Anchoring the **XS FIX** system to T11 and T12 was problematic and sometimes impossible as the cables slipped off the transverse processes when tightened. Although mean strength difference between **XS FIX** and PSA in both lateral loading and in axial torsion appeared large, differences showed no significance due to the small sample size in the LT region.

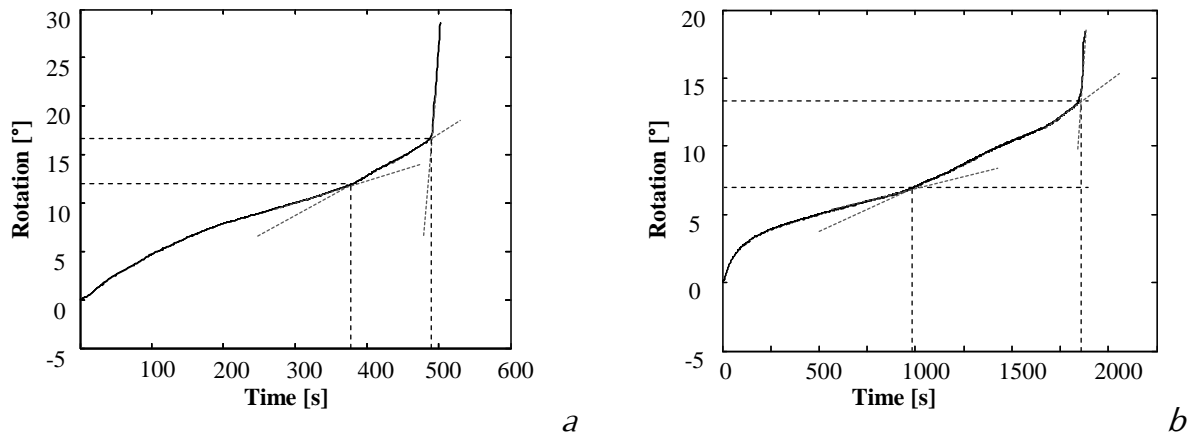


Figure 5.5: Typical rotation-time curves

(a) Typical rotation-time curve of a **XS FIX** fixation. The rotation-time curve shows a sudden increase in rotation at time=385 s, indicating a collapse of structures. At time=488 s one of the transverse process is separated from the vertebral arc resulting in a sharp increase in rotation. (b) Typical rotation-time curve of a PSA fixation. Also here, at time=998 s, a sudden increase of rotation can be seen in the curve (defined as the failure point). At time=1851 s, the vertebral body ruptured.

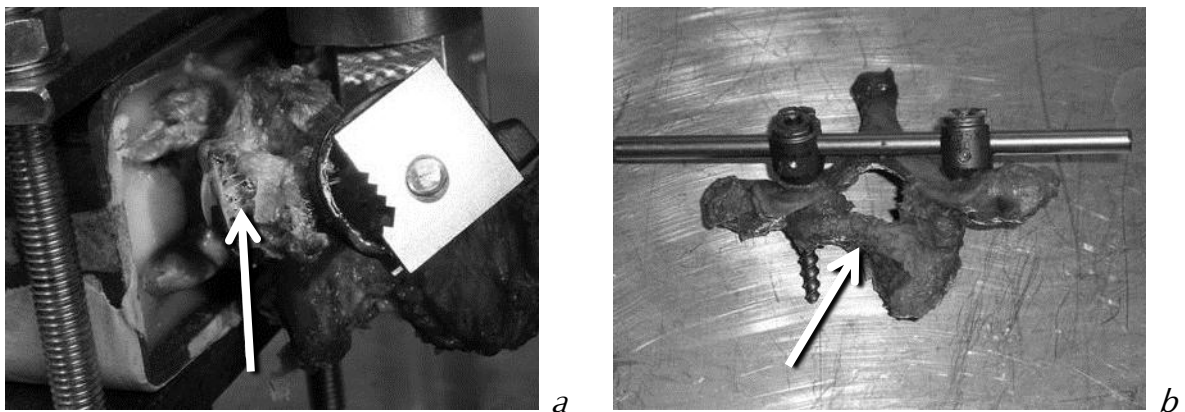


Figure 5.6: Typical failure

(a) Transverse process rupture, indicated with a white arrow, in torsion test with **XS FIX**.
 (b) Vertebral body rupture in torsion test with PSA (black arrow).

		<i>HT</i>		<i>MT</i>		<i>LT</i>		<i>L</i>	
		Mean	SE	Mean	SE	Mean	SE	Mean	SE
Force [N]	XS FIX	341.3	61.3	402.2	97.8	317.5	112.5	451.0	79.1
	PSA	702.7	92.1	506.7	60.7	594.6	28.8	631.8	14.1
Torque [Nm]	XS FIX	13.9	2.2	12.3	1.8	5.0	1.8	4.5	1.5
	PSA	9.6	1.9	13.1	3.4	14.0	4.0	16.2	2.8

Table 5.3: Fixation failure strength

Mean fixation strengths and standard errors of the two fixations at all different vertebral levels.

5.2.a. Lateral force

In lateral loading, both the PSA and the **XS FIX** demonstrated fixation strengths above 200 N that are typically expected for a non-fusion implant system such as the **XS LATOR**. The fixation strength of the **XS FIX** is significantly lower than that of the PSA in both the high thoracic region ($p=0.019$) and the lumbar region ($p=0.045$). In the mid and low thoracic levels the mean strength of **XS FIX** is not significantly different from the strength of the PSA system ($p>0.05$, Table 5.3 and Figure 5.7). The small sample size of the LT region level causes the mean difference to be not significant (Figure 5.7a).

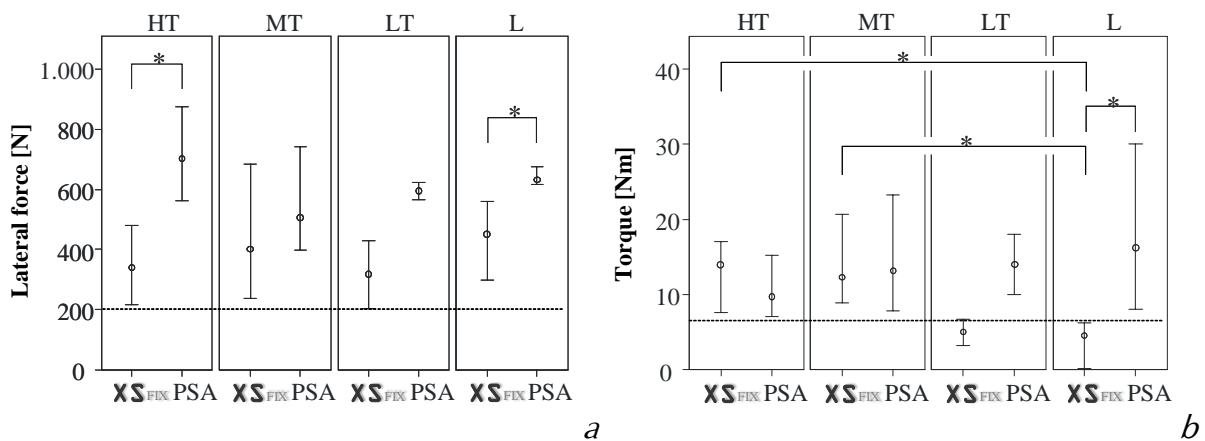


Figure 5.7: Failure load plots

High-low plots with mean failure loads in lateral loading (a) and axial torsion (b) at the different vertebral levels. The symbol * indicates significant difference. Dashed lines indicate lower limit values required for use in the non-fusion implant system.

5.2.b. Axial rotation

In all spinal regions, the PSA demonstrated fixation strengths in torsion above 7 Nm, which was estimated to be maximally generated by the non-fusion implant system. The **XS FIX** demonstrated fixation strengths in torsion above 7 Nm only in the high and mid thoracic regions. In the lumbar region, the fixation strength of the **XS FIX** significantly lower than that of the PSA ($p=0.015$) and lower than 7 Nm.

In each of the thoracic levels the mean strength of the **XS FIX** is not significantly different from the strength of the PSA system ($p>0.05$). The fixation strength of the **XS FIX** was significantly lower in the lumbar region compared to both the high thoracic ($p=0.024$) and mid thoracic region ($p=0.041$, Table 5.3 and Figure 5.7). In the mid thoracic region, mean fixation strength difference is large, however not significant caused by small sample size (Figure 5.7b).

5.3. DISCUSSION

Some limitations apply to this study. First, all tested vertebrae were osteoporotic; the results may differ for healthy vertebrae. However, both the PSA and the **XS FIX** obtain their strength from bone structures of the vertebral arc, which are relatively unaffected by osteoporosis.¹⁴

Second, both the **XS FIX** and the PSA were placed without the physical limitations that are present during *in vivo* surgery. Pedicle screws were placed using visual cues not available during surgery. The **XS FIX** was also easier to attach, due to the removal of the ribs. If the clinical reality prevents proper placement of these systems, failure strengths may be different.

Third, in this experiment the pedicle screw fixation (PSA) consisted of a bridge construction. Clinically, pedicle screws are used as stand-alone systems. A single screw will transfer a torque directly to the vertebra, resulting in high peak pressures and increased risk of early fixation failure. Our test results for the PSA cannot be compared to single pedicle screw arrangements; though it can be stated our results will give much higher strength values.

We defined failure strength as the point at which a sudden increase in displacement (rotation) took place. Because the PSA showed migration of the screws and the **XS FIX** showed large unrecoverable deformation of the vertebral arc before actual rupture of the structures, we attribute the sudden increase in deformation to microscopic bone failure. Nonetheless, the failure strength criterion we used seems clinically most relevant.

In some cases, premature **XS FIX** failure occurred in the small ratchet of a cable tie. An improved version of the ratchet that consists of high strength materials will prevent early fixation failure. In addition, the material aspect needs further attention because the

material used in our ties (Polyamide 6/6) is not suitable for implantation due to issues with creep, relaxation, and biocompatibility. Replacing the material for a creep resistant and biocompatible material such as carbon fibre reinforced PEEK (polyetheretherketone) may well be considered.^{15,16}

In the high and mid thoracic regions the torsion strength of the **XS FIX** is higher than the required value of 7 Nm for use with the non-fusion implant system such as the **XS LATOR**. In the low thoracic and lumbar regions, the torsion strength of the **XS FIX** is lower than the required 7 Nm, but in these regions, the PSA is strong enough. Lateral fixation strength of the **XS FIX** meets the requirement of 200 N for use with the non-fusion implant system for all spinal regions. However, the anchoring of the **XS FIX** to T11 and T12 is problematic, due to the poorly pronounced transverse processes of those vertebrae. Consequently, the **XS FIX** is not very suitable for those vertebrae. Similarly, the lumbar vertebrae have long transverse processes that are very slender and fragile, making the lumbar vertebrae not suited for use of the **XS FIX**. In fact, some of the lumbar transverse processes broke during tensioning of the cable ties. Fortunately, pedicle screws can be inserted easily into these vertebrae without obstructing or damaging the facet joints.

In Table 5.4, a schematic overview is given of the assessment of the **XS FIX** and PSA in respect to the different spinal regions. Four grades ('poor', 'sufficient', 'good' and 'very good') were used to evaluate the fixations on fixation strength, facet joint damage, and placement. Fixation strength was assessed using the mean (*Mean*) and standard error (*SE*) values for each VB level.

		<i>HT</i>	<i>MT</i>	<i>LT</i>	<i>L</i>
XS FIX	Fixation strength	□	+	-	-
	Facet joint damage	+	+	+	+
	Placement	+	+	-	□
PSA	Fixation strength	□	□	□	+
	Facet joint damage	-	-	□	□
	Placement	□	□	+	++

Table 5.4: Assessment of fixations

*Evaluation of fixations on basis of three criteria (strength, facet joint damage, and placement) shows that the **XS FIX** scores well on all criteria in the high and mid thoracic regions. The PSA scores best in the low thoracic and lumbar regions. Grades used for assessment are 'poor' (-), 'sufficient' (□), 'good' (+) and 'very good' (+ +).*

For each loading condition, the fixation strength was graded:

- 'poor' if $\text{Mean} - \text{SE} < RV$,
- 'sufficient' if $1 \cdot RV \leq \text{Mean} - \text{SE} < 1.5 \cdot RV$,
- 'good' if $1.5 \cdot RV \leq \text{Mean} - \text{SE} < 2 \cdot RV$, and
- 'very good' if $2 \cdot RV \leq \text{Mean} - \text{SE}$,

where RV is the required value ($RV = 200 \text{ N}$ for lateral force and $RV = 7 \text{ Nm}$ for torsion).

For all four VB levels, the lowest grades of PSA and **XS FIX**, which represent the limiting factor in fixation strength, were selected. For example, if a grade for **XS FIX** at the LT level was 'poor' for torsion and 'sufficient' for lateral force, then fixation strength was rated 'poor'.

Facet joint damage was graded:

- 'poor' if the facet joint was intrinsically damaged,
- 'sufficient' if the facet joint was not damaged but mobility was seriously obstructed,
- 'good' if the facet joint remained unharmed but with minor risk of joint obstruction, and
- 'very good' if no damage or possible obstruction occurred.

Placement of the fixation was graded:

- 'poor' if fixation was not possible,
- 'sufficient' if proper placement was possible but with high risk of damaging essential structures (*e.g.* spinal canal, transverse process),
- 'good' if placement was possible and straightforward with reduced risk of structural damage, and
- 'very good' if placement was very easy with very low risk of structural damage.

Table 5.4 shows that the **XS FIX** is an excellent fixation for the high and mid thoracic regions. In contrast, grades for fixation strength and placement of **XS FIX** in the low thoracic and lumbar region are valued much lower, whereas PSA produced decent grades for those regions.

In summary, this experiment showed that the **XS FIX** is a solid fixation with strength that is comparable to the PSA strength, when placed on a vertebra in the T2-T10 region. Fixation strength of **XS FIX** is sufficient for use with a non-fusion implant system, such as the **XS LATOR**, in mid and high thoracic regions. For the low thoracic and lumbar region, the PSA is a more rigid fixation. Therefore, in the lower thoracic and lumbar vertebrae, pedicle screws should be used.

5.4. ACKNOWLEDGEMENTS

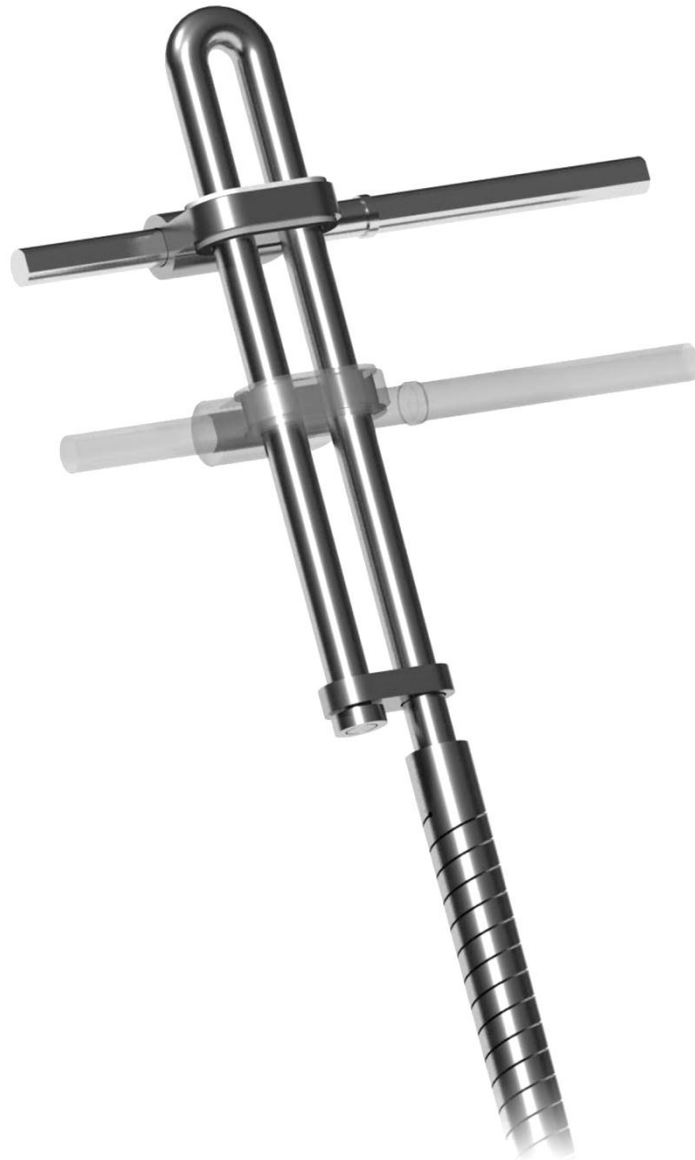
We would like to acknowledge the assistance of Willem van Wijdeven from the Orthopaedic Research laboratory and René Aquarius from the St. Radboud University Nijmegen Medical Centre, The Netherlands.

5.5. REFERENCES

1. Steffee, D., Biscup, S. & Sitkowskj, D.J. Segmental spine plates with pedicle screw fixation - a new internal fixation device for disorders of the lumbar and thoracolumbar spine. *Clin Orthop Relat Res* **203**, 45-53 (1986).
2. Gaines, R.W., Jr. The use of pedicle-screw internal fixation for the operative treatment of spinal disorders. *J Bone Joint Surg Am* **82**, 1458-1476 (2000).
3. Cotrel, Y., Dubousset, J. & Guillaumat, M. New universal instrumentation in spinal surgery. *Clin Orthop Relat Res* **227**, 10-23 (1988).
4. Zeiller, S., Lee, J., Lim, M. & Vaccaro, A. Posterior thoracic segmental pedicle screw instrumentation: evolving methods of safe and effective placement. *Neurology India* **53**, 458-465 (2005).
5. Mattei, T., Meneses, M., Milano, J. & Ramina, R. "Free-hand" technique for thoracolumbar pedicle screw instrumentation: critical appraisal of current "state-of-art". *Neurology India* **57**, 715-721 (2009).
6. Vaccaro, A.R., *et al.* Placement of pedicle screws in the thoracic spine. Part I: morphometric analysis of the thoracic vertebrae. *The Journal of bone and joint surgery. American volume* **77**, 1193-1199 (1995).
7. Vaccaro, A.R., *et al.* Placement of pedicle screws in the thoracic spine. Part II: an anatomical and radiographic assessment. *J. Bone Joint Surg. Am* **77**, 1200-1206 (1995).
8. Xu, R., Ebraheim, N.A., Ou, Y. & Yeasting, R.A. Anatomic considerations of pedicle screw placement in the thoracic spine. Roy-Camille technique versus open-lamina technique. *Spine* **23**, 1065-1068 (1976).
9. Lonstein, J.E., *et al.* Complications associated with pedicle screws. *J Bone Joint Surg Am* **81**, 1519-1528 (1999).
10. Rampersaud, Y.R., Simon, D.A. & Foley, K.T. Accuracy requirements for image-guided spinal pedicle screw placement. *Spine* **26**, 352-359 (1976).
11. Papadopoulos, E.C., Girardi, F.P., Sama, A., Sandhu, H.S. & Cammisa, J.F.P. Accuracy of single-time, multilevel registration in image-guided spinal surgery. *The Spine Journal* **5**, 263-267 (2005).

12. Chung, K., Suh, S., Swapnil, K., Yang, J. & Song, H. Facet joint violation during pedicle screw insertion: a cadaveric study of the adult lumbosacral spine comparing the two pedicle screw insertion techniques. *International Orthopaedics* **31**, 653-656 (2007).
13. WHO. Assessment of fracture risk and its application to screening for postmenopausal osteoporosis. Report of a WHO Study Group. *World Health Organ Tech Rep Ser* **843**, 1-129 (1994).
14. Riggs, B.L. Overview of osteoporosis. *West J Med.* **154**, 63-77 (1991).
15. Kurtz, S.M. & Devine, J.N. PEEK biomaterials in trauma, orthopedic, and spinal implants. *Biomaterials* **28**, 4845-4869 (2007).
16. Toth, J.M., *et al.* Polyetheretherketone as a biomaterial for spinal applications. *Biomaterials* **27**, 324-334 (2006).

Chapter 6



**MECHANICAL BEHAVIOUR OF THE NON-FUSION
SCOLIOSIS CORRECTION DEVICE**

CONTENTS

CHAPTER 6. MECHANICAL BEHAVIOUR OF THE NON-FUSION SCOLIOSIS CORRECTION DEVICE 115

- 6.1. ABSTRACT..... 115
- 6.2. INTRODUCTION..... 117
- 6.3. MATERIALS AND METHODS 117
- 6.4. RESULTS..... 122
- 6.5. DISCUSSION 126
- 6.6. CONCLUSION..... 128
- 6.7. REFERENCES..... 128

CHAPTER 6. MECHANICAL BEHAVIOUR OF THE NON-FUSION SCOLIOSIS CORRECTION DEVICE

6.1. ABSTRACT

Introduction

We developed an innovative non-fusion correction system (**XS LATOR**) consisting of two individual implants that are extendable and extremely flexible. One implant, the **XS LAT** generates a lateral bending moment and one implant, the **XS TOR** generates a torsion moment. Two 'inverse' implants were developed for generating torsion and lateral bending in a porcine model were tested for force delivery. An *in vitro* experiment was set up to describe the mechanical behaviour of both implants.

Materials and methods

Narrow and wide ('inverse') versions of the **XS TOR** and **XS LAT** were mounted on an apparatus that was able to simulate different spinal geometries. The implants were anchored to three artificial vertebrae with integrated 6D force sensors, after which the vertebrae were rotated and translated towards the demanded position. The reaction forces and moments were recorded in all configurations. The maximal (lateral) bending moment, which occurred at the middle vertebra, was determined and similarly, torque applied at the centre of rotation of the middle vertebra was calculated.

Results

As expected, the wide and the small version of the **XS TOR** generate a torque that increases during growth of the system (Figure 6.6). Similarly, the **XS LAT** generates a bending moment that slightly increases during growth of the system (Figure 6.7). The produced moments approximate the theoretically predicted ones. The contribution to the spinal stiffness ranges between 0.01 Nm/° and 0.04 Nm/° in bending and between 0.03 Nm/° and 0.08 Nm/° in torsion.

Discussion and conclusions

The **XS TOR** and the **XS LAT** are able to generate a torque and a bending moment that remain (fairly) constant during spinal growth when a shape change due to the generated moment/torque is achieved. The stiffness of the implants is extremely low, being only a fraction of the stiffness of conventional spinal fusion constructs. Current fusion systems, such as non-segmental spinal constructs generally have 11 times higher stiffness in torsion and 6 times higher stiffness in lateral bending. Implantation of the **XS LATOR** adds 9% stiffness in axial rotation and 17% stiffness in lateral bending (to the original spinal stiffness). By preserving the flexibility of the spine after implantation, fusion of the vertebrae in the instrumented region is likely to be prevented.

Key terms

Non-fusion, scoliosis, implant, lateral bending, Cobb-angle, moment, torsion, torque

6.2. INTRODUCTION

Surgical treatment of scoliosis generally consists of performing spondylodesis, a technique that invokes vertebral fusion.¹ Complications related to this technique are reduction of spinal flexibility and obstruction of growth. For that reason, non-fusion surgery is increasingly explored,² however results are still not satisfying. We developed an innovative non-fusion correction system (**XS LATOR**) consisting of two individual implants that are extendable and extremely flexible (Figure 6.1). One implant, the **XS LAT**, generates a lateral bending moment to correct the lateral curvature. The other implant, the **XS TOR**, generates a torque to correct the axial rotation of the spine. The two ends of the implants are bent backwards and retained in anchors. This construction makes it possible that the correction moments increase during growth, which is necessary to compensate for a decrease in correction moment due to rotational and lateral correction of the spine.

The **XS TOR** mainly comprises Ti6Al4V parts and sliding anchors containing UHMWPE bushings to allow growth of the spine. The **XS LAT**, with similar sliding anchors, has a functional NiTi unit (a Ø4 mm rod). The NiTi rod is pseudo-elastic (austenitic) at body temperature. Both implants span five or six vertebrae and are anchored to the two outer vertebrae (cranially and caudally) and the middle one. Application of torque and bending moment is facilitated by using transverse bridges that are anchored to the three vertebrae. To deliver the appropriate moment/torque, both implants are mounted in a pre-stressed state.

For *in vivo* animal experiment applications, two 'inverse' versions of both implants (**XS TOR** and **XS LAT**) were designed. These 'inverse' versions are intended to induce scoliosis in a straight porcine spine model, since representative (idiopathic) scoliotic animal models do not exist. Both implants were provided in two versions, one with a narrow and one with a wide curve at both outer ends (Figure 6.1) to adjust to variations in vertebral geometries. The bending moment and torque are required to be about 2 Nm (see Chapter 1).

This experiment was set up to determine if the required bending moments and torques can be delivered by the 'inverse' versions of the **XS TOR** and the **XS LAT** in different spinal configurations.

6.3. MATERIALS AND METHODS

For the experiment, four implants were manufactured (Figure 6.1), one narrow and one wide version of both 'inverse' implants. The four implants were tested on torque and moment delivery using an experimental set-up that is able to simulate various spinal configurations and to measure forces and torques on the anchors of the implant (Figure 6.2a).

The apparatus, consisting of a frame on which four artificial vertebrae were mounted, is able to facilitate different spinal configurations using multiple sliding connections by which the vertebrae can be manoeuvred in the desired positions (Figure 6.3). The artificial vertebrae can be translated and rotated in three orthogonal directions x , y , z (Figure 6.2b). The implants were anchored to three artificial vertebrae (Figure 6.2c, a fourth available artificial vertebra was not used in this experiment), after which the vertebrae were rotated and translated towards the demanded position. As intended in normal scoliosis correction, the three vertebrae in the experimental set-up represent the instrumented vertebrae and simulate the instrumentation over five or six segmental levels (for example T9-T12-L2).

With the apparatus, all functional movements of the spine can be simulated. Lateral bending is simulated by lateral translation of the middle vertebra and tilting the cranial and caudal vertebrae into the desired Cobb-angle. Axial rotation is simulated by the axial rotation of the middle vertebra (Figure 6.5). The axis of rotation of the artificial vertebra is positioned with an offset of 20 mm from the anchor level, simulating the location of the physiological axis of rotation in the spinal canal. Thus, axial rotation of a vertebra results in a lateral displacement of the anchor and an accompanied lateral bending (Figure 6.5d). Similarly, this rotation is accompanied by a small translation of the anchor in z -direction resulting in (minor) flexion/extension of the implant. Pure flexion/extension of the implant can be achieved by displacement of the middle vertebra in the z -direction orthogonal to the frontal plane.

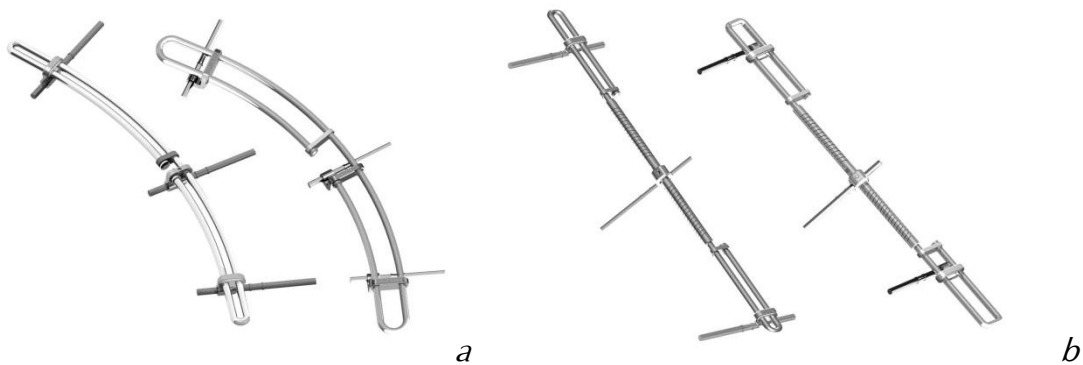


Figure 6.1: The 'inverse' implants

(a) The tested 'inverse' lateral bending implants (XS LAT) were manufactured in two versions: a wide and a narrow implant version. (b) Similarly, two versions of the torsion implants (XS TOR), wide and narrow, were tested. The implants were pre-shaped in order to generate the required bending moment and torque.

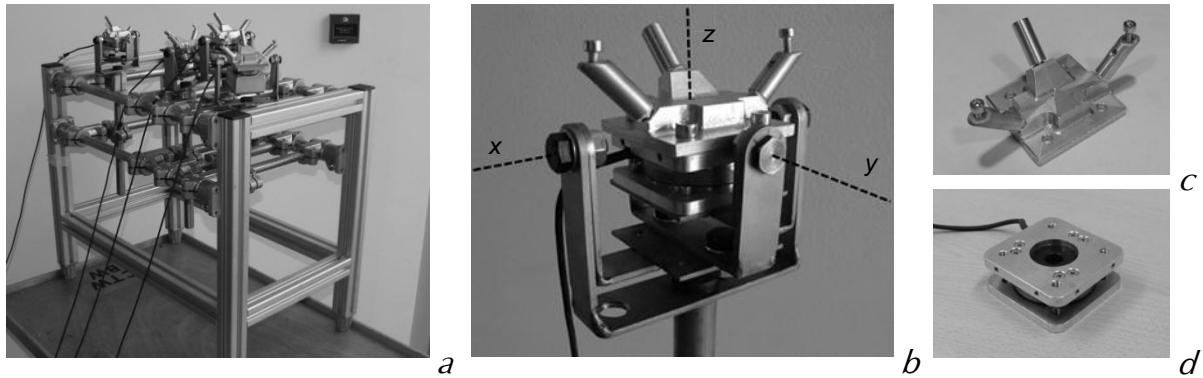


Figure 6.2: Spinal implant measuring apparatus

(a) Four artificial vertebrae mounted on a frame can be manoeuvred in various positions representing spinal configurations. (b) The artificial vertebrae were each bolted to a 6D force/torque sensor that measures three forces and three torques (F_x , F_y , F_z , T_x , T_y , T_z). The vertebrae can be rotated and translated in three orthogonal directions. (c) Artificial vertebra with two lateral pins (representing transverse processes) each contained a hole for insertion of a transverse bridge. The bridge can be anchored with two fasteners. (d) ATI Mini45 F/T sensor.

First, the vertebrae were positioned in a straight spinal configuration (0 mm displacements in x - and y - direction and 0° rotation) to determine the instant moment/torque delivery of the implant (Figure 6.5a). Second, growth of the spine was simulated by translating the cranial and caudal vertebrae axially (Figure 6.5b). This procedure is repeated for different configurations in bending, lateral bending and torsion. The additional lateral bending and flexion/extension configurations included middle vertebra displacements of 10 mm and -10 mm (-9 mm lateral displacement for the wide **XS_{LAT}**). Additional configurations simulating torsion included rotations of 10° and -10° (-5° for the narrow **XS_{TOR}**). All force and torque measurements represented a static configuration. Because the implants were designed to induce scoliosis by implementation of a bending moment/torque, it is expected that during growth of the spine, when length of the system increases, the spine slowly changes shape. The static measurements were used to estimate bending moment/torque delivered by implant during spinal growth and shape change.

Forces/moments were measured by three ATI mini45 multi-axis (6D) force/torque sensors with DAQ F/T interfaces/power supplies and recorded using a National Instruments data acquisition (NI-DAQ™) device connected to a laptop running Matlab® (R2009b). Data analysis was performed using Microsoft Excel®. Both **XS_{LAT}** versions were tested in a room heated to body temperature (37°C) to bring the NiTi rod of the implants in the intended austenitic state. Both versions of the **XS_{TOR}** were tested at room temperature.

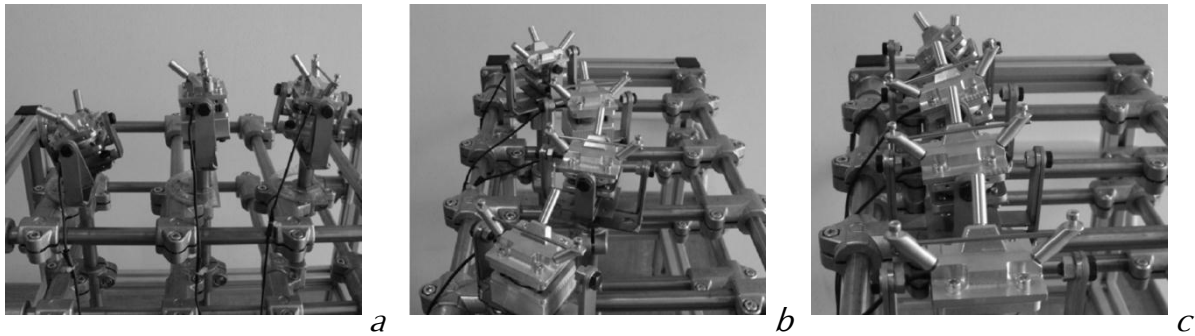


Figure 6.3: Various configurations

(a) Spinal configuration with three artificial vertebrae representing flexion. (b) Configuration with four artificial vertebrae representing lateral bending. (c) Configuration representing axial rotation.

Delivered correction moment and torque were determined in all spinal configurations using the lateral force F_c and torque T_c at the middle vertebrae and variable length L (distance between the anchors of cranial and caudal vertebrae). L_{max} is defined as the maximal length of the implant. It is assumed that $M_c = \frac{1}{4} F_c \cdot L$ (Figure 6.4). Torque generated on the middle vertebra (T_c) by the **XS TOR** is negative in y -direction. Lateral bending moment is positive if the F_c (force at the middle vertebra) is positive in x -direction.

Stiffness of the implant in torsion and lateral bending and flexion/extension was calculated by dividing measured moment/torque by the accompanied deviation/axial rotation. Flexion angle α (Cobb-angle for lateral flexion) was calculated by $\alpha \approx \theta \cdot d / L$, with d defined as deflection (lateral/sagittal).

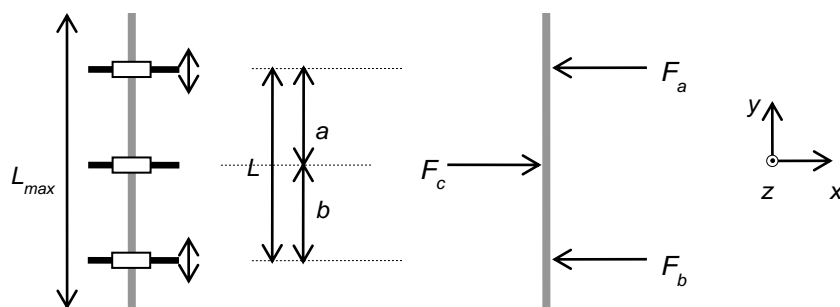


Figure 6.4: Determination of bending moments

The variable implant length, defined by L , is adjustable to facilitate growth using sliding anchors at both ends of the implant. Maximal moment in the implant, which occurs at the centre of the implant, is defined by $M_c \approx F_c \cdot (a + b) / 4.0$, if a is between $0.80 \cdot b$ and $1.25 \cdot b$. Therefore, F_c and L were used to determine M_c .

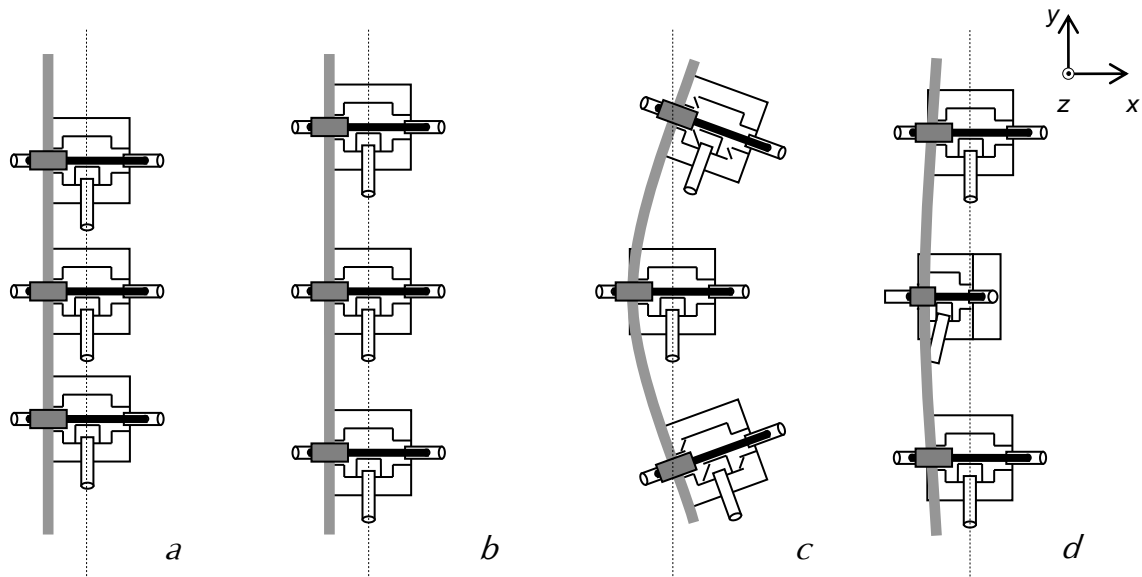


Figure 6.5: Positions of artificial vertebrae

A schematic frontal view shows displacements of the artificial vertebrae in lengthening (growth), lateral flexion, and torsion. Accordingly, flexion/extension of the implant is achieved by displacement of the middle vertebra in the direction orthogonal to the frontal plane. Axial rotation of the middle vertebra shows a coupled lateral motion of the anchor resulting in lateral flexion.

	<i>Torsion [Nm/°]</i>	<i>Lat flex [Nm/°]</i>	<i>Flex/ext [Nm/°]</i>
Spine + construct	2.1	1.8	1.8
Spine	1.5	0.6	1.4
Construct	0.6	1.2	0.4

Table 6.1: Stiffness of a non-segmental spinal fusion construct

The stiffness of this typical spinal fusion instrumentation was determined after subtraction of the stiffness of the spinal region from the stiffness of corresponding instrumented spinal region using a porcine model.^{3,4}

For evaluation of the stiffness at a certain length L , the values for a wide and a narrow version were averaged for each implant, resulting in one value for \mathbf{XS}_{TOR} and one value for the \mathbf{XS}_{LAT} . The determined stiffness of the implants was compared to the (estimated) stiffness of a human spinal five-vertebra segment and with the stiffness of a non-segmental spinal fusion construct.³ The stiffness of this typical spinal fusion instrumentation was determined after subtraction of the stiffness of the spinal region from the stiffness of corresponding instrumented spinal region using a porcine model (Table 6.1).^{3,4}

6.4. RESULTS

Both versions of the **XS TOR** generate a torque at the middle vertebra, which increases during growth of the system. Figure 6.6 shows the increasing torque in a straight and non-axially rotated spine with increasing length L of the system (due to spinal growth). The narrow version, which produces a lower instant torque, shows a higher increase in torque than the wide version. The dotted arrows demonstrate estimations of the torque developments expected to occur after slow induction of torsion from 0° to 10° axial rotation and a simultaneous length increase from 170 mm to 220 mm.

Lengthening of the **XS LAT** results in an increase in bending moment. For instance in a straight spine the bending moment increases from 2.8 Nm to 3.2 Nm for the wide system and from 2.5 Nm to 2.8 Nm for the narrow system (Figure 6.7). Similar to the mechanism described for the **XS TOR**, the *in vivo* spine is expected to adjust to the bending moment applied by the **XS LAT**. The dotted arrows demonstrate the bending moment development with a Cobb-angle progression from 0° to 21° and increasing length (170 mm to 220 mm). The narrow version of the **XS LAT** shows smaller bending moments than the wide version.

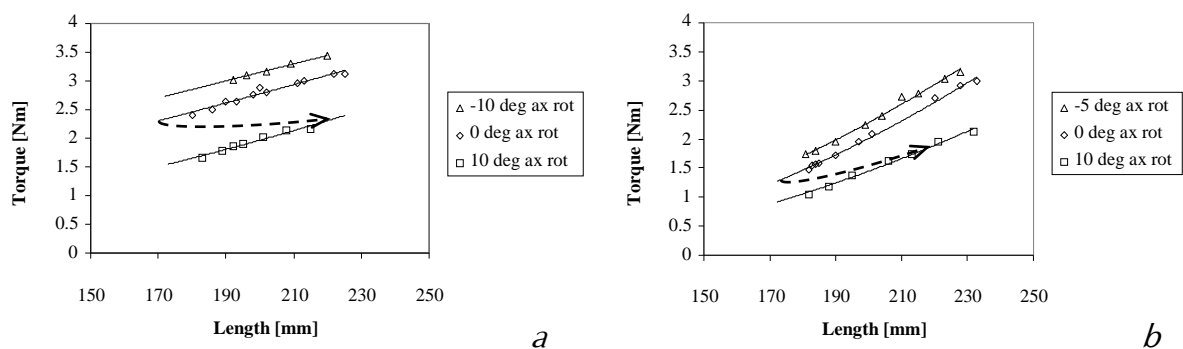


Figure 6.6: Torque delivery of **XS TOR**

Both versions of the **XS TOR** generate a torque (T_c) which increases during lengthening of the implant. (a) The by the wide version generated torque, in a straight and not axially rotated spine, increases during lengthening of the system. *In vivo*, the spine will respond to the generated torque by rotating the middle vertebra axially relative to the other to vertebrae. The resulting axial rotation will increase over time (during growth). The dotted arrow illustrates an estimation of a torque development from 0° to 10° axial rotation. (b) The narrow version shows a higher increase in torque.

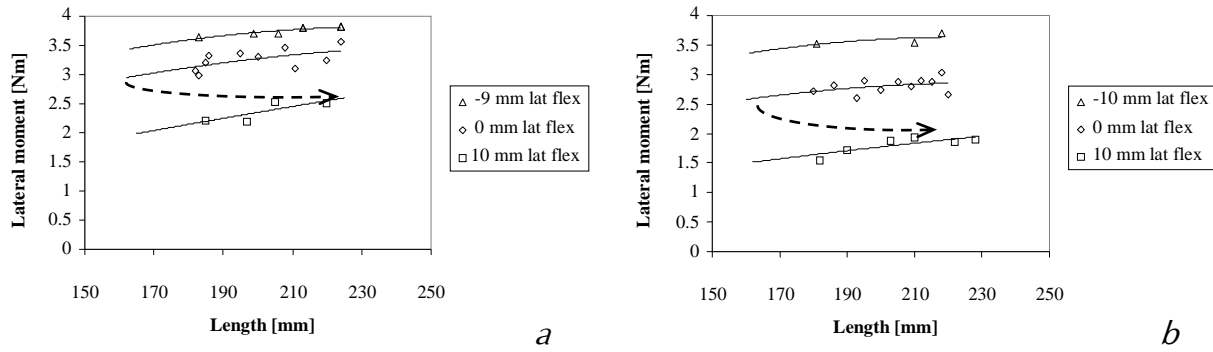


Figure 6.7: Lateral bending moment of **XS LAT**

(a) The wide version of the **XS LAT** generates a bending moment (M_c) that increases during extension in a straight spine (deviation flexion of 0 mm). In reality, the spine adjusts to the applied bending moment such that during growth (extension), when length of the system increases, the applied moment follows a different path. The dotted arrow demonstrates an estimation of a bending moment development with a Cobb-angle progression from 0° to 21° and increasing length (from 160 mm to 222 mm). (b) The narrow version of the **XS LAT** showed smaller bending moments.

As a result of lengthening, the torsion stiffness of the **XS LAT** decreases whereas the torsion stiffness of the **XS TOR** increases. Bending stiffness of the **XS TOR** and the **XS LAT** decreases during lengthening (Table 6.2). The stiffness (relative to the spinal cord) was measured at the centre of rotation of the vertebrae. The lateral force exerted by the **XS LAT** creates a (admittedly small) moment around the centre of rotation of the vertebra, which lies in the spinal canal. The contribution of both implants to the spinal stiffness ranges between $0.01 \text{ Nm}/^\circ$ and $0.04 \text{ Nm}/^\circ$ in (lateral) flexion and between $0.03 \text{ Nm}/^\circ$ and $0.08 \text{ Nm}/^\circ$ in torsion. The minimal and maximal stiffness for all directions are presented in Table 6.2.

The stiffness of the **XS LATOR** is considerably lower than the stiffness of non-segmental spinal fusion constructs. The stiffness of an isolated non-segmental spinal fusion construct (spanning five vertebrae) was determined to be $0.6 \text{ Nm}/^\circ$ in torsion, $0.4 \text{ Nm}/^\circ$ in flexion/extension and $1.2 \text{ Nm}/^\circ$ in lateral flexion (Table 6.1). The stiffness of the **XS TOR** and the **XS LAT** relative to a non-segmental spinal fusion construct³ (spanning 5 vertebrae) are shown in Table 6.3. Stiffness of the **XS LATOR** in lateral flexion and flexion/extension is at most 6% of the stiffness of the non-segmental spinal fusion construct. Torsion stiffness of the **XS TOR** is less than 13%. The **XS LAT** shows lower torsion stiffness, with a maximum of 6%.

	Torsion [Nm/°]		Lat flex [Nm/°]		Flex/ext [Nm/°]	
	Min	Max	Min	Max	Min	Max
XS TOR	0.05	0.08	0.01	0.03	0.01	0.02
XS LAT	0.03	0.04	0.03	0.04	0.01	0.01

Table 6.2: Stiffness of the implants

Mean stiffness contribution of the **XS TOR** and **XS LAT** in torsion, flexion and lateral flexion [Nm/°], measured at the centre of rotation of the vertebrae. The **XS LAT** does not generate significant torque at the anchors, but the lateral forces create a moment at the centre of rotation of the vertebra (which lies in the spinal canal). Stiffness of both implants is dependent on the length L . Except for the torsion stiffness of the **XS TOR**, maximal stiffness of the implants occurs at minimal length and minimal stiffness at maximal length. The **XS TOR** shows maximal torsion stiffness at maximal length.

	Torsion		Lat flex		Flex/ext	
	Min	Max	Min	Max	Min	Max
XS TOR	8%	13%	1%	2%	2%	4%
XS LAT	5%	6%	3%	3%	2%	2%
XS LATOR	13%	19%	4%	6%	3%	6%

Table 6.3: Relative stiffness of the implants

The table shows the stiffness range of the **XS TOR** and the **XS LAT** relative to conventional non-segmental spinal constructs (spanning five vertebrae). Stiffness in lateral flexion and flexion/extension, which depends on the variable length L of the implant, is less than (or equal to) 6%, respectively. Torsion stiffness of the **XS TOR** is less than 13%. The **XS LAT** shows lower torsion stiffness, with a maximum of 6%. Similar to Table 6.2, minimal and maximal stiffness represent the stiffness for the range of tested lengths.

Table 6.4 shows that the total system adds stiffness to the human spine of about 9% in torsion, 17% in lateral flexion, and 4% in flexion/extension. In contrast, we calculated that the non-segmental spinal fusion construct adds stiffness of app. 58% in torsion, 91% in flexion/extension, and 361% in lateral flexion (Table 6.4).

As was already shown in Figure 6.5d, torsion in the spine and thus in the implant generates bending of the implant which will in effect cause a lateral bending moment. In fact, variations in spinal configurations in each direction created variation in moments in all other directions.

	<i>Torsion</i>	<i>Lat flex</i>	<i>Flex/ext</i>
XS TOR	6%	6%	2%
XS LAT	3%	11%	2%
XS LATOR	9%	17%	4%
NS Construct	58%	361%	91%

Table 6.4: Stiffness contribution to the human spine

The stiffness contribution by a non-segmental (NS) construct to the human spine is much higher than by the XS LATOR.

Table 6.5 shows the range in which the torques and moments of the XS LAT and XS TOR change as a result of torsion (10°), lateral bending (20°) and flexion (20°) in related and non-related directions. With this table, the decrease in moment/torque and the generated moment/torque in other directions can be estimated. For example, the lateral flexion moment delivered by the XS TOR is 0.0 Nm for zero torsion of the spine (0°) and increases to a value between 0.03 Nm/° and 0.13 Nm/° for 10° torsion.

		<i>Torque [Nm]</i>		<i>Lat flex moment [Nm]</i>		<i>Flex moment [Nm]</i>	
		Min length	Max length	Min length	Max length	Min length	Max length
XS TOR	10° Torsion	0.50	0.80	0.13	0.03	0.27	0.19
	20° Cobb-angle	0.55	0.20	0.55	0.20	0.02	0.00
	20° Flexion	0.34	0.20	0.02	0.00	0.31	0.15
XS LAT	10° Torsion	0.40	0.30	0.75	0.63	0.32	0.22
	20° Cobb-angle	0.62	0.49	0.79	0.70	0.03	0.01
	20° Flexion	0.09	0.05	0.09	0.02	0.16	0.15

Table 6.5: Change in moments as a result of spinal motion

The (lateral/sagittal) bending moments and torque of the implants change as a result of (lateral/sagittal) flexion and torsion in related and non-related directions. This table shows the range in which the torques and moments of the XS LAT and XS TOR change as a result of torsion (10°), lateral bending (20°) and flexion (20°) for minimal and maximal length in different directions.

6.5. DISCUSSION

With this study, we intended to demonstrate the mechanical properties *i.e.* the force/torque delivery by and stiffness of our innovative non-fusion scoliosis correction system (the **XS LATOR**). The implant system was designed to generate a significant amount of torque/bending moment while keeping the stiffness of the implant low. We compared the stiffness of the **XS LATOR** with the (estimated) stiffness of a non-segmental fusion system. The stiffness of non-segmental and other conventional fusion systems is very high, which is required to immobilise the vertebrae to invoke fusion of the spinal segments. We found that the stiffness of a non-segmental spinal construct is app. 22 times higher in flexion/extension and lateral flexion and 6 times higher in axial rotation. The stiffness of segmental spinal constructs is even higher.

Because the highly flexible **XS LATOR** is pre-strained, loss of correction moment will be much less than observed in conventional fusion constructs. Both implants (**XS TOR** and **XS LAT**) not only generate the bending moment/torque they were designed to deliver, they also generated coupled moments in other directions. Although the generated torque/moment could interfere with the torque/moment necessary for optimal scoliosis correction, the contribution of **XS TOR** and **XS LAT** to the spinal stiffness is very low, given that the stiffness of the instrumented thoracolumbar region is roughly estimated to be between 0.5 Nm/° and 1.0 Nm/° in flexion, lateral flexion and torsion,^{4,5} when the instrumented region covers 5 vertebrae and consists of 4 functional spine units (vertebra-disc-vertebra). When anchored to the thoracolumbar spine, due to the extreme low stiffness contribution, the **XS LATOR** is able to adjust to the full range of motion of the instrumented spine without obstructing the spinal motion. By preserving the flexibility of the spine after implantation, fusion of the vertebrae in the instrumented region due to limited vertebral motion is likely to be prevented.

Some limitations apply to this study. First, we determined the stiffness of the non-segmental spinal constructs by using the stiffness of a porcine spine segment (L1-L6) as determined by Wilke *et al.*⁴ and the stiffness of an instrumented porcine spine segment (L1-L6) as determined by Hart *et al.*³ Evidently, the values for relative stiffness in Table 6.3 may not be exact, since the results from two different studies were used. However, the table was presented to merely give an indication for the relative stiffness of the **XS TOR**.

Second, the range of axial motion of the artificial vertebrae was limited by the testing device. The actual minimal implant length was 150 mm. The minimal distance L between the artificial vertebrae was 180 mm. Therefore, we were not able to test the implant length L in the range between 150 mm and 180 mm. As a result, the torque/moment delivery for this range is determined by extrapolation.

Two versions of each implant were tested: a narrow and a wide version. These versions were designed to deliver comparable moment or torque. A difference however was observed in the generated torque between the narrow and the wide version of the **XS TOR**. This difference, which is largest at minimal length, is originated in the magnitude of the forces that act on the implant. Both versions of the **XS TOR** have a torsion generating element (torsion spring) and torsion transfer element (U-loop). The U-loop transfers torque via a couple to the spine. Given a torque T , the force F acting on the U-loop is defined as $F = T/d$, with d defined as the distance between the legs of the U-loop. Since the distance between the legs is smaller for the narrow version than for the wide version ($d_n < d_w$), the force F_n acting on the narrow version is higher than the force F_w acting on the wide version for similar torque T . The higher force F_n creates a larger (bending) deformation of the U-loops. The larger deformation of the U-loops results in a larger torsion of the system, which means that the narrow **XS TOR** exhibits lower torsion stiffness. Consequently, at similar torsion (axial rotation) and length L , the torque generated by the narrow **XS TOR** is smaller than the torque generated by the wide **XS TOR**.

The difference in torsion stiffness between the two versions is largest at small length L . At increasing length L , the difference becomes smaller. Therefore, the generated torque follows a different course for each **XS TOR** version during extension (lengthening) of the implant (Figure 6.6). See Chapter 1 for a detailed description of the functioning of the **XS TOR**. The *in vivo* study (Chapter 1) will show whether the difference in generated torque will result in different outcomes regarding the generation of a spinal shape change.

Furthermore, a difference in lateral bending moment was observed between the wide and the narrow version of **XS LAT**. The difference in moment delivery and thus mechanical behaviour of the two versions of the **XS LAT** may be attributed to the difference in length. The wide version was 20 mm smaller (in maximal length L_{max}) than the narrow version. This variation in length occurred due to manual preparation of the rods, which may have caused increased flexibility of the narrow version resulting in a smaller generated bending moment. Another possible explanation of the difference between generated bending moments may be explained from differences in transformation temperatures of the NiTi rods that are integrated in the **XS LAT**. These differences in transformation temperatures were not examined though. The forces/moments delivered by **XS LAT** showed a higher spread in values (hence lower accuracy) than the forces/moments delivered by **XS TOR**. Since the mechanical behaviour of the NiTi element in the **XS LAT** is highly temperature dependent, small variations in temperature might be responsible.

After fixation of the implants, the remaining moment is dependent on the obtained correction and will decrease post-operatively. Post-operatively, the applied moment could be kept fairly constant over time if for example the corrected torsion does not

exceed 10° (Figure 6.6). If a larger shape change occurs, correction moment/torque will be diminished over time (and over spinal growth).

The implant system, which is designed to induce a shape change, will generate an axial rotation of the middle vertebra (apex) relative to the caudal and cranial vertebrae. The axial rotation is expected to increase over time while the spine continues growing and the implant lengthens. However, the degree of shape change (correction/induction of scoliosis) as a function of time and thus spinal growth is not known. Therefore, the dotted arrows in Figure 6.6 and Figure 6.7, which illustrate a path that the system possibly follows regarding moment delivery, do not necessarily give a valid representation of the delivered moment during implantation.

Although the implants (**XS TOR** and **XS LAT**) are originally designed to work together, they are tested separately. The rationale for separate testing is to determine the characteristics of a single implant. For correction of idiopathic scoliosis, the separate implants can be placed at different levels, hence (partly) overlapping. In future research, various combinations of original implants, instead of 'inverse' versions, should be tested *in vitro* to determine the effect of combining implants on scoliosis correction.

To determine the actual contribution of the **XS LATOR** to the spinal flexibility and to verify the principles of the mechanical behaviour of the implants and the effect toward correction of a scoliotic spine, porcine or (scoliotic) humane spinal segments may be tested *in vitro*. In addition, *in vivo* experiments in preferably a porcine model should be performed to examine long-term visco-elastic behaviour of the implanted spine and the effect of the implant on vertebral fusion. Accordingly, in Chapter 1, the results of the *in vivo* study of the 'inverse' versions of the **XS LAT** and the **XS TOR**, implanted in a porcine model, are presented.

6.6. CONCLUSION

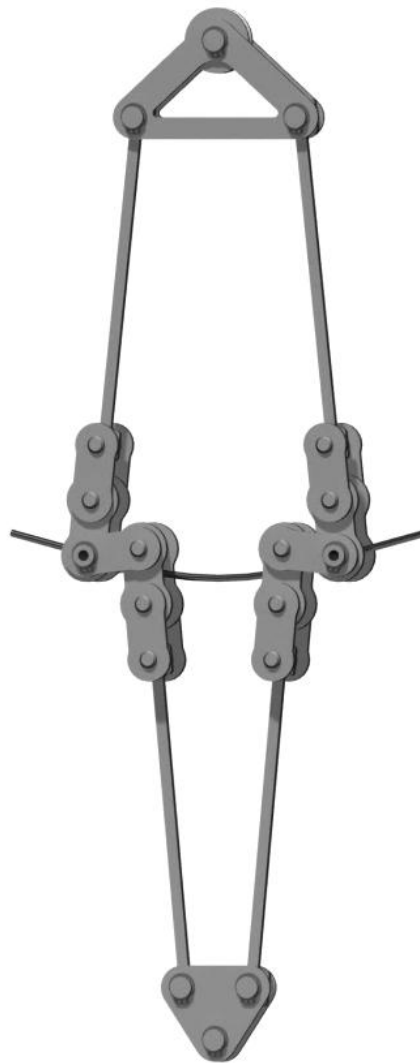
The **XS TOR** and the **XS LAT** are able to generate a moment and torque that remains (fairly) constant during spinal growth when a shape change due to the generated moment/torque is achieved. The stiffness of the implants is extremely low, being only a fraction of the stiffness of conventional spinal fusion constructs.

6.7. REFERENCES

1. Deyo, R.A., Nachemson, A. & Mirza, S.K. Spinal-fusion surgery - the case for restraint. *The Spine Journal* **4**, S138 (2004).
2. Maruyama, T. & Takeshita, K. Surgical treatment of scoliosis: a review of techniques currently applied. *Scoliosis* **3**, 6 (2008).

3. Hart, R., Hettwer, W., Liu, Q. & Prem, S. Mechanical stiffness of segmental versus nonsegmental pedicle screw constructs: the effect of cross-links. *Spine* **31**, E35-E38 (2006).
4. Wilke, H.-J., Geppert, J. & Kienle, A. Biomechanical *in vitro* evaluation of the complete porcine spine in comparison with data of the human spine. *European Spine Journal* **20**, 1859-1868 (2011).
5. Panjabi, M.M., Brand, R.A. & White, A.A. Mechanical properties of the human thoracic spine as shown by three-dimensional load-displacement curves. *J Bone Joint Surg Am* **58**, 642-652 (1976).

Chapter 7



**BENDING FATIGUE OF PSEUDO-ELASTIC NiTi ROD
IMPLANTS**

CONTENTS

CHAPTER 7. BENDING FATIGUE OF PSEUDO-ELASTIC NITI ROD IMPLANTS..... 133

- 7.1. ABSTRACT..... 133
- 7.2. INTRODUCTION..... 135
- 7.3. MATERIALS AND METHODS 136
- 7.4. RESULTS..... 140
- 7.5. DISCUSSION 145
- 7.6. CONCLUSIONS 148
- 7.7. REFERENCES..... 148

CHAPTER 7. BENDING FATIGUE OF PSEUDO-ELASTIC NITI ROD IMPLANTS

7.1. ABSTRACT

Introduction

NiTi alloys are extensively used in medical applications. In long-term implantation, fatigue life of materials is crucial. Stress- and temperature-induced phase transformations make NiTi fatigue behaviour unpredictable since it depends on the type of loading, dimensions, test temperature, environment, and processing parameters such as the amount of cold work and heat and surface treatment. The fatigue behaviour in non-zero mean strain loading conditions that apply in for instance non-fusion correction of scoliosis is unknown. Goal of this study is to determine how different pre-strains, heat, and surface treatments influence this behaviour.

Methods

In a phosphate buffered saline (PBS) solution of 37°C, pseudo-elastic Ø4 mm NiTi rods (55.8wt% Ni; A_f temperature between 32°C and 38°C) were bent uni-axially at a frequency of 3 Hz. Four supports, of which the middle two were fixed vertically and the outer two were pulled vertically, introduced a pure bending moment. The alternating strain for a fatigue life of 1.5 million cycles (referred to as fatigue limit) was determined. Tested parameters included pre-strain, heat treatment, surface treatment, and batch from manufacturer. Heat treatments of 400°C/15 min (T1), 400°C/30 min (T2), 350°C/15 min (T3), 450°C/15 min (T4) and a double treatment of 520°C/60 min (shape setting) and 400°C/22 min (T5) were applied. Surface treatments included axial grinding prior to mechanical super-polishing (AS), mechanical super-polishing after tangential grinding (TS), plasma polishing (PP) and shot peening (SP). Pre-strain was varied between 1% and 2.5%. Two batches (B1, B2) of the same manufacturer were tested for consistency.

Results

Varying pre-strain in intermediate regions (1.5%-2.5%) did not alter the fatigue limit. Lowering the pre-strain from 1.5% to 1% increased the fatigue strain limit for 1.5 million cycles. Small changes in heat treatment time and temperature (T1-T4) did not result in altered fatigue behaviour. Double heat treatment (T5) and PP increased the fatigue limit compared to mechanical super-finishing. SP did not increase the fatigue limit. Compared to axial grinding (AS), tangential grinding (TS) lowered fatigue life at given alternating strain of 0.10% and pre-strain of 2%; the second batch (B2) obtained from the manufacturer exhibited a higher alternating strain limit.

Discussion and conclusion

Fatigue resistance in (large diameter) rods is lower than in small diameter wires. This could be explained by residual stresses that are generally present in large diameter rods. Generally, wires show lower fatigue resistance if mean strain loading is higher than zero since cyclic bending in pre-strained rods induces phase transition when strained above 0.7%. Conversely, for cyclic strains in the pseudo-elastic region (pre-strains of 1.5%-2.5%), fatigue life is independent of pre-strain. Slight changes in heat treatment temperature ($\pm 50^\circ\text{C}$) or increase in heat treatment time (+15 min) does not have an effect on fatigue properties if austenite finish temperature (A_f) remains unchanged. Prior to super-finishing, axial grinding shows higher fatigue resistance than tangential grinding. Whereas plasma polishing improves the fatigue resistance, shot peening does not, compared to mechanical super-finishing. A shape-setting heat treatment prior to the default heat treatment (at lower temperature) can improve fatigue resistance in certain cases, depending on the state of the material 'as received' from manufacturer. However, the fatigue behaviour of NiTi is highly dependent on quality realised by the manufacturer.

Key terms

Fatigue, NiTi, pre-strain, alternating strain, surface treatment, heat treatment, pseudo-elasticity,

7.2. INTRODUCTION

NiTi alloys are extensively used in medical applications, because of their excellent biocompatibility and mechanical properties.^{1,2} Examples of implementations are endoscopic guide wires, cardiovascular stents and orthodontic arch wires.¹⁻³ Stimuli for exploitation of NiTi are its shape memory effect and in particular its superior pseudo-elasticity.^{1,2} The remarkable mechanical behaviour of NiTi is originated in the austenite-martensite transformation under influence of strain and temperature. In case high implant flexibility is required, an option would be to use NiTi alloy. An example of an application is an implantable NiTi rod to correct scoliosis.^{4,6} Another example in spine surgery is the use of pseudo-elastic NiTi wires for stabilisation of lumbar segments.⁷

We designed a highly flexible non-fusion scoliosis correction implant system (**XS LATOR**) which is able to adjust to spinal flexion. The implant, containing a Ø4 mm NiTi rod element, is pre-strained during surgery. Post-operative spinal flexion carried out during daily activities results in non-zero mean strain cyclic loading. Like in the other spinal implants, the fatigue behaviour of NiTi is crucial for successful long-term implantation. The fatigue behaviour of NiTi, however, is complex and difficult to predict, particularly due to the phase transformations the material exhibits.⁸⁻¹⁰ Several studies confirmed that this phase transition accelerates fatigue crack growth thereby limiting fatigue life.^{8,11-13}

Fatigue life is dependent on magnitude, type, and history of loading and on the geometry of the NiTi material, but also on other factors. For example, rotary bending experiments on guide wires showed fatigue behaviour is dependent on test temperature, surface condition, and testing environment as well.^{14,15} Important is the difference between phase transition temperature and test temperature.¹⁶ The transition temperature is dependent on various process parameters of the specimen such as melt practice,¹⁷ amount of cold work,^{18,19} annealing time and annealing temperature.^{10,20}

Because there is no generic S-N curve for NiTi, a fatigue study of a specific NiTi application must be performed under its typical loading conditions.¹⁴ In most studies determining fatigue behaviour of NiTi, a rotary bending technique is applied in which wires are subjected to zero mean stress cyclic bending.^{9,21-24} Diameters of such wires, generally used in endoscopy and orthodontics range from 0.3 mm to 1.4 mm.^{9,17} For non-zero mean stress loads, only a few studies exist,²⁵ and little is known about the fatigue life of pre-bent rods subjected to cyclic uni-axial bending. One study indicated that the fatigue limit in a four-point-bending experiment is lower than in a rotational bending experiment.²⁶ Another study that reported on fatigue life of NiTi wires in a four-point-bending test with non-zero mean strain, indicated that for cyclic strains in the pseudo-elastic region, fatigue life is virtually independent of mean strain.²⁶ This finding is fairly consistent with the results of a study about fatigue of NiTi cardiovascular stents.²⁵ All studies concentrate on small-diameter wires though. No studies have been found on bending wires with a large (>3 mm) diameter. Accordingly, the fatigue behaviour under non-zero mean strain loading conditions that apply in for instance non-

fusion scoliosis correction devices is still unknown. Goal of this study is to determine the fatigue behaviour of NiTi rods subjected to four-point-bending as a function of pre-strain and different heat and surface treatments.

7.3. MATERIALS AND METHODS

Hot rolled NiTi rods (55.8w% Ni) with diameter of 4 mm and length 167 mm were obtained from a single supplier (Nimesis Technology, France). The specimens were heat treated and polished under various conditions. Heat treatments of 400°C/15 min (T1), 400°C/30 min (T2), 350°C/15 min (T3), 450°C /15 min (T4), and a double treatment of 520°C/60 min and 400°C/22 min (T5) were performed in a hot air furnace followed by water quenching at room temperature. The resulting austenite finish temperature (A_f) was for all specimens between 32°C and 38°C, which were determined using Differential Scanning Calorimetry (DSC, Table 7.1).

Surface treatments included axial grinding followed by mechanical super-polishing (AS), mechanical super-polishing after tangential grinding (TS), plasma polishing (PP), and shot peening (SP). Grinding of the specimens was performed using sandpaper with grain 300, 600, 1200 and 2500, successively. Surface roughness (R_a) was determined using confocal laser scanning microscopy. Pre-strain was varied between 1% and 2.5%. Two batches (B1, B2) of the same manufacturer were tested for consistency.

<i>Heat tr</i>	<i>Temp/time</i>	<i>As</i>	<i>Apeak</i>	<i>Af</i>	<i>Ms</i>	<i>Mf</i>	<i>Rs</i>	<i>Rf</i>
T1	400°C/15 min	29	34	37	-16	-27	32	16
T2	400°C/30 min	29	36	38	-7	-23	29	20
T3	350°C/15 min	32	35	38	xxx	xxx	37	21
T4	450°C/15 min	21	28	32	-29	-43	23	11
T5	520°C/60 min and 400°C/15 min	31	35	37	-19	-25	30	19

Table 7.1: Transformation characteristics

The transformation temperatures (start, finish, and peak) were determined using Differential Scanning Calorimetry (DSC). Austenite (A_s , A_f , A_{peak}), Martensite (M_s , M_f) and R-phase (R_s , R_f) transformation temperatures are listed. All heat treatments resulted in austenitic phase at body temperature. For T3, M_s and M_f temperature could not be determined in the range between -50°C and 10°C.

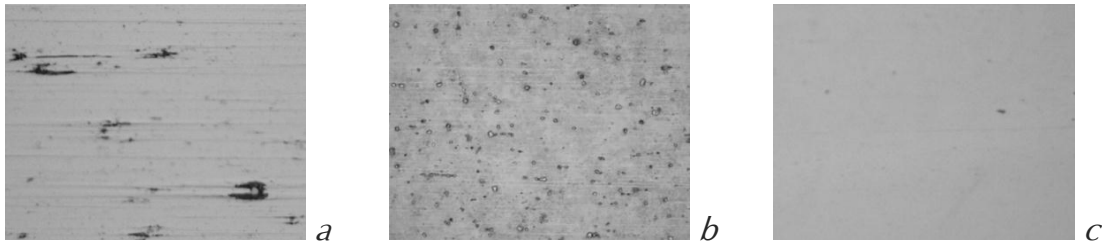


Figure 7.1: Different polished surfaces (magnification 50x)

(a) Image of a typical axially grinded and mechanically polished surface of a batch 1 rod shows major inclusions and irregular surface. (b) Typical plasma polished surface of a batch 1 rod also shows irregular surface but smaller inclusions. (c) Typical (axially grinded and mechanically polished) surface of a batch2 rod shows a smooth surface with minute inclusions.

Although the two batches were obtained from the same manufacturer, claiming similar processing procedures and equal mechanical properties, the confocal laser scanning microscope revealed differences between the two batches (Figure 7.1a, c). Batch 1 (B1) showed large inclusions in the surface and in the bulk material whereas batch 2 (B2) showed fewer and smaller inclusions. As a result, equal surface treatment resulted in different surface roughness (Table 7.2) between the batches. Plasma polished rods (B1) showed smaller inclusion sizes and a higher surface roughness than the mechanically polished rods (B1). Figure 7.1b shows a typical plasma polished surface.

Thirteen experiments were performed, each with 15 samples and each with different parameter values (Table 7.2). Experiment X1 was the reference experiment with basic values for all parameters. In all following experiments, each time only one parameter was changed. Shot peening treatment was added as a supplementary surface treatment. Because B1 ran out of specimens, the shot peening treatment was performed on specimens of B2. To check the surface and bulk composition, confocal laser scanning microscopy was performed.

In a four-point-bending set-up (Figure 7.2), the rods were tested in a phosphate buffered saline (PBS) solution maintained at body temperature of (37°C) at which all rods were in austenitic state. With a 3 Hz frequency, cyclic bending of a rod was facilitated by four supports, the middle two of which were constrained vertically whereas the outer two supports underwent a cyclic vertical translation. Vertical translation of these supports was initiated by an electromotor and a camshaft mechanism, which introduced an alternating strain. Before introduction of the cyclic motion, the supports were positioned in such a way that the rods were pre-strained. Bending strain at the rod surface was calculated from the displacements of the supports. Unless otherwise indicated, the reported pre- and alternating strains occurred at the surface on the convex side of the bent rod.

Exp	Heat tr	Surface tr	Pre-strain	Batch	Ra
X1	T1	AS	2.0%	B1	0.11
X2	T1	AS	2.5%	B1	0.11
X3	T1	AS	1.5%	B1	0.11
X4	T1	AS	1.0%	B1	0.11
X5	T2	AS	2.0%	B1	0.11
X6	T3	AS	2.0%	B1	0.09
X7	T4	AS	2.0%	B1	0.08
X8	T5	AS	2.0%	B1	0.10
X9	T1	TS	2.0%	B1	0.10
X10	T1	PP	2.0%	B1	0.29
X11	T1	AS	2.0%	B2	0.06
X12	T1	SP	2.0%	B2	0.55
X13	T5	SP	2.0%	B2	0.58

Table 7.2: Overview of tested parameters and values

The influence of four parameters was tested: heat treatment, surface treatment, pre-strain and batch number. Five different heat treatments were performed, varying temperature and time. Surface treatment consisted of shot peening (SP), plasma polishing (PP) or mechanical super-finishing after axial (AS) or tangential grinding (TS). The rods were pre-strained with 1%, 1.5%, 2.0%, and 2.5%. The right column shows the mean R_a surface roughness of the rods in the various experiments.

During cyclic motion, the pre-strain (minimal strain) was always kept above zero (Figure 7.3). Four different pre-strain values were applied: 1.0%, 1.5%, 2.0%, and 2.5 %. A sensor recorded each bending cycle. Fatigue failure detection was carried out by mechanical levers that switched off if a rod failed. Cycle and failure data of each rod were digitally stored.

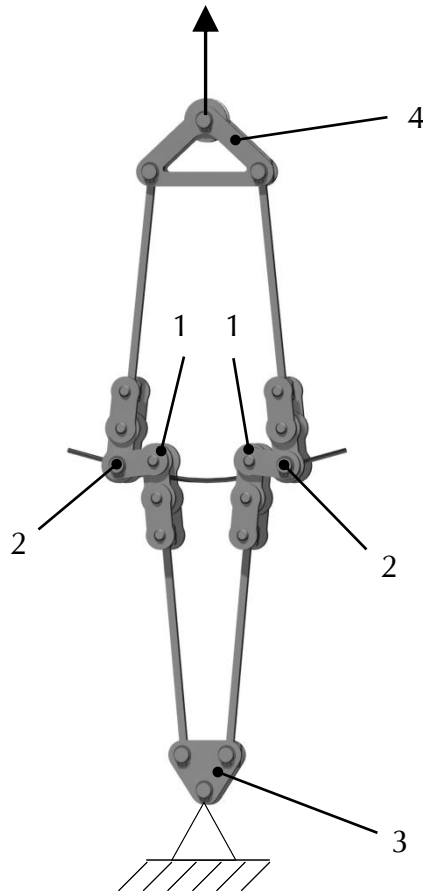


Figure 7.2: Bending test set-up

Four supports facilitated the bending of a NiTi rod. Two outer supports (2) translated vertically, initiated by a vertical translation of the upper triangle (4) which was pulled by a wire connected to a camshaft. The inner two supports (1) were restrained vertically by the lower triangle (3) that was fixed to a frame.

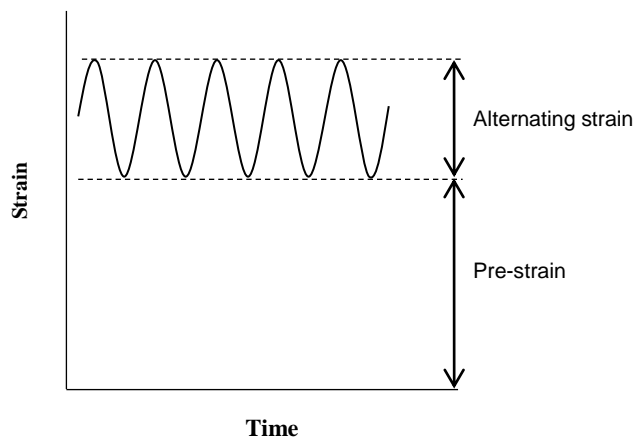


Figure 7.3: Applied bending surface strain

Each rod was pre-strained prior to the application of alternating strain. The referred pre- and alternating surface strains represent the maximal calculated surface strain in the rod.

To determine alternating strain limits, we used the 'staircase method', a method described in detail by Dixon and Mood.²⁷ The staircase method has been shown very effective and efficient in determining the fatigue limit for a specific amount of cycles.²⁸ Using this technique, the alternating run-out strain for 1.5 million cycles (referred to as fatigue limit) was determined in each experiment. In total, 13 experiments were performed. In each experiment, a specimen was initially tested on an arbitrarily chosen alternating strain. The next specimen was tested using increased alternating strain if the specimen survived the 1.5 million cycles and decreased alternating strain if the specimen failed. A variable step size in terms of alternating strain was used. These variable step sizes were dictated by the test set-up and could not be influenced. The specimens were tested at strains of 0.03%, 0.10%, 0.21%, and 0.37%. A test run was stopped if a rod survived 1.5 million cycles. If for example, a specimen survived 1.5 million cycles of 0.10% alternating strain, the strain was altered to 0.21% for the next specimen. If the specimen broke, the strain was set to 0.03% for the next specimen. The chosen fatigue strain limit for 1.5 million cycles was based on the estimated maximum number of significant bends (flexion/extension) of adolescents during an implantation period of ten years.²⁹⁻³¹ Run-out strain amplitude was tested on four different parameters including heat treatment, surface treatment, pre-strain and batch from manufacturer (Table 7.2).

Statistical significance was examined using two techniques. First, the mean alternating strain limits for a fatigue life of 1.5 million cycles (fatigue limit) and their confidence intervals were determined using the procedures described by Dixon and Mood (staircase method).²⁷ A difference between means was identified as significant ($p < 0.05$) if the 84% confidence intervals (CI) did not overlap. This procedure was proposed by Payton *et al.* if only an estimate of the means and their confidence intervals are known.^{32,33} Second, the fatigue lives of the rods for alternating strains of 0.10% and 0.21% were determined. For comparison, multiple *t*-tests (for independent samples with equal variances not assumed) were performed for alternating strains of 0.10% and 0.21% using the log cycles-to-failure of the rods. In these *t*-tests, for samples that survived, the maximum of (log) 1.5 million cycles was used.

7.4. RESULTS

An overview of the fatigue limit of each experiment, as determined by the staircase method, is shown in Figure 7.4 and Table 7.3. The fatigue limit (for 1.5 million cycles) of the X1 (batch 1) rods with the default heat and surface treatments (T1, AS) and pre-strain (2%) was 0.06%. The fatigue limit of the rods of batch 2 (X11) with identical heat and surface treatments was 0.15%. In this staircase method, the difference between fatigue limit of the two batches B1 and B2 was considered significant since the 84% confidence intervals did not overlap (Figure 7.4). Likewise, the X4 (1% pre-strained) and X8 (double heat-treated) rods showed significantly higher fatigue limits than X1 rods. Both these X4 and X8 rods showed a fatigue limit of 0.19% (Figure 7.4). Fatigue lives for

0.10% alternating strain of X4, X8, and X11 rods were not used in the t -tests for comparison because none of the specimens tested at 0.10% strain failed.

Figure 7.4 illustrates that the fatigue limit was 0.06% for the X2, X9, and X6 rods, which is similar to the fatigue limit for the X1 rods (the default experiment). The X3, X5, X7, and X10 rods showed higher fatigue limits but these differences were not significant. Despite the fact that no significant difference in fatigue limit could be observed for X10 and X9, the t -test for 0.10% alternating strain showed a significant difference in fatigue life. This t -test showed that the log cycles to failure (fatigue life) for X10 rods (plasma polished) was significantly higher ($p=0.010$) than for X1 rods (Figure 7.5a, Table 7.4a). Furthermore, at 0.10% alternating strain, significant difference in fatigue life between X9 (tangentially grinded) and X1 (axially grinded) rods ($p=0.003$) was observed. The t -tests for 0.10% alternating strain did not show differences in fatigue life between X2, X3, X5, X7, X6 rods, and X1 rods.

Rods of batch 2 (X11) with the default parameters showed a fatigue limit of 0.15%. The X13 (double heat-treated, shot peened) rods showed a significantly lower fatigue limit (Figure 7.4). The shot peened rods (X12) of B2 with default heat treatment also showed a lower fatigue limit than X11 rods, though not statistically significant. Additionally, the t -tests for alternating strain of 0.21% demonstrated no significant difference in fatigue life between the X11 and X12 rods (Figure 7.5b, Table 7.4b). Both the staircase method and the t -test however demonstrated a significant difference between X13 and X12 rods. In fact, the X13 rods showed significantly lower fatigue limit (Figure 7.4) and a significantly lower fatigue life at 0.10% alternating strain ($p=0.05$) than X12 rods (Figure 7.5a).

Furthermore, when we compared the X13 (double heat treated, shot peened, B2) rods with X8 (double heat treated rods, mechanically polished, B1) rods, we observed a significant lower alternating strain limit for the X13 rods than for the X8 rods, despite the fact that the X11 (B2) rods showed higher alternating strain limit than X1 (B1) rods.

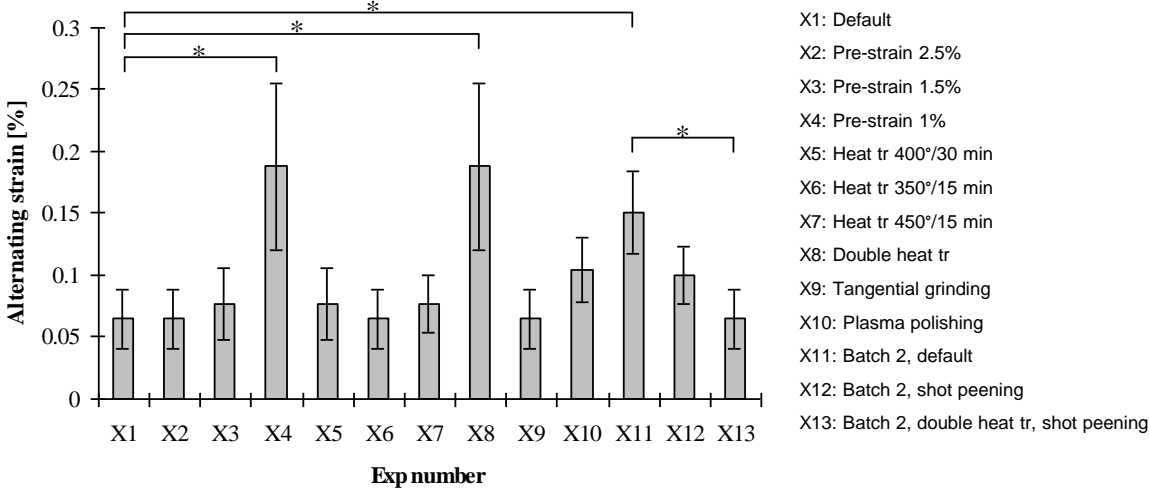


Figure 7.4: Alternating strain limit

Mean strain limits and 84% CI levels for a fatigue life of 1.5 million cycles. Default parameters are heat treatment of 400°C/15 min, axial grinding, mechanical super-finish, and pre-strain of 2%. The figure shows that compared to X1 (default), large increase in alternating strain limit was achieved by lowering pre-strain to from 2% (X1) to 1% (X4), adding a shape setting anneal of 520°C/60 min (X8) and testing another batch (B2) with default values (X11). Double heat-treated and shot peened rods of batch 2 (X13) demonstrated a decrease in fatigue limit when compared to X11 (default parameters, B2).

<i>Exp</i>		<i>Mean [%]</i>	<i>SE [%]</i>
X1	Default	0.06	0.02
X2	Pre-strain 2.5%	0.06	0.02
X3	Pre-strain 1.5%	0.08	0.02
X4	Pre-strain 1%	0.19	0.03
X5	Heat tr 400°/30 min	0.08	0.02
X6	Heat tr 350°/15 min	0.06	0.02
X7	Heat tr 450°/15 min	0.08	0.02
X8	Double heat tr	0.19	0.03
X9	Tangential grinding	0.06	0.02
X10	Plasma polishing	0.10	0.02
X11	Batch 2, default	0.15	0.02
X12	Batch 2, shot peening	0.10	0.02
X13	Batch 2, double heat tr, shot peening	0.06	0.02

Table 7.3: Alternating strain limit

An overview of the determined mean alternating strain (mean and standard error ¹⁵) values for a fatigue life of 1.5 million cycles for each group of rods (X1-X13).

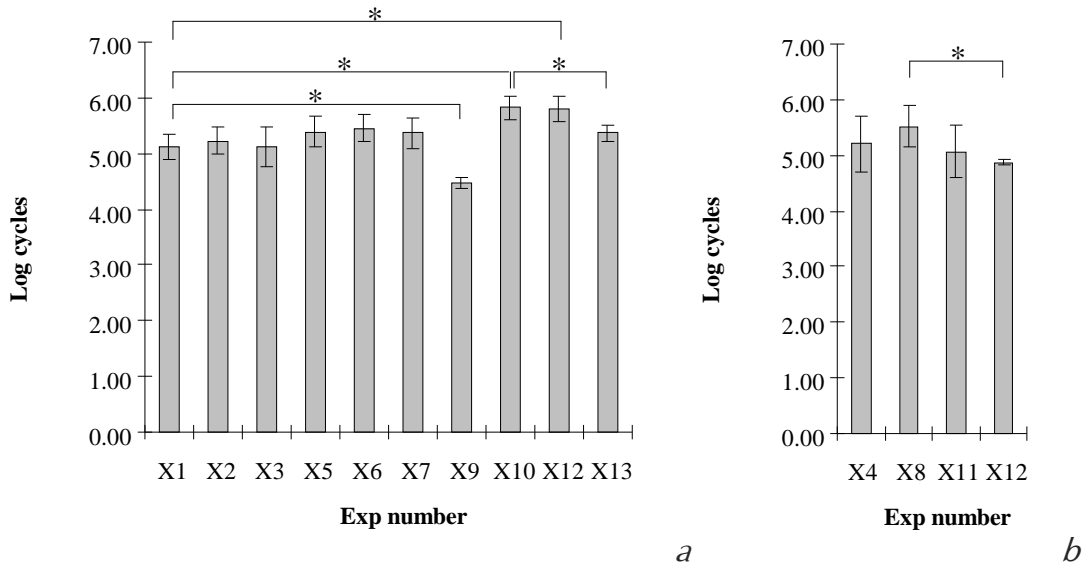


Figure 7.5: Cycles to failure at given strain

The figures show the mean log cycles to failure (with 84% confidence intervals) at 0.10% (a) and 0.21% (b) alternating strains. (a) *t*-Tests showed that the log cycles to failure (fatigue life) at 0.10% alternating strain was significantly higher for X12 and X10 rods than for X1 rods. Additionally, X9 rods demonstrated significant lower fatigue life than X1 rods. At 0.10% alternating strain, X4, X8 and X11 rods were not used for comparison because none of the specimens tested at 0.10% strain failed. (b) *t*-Test for 0.21% alternating strain demonstrated no statistical difference in fatigue life between X12 (shot peened, B2) rods and X11 (default, B2). Rods X8 showed significantly higher fatigue life than X12 rods at 0.21% alternating strain.

<i>Exp</i>	<i>Mean [%]</i>	<i>SE [%]</i>	<i>Exp</i>	<i>Mean [%]</i>	<i>SE [%]</i>
X1	5.12	0.17	X4	5.20	0.36
X2	5.23	0.17	X8	5.52	0.26
X3	5.13	0.25	X11	5.07	0.33
X5	5.39	0.20	X12	4.88	0.04
X6	5.46	0.18			
X7	5.36	0.20			
X9	4.48	0.07			
X10	5.82	0.15			
X12	5.79	0.17			
X13	5.36	0.10			

Table 7.4: Log cycles to failure at various alternating strains

(a) Cycles to failure at 0.11% alternating strain for various experiments. (b) Cycles to failure at 0.21% alternating strain.

7.5. DISCUSSION

NiTi is a fascinating material because of its shape memory properties, its biocompatibility, and pseudo-elasticity. Elastic (recoverable) strains up to 8% have been reported.³⁴ Because of these properties, the use of NiTi in implants and medical devices is appealing. Unpredictable behaviour regarding fatigue at high strains makes it challenging to use NiTi in high performance medical applications. This study attributes to a better understanding of the fatigue behaviour of austenitic (pseudo-elastic) NiTi.

The influence of surface finish on fatigue properties of pseudo-elastic NiTi wire was previously investigated by for example Patel *et al.* and Polinski *et al.*^{15,35} They examined mechanically polished, light oxide, electro polished, pickled, etched, dark oxide and black oxide surfaces. No consensus however on the optimal surface treatment has been achieved.

Fatigue limit in metals is known to be dependent on the quality of the surface finish, which is usually determined by the surface roughness (R_a) value.^{36,37} Decreasing surface roughness can increase the fatigue limit due to lowered stress-peaks. However, non-metallic inclusions such as oxygen and carbon are mainly responsible for crack initiation.^{22,38} In NiTi for example, $Ti_4Ni_2O_x$ inclusions formed by oxygen contaminants can depress martensite start temperature (M_s) which may have an adverse effect on fatigue resistance.³⁹

In our study, the alternating strain limit of the axially ground and (mechanically) polished rods was different between the two batches. Although the mechanical polishing procedures were equal for both batches, surface roughness (R_a) of B1 rods was higher. The lower fatigue resistance of the B1 rods, compared to B2 may be the result of the larger inclusion size in the B1 rods.

The plasma polished specimens showed higher surface roughness than the mechanically polished specimens did. Despite the higher surface roughness, the determined fatigue limit was higher than for the mechanically polished rods. Plasma polishing may have altered the martensite transformation characteristics and/or decreased the size of inclusions at the surface due to local increase in temperature.

Besides surface roughness, surface texture influences fatigue behaviour.⁴⁰ Tangential grinding introduces scratches that are in the direction orthogonal to the main stresses in bending, which increases stress concentrations during bending. The results in our study show that axial grinding increases the fatigue limit in bending of NiTi rods. Generally, in metals such as stainless steel, shot peening improves fatigue behaviour as a result of compressive residual surface stresses.⁴¹ In our study, shot peening showed no improvement of fatigue resistance of 2% pre-strained rods. The change in phase transformation characteristics of the surface, a consequence of shot peening,⁴² may have neutralised the positive effect of shot peening on stress-peak reduction. At lower pre-strain, when surface strains remain low ($< 1\%$), shot peening may still be beneficial for fatigue behaviour because martensite transition in the surface, which is known to accelerate fatigue crack growth,¹³ will be avoided.

The amount of cold work as a result from the rod processing influences fatigue behaviour. Hot rolled large diameter NiTi rods show significantly lower fatigue crack growth rate than cold drawn (following initial hot rolling) specimen.¹⁹ The resulting residual stresses in cold drawn specimens are likely to be responsible for the lower fatigue resistance.¹⁹ Heat treatment may be performed to reduce these residual stresses. However, because heat treatment also influences phase transition temperature, determination of optimal heat treatment is challenging. In our study, we compared five different heat treatments. Small variations in heat treatment temperature ($\pm 50^\circ\text{C}$) and time (+ 15 min) did not result in altered fatigue resistance. However, the addition of a heat treatment ($520^\circ\text{C}/60$ min) prior to the final heat treatment ($400^\circ\text{C}/15$ min) resulted in altered fatigue behaviour. Whereas the double heat treatment showed increased fatigue resistance in mechanically polished B1 rods, similar heat treatment showed a reduced fatigue resistance in shot peened B2 rods. Introduction of compressive stresses by shot peening, after a double heat treatment, did not result in improvement of fatigue resistance (B2). Nevertheless, we conclude that the addition of a shape setting annealing treatment increases the fatigue behaviour in certain cases. The actual effect on the fatigue properties may depend on the composition of the alloy and properties achieved

by processing such as the amount of cold work, inclusions *etc.* The quality and state of NiTi obtained from the manufacturer is crucial for its fatigue properties.

Austenitic NiTi exhibits stress-induced martensite transition resulting in pseudo-elastic behaviour. Stress-induced phase transition is regarded as a fatigue augmentation factor,¹³ caused by high shear stresses accompanying these transitions.⁸ However, when stresses do not impose phase transition, fatigue life will improve drastically.^{12,13} This can be achieved by limiting the cyclic strains to 0.7%, the onset of martensite forming,¹⁷ or by keeping the surface strain in the rods during cyclic bending high enough to maintain the stress-induced martensite. In our study, increasing pre-strain from 1.5% to 2.5% did not decrease fatigue resistance. This result is in correspondence with other studies that showed little influence of pre-strain on fatigue in the range between 2% and 6%. At lower strains, fatigue resistance becomes higher,^{13,25} which is confirmed by our study. The rods with a pre-strain of 1% showed significant higher alternating strain limit than the rods with intermediate pre-strains (1.5%, 2%, and 2.5%).

The alternating strain limits determined in our (large diameter) NiTi rods are considerably lower than would be expected from the results of other small diameter wire experiments.^{17,24,26} Most of these studies performed their fatigue tests at frequencies that are one hundred to one thousand times higher than in our experiment.^{17,21,24,35} In these studies, a non-corrosive in silicon-oil environment or a corrosive water bath was used to keep the temperature constant at these high frequencies. An aqueous medium such as water and hypochlorite solution adversely affects fatigue crack propagation.^{43,44} The corrosive environment in our experiment, a PBS solution maintained at 37°C, may have an even greater influence on fatigue behaviour since the relative exposure time is longer as a result from the low testing frequency. This will contribute to a lower fatigue strain limit. Another explanation of the relatively low fatigue resistance in our experiment can be found in the large wire diameter. Norwich *et al.* found that an increase in wire diameter lowers NiTi fatigue resistance.¹⁴ In addition, the fatigue resistance in four-point-bending is reportedly lower than in rotational bending.^{26,45}

Local stabilisation of martensite can be helpful in optimizing the fatigue properties.³⁹ To improve the bending fatigue resistance in pseudo-elastic rods, austenite in the surface of the rods may be transformed to martensite and stabilised. As a result, bending the rods will not induce a phase transformation in the surface of the rods, thereby increasing alternating strain limit for high cycle bending. Plasma polishing, in which only the surface is locally heated, can be helpful in generation of stable martensite structure without affecting the pseudo-elasticity of the austenite core of the rod. In a follow-up study, optimal fatigue heat and surface treatment will be determined. Plasma polishing will be carried out on double and single heat-treated rods of the second batch (B2).

In our testing procedure, we used the staircase method to determine the alternating strain limits for pre-bent rods. The staircase method for analysing sensitivity data is

introduced by Dixon and Mood²⁷ and recommended by Collins to obtain the fatigue limit at a certain life.²⁸ Although this method can be very efficient, in our study the determination of confidence intervals was complicated by the variable step sizes. At higher alternating strains, this resulted in relatively large confidence intervals, which makes it more difficult to identify statistical significance for the higher strain levels. The large step sizes was a limitation of the fatigue testing machine, which was originally designed to examine fatigue at much higher alternating strain levels (range between 1.5% and 2.5%). By using the *t*-tests to compare of the log cycles to failure for alternating strain levels (0.10% and 0.21%), significant differences in fatigue life between groups could be identified.

7.6. CONCLUSIONS

The following conclusions can be drawn concerning 2% pre-strained large diameter (4 mm) NiTi wires (55.8w% Ni) in high cycle four-point-bending dynamics.

For intermediate pre-strain levels (1.5%-2.5%), fatigue resistance does not change with altering the pre-strain.

Fatigue resistance of austenitic NiTi becomes higher at a lower pre-strain level of 1%.

Slight changes in heat treatment temperature (+/-50°C) or increase in heat treatment time (15 min) does not have an effect on fatigue properties if the austenite finish temperature (A_f) remains unchanged.

Axially ground rods show higher fatigue resistance than tangentially ground rods, in spite of super-finishing procedures.

Shot peening does not show improved fatigue resistance compared to mechanical super-finishing.

In pre-strained rods, plasma polishing, compared to mechanical super-finishing, improves the fatigue resistance.

A shape-setting heat treatment prior to the default heat treatment at lower temperature can improve fatigue resistance in certain cases, depending on the state of the material 'as received' from manufacturer.

The quality and state of NiTi retrieved from the manufacturer is crucial for its fatigue properties.

7.7. REFERENCES

1. Stoeckel, D. Nitinol medical devices and implants. *Minimally Invasive Therapy and Allied Technologies* **9**, 81 - 88 (2000).
2. Duerig, T., Pelton, A. & Stöckel, D. An overview of nitinol medical applications. **273-275**, 149 (1999).

3. Thompson, S.A. An overview of nickel-titanium alloys used in dentistry. *International Endodontic Journal* **33**, 297-310 (2000).
4. Veldhuizen, A.G., Sanders, M.M. & Cool, J.C. A scoliosis correction device based on memory metal. *Medical Engineering & Physics* **19**, 171-179 (1997).
5. Schmerling, M.A., Wilkov, M.A., Sanders, A.E. & Woosley, J.E. Using the shape recovery of nitinol in the Harrington rod treatment of scoliosis. *Journal of Biomedical Materials Research* **10**, 879-892 (1976).
6. Newton, P.O., *et al.* Dual and single memory rod construct comparison in an animal study. *Spine* **36**, E904-E913 (2011).
7. Kim, Y.-S., *et al.* Nitinol spring rod dynamic stabilization system and Nitinol memory loops in surgical treatment for lumbar disc disorders: short-term follow up. *Neurosurgical FOCUS* **22**, 1-9 (2007).
8. Dauskardt, R.H., Duerig, T.W. & Ritchie, R.O. Effects of in situ phase transformation on fatigue-crack propagation in titanium-nickel shape-memory alloys. *Shape Memory Materials* **9**, 243-249 (1989).
9. Eggeler, G., Hornbogen, E., Yawny, A., Heckmann, A. & Wagner, M. Structural and functional fatigue of NiTi shape memory alloys. *Materials Science and Engineering A* **378**, 24 (2004).
10. Robertson, S.W., Stankiewicz, J., Gong, J.M. & Ritchie, R.O. Cyclic fatigue of Nitinol. *Proceedings of the International Conference on Shape Memory and Superelastic Technologies* (2004).
11. Humbeeck, J.V. Cycling effects, fatigue and degradation of shape memory alloys. *J. Phys. IV France* **01**, 189-197 (1991).
12. Tobushi, H., Hachisuka, T., Yamada, S. & Lin, P.-H. Rotating-bending fatigue of a TiNi shape-memory alloy wire. *Mechanics of Materials* **26**, 35 (1997).
13. Tabanli, R.M., Simha, N.K. & Berg, B.T. Mean stress effects on fatigue of NiTi. *Materials Science and Engineering A* **273-275**, 644 (1999).
14. Norwich, D. & Fasching, A. A study of the effect of diameter on the fatigue properties of NiTi wire. *Journal of Materials Engineering and Performance* **18**, 558-562 (2009).
15. Polinski, M., Norwich, D. & Wu, M. A study of the effects of surface modifications and processing on the fatigue properties of NiTi wire. *Proceedings, SMST-2006, Pacific Grove, California*, 1-17 (2006).

16. References, S. Growth of human intervertebral discs and vertebral bodies. *Journal of anatomy* **120**, 49 (1975).
17. Reinoehl, M., Bradley, D., Bouthot, R. & Proft, J. The influence of melt practice of final fatigue properties of superelastic NiTi wires. *SMST 2000* (2000).
18. Schaffer, J. & Plumley, D. Fatigue performance of Nitinol round wire with varying cold work reductions. *Journal of Materials Engineering and Performance* **18**, 563 (2009).
19. Gall, K., *et al.* Effect of microstructure on the fatigue of hot-rolled and cold-drawn NiTi shape memory alloys. *Materials Science and Engineering: A* **486**, 389 (2008).
20. Huang, X. & Liu, Y. Effect of annealing on the transformation behavior and superelasticity of NiTi shape memory alloy. *Scripta Materialia* **45**, 153-160 (2001).
21. Miyazaki, S., Mizukoshi, K., Ueki, T., Sakuma, T. & Liu, Y. Fatigue life of Ti-50 at.% Ni and Ti-40Ni-10Cu (at.%) shape memory alloy wires. *Materials Science and Engineering A* **273-275**, 658-663 (1999).
22. Sawaguchi, T., Kausträter, G., Yawny, A., Wagner, M. & Eggeler, G. Crack initiation and propagation in 50.9 at. pct Ni-Ti pseudoelastic shape-memory wires in bending-rotation fatigue. *Metallurgical and Materials Transactions A* **34**, 2847-2860 (2003).
23. Figueiredo, A.M., Modenesi, P. & Bueno, V. Low-cycle fatigue life of superelastic NiTi wires. *International Journal of Fatigue* **31**, 751 (2009).
24. Patel, M. Characterizing fatigue response of nickel-titanium alloys by rotary beam testing. *J ASTM Int* **4**, 1-11 (2007).
25. Tolomeo, D., Davidson, S. & Santinoranont, M. Cyclic properties of superelastic Nitinol: design implications. In: *Russell SM, Pelton AR, editors. Proceedings of the international conference on shape memory and superelastic technologies. Menlo Park, CA: SMST Society, Inc, 471-476* (2000).
26. Wick, A., Gong, X.-Y., Fino, J., Sherrif, J. & Pelton, A.R. Bending fatigue characteristics of Nitinol. *Proceedings of SMST-2004, ed. M. Mertmann, Baden-Baden, Germany, 361-366* (2006).
27. Dixon, W.J. & Mood, A.M. A method for obtaining and analyzing sensitivity data. *Journal of the American Statistical Association* **43**, 109-126 (1948).
28. Collins, J. *Failure of materials in mechanical design: analysis, prediction, prevention*, (John Wiley & Sons, Inc. , New York, 1993).

29. Morlock, M.M., *et al.* Determination of the *in vivo* loading of the lumbar spine with a new approach directly at the workplace - first results for nurses. *Clinical Biomechanics* **15**, 549-558 (2000).
30. Hedman, T.P., Kostuik, J.P., Fernie, G.R. & Heller, W.G. Design of an intervertebral disc prosthesis. *Spine* **16**, S256-S260 (1991).
31. ASTM Standard F2624 - 07 (2008). Standard test method for static, dynamic and wear assessment of extra-discal spinal motion preserving implants. ASTM International, West Conshohocken, PA, 2008, DOI: 10.1520/F2624-07, www.astm.org.
32. Payton, M.E., Greenstone, M.H. & Schenker, N. Overlapping confidence intervals or standard error intervals: what do they mean in terms of statistical significance? *J Insect Sci* **3**, 30 (2003).
33. Julious, S.A. Using confidence intervals around individual means to assess statistical significance between two means. *Pharmaceutical Statistics* **3**, 217-222 (2004).
34. Shabalovskaya, S.A. Surface, corrosion and biocompatibility aspects of Nitinol as an implant material. *Bio-Medical Materials and Engineering* **12**, 69 (2002).
35. Patel, M. & Gordon, R. An investigation of diverse surface finishes on fatigue properties of superelastic nitinol wire. *Presented at the International Conference on Shape Memory and Superelastic Technologies (SMST)* (2006).
36. Bayoumi, M.R. & Abdellatif, A.K. Effect of surface finish on fatigue strength. *Engineering Fracture Mechanics* **51**, 861-870 (1995).
37. McKelvey, S.A. & Fatemi, A. Surface finish effect on fatigue behavior of forged steel. *International Journal of Fatigue* **36**, 130-145 (2012).
38. Saberifar, S., Mashreghi, A.R., Mosalaeepur, M. & Ghasemi, S.S. The interaction between non-metallic inclusions and surface roughness in fatigue failure and their influence on fatigue strength. *Materials & Design* **35**, 720-724 (2012).
39. Biscarini, A., Mazzolai, G. & Tuissi, A. Enhanced nitinol properties for biomedical applications. *Recent Patents on Biomedical Engineering* **1**, 180-196.
40. Arola, D. & Williams, C.L. Estimating the fatigue stress concentration factor of machined surfaces. *International Journal of Fatigue* **24**, 923-930 (2002).
41. Mahagaonkar, S.B., Brahmankar, P.K. & Seemikeri, C.Y. Effect on fatigue performance of shot peened components: an analysis using DOE technique. *International Journal of Fatigue* **31**, 693-702 (2009).
42. McNichols, J.J.L., Brookes, P.C. & Cory, J.S. NiTi fatigue behavior. *Journal of Applied Physics* **52**, 7442 (1981).

43. Cheung, G.S.P. & Darvell, B.W. Fatigue testing of a NiTi rotary instrument. Part 1: strain-life relationship. *International Endodontic Journal* **40**, 612-618 (2007).
44. Cheung, G.S.P., Shen, Y. & Darvell, B.W. Effect of environment on low-cycle fatigue of a Nickel–Titanium instrument. *Journal of Endodontics* **33**, 1433-1437 (2007).
45. Melton, K.N. & Mercier, O. Fatigue of NITI thermoelastic martensites. *Acta Metallurgica* **27**, 137 (1979).

Chapter 8



NON-FUSION SCOLIOSIS INDUCTION IN AN *IN VIVO* PORCINE MODEL

CONTENTS

- CHAPTER 8. NON-FUSION SCOLIOSIS INDUCTION IN AN *IN VIVO* PORCINE MODEL 155**
- 8.1. ABSTRACT..... 155
- 8.2. INTRODUCTION..... 157
- 8.3. MATERIALS AND METHODS..... 158
 - 8.3.a. *The non-fusion scoliosis correction device* 158
 - 8.3.b. *Surgical procedure*..... 161
 - 8.3.c. *Postoperative period* 162
 - 8.3.d. *Post-terminal period*..... 162
- 8.4. RESULTS..... 165
 - 8.4.a. *Induced deformity* 165
 - 8.4.b. *Amount of growth* 167
 - 8.4.c. *Ossification* 168
 - 8.4.d. *Status of the implant*..... 168
 - 8.4.e. *Facet joints* 170
 - 8.4.f. *Overall tissue response*..... 171
- 8.5. DISCUSSION 172
- 8.6. CONCLUSION..... 176
- 8.7. ACKNOWLEDGEMENTS 177
- 8.8. REFERENCES..... 177

CHAPTER 8. NON-FUSION SCOLIOSIS INDUCTION IN AN *IN VIVO* PORCINE MODEL

8.1. ABSTRACT

Study design

In an experimental design, a non-fusion scoliosis correction device was tested on its functionality in (female) Dutch Landrace pigs by inducing a scoliotic deformation.

Objective

The aim of this study is to analyse the functionality of the **XS LATOR**, a non-fusion scoliosis correction system in an *in vivo* animal model. The system consists out of two different implants: one that addresses the lateral deformation, and one the axial rotation. Main investigated parameters are the amount of growth, amount of fusion, amount of tissue response and the actual amount of deformation caused by these two implants.

Material and methods

Scoliosis was induced in twelve normal Dutch Landrace pigs; six pigs received the **XS LAT**, an implant applying a lateral bending moment and six pigs received the **XS TOR**, an implant applying (axial) torque. The implants were placed posteriorly on the spine between T12 to L2 and each fixed to three vertebrae: T12, T15, and L2. To control the status of the porcine spine and the implant itself, radiographs were taken preoperatively, peroperatively and 1, 4 and 8 weeks postoperatively. After 8 weeks the pigs were euthanised and macro- and micro-biological analyses were performed to collect results concerning fusion, growth, tissue response, actual induced deformation and status of the implant.

Results

Induced deformities by the **XS TOR** are a mean cranial torsion of 11.9° and a mean caudal torsion of 7.1°. The mean Cobb-angle induced by the **XS LAT** is 18.6°. Measured (mean) kyphosis angle was 7.8° in the spines instrumented with **XS TOR** and 6.4° in spines instrumented with the **XS LAT**. Mean length progression was 20% in 8 weeks. On microscopic scale, cartilage degeneration was observed in the facet joints instrumented with pedicle screws. The vertebrae in the instrumented region had not fused.

Conclusions

The system is capable of inducing significant deformities in two different directions. Although inducing axial rotation could cause a mild associated lateral deviation, the system parts mainly effect the intended directions. The results suggest that splitting up the functionality of the implants in two parts will have advantages over the single action

implants, in which surgery mainly focuses on lateral and sagittal deformity. Avoidance of spinal fusion is possible with minimal invasive techniques. Heterotopic ossification can be limited by preserving periosteum. The system does not inhibit spinal growth.

Key terms

Scoliosis, induction, implant, torsion, Cobb-angle, pigs, *in vivo*, non-fusion, fusion, flexibility

8.2. INTRODUCTION

Scoliosis is a three-dimensional deformity in which a lateral deviation of the spine is accompanied by an axial rotation of vertebrae. Furthermore, a flattening of the spine in the sagittal plane occurs, characterised by a reduction in thoracic kyphosis and/or lumbar lordosis. Scoliosis develops most frequently during adolescence in 5% of the total population of which 80% is female. The cause for gender predominance is unknown. About 80% of all scoliotic cases are idiopathic. Research shows that biomechanical and neuromuscular misbalance seem to play a role in developing a first minor curve, which progresses during adolescence.¹ Essential problem related to scoliosis is progression of the deformity. If the deformity progresses to a lateral deviation of 45° Cobb-angle or more, surgery will be performed. The prevalence of a minimal Cobb-angle of 45° is 0.1%.

Scoliosis can reduce the quality of life significantly.^{2,3} Cosmetic deformation is likely to have a major mental impact on the adolescent patient.⁴ In addition, patients with curve progression are more likely to experience significant pain.^{5,6} Decreased pulmonary volume and compression of the heart are seen in extreme cases of scoliotic deformation.

Nowadays, surgery is performed to correct the three-dimensional deformity and to prevent its progression by realising a solid fusion of spine segments. First generation surgical procedures originate from 1962, when Harrington published his new surgical treatment for scoliosis.⁷ Second generation procedures include the application of Cotrel-Dubousset (CD) instrumentation in combination with rod derotation manoeuvres. Third generation systems apply multi-segmental instrumentation with thoracic pedicle screw anchors and use a technique called direct vertebral derotation (DVR).⁸ The second and third generation systems were able to offer major improvements in surgical techniques. Recent development in scoliosis surgery that looks promising is the usage of shape-memory metal for enhanced post-operative correction.^{9,10} Although the surgical therapies, which are based on principles of correction by applying forces and moments, have improved considerably, no system has been able to correct the torsion in scoliosis satisfyingly.

Spinal surgery aims for a solid fusion of the spine to acquire spinal strength. Main disadvantages of surgery however are loss of flexibility and inhibition of growth. In addition, a phenomenon called 'crankshafting' can take place, which means that a posterior fusion causes a new deformation induced by anterior growth.¹¹ Because of this, proper correction surgery can take place only after the spine has its full-grown length. During the growth period, patients have to depend on other treatment options for scoliosis, such as bracing, to minimise the progression of scoliosis.¹²⁻¹⁴

A system that avoids fusion, allows growth and results in full correction is requested. It serves the purpose to facilitate the spinal growth of the scoliotic patient and to redirect it

for enhanced correction. Non-fusion surgery can be applied already when the patients are in their adolescence.

The overall demand for a non-fusion scoliosis device is to apply forces that are high enough to correct the deformity and low enough to preserve flexibility in order to prevent fusion and to allow growth.

The University of Twente, in collaboration with the UMC Groningen and the VU Medical Center in Amsterdam, developed the **XS LATOR**, a novel non-fusion scoliosis correction system. This non-fusion scoliosis system, consisting of two correcting implants (**XS LAT** and **XS TOR**), is extendable to allow growth. The system is designed to correct axial rotation and lateral bending.

The aim of this study is to analyse the functioning of the **XS LAT** and the **XS TOR**, both part of the non-fusion scoliosis correction system, in an *in vivo* animal model. Because there is no animal model with a scoliotic deformation, an 'inverse' approach was used. We assume that if scoliosis can be induced by a system applying torque and a lateral bending moment in animals, actual scoliosis can be corrected using a similar but 'inverse' system in humans.

8.3. MATERIALS AND METHODS

8.3.a. The non-fusion scoliosis correction device

The double implant system (**XS LATOR**) consists of a torsion implant (**XS TOR**, Figure 8.2) and a lateral bending implant (**XS LAT**, Figure 8.3). The **XS TOR** and the **XS LAT** are placed on the posterior side of the spine and attached to three transverse bridges that are each fixed to a vertebra using two pedicle screws, one on each side (Figure 8.1). In both systems, a wide version and a narrow version were realised using different anchoring configurations. A narrow version is placed between two pedicle screws whereas a wide version is attached laterally to the pedicle screws. Connections between the bridges and the functional implant are created by fixation parts. These fixation parts, slide-bearing systems basically, which contain polyethylene (UHMWPE) bushings, are fixed to the bridges while being able to slide axially over two U-shaped loops in order to adapt to growth and functional daily motion. At the end of both loops of each implant, ring are attached to prevent the bearings for detachment (Figure 8.2b). Each implant is capable of allowing 35% axial spinal growth.

Torsion implant

The narrow and wide **XS TOR** versions, manufactured from titanium grade 5 ELI (Ti6Al4V), consist of two springs, two loops, and three fixation parts (Figure 8.2). The implants were created in two different versions with a comparable functionality. After anchoring of a torsion implant by connecting the fixation parts to the bridges, torsion is

induced by a specially developed tool. The tool is able to introduce torsion in the springs and preserve it by shifting the implant downwards into the centre fixation, which contains a square hole (see Chapter 4 for details).

Lateral implant

The **XS LAT** mainly consists of a NiTi shape memory rod (55.8 wt% Ni) with double U-loops; the rod is slidably anchored with similar elements in a similar fashion as the torsion implant. Again, two different versions were created: a narrow and a wide version (Figure 8.3). The centre part contains two PEEK (polyetheretherketone) elements. After anchoring, a bending moment is induced by allowing the implant to warm up to body temperature. The NiTi rod has reached full phase transition at body temperature.

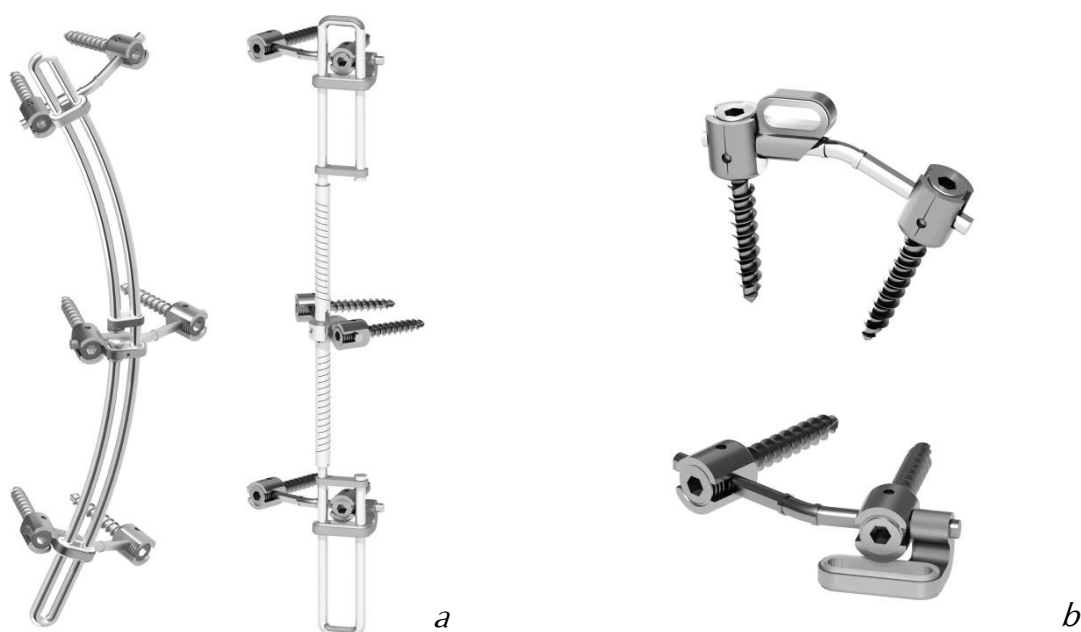


Figure 8.1: Implants designed in various configurations

(a) The XS TOR and XS LAT are attached to transverse bridges, which are anchored to the vertebrae by means of pedicle screws. A wide version of the XS TOR and a small version of the XS LAT are shown in the figure. (b) The bearings of a narrow system are located between the pedicle screws; Bearings of a wide system are attached laterally to the screws.

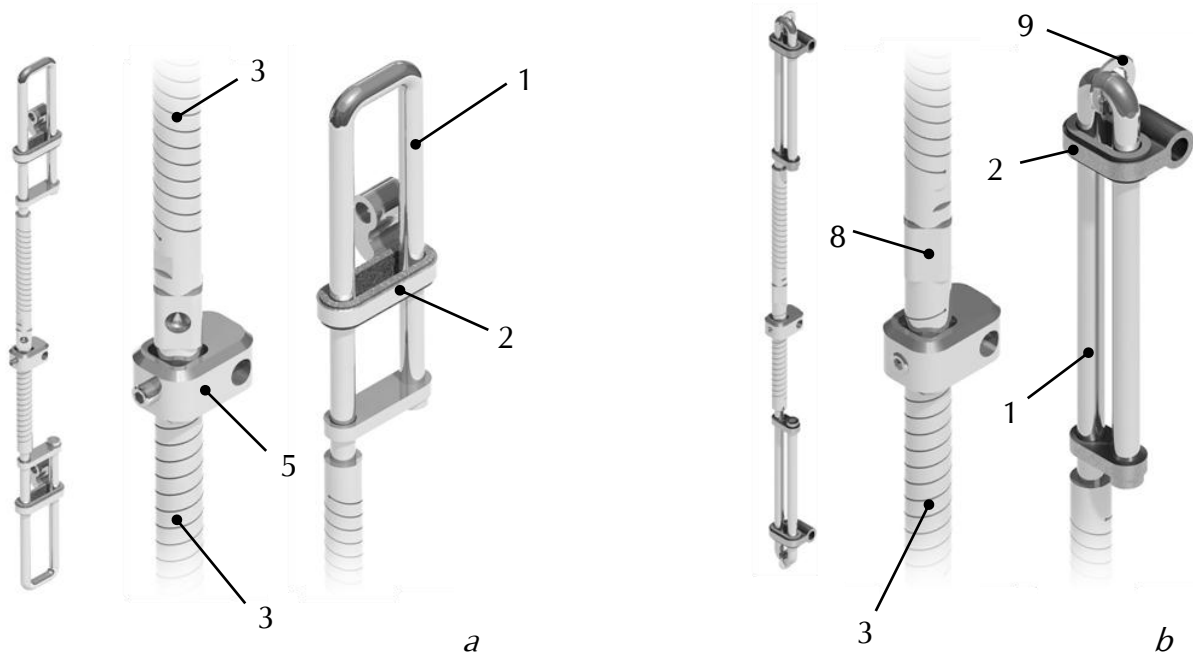


Figure 8.2: Torsion implants

The XS_{TOR} (main material Ti6Al4V) consists of two (double helical) springs (3), two U-loops (1) and two bearing systems (2) with the ability to slide (using UHMWPE bushings) over the loops. At the centre of the implant, torsion is generated by twisting and sliding the square part (8) into the square hole of a box-shaped centre part (5). Fixation to the spine is established by securing the three elements (bearings and centre part) to transverse bridges that are anchored with pedicle screws. A ring (9) is attached at the end of the U-loop to stop the bearing from detachment. (a) Wide system (XS_{TOR} -wide) with two close-ups. (b) Narrow system with two close-ups (XS_{TOR} -narrow).

Pig 1	Pig 2	Pig 3	Pig 4	Pig 5	Pig 6	Pig 7	Pig 8	Pig 9	Pig 10	Pig 11	Pig 12
NT	NL	WL	WT	NT	NL	WT	WL	WT	WL	NT	NL

Table 8.1: Overview pigs and implants

The pigs were implanted with four different implants: NL = Narrow Lateral implant (XS_{LAT} -narrow), WL = Wide Lateral implant (XS_{LAT} -wide), NT = Narrow Torsion implant (XS_{TOR} -narrow), WT = Wide Torsion implant (XS_{TOR} -wide).

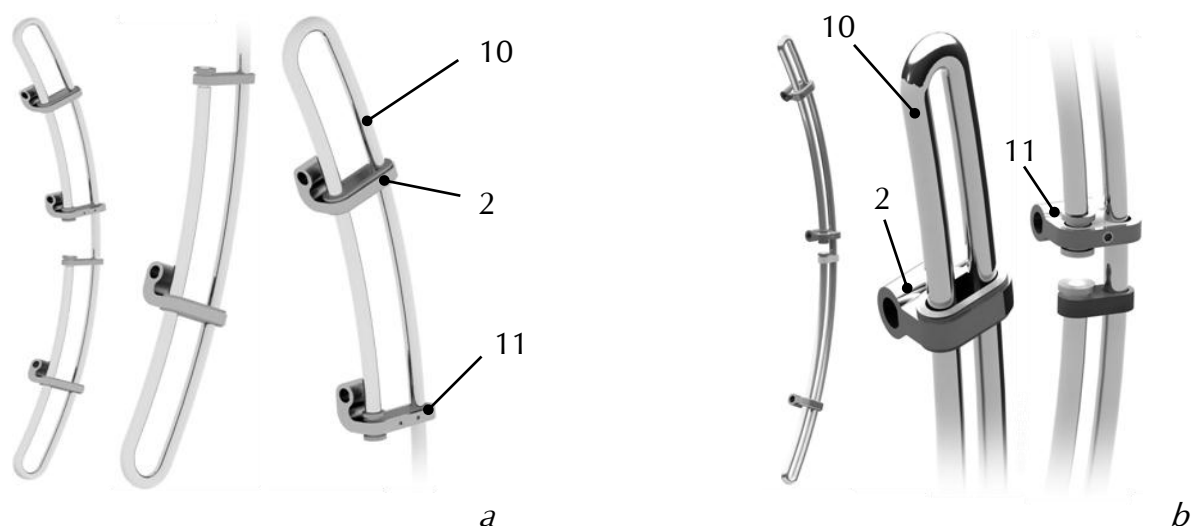


Figure 8.3: Lateral bending implants

The XS_{LAT} is composed of a pre-bent pseudo-elastic NiTi rod (10), two Ti6Al4V bearing systems (2) with UHMWPE bushings that are able to slide over the rod, and a central part (11). The bearing systems are secured to transverse bridges that are fixed to the spine using pedicles screws. (a) The wide version (XS_{LAT}-wide) consists of a wide rod and corresponding parts; (b) the narrow version (XS_{LAT}-narrow) consists of smaller parts and a narrow NiTi rod.

In this study, the newly designed non-fusion scoliosis devices were implanted in twelve normal female land pigs (age four months, weight 55-60 kg). Similarities in the human and porcine spine regarding to the biomechanical behaviour and geometrical dimensions makes the pig a representative model.^{15,16}

Six pigs received the system inducing lateral bending and six receiving the torsion inducing system. Wide and the narrow versions of the implants were used, three implants of each version (Table 8.1).

Because of the high resemblance between the porcine and the human thoracolumbar spine,¹⁶ the implants for the porcine model were implanted in this region spanning a total of six vertebrae. The porcine spine consists of 15 thoracic vertebrae; T12, T15, and L2 were selected for anchoring.

8.3.b. Surgical procedure

Surgical procedures were similar for all twelve pigs, with the only difference that the lateral implants were placed on the left side of the spinous process and the torsion implants were placed on the right side of the spinous processes.

Before surgery, the pigs were placed in prone position. Radiographs were taken to determine the pre-operative situation of the porcine spine and location of the instrumented vertebrae. After skin incision, the posterior spine was prepared for instrumentation by blunt dissection, following the facial planes, to minimise soft tissue injury and to prevent heterotopic ossification by preserving the periosteum. Heterotopic ossification¹⁷ should be avoided because bone overgrowth can counteract the induced deformation.

The laminae of vertebrae T12, T15 and L2 were prepared free of muscle tissue, followed by pedicle screw insertion. For determination of the position and direction of the screws, an awl was inserted into cortex of the pedicle and a (lateral) radiograph was taken. Each pair of pedicle screws was interconnected with a transverse bridge crossing the spinous processes. The implant was attached to the three bridges. In case a torsion-inducing device was implanted, torque was induced by using a tool that was designed exclusively for this implant and finally the implant was secured to the bridge at T15. In case a lateral system was implanted, the implant was stored at 0°C, well below the transition temperature, before attaching it to the bridges. The easily deformable low temperature state enables to the implant to be attached with less effort. Unlike in the implant of Wever *et al.*,⁹ lateral bending moment was induced by the slow (passive) rise of implant temperature to the pig's body temperature.

8.3.c. Postoperative period

In the postoperative period, the pigs were housed for two months in the central animal facility of the University Medical Center Groningen. During this period, the pigs experienced a growth spurt. In the first week of the postoperative period, the pigs were housed alone, to provide for optimal wound healing. They were checked daily on pain behaviour, mobility, temperature and the progress of their wound recovery. After the first week, they shared cages in couples of two to improve mobility and social interaction. Radiographs were taken at 1 week, 4 weeks, and 8 weeks post-operatively. Eight weeks post-operatively, the pigs were euthanised with an injection of Euthasol® (20%). The spines were harvested for macroscopic and microscopic research on the presence of heterotopic ossification, status of the implant, amount of growth and induced deformity.

8.3.d. Post-terminal period

Post-terminal analysis was performed using radiographs and CT (computed tomography) data collected immediately after the spines were harvested. The spines with the attached implants were conserved in an environment of 38°C during the period between harvesting and performing the scans. Afterwards, the spines were fixated as a whole in 4% Formaldehyde solution for seven days. After complete fixation, tissue samples were collected. The samples were taken from various areas adjacent to the bridges and screws

and from the areas adjacent to the bending and torsion springs. Special attention was paid at areas that showed dark colouration. For control, tissue samples were taken from a location outside the area of implantation. Tissue reaction and the amount of wear particles in the surrounding tissue were examined. Furthermore, all facet joints adjacent to the pedicles screws were harvested and several joints between the bridged vertebrae. Again for control, a few joints outside (caudally and cranially) the implanted area were collected. The status of the facet joints after termination was examined by determination of the quality of the cartilage using the Mankin classification.¹⁸

CT scans and radiographs

For determination of the amount growth, induced deformity and the presence of heterotopic ossification, CT scans, with a z-axis resolution (slice thickness) of 0.6 mm, were analysed. Analysis was performed using 3D Slicer (version 3.6.31.0), a software distribution under open source licence. Since scoliosis is a three-dimensional curvature, the axial rotation, lateral curvature and kyphosis angle were calculated. In each of the vertebrae T12, T15, and L2, a slice was selected at the level of the screw fixation. In this slice, the rotation angle of the vertebra was determined by drawing an anterior-posterior line of symmetry (Figure 8.4b).

After creating a 3D reconstruction of the spine, the lateral deformation was quantified by determining the Cobb-angle. The Cobb-angle, which is an established measure of lateral scoliotic deformation, was determined measuring the angle between the endplates of the instrumented vertebrae T12 and L2 in a frontal view (Figure 8.4a). The kyphosis angle was calculated in a similar fashion using a sagittal view.

The amount of spinal growth was determined from the radiographs taken 1 week, 4 weeks, and 8 weeks post-operatively by measuring the distance between the superior and inferior endplates of the instrumented vertebrae. The implant was designed to adapt to spinal growth during the implantation period. By measuring the distance between the outer pedicles screws, functional length of the implant was determined (Figure 8.4c). It was calculated that the implants have the ability to show a progression in length facilitating 35% of spinal growth.

Analysis of ossification (bone formation due to activation of osteoblasts) was done using the CT scans by optical investigation. From the CT slices, the extent of (heterotopic) ossification was determined on each spinal level. Tissue for microscopic research was harvested including the facet joints.

Status of the implant

After detaching the implant from the porcine spine, different parts of the implant were carefully checked on failure and signs of wear, especially the sliding interfaces. In addition, the implant was investigated on plastic deformation. Plastic deformation of a spring, a loop, or a NiTi rod indicates a loss of functionality.

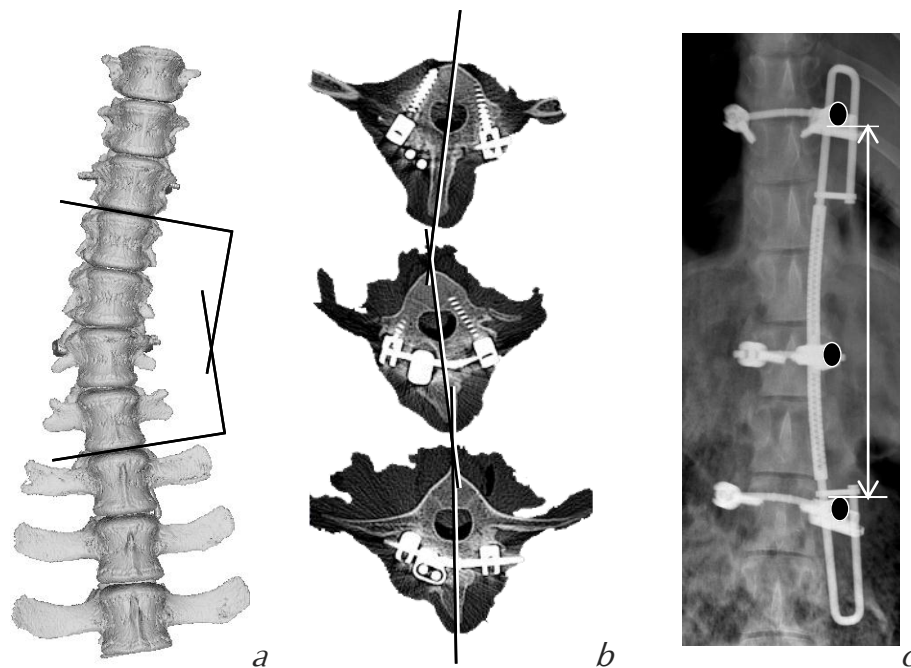


Figure 8.4: Measurement of deformations

(a) The Cobb-angle (frontal view) was determined from the CT scan (3D reconstruction) of the spine using guidelines parallel to the endplates. (b) Axial rotation angle was determined from lateral slices using guidelines running from posterior to posterior dividing the vertebrae in equivalent parts. (c) Growth of the system was determined using radiographs by measurement of the distance between the pedicle screws at the various instrumented levels.

Damage	Mankin grade	Interpretation
Mild	$0 < \text{grade} \leq 4$	Good
Moderate	$4 < \text{grade} \leq 9$	Intermediate
Severe	$9 < \text{grade} \leq 14$	Bad

Table 8.2: Legend of Mankin grades

The obtained scores were ranked using three grades: mild, moderate, and severe damage. Cartilage graded as 'mild' may be interpreted as good and normal cartilage, 'severe' as bad cartilage. Obviously, 'moderate' damage is the intermediate between good and bad.

Facet-joints and Mankin score

The different facet-joints that were harvested from all twelve porcine spines were decalcified with Propylene Diamine Tetra-acetic Acid (PDTA) solution (10%) for a period of three weeks. After total decalcification, the facet joints were embedded in a

glycol methacrylate resin (Technovit 7100). After cutting, the coupes (3 μm) were stained with Toluidine Blue (1%) for 20 seconds.

Finally, the quality of the facet joint cartilage was quantified on a scale of 0-13 (Mankin score). The Mankin score, which gives a representative outcome concerning the cartilage quality, grades the cartilage structure, the amount of cells and organization of the cartilage cells and the staining of the cartilage tissue. Two observers graded the harvested joints. The mean of each score was used for evaluation. A score of zero represents undamaged cartilage; a score of thirteen indicates severely damaged cartilage. A total of 83 facet joints of vertebrae inside and outside the implanted region as well as all instrumented vertebrae were harvested.

The harvested joints were divided into three categories: the (by screws) instrumented joints, the (un-instrumented) complementary joints inside the instrumented area and the joints outside the instrumented (control). Finally, the obtained scores were ranked using three final grades: mild, moderate, and severe damage. Legend of the Mankin grades is presented in Table 8.2.

Tissue surrounding the implant

The tissue surrounding the implant is harvested at locations adjacent to pedicle screws, bridges, and bearings. As the porcine spine had already been fixated with Formaldehyde 4%, the tissue was embedded in paraffin and cut into coupes (5 μm) afterwards. These coupes were stained with Toluidine Blue (1%) and Haematoxylin & Eosin (H&E) showing the cellular reaction of the surrounding tissue.

8.4. RESULTS

All twelve pigs that underwent the surgical procedure survived the implantation period. The implants that were placed in the first two pigs showed a remaining growth potential that was considerable after eight weeks. To get a better overall result concerning the progression in length the next two pigs (Pig 3 and pig 4) were euthanised after a total of 12 weeks. In pig 1, preoperative measurement was taken of initial axial rotation, by means of metal pins that were attached to the pedicle screws before and after application of torque. The measurement showed axial rotation of 2° for the thoracic (cranial) part and 1° for the lumbar (caudal) part.

8.4.a. Induced deformity

Measurements showed spine deformations corresponding with the intended direction (Figure 8.5b). Each torsion implant (**XS TOR**) induced torsion between T12 and T15 and between T15 and L2. Torsion induced by the **XS TOR** range from 3° to 15° . Torsion in the upper (cranial) section of the instrumented area was always higher, because more vertebrae were involved. The mean cranial torsion angle is 11.9° and the mean caudal torsion angle is 7.1° . Mean thoracic torsion is 5.8° per motion segment (vertebra and

intervertebral disc) and the mean lumbar torsion is 3.6° per motion segment. The maximum torsion was observed in pig 9 (15° cranial and 11° caudal).

The mean Cobb-angle in the porcine spine induced by the **XS L_{AT}** was 18.6° . Analysing the results showed that the narrow **XS L_{AT}** created a maximum Cobb-angle of 22° and a minimum Cobb-angle of 19° . The results concerning the wide version of the **XS L_{AT}** show a maximum Cobb-angle of 18° and a minimum of 14° . The lateral deformity progressed during the 8 weeks implantation period (Figure 8.5a). In all lateral implants, the largest relative deformation was seen in the region adjacent to the middle instrumented vertebra. In this area, slight wedging of the vertebrae was observed. Relative deformation of the segments increased with the increase of the bending moment. Spines, implanted with the **XS L_{AT}** showed no significant torsion. Mean cranial torsion was 1.1° and mean caudal torsion was -0.8° .

Spines implanted with the **XS T_{OR}** showed a mean Cobb-angle of 2.8° and a maximum Cobb-angle of 6° . Deformation was highest in the areas adjacent to the middle instrumented vertebrae (T15-T15-L1). Average kyphosis angle was bigger in the spines instrumented with a **XS T_{OR}**. After eight weeks, the mean kyphosis angle for the torsion implant was 7.8° . Mean kyphosis and for the lateral bending implant was 6.4° .

Pig 3, instrumented with a wide **XS L_{AT}** and pig 4 instrumented with a wide **XS T_{OR}**, carried the implant for 12 weeks. After 12 weeks, the Cobb-angle in the porcine spine of pig 3 was 18° (Figure 8.5a). The torsion induced in pig 4 was 13° for the cranial part and 10° for the caudal part. Kyphosis angle in pig 3 was 8° and 14° in pig 4.

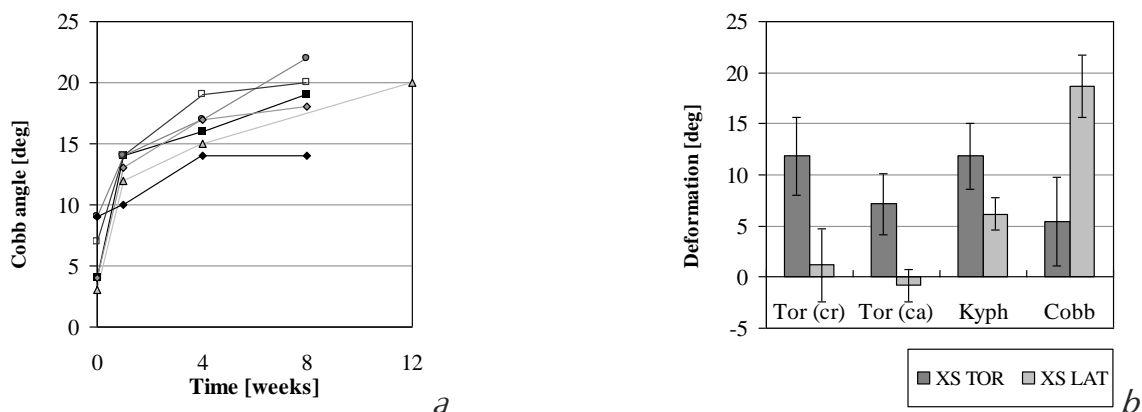


Figure 8.5: Cobb-angle progression

(a) The pigs instrumented with **XS L_{AT}** all show progression of lateral deformity during 8 weeks. Lateral deformity was determined by Cobb-angle. Pig 3, which carried the implant for 12 weeks, showed a Cobb-angle of 18° after termination. (b) The **XS T_{OR}** shows significant torsion of the vertebrae (both in the cranial Tor (cr) and caudal Tor (ca) part) while the **XS L_{AT}** shows a significant Cobb-angle. Average kyphosis angle is higher for the torsion system.

Minor wedging of vertebrae was observed in all pigs that were instrumented with the **XS LAT**, which was best visible in the middle instrumented vertebrae. Furthermore, five of the twelve pigs showed (minor) spinous process deformation. Two of which had been instrumented with a torsion implant (**XS TOR**) and the other three had been instrumented with a lateral bending implant (**XS LAT**).

8.4.b. Amount of growth

All implants showed progression in length, with a minimum of 14% and a maximum of 22% increase in length in 8 weeks (Figure 8.6a). An even bigger progression is observed in the 12-week implantation period of pig 3 and pig 4, with a maximum of 25%. Mean length progression in 8 weeks was 19.5% and mean length progression in 12 weeks was 24.4%. The post-terminal x-ray of pig number 3 and 4 showed that the implants had not reached their final length yet. Figure 8.6b shows the increase in Cobb angle *vs.* length growth.

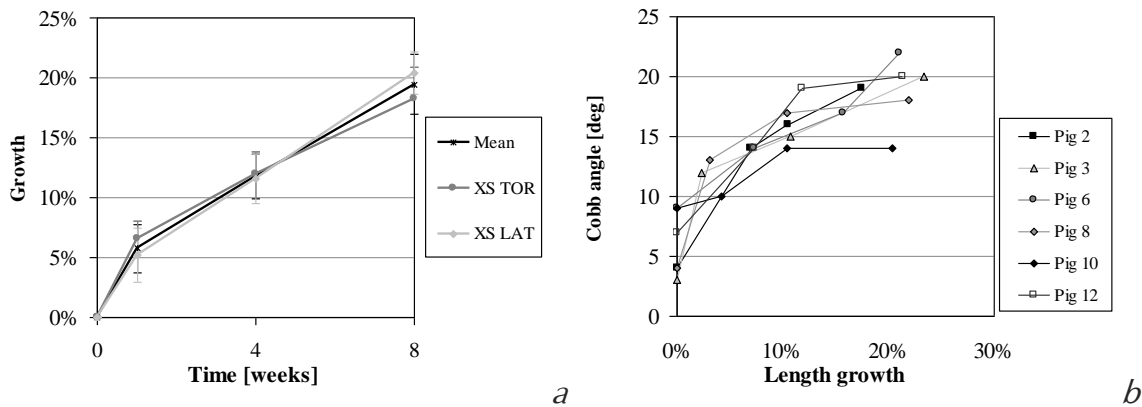


Figure 8.6: Growth and final deformation

(a) Both the **XS TOR** and **XS LAT** were able to adapt to growth. Length growth speed reduced, as would be expected from normal growth curves of porcine models.¹⁹ No significant difference between the systems can be observed. (b) Cobb-angles increased with length growth during the implantation period of 8 weeks.

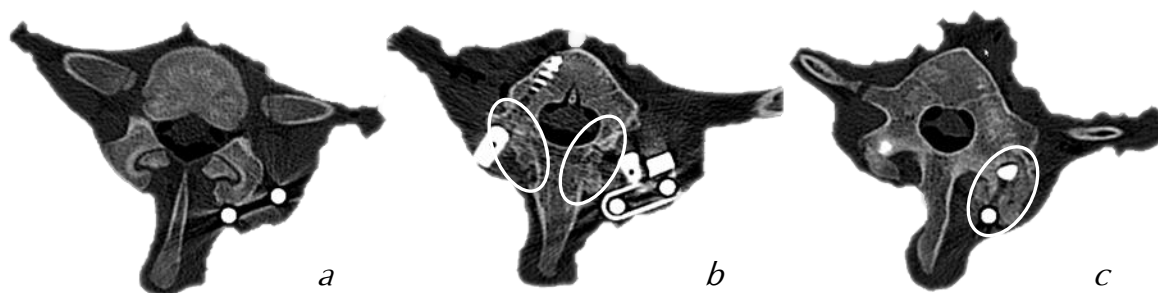


Figure 8.7: Ossification of vertebrae

CT scans showed ossification at vertebrae instrumented with pedicle screws (b, c). The vertebrae between the pedicle screw fixations showed much less ossification (a). Though some spines showed ossification surrounding the implants at various levels, vertebral fusion was not observed.

8.4.c. Ossification

The CT scans showed much scattered radiation caused by the instrumentation (implant/screws/bridges), interfering with bone visualization. Ossification was observed in small amounts in tissue surrounding the pedicle screws and at places where the implant was in contact with bone tissue (Figure 8.7). In addition, during harvesting of the samples for microscopic research and removal of the implant, ossification was seen in some additional posterior parts of the spines in pig 1, pig 4, and pig 5. In pig 1 and pig 4, the lateral implants (**XS LAT**) showed ossification over the middle part of the implant. The torsion implant (**XS TOR**) in pig 5 showed ossifications over the end of the U-loops.

8.4.d. Status of the implant

Though all bearings endured friction because of the sliding movements during daily motion and growth, most of the implants were in good condition and showed only some minor scratches. With the exception of scratches near failing bushings, these scratches had most likely occurred during implantation. Signs of wear were only visible in cases of bearing failure. Although none of the torsion implants failed, two **XS TOR** implants showed bearing damage: one bushing deformation (Figure 8.8b) and one bearing malfunctioned by a displacement of a bushing (in pig 1 and pig 4). Furthermore, none of the lateral bending implants failed. Only in one **XS LAT**, a bearing malfunctioned due to a detachment of a PEEK bushing (Figure 8.8c) and one welded ring was detached from the end of the loop. These failures however did not show a decrease in functionality.

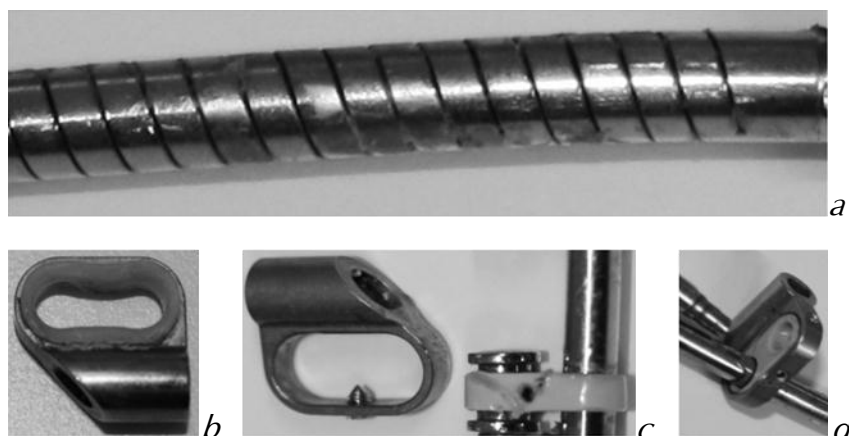


Figure 8.8: Failed implant parts

(a) One torsion spring showed plastic deformation. (b) Two bearings showed deformed or shifted PE bushings. (c) In one centre fixation of a lateral system, the PEEK bushing was de-attached from the bearing house. (d) One end ring of a lateral implant was de-attached due to a welding failure.

One **XS TOR**, which was fixated for a period of twelve weeks, showed a plastic deformation in one spring (Figure 8.8a), the only plastic deformation seen in all implant. All the other implants have proven their elastic capacities by returning to their original shape. A complete overview is given in Table 8.3.

Analysis of the condition of the implant and the final progression in length in the torsion implant in pig 4 did not show inhibition in growth progression because of the failing bearing (length progression of 25 %). Analysing the status of the implant and the final induced Cobb-angle in the **XS LAT** of pig 2 and pig 12 also did not show inhibition of growth which might have resulted from the failing centre bearing or damaged welding in the middle of the lateral implant (Cobb-angle of 19° and 20°). The torsion implant of pig 2, which had the least progression in length, showed some minor wear scratches and one deformed bearing.

Pig	PE/PEEK bearings	Metal parts	Plastic deformation	Implant failure
Pig 1	One bearing deformed	Minor wear scratches	None	No
Pig 2	Bearing at apex failed	No visible damage	None	No
Pig 3	Intact	Minor wear scratches	None	No
Pig 4	One bearing failed	Wear scratches	1 Bent spring	No
Pig 5	Intact	No visible damage	None	No
Pig 6	Intact	No visible damage	None	No
Pig 7	Intact	No visible damage	None	No
Pig 8	Intact	No visible damage	None	No
Pig 9	Intact	No visible damage	None	No
Pig 10	Intact	No visible damage	None	No
Pig 11	Intact	No visible damage	None	No
Pig 12	Intact	Damage at detachment of locking ring	None	No

Table 8.3: Status of implants after explantation

Examination of the bearings and other parts after explantation showed damage to the implant systems was low. Although some damage was seen, none of the implants failed.

8.4.e. Facet joints

The mean scores of each category (with standard deviations) are presented Figure 8.9. Three facet joints of pig 1 and pig 2 served as control. The L3 joints of pig 2 (L3-R and L3-L) and the right side T11 joint of pig 1 (T11-R), which lie outside the area of implantation, were graded with a mean score of 1.83. From 61 joints adjacent to pedicle screws, three joints adjacent to pedicle screws showed mechanical destruction, one joint showed bone atrophy and only one facet joint showed total fusion of the joint. The facet joints inside the area between the instrumented vertebrae show higher scores than the control group, and are comparable with scores of the joints adjacent to the instrumented vertebrae. Furthermore, no difference in scores between the two implant systems was observed.

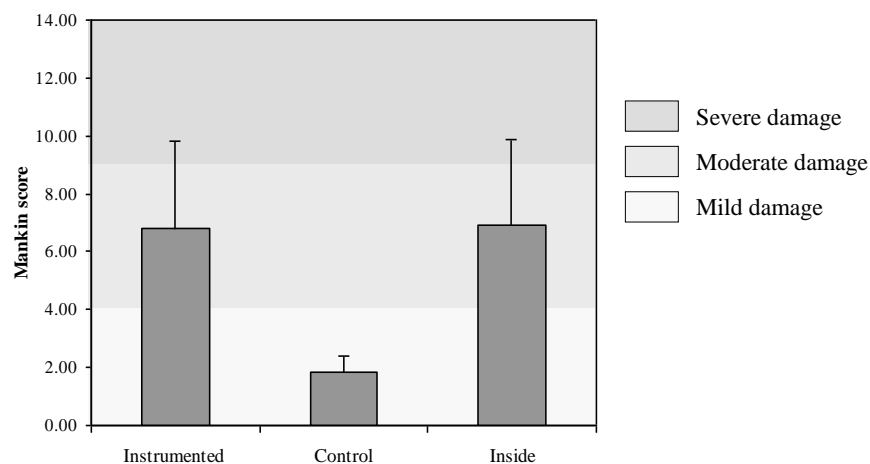


Figure 8.9: Mankin scores of the joints

The Mankin scores of the instrumented and remaining joints inside the instrumented area show comparable values for the mean and for the standard deviation. The three facet joints that were used for control show a lower mean score. The damage of these joints is classified as 'moderate'. Damage of the joints of the control group is classified as 'mild'.

8.4.f. Overall tissue response

The surrounding tissues gave a healthy overall tissue response towards the implants although the amount of macrophages, scar tissue, muscle tissue, and the formation of blood vessels showed a clear response. Polyethylene particles were observed adjacent to the bearings, most likely due to wear. The surrounding tissue showed dark spots, which could be caused by Ti alloy particles or by damaged red blood cells (Figure 8.10). The tissue surrounding the pedicle screws and the bearings showed most of the dark particles, probably because of the wear of sliding parts and because the amount of material is concentrated at the bearings (screws, bridges, implant, bearing). By analysing this tissue, using a TEM (Transmission Electron Microscope) the dark particles appeared to be phagocytised, thereby inactivating the debris/particles.

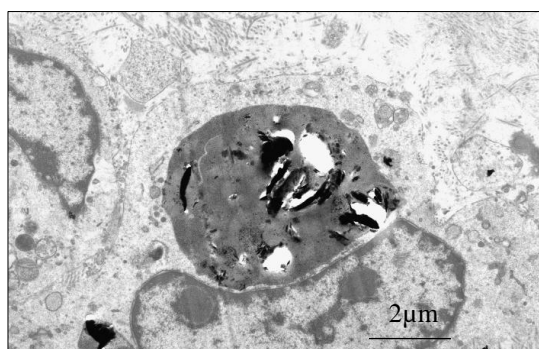


Figure 8.10: Tissue response

Tissue surrounding the implants showed dark coloration. Particles were phagocytised.

8.5. DISCUSSION

Ossification

In all pigs, bone formation in tissue surrounding the pedicle screw fixations was observed. This bone formation is very likely caused by damaging the periosteum during insertion of the screws and placement of the transverse bridges. Although excessive bone formation should be avoided because of the increased risk of spinal fusion, this minor bone formation can be interpreted as acceptable and perhaps preferable because it will consolidate the fixation. In some pigs minor bone formation in tissue surrounding the implant was found at other locations. Periosteum damage caused by implants rubbing against the spinous processes, lamina, and facet joints during daily movements could have triggered the bone formation in those areas. It should be noted that osteoinductive response in spine surgery in lower animal models, such as dogs, sheep, and goats is commonly higher than in humans. Merely surgical exposure of the spine and periosteal stripping will generally result in facet joint and interlaminar (posterior) fusion. In fact, despite decortication and addition of bone graft, posterior spine segments often fail to fuse. Therefore, this experiment can be considered as a worst case regarding osteoinduction.

Facet joints

The pedicles of vertebrae T12, T15, and L2 were instrumented with pedicle screw increasing the risk of adjacent facet joint damage. Although 'moderate' damage was observed in these joints, insertion of the screws itself seems not to damage the joints since the joints adjacent to the un-instrumented vertebrae inside the implanted area are damaged to the same extent.

Despite the fact that all joints in the implanted area showed damage to the cartilage layer, only one of all examined joints showed complete fusion. Both implants are highly flexible compared to current fusion systems. The flexibility of the **XS LAT** and the **XS TOR** are comparable with motion preserving implants that are capable of avoiding vertebral fusion. Therefore, our results indicate that fusion of the joints can be avoided in long-term implantation. Since we can consider the implantation in the porcine model as a worst case, these results are very promising towards long-term non-fusion in human adolescents.

Mankin grading

The Mankin grading was used for determination of cartilage damage of the facet joints. Three joints of the vertebral levels outside the instrumented area were used as a control. However, a mean control score of 1.83 is interpreted as 'mild damage'. This may be explained by the fact that in fast growing pigs, the cartilage of the facet joints is under a constant renewal, resulting in surface irregularities, hyper-cellularity and different cartilage composition. Theoretically, these joints could have been damaged during surgery and/or during the implantation period. However, it is highly unlikely that these

were damaged during surgery because the tissue surrounding the joints was not removed. Damage of the joints during the implantation period is possible; however, this would be caused by excessive loading of the vertebrae. Excessive loading of adjacent vertebrae is not likely because of the flexibility of the implant systems allows for a large range of motion in the instrumented area. To rule out this possibility, the control scores should be compared with scores of joints harvested from healthy (un-instrumented) young porcine spines.

Despite the fact that the Mankin grading system is widely used in research regarding osteoarthritis, the inter- en intra-observer reliability of this rather subjective method has been questioned.²⁰ Our study confirms this. In fact, the articular cartilage of the harvested facet joints, which was examined by two observers, showed a considerable inter-observer variability.

Induced deformity

The **XS TOR** induced torsion ranging from 3° to 15° between the anchored vertebrae. The neutral zone (NZ), as determined by Busscher *et al.* for thoracic porcine spine (T11-T14) is 0.8° and for the lumbar spine (T14-L2) 0.5° in left or right torsion.¹⁶ Range of motion (ROM) for same segments (achieved by a 2Nm torque) is about 2.2° and 1.3°, respectively. These NZ and ROM reflect only one-half of the totals because torsion in one direction is considered. Mean induced thoracic torsion in the **XS TOR** is 11.9°, the mean lumbar torsion is 7.1°, which is far beyond the neutral zone, and ROM. Fig 1 was measured on initial axial rotation by means of metal pins that were attached to the pedicle screws before and after application of torque. Axial rotations of the vertebrae were about 1° for the thoracic (cranial) part and 1° for the lumbar (caudal) part, which suggests that, like the Cobb-angle in lateral bending, the axial rotation increased during the implantation period.

For the instrumented area in our experiment, the mean NZ in a one-side lateral bending is 2.5° for the low thoracic and 1.1° for the lumbar region in pigs.¹⁶ One-side ROM in lateral bending (bending moment of 2Nm) is 5.6° and 2.5°, which adds up to 8.1°. Measured (mean) induced Cobb-angle using the **XS LAT** is 15.8°. The induced deformity is almost twice the total ROM of the instrumented area. Observed relative deformation of the segments however was not equal but increased correspondently with the increase of the bending moment (characteristic for a three-point-bending mechanism). In all lateral implants, largest relative deformation was seen in the region adjacent to the middle instrumented vertebra. Together with the observation of slightly wedged vertebrae, it seems reasonable to conclude that structural changes in the spine occurred.

Kyphosis angle

In this study, after the implantation period of 8 weeks, a mean kyphosis angle (measured between the endplates of T12 and L2) of 7.8° was found for the **XS TOR** and 6.4° for the **XS LAT**. Comparing these results with another study with a porcine spine model, in

which a mean thoracic (T1-T15) kyphosis of 15.6° and a lumbar (L1-L5) lordosis of 7.9° was found,¹⁵ shows that the measured kyphosis angle is small. However, we measured the angles in a smaller spine fragment of six vertebrae. In addition, in our study the determined kyphosis angle is measured in an area of transition between lumbar lordosis and thoracic kyphosis, hence a major kyphosis would not be expected.

A small kyphosis angle ranging between 6° and 8° may be interpreted as normal. Although range of distribution of kyphosis angle was considerable, the mean kyphosis angle appeared constant between 1 and 8/12 weeks after surgery. Interestingly, the largest change in kyphosis angle occurred within the first week after surgery. Possible explanation could be that (axial) friction in the bearings in some way inhibited the extension, a result of the prone position during taking of the radiographs, of the porcine spine. Besides that, it appeared that kyphosis is not influenced by the deformation angle (lateral bending or torsion) itself.

Growth and progression

The progression in length of all twelve pigs shows a similar pattern. The length progression with a mean of 19.5 % and standard deviation of 2.5 % shows that all pigs except one (pig 1; 14 %) are in between two standard deviations of one another. The difference in growth may be caused by the fact that the progression of the individual growth spurts pigs is not similar in pigs during a research period of 8 to 12 weeks. Growth inhibition caused by the implant seems to have occurred since the sliding bushing were still intact after explantation and secondary curves, which usually result from mechanical growth obstruction, did not develop.

Cobb-angle of spines implanted with **XS LAT** progressed but progression diminished during growth. Undoubtedly, short-term (minutes to hours) and intermediate-term (several days) viscoelastic effects, which provide for the main contribution of shape change, have faded after 1 week. This suggests that a long-term visco-elastic response is present.

One cause for long-term progression response would be the increased relative flexibility of the spine because of growth of the spine. The implant was designed to generate a fairly constant bending moment, which could have induced sustained progression.

From the radiographs, it was impossible to determine the torsion angle. CT scan analysis provided the only valid measurement, but was only carried out post-terminally. Therefore, progression in torsion could not be determined, only the final status was determined.

Wide versus narrow implants

Cobb-angle measurements from the radiographs showed that the narrow **XS LAT** implants created larger deformities than the wide lateral implants. Torsion measured from CT scans showed that torsion created by the wide **XS TOR** implants was higher than created

by the narrow torsion implants. Although these differences are not significant, it seems that the sizes of the implants may have an influence on the size of the deformation. Generated moments may be different for different sizes. *In vitro* measurements relating to the lateral implants did not show difference in bending moment. Therefore, an explanation for the observed difference in lateral bending has not been found. *In vitro* measurements of torque delivery by the **XS TOR** showed higher torque for the wide system, which could be a valid explanation of the difference in torsion angles.

One aspect from a clinical perspective is that an implant should be as small as possible. Although surgery performed by using blunt dissection, keeps damage of the surrounding tissue low, application of small implant is preferable. A reliable implant that generates enough bending moment or torque requires certain minimal geometrical dimensions. Optimal implant dimensions should be determined in future research.

Motivation for the porcine model

The results of this study show the ability of the **XS LATOR** non-fusion system to induce a deformation similar to scoliosis in a porcine model. The system is also capable of adapting to spinal growth of a pig in a period of 12 weeks, and of avoiding spinal fusion. Due to differences between human and porcine spines in geometry and loading, formulation of statements about scoliosis correction in human adolescents is challenging. Humans are bipedal and thus walk in an upright position whereas all available animal models, including the pigs, walk on four feet. The result is an entirely different loading of the spine. Therefore, results in an animal model may not be generalised to humans *per se*. Nevertheless, Busscher *et al.* stated that the porcine spine is a valid model for the human spine in research.¹⁶

The pigs used in this experiment experienced a growth spurt, which can be interpreted as a resemblance to the growth spurt observed in human adolescents. By merely testing this newly designed non-fusion implant on its ability to adapt to growth and on the possibility to avoid fusion during a rapid growth phase, the use of the scoliosis induction strategy in a young porcine model is more acceptable. Although there has been some research on scoliosis induction and correction in goats, idiopathic scoliosis does not exist in animal models.²¹ Therefore, the approach of inducing a scoliosis in an animal model seems the only available option to test the new implant and correction strategies at this point.

General

Scoliosis surgery is generally performed once the lateral curvature has progressed to a 45° Cobb-angle. In this experiment, maximal induced lateral deformity is 22° (Cobb-angle), suggesting the **XS LATOR** will not be able to correct such a scoliosis of 45°. However, our expandable non-fusion system can be implanted in a growing spine when deformity is still small, because flexibility of the spine is preserved and spinal growth is allowed

limiting the impact on spine functionality. The scoliotic deformity to be corrected will be smaller and hence the chance for complete correction will be higher.

In this experiment, two different aspects of the non-fusion scoliosis correction system were tested. Six pigs received a lateral implant and six pigs received a torsion implant. Although there is a small indication for coupled motions, the two different implants are able to generate deformity mainly in their intended direction. To generate a 3D shape change such as in scoliosis correction, in which axial rotation is combined with a lateral bending, the implants must preferably be combined in one patient. Further experiments must reveal whether combining the systems will accumulate or perhaps obstruct their individual effect.

Using a Finite Element (FE) model of an adolescent human spine, Meijer compared scoliosis induction with scoliosis correction.²² It was found that when a torque is applied to a normal spine in a similar fashion as in our **XS TOR**, a very small coupled lateral deformation (Cobb-angle) was generated. When opposite torque was applied in a scoliotic spine, lateral shape change (correction) was higher, in fact four times. Despite the fact that the amount of correction in torsion by the **XS TOR** in a scoliotic spine was comparable to the amount of induced torsion in a healthy spine, the induced Cobb-angle was 62% of the induced torsion. These findings emphasise the presence of coupled motions between torsion and bending, which is often observed during spinal movements.²³⁻²⁵ However, the model did not demonstrate significant coupling of motions between lateral bending and sagittal bending (flexion/extension) and between torsion and sagittal bending.

These results suggest that when we look at the amount of scoliosis induced by the non-fusion system (**XS LATOR**) in the porcine model, a good result may be expected in correction of an idiopathic scoliosis in human adolescents. In addition, implantation of a single torsion system (the **XS TOR**) may still be enough to correct a scoliosis.

8.6. CONCLUSION

Although on microscopic scale cartilage damage was seen in facet joints of the instrumented vertebrae, fusion of the joints was not observed. By limiting ossification and facet joint damage, fusion of spine was prevented, at least in our research period of 12 weeks. The tissue surrounding the implant showed a healthy response toward the implant. This study indicates that avoidance of spinal fusion is possible with minimal invasive techniques. Bone growth can be limited by preserving periosteum. The system does not inhibit spinal growth during the 8/12 weeks research period. The study also indicates that it is possible with our non-fusion system, the **XS LATOR**, to correct a lateral curve with the lateral system (**XS LAT**) and an axially rotated spine with the torsion system (**XS TOR**). The **XS LATOR** is capable of inducing significant deformities in two different directions. Although inducing axial rotation appears to cause an associated lateral

deviation, the system parts mainly effect the intended directions. The results suggest that this complementary functioning can have advantages over the single action implants, in which surgery mainly focuses on lateral and sagittal deformity.

8.7. ACKNOWLEDGEMENTS

The authors would like to acknowledge the assistance of prof. dr. G. Rakhorst from the Department of Biomedical Engineering and the surgical staff from the Central Animal Facility, UMC Groningen, The Netherlands.

8.8. REFERENCES

1. Veldhuizen, A.G., Wever, D.J. & Webb, P.J. The aetiology of idiopathic scoliosis: biomechanical and neuromuscular factors. *European spine journal* **9**, 178-184 (2000).
2. Freidel, K., *et al.* Quality of life in women with idiopathic scoliosis. *Spine* **27**, E87-91 (2002).
3. Freidel, K., *et al.* Idiopathic scoliosis and quality of life. *Studies in Health Technology and Informatics* **88**, 24-29 (2002).
4. Theologis, T.N., Jefferson, R.J., Simpson, A.H., Turner-Smith, A.R. & Fairbank, J.C. Quantifying the cosmetic defect of adolescent idiopathic scoliosis. *Spine* **18**, 909-912 (1993).
5. Nachemson, A. Adult scoliosis and back pain. *Spine* **4**, 513-517 (1979).
6. Li, M., *et al.* Surgical treatment of adult idiopathic scoliosis: long-term clinical radiographic outcomes. *Orthopedics* **34**, 180-20110124-20110114 (2011).
7. Harrington, P.R. Treatment of scoliosis: correction and internal fixation by spine instrumentation. June 1962. *J bone Joint Surg Am* **84-A**, 316 (2002).
8. Kadoury, S., *et al.* A three-dimensional retrospective analysis of the evolution of spinal instrumentation for the correction of adolescent idiopathic scoliosis. *European spine journal* **18**, 23-37 (2009).
9. Wever, D.J., Elstrodt, J.A., Veldhuizen, A.G. & v Horn, J.R. Scoliosis correction with shape-memory metal: results of an experimental study. *Eur Spine J* **11**, 100-106 (2002).
10. Wang, Y., *et al.* Temporary use of shape memory spinal rod in the treatment of scoliosis. *Eur Spine J* **20**, 118-122 (2011).

11. Tao, F., *et al.* The effect of differing spinal fusion instrumentation on the occurrence of postoperative crankshaft phenomenon in adolescent idiopathic scoliosis. *Journal of Spinal Disorders & Techniques* **23**, e75-80 (2010).
12. Sponseller, P.D. Bracing for adolescent idiopathic scoliosis in practice today. *Journal of pediatric orthopedics* **31**, S53-60 (2011).
13. Grivas, T.B. & Kaspiris, A. The classical and a modified boston brace: description and results. *Physiotherapy theory and practice* **27**, 47-53 (2011).
14. Zaborowska-Sapeta, K., Kowalski, I.M., Kotwicki, T., Protasiewicz-Faldowska, H. & Kiebzak, W. Effectiveness of Cheneau brace treatment for idiopathic scoliosis: prospective study in 79 patients followed to skeletal maturity. *Scoliosis* **6**, 2 (2011).
15. Busscher, I., Ploegmakers, J., Verkerke, G. & Veldhuizen, A. Comparative anatomical dimensions of the complete human and porcine spine. *European Spine Journal* **19**, 1104-1114 (2010).
16. Busscher, I., *et al.* *In vitro* biomechanical characteristics of the spine: a comparison between human and porcine spinal segments. *Spine* **35**, E35-42 (2010).
17. Shebab, D., Elgazzar, A. & Collier, B. Heterotopic ossification. *J Nucl Med.* **43**, 346-353. (2002).
18. Mankin, H.J. & Lippiello, L. Biochemical and metabolic abnormalities in articular cartilage from osteo-arthritic human hips. *The Journal of bone and joint surgery.American volume* **52**, 424-434 (1970).
19. Robison, O.W. Growth patterns in swine. *Journal of Animal Science* **42**, 1024-1035 (1976).
20. van der Sluijs, J.A., *et al.* The reliability of the Mankin score for osteoarthritis. *J Orthop Res* **10**, 58-61 (1992).
21. Braun, J.T., *et al.* Three-dimensional analysis of 2 fusionless scoliosis treatments: a flexible ligament tether versus a rigid-shape memory alloy staple. *Spine* **31**, 262-268 (2006).
22. Meijer, G.J.M. Development of a non-fusion scoliosis correction device - numerical modelling of scoliosis correction. PhD-thesis, University of Twente, Enschede. (2011).
23. Sizer, P.S., Brismée, J.-M. & Cook, C. Coupling behavior of the thoracic spine: a systematic review of the literature. *Journal of manipulative and physiological therapeutics* **30**, 390-399 (2007).

24. Stokes, I.A. Axial rotation component of thoracic scoliosis. *J Orthop Res* **7**, 702-708 (1989).
25. Stokes, I.A.F. & Gardner-Morse, M. Analysis of the interaction between vertebral lateral deviation and axial rotation in scoliosis. *J Biomech* **24**, 753-759 (1991).

Chapter 9



GENERAL DISCUSSION

CONTENTS

- CHAPTER 9. GENERAL DISCUSSION 183**
- 9.1. INTRODUCTION..... 183
- 9.2. FEEDBACK TO THE REQUIREMENTS..... 184
 - 9.2.a. *Architecture*..... 184
 - 9.2.b. *In vitro experiments*..... 186
 - 9.2.c. *In vivo experiments* 187
- 9.3. FAILURE MODE EFFECT ANALYSIS (FMEA)..... 193
 - 9.3.a. *Possible failures and their effects*..... 194
 - 9.3.b. *Necessary improvements* 195
- 9.4. RECOMMENDATIONS 198
 - 9.4.a. *Preservation of bone structures* 198
 - 9.4.b. *Improvements on the design*..... 198
 - 9.4.c. *Topics for future research* 199
- 9.5. CONCLUSIONS 201
- 9.6. REFERENCES..... 202

CHAPTER 9. GENERAL DISCUSSION

9.1. INTRODUCTION

In the previous chapters, the design of a novel non-fusion correction system (**XS LATOR**), comprising two separate implants thus splitting up functions for scoliosis correction, was presented and tested *in vitro* and *in vivo*. One implant (**XS TOR**) was designed to correct the axial rotation of the vertebrae and the other implant (**XS LAT**) to correct the lateral curvature. The **XS TOR** is a torsion-generating element that applies mainly a torque on the spine to generate torsion. The **XS LAT** is a lateral bending implant that mainly applies a bending moment to generate lateral bending. The imposed corrective forces and torque on the spine are small, but remain present within a large range of motion (ROM). Unlike current fusion systems, the system is highly flexible thus avoiding fusion of the vertebrae. The flexibility of the system is not only provided by the method of fixation, but also by the material and geometry. In addition, sliding bearings facilitate daily motion and growth adaptation.

The implants can be used together in such a way that an optimal configuration for each patient can be implemented. To facilitate the implantation of the total system, various instruments, such as the **iXS BEN**, the **iXS ANG** and the **iXS SET** have been designed and manufactured. For implantation in adolescents, a new anchor has been designed (**XS FIX**). This anchoring system can be placed in the high and mid thoracic spine (T1 to T9) to avoid facet joint damage.

Plain bearings facilitate axial motion of the anchors of the **XS LATOR**. The associated variation in implant length is supplied by U-loops. In fact, the **XS LATOR** is able to extend 85% in length (minimal to maximal length). This high range was created to cover three aspects. First, spinal growth of 35% is facilitated. Second, variations in lengths of the human spines (between -20% and +20% for 95% of the patients)¹ is facilitated. Third, daily activities result in axial motion of the instrumented vertebrae, which is estimated between -10% and 18% of the original length. These axial motions are compensated as well.

In our approach to realise non-fusion scoliosis correction, we chose a surgical solution in which small correctional forces/moments are applied using an implant that allows spinal motion and growth. Performing non-fusion surgery to correct scoliosis by long-term implantation of an extremely flexible and extendable implant has not been applied yet clinically. Current surgical non-fusion strategies, such as stapling,² have different aims. Staples are used for steering the direction of growth. Other strategies, in which juvenile scoliosis is treated with the implementation of growing rods or ribs, are developed to only postpone fusion or to increase the volume of the thorax.^{3,4} In clinical

practice, overall (and permanent) avoidance of fusion is currently only targeted by performing vertebral wedge osteotomies,⁵ which evidently is a completely different approach than ours. Although non-fusion correction may be pursued using other surgical strategies such as use of an orthosis, the implantation of a highly flexible prosthesis, which applies correctional forces directly on the spine, seems more promising.

9.2. FEEDBACK TO THE REQUIREMENTS

After creation of a novel design and testing of its prototypes, it is essential to evaluate these results regarding functional performance and other features. The extent to which the requirements are fulfilled gives an indication of the quality of the design. Therefore, we will evaluate the design of the **XS LATOR** by comparing it to the requirements that were set up in Chapter 1. Table 9.1 shows an overview of essential requirements and the specifications achieved by the implant system.

9.2.a. Architecture

Due to the small corrective bending moments and torque, the implants could be kept small and the mass of the system low. The upper mass limit for the system was determined at 900 g. The total mass of the **XS LAT** is between 117 g and 152 g for the combined system, depending on the shared use of bridges and screws. The maximal mass of a separate implant is 79 g (73 g for **XS TOR** and 79 g for **XS LAT**).

The implant as a whole can be steam sterilised using an autoclave. All parts are corrosion-resistant and heat-resistant up to a temperature of 134°C; however, difficulties in long-term implantation may rise after the sterilisation of UHMWPE parts.⁶

The materials (Ti6Al4V, UHMWPE, NiTi, and PEEK), known for their biocompatibility, are resistant to pH levels between 6 and 8 and are widely used as implant materials.⁷⁻¹² The various parts of the **XS LATOR** can be super-finished to a maximal surface roughness (R_a) of 0.20 μm . The large implant parts can be mechanically polished even further to a mirror super-finish with a surface roughness of maximal 0.1 μm to prevent osseointegration. The screws can be implemented using a slightly higher surface roughness of *e.g.* 0.50 μm to stimulate adhesion of bone to the screws (osseointegration) to secure anchoring which is crucial for safe and proper functioning of the implant. However, a disadvantage is that osseointegration complicates removal of the implant.

<i>Constraint</i>	<i>Required</i>		<i>Obtained</i>		<i>Tested</i>
	Min	Max	Min	Max	
Growth (T1-L4)	x	85 mm	x	85 mm	Architecture
Implant length	20 mm	260 mm	141 mm	260 mm	Architecture
Fabrication costs	x	1000 Euro	900 Euro	1000 Euro	Architecture
Weight	x	900 g	117 g	152 g	Architecture
Axial translation posterior	-10%	18%	-10%	18%	Architecture
Life span	10 years	x	3 months	Unknown	<i>In vivo/vitro</i>
Lateral flexion stiffness	x	0.5 Nm/°	0.04 Nm/°	0.07 Nm/°	<i>In vitro</i>
Torsion stiffness	x	1.1 Nm/°	0.08 Nm/°	0.12 Nm/°	<i>In vitro</i>
Lateral correctional moment	0.6 Nm	4.0 Nm	3.0 Nm	3.5 Nm	<i>In vitro</i>
Axial torsion moment	0.6 Nm	4.0 Nm	2.5 Nm	3.0 Nm	<i>In vitro</i>
Surface roughness implant	x	0.5 µm	0.1 µm	0.2 µm	<i>In vitro</i>
Environmental temperature	0°C	134°C	0°C	134°C	<i>In vivo</i>
Generated temperature	35°C	45°C	35°C	40°C	<i>In vivo</i>
Blood loss	x	1000 ml	80 ml	120 ml	<i>In vivo</i>
Surgery time	x	4 hours	2.5 hours	3.5 hours	<i>In vivo</i>
Implant failure risk	x	1%	x	Unknown	<i>In vivo</i>
Risk of neurological injury	x	0.3%	x	0.3%	<i>In vivo</i>
Mortality risk	x	0.1%	x	0.1%	<i>In vivo</i>

Table 9.1: Implant specifications

This table shows an overview of essential requirements and the specification achieved by the implant system. Fulfilment of the requirements was assessed by the architecture, in vitro and in vivo experiments.

The prototypes of the implant, used in the *in vivo* and *in vitro* experiments, were manufactured in a small quantity. An estimate for the price of one torsion implant (**XS TOR**) is €1,500. For one lateral bending implant (**XS LAT**) a price of €1,000 was paid. Screws and bridges are included in these prices. So, a total of €2,500 is estimated for the total system. When placed at the same vertebral level, the implants will share bridges and screws, which results in a total price of about €2,000. The manufacturing cost of these prototypes was thus higher than the limit of €1,000 that was set for the

implants. For commercial quantities of the implants, the prices will obviously be lower. Since all materials and components of the **XS LATOR** can be manufactured using standard techniques such as milling, drilling, laser cutting, or spark erosion, it should be possible to produce the system for a price under €1,000. The selling price of fusion implants (price levels of 2004) ranges between \$3,500 and \$4,500.¹³ We assume that the costs of manufacturing is approximately 40% of the selling price, which results in manufacturing costs between \$1,400 and \$1,800 for current fusion implants. Consequently, for a large lot, the total cost will be lower than current (fusion) systems.

There is another aspect concerning the costs of surgery, which is hospitalisation time. Fusion surgery requires the patient to be inactive for a few weeks to let the spine recover and fuse, which will usually take place in the hospital. After non-fusion surgery, however, the patient needs to be active as soon as possible to help prevention of fusion. The minimal invasive surgery that is used in implantation of the **XS LATOR** allows shorter recovery time. The resulting limited hospitalisation time will significantly reduce the costs of the **XS LATOR** implantation compared to commercially available fusion systems.

9.2.b. *In vitro* experiments

The results in Chapter 6 show that the *in vitro* mechanical behaviour of the **XS LATOR** regarding moment delivery conforms to the requirements. The upper limit for bending moment/torque was determined at 3.5 Nm (lower limit: 0.6 Nm). The **XS LAT** generates a lateral bending moment between 3.0 Nm and 3.5 Nm, which varies with the length of the system. The **XS TOR** generates torsion (on the middle instrumented vertebrae) between 2.5 Nm and 3.0 Nm, which varies with the length of the system. After fixation of the system, the remaining bending moment and torque will be lower, depending on the amount of (instant) shape correction.

The high flexibility of the **XS LATOR** results in a very low contribution to the total bending stiffness (lateral and sagittal) and axial rotation stiffness of the spine. The total stiffness of the human spine (5 segments) is about 1.1 Nm/° in torsion and 0.4 Nm/° in bending.¹⁴⁻¹⁶ Torsion stiffness after instrumentation with the **XS LATOR** will increase only by approximately 9%. Total bending stiffness will increase with 17% in lateral flexion and with 4% in flexion-extension (Table 9.2). This high flexibility, essential in preservation of motion to avoid fusion, is realised by the geometry of the implants, the implementation of flexible materials and the use of plain bearings enabling sliding motions.

Fatigue behaviour of the elements in the **XS LATOR** that are strained during flexion of the spine becomes an issue in long-term implantation. Especially the long-term behaviour of the **XS LAT** concerning fatigue may be critical, since the pre- and alternating strains are highest in the NiTi rod.

	<i>Torsion</i>	<i>Lat flex</i>	<i>Flex/ext</i>
XS-TOR	6%	6%	2%
XS-LAT	3%	11%	4%
XS-LATOR	9%	17%	4%

Table 9.2: Mean relative stiffness in torsion and bending

Contribution of the implants to the total stiffness of the isolated spine is very low (see Chapter 6). The joint system will increase the stiffness with 9% in torsion, 17% in lateral bending, and only 4% in sagittal bending (flexion/extension).

Only limited data of *in vivo* vertebral motion is available. The actual spinal dynamics during daily activities have not been determined yet. Despite these limited data, estimations were made about the number of flexions that occur *in vivo* throughout the total period of implantation. Data by Morlock *et al.* who measured the number of ‘significant bends’ (flexion/extension) of nurses in one hour was used.¹⁷ Extrapolating the results, 98% of the population would bend about 100,000 times per year. In ten years, which is the lifetime of our system, a spinal implant should thus survive 1 million cycles. These findings correspond highly with the estimation of Hedman *et al.* who estimated 1.24 million significant bends in ten years.¹⁸ The standard test method for static, dynamic and wear assessment of extra-discal spinal motion preserving implants: ASTM F 2624–07, used the data of Hedman *et al.* and Morlock *et al.* as rationale for the test method.¹⁰

For the fatigue experiments performed in Chapter 7, we chose to determine the alternating strain limit for 1.5 million cycles to include a margin of safety. The **XS LATOR** appeared to survive only when the alternating strain was limited to 0.10%. The definition of ‘significant bends’ is arbitrary in the literature. Therefore, an accurate estimation of the survival chance of the **XS LATOR** cannot be made.

In Chapter 5, the **XS LFIX** was tested and proved a solid fixation. The forces and moments applied by the **XS LATOR** on the **XS FIX** are low and are within the boundaries tested (and required) for long-time fixation. This outcome indicates that the fixation will not be a limiting factor for long-time performance.

9.2.c. *In vivo* experiments

The **XS LAT** and the **XS TOR** were implanted using pedicle screw anchors. The **XS FIX** was not used because the porcine vertebrae do not have large transverse processes like human vertebrae do. Therefore, functional performance of the **XS FIX** could not be assessed. However, the performance of the **XS LATOR** in terms of correctional moment will be similar.

Despite the fact that correction of scoliosis is not similar to induction,¹⁹ the *in vivo* tests strongly suggest that the **XS LATOR** is capable of realising shape correction. During the *in vivo* experiments, the mean induced lateral deformation by the 'inverse' **XS LAT** was 18.6° (Cobb-angle). The generated bending moment and torque were high enough to generate a gradual and permanent shape change in soft tissue structures and to induce bone remodelling. Clinically, curve reduction to 5° Cobb-angle is considered full correction. Not taking into account the differences between the porcine and (adolescent) human spine and the difference between scoliosis correction and induction, the results suggests that a curve up to $18.6^\circ + 5^\circ = 23.6^\circ$ Cobb-angle can be corrected by the **XS LATOR** in three months. Full correction of the lateral deviation of a (human) scoliosis is thus not achieved at three months, since the patient group has a scoliotic curve between 15° and 45° Cobb-angle. Since all deformities start with a minor curve, full correction of scoliosis is possibly provided if it is detected and treated in an early stage. The 'inverse' **XS TOR** showed mean induced axial rotation of 10°, which is more than five times the (one-side) rotation, which can be instantaneously achieved by 2.0 Nm, and about two times the rotation achieved by 7.5 Nm.^{14,16} In the lumbar area the torsional stiffness of the human spine is comparable to that of the porcine spine. In torsion, the human thoracic spine is more flexible than the porcine thoracic spine.¹⁶ In a typical scoliotic curve, the axial rotation is about half the Cobb-angle.²⁰ Therefore, again ignoring the difference between scoliosis induction and correction, the results from the *in vivo* experiments suggest that full axial derotation in scoliosis can be achieved. A scoliosis of 15° to 45° Cobb-angle is typically accompanied with an axial rotation of 7.5° to 22.5°.²⁰ Mean induced axial rotation by the system is 9°, which suggests that a maximal axial rotation of $9 + 5 = 14^\circ$ can be corrected to an axial rotation of 5°. As in lateral bending, it is expected that axial rotation in starting cases of scoliotic deformities can be corrected by the implant. Again, early detection and surgery is essential for optimal (full) correction using the **XS LATOR**.

Unlike in our *in vivo* experiments, the post-surgical period of scoliosis correction in patients can last up to several years. Because the bending moment and torque are fairly constant during growth (and moderate shape change), correction is expected to persistently increase due to remodelling.

In the *in vivo* experiments, normal spinal growth was observed and segmental fusion did not occur. No ossification in facet joints and in intervertebral discs occurred. Since axial friction and thus extendibility of the system is equal for the scoliosis induction system and for the scoliosis correction system, we can conclude that the **XS LATOR** does not obstruct spinal growth and, thus, does not induce fusion for at least three months.

The plain bearing joints of the **XS TOR** and the **XS LAT** containing UHMWPE bushings, with friction coefficients of the sliding materials between 0.18 and 0.12,²¹ were tested *in vivo* and showed no significant wear since wear debris of UHMWPE bushings was not

found. However, at two locations at which bearings had failed, high concentrations of metal particles in the surrounding tissue were found and large scratches were visible on the U-loop of the implants. These scratches and wear particles were likely caused by metal-on-metal motion of the surface of the U-loop and the bearing house after a bushing failure.

Statements concerning the life span of the implants and their reliability in long-term performance are not easy to make. In the post-operative period of two and three months, the implants used in the *in vivo* experiment did not show functional failures; however, some implants showed a damaged bushing that would give problems in long-term implantation. Small improvements in the design, for example increase in bushing strength by either altered dimensions or geometry, will be needed to increase the long-term reliability. Additional (clinical) experiments must be performed to conclude whether the required ten years life span of the system can be realised.

Compared to current fusion implant systems, the highly flexible structure of the **XS LATOR** and its capability of adjusting to spinal motion/growth reduce stress peaks and therefore reduce the chance of implant failure. Furthermore, the lower stresses will reduce the risks regarding mortality and neurological injuries. Preservation of ROM is beneficial in prevention of spinal fusion in long-term implantation. Furthermore, preservation of bone and muscle structure integrity in long-term implantation following minimal invasive surgery may assist in avoidance of fusion on all vertebral levels. Non-fusion scoliosis correction by **XS LATOR** implantation will therefore result in preservation of full functionality.

In our project, we chose for a mechanical and surgical solution. Non-mechanical and/or non-surgical solutions to correct the scoliosis may also be possible, but were not the topic of this research. A surgical solution always implies tissue damage and introduces risks for the patient. However, minimal invasive surgical procedures will limit damage and risks. In addition, spinal fusion can be avoided.

To illustrate this, we observed a drastic reduction of heterotopic bone growth in the porcine model when we changed the surgical procedure for the final experiments. In a pilot experiment, the **XS LATOR** was implanted by performing a standard surgical (fusion) procedure that resulted in highly reactive bone and excessive bone growth (Figure 9.1). The minimal invasive procedure we used in our actual *in vivo* experiment limited the bone growth significantly. Despite this, some bone growth was observed in the porcine spine model. This heterotopic bone growth seemed to be activated by periosteal damage.

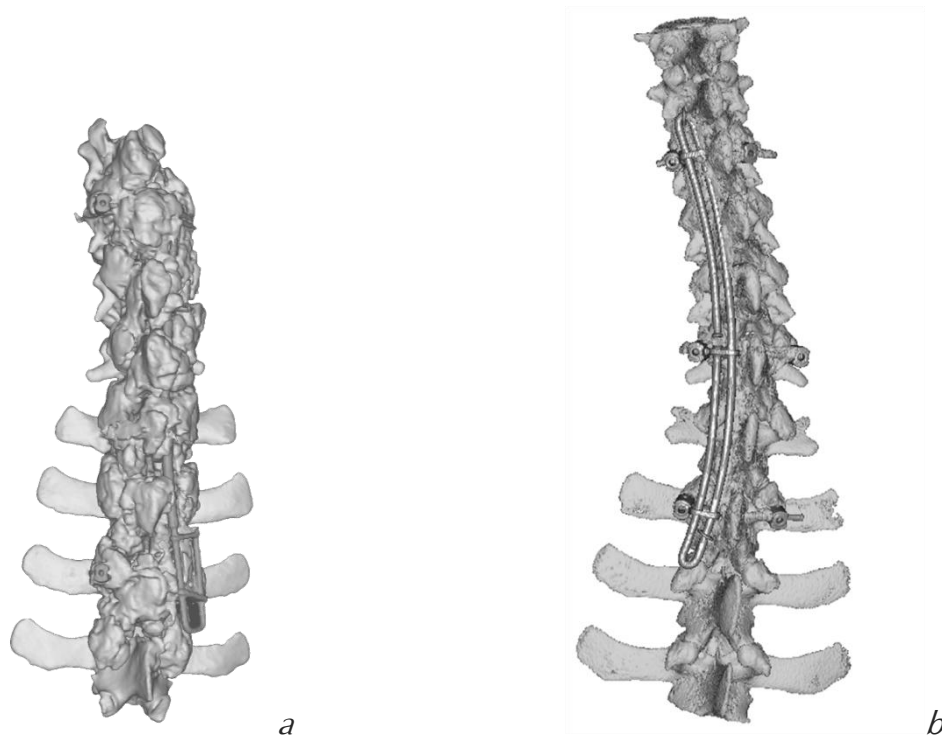


Figure 9.1: Ossification after surgery

(a) Large amount of ossification in a porcine model is observed after implantation of **XSTOR** using surgical procedures that are commonly used in fusion surgery. (b) Ossification observed after implantation of **XSLAT** using minimal invasive procedures is much less.

Domestic pigs and in particular young pigs such as used in our *in vivo* experiment are fast growing animals. Plexiform bone, a type of cortical bone adjacent to the periosteum,²² is found in large mammalian animals such as pigs. Humans generally do not show this type of bone formation, except occasionally in children during periods of rapid growth.²³ Therefore, bone formation after spine surgery in pigs can be expected to be more abundant than in (adolescent) humans. This is in agreement with Ferretti *et al.* who stated that osteoinduction in pigs more likely than in humans.²⁴ For our experiments, the pigs thus represented a worst-case scenario. The fact we did not observe major heterotopic bone growth in our pigs holds promise for application of our implants in humans.

Application of the lateral bending moment mainly achieved a lateral bending without creating significant torsion. Application of torque mainly created torsion but also created a small but significant lateral bending. These results suggest that correction of scoliosis can be controlled using two separate implants (**XSLAT** and **XSTOR**) each affecting only one mode of deformation. Additionally, separation of functionality can be beneficial for the location of force application. The separate implants can be anchored at different vertebral levels to further adapt the system to the patient's deformity, in order to

establish the optimal locations of lateral and rotational correction moment along the spine. In clinical practise, the necessity for instrumentation with both implants of the **XS LATOR** may be determined. Due to the coupled motions, it could be possible that the **XS TOR** creates enough correction of lateral deformity as well as the axial torsion. In that case, only the separate **XS TOR** is required for implantation.

Fulfilment of the requirements concerning the surgical aspects was assessed using the results of the *in vivo* experiments. Mean surgery time in the *in vivo* experiments was between 150 minutes and 180 minutes from first incision to wound closure. Including intubation *etc.*, surgery time was 30 minutes more. This is in conformity with the requirements. A maximal surgery time of 240 minutes (4 hours) was demanded, which is comparable with the duration of posterior spondylodesis surgery.²⁵ In our *in vivo* experiments, mean surgery time was shorter, which is likely achieved by the fact that the **XS LATOR** is much more flexible than current fusion systems as well as by the fact that fewer vertebrae need to be instrumented. In addition, the implants are stressed only *after* fixation, which simplifies instrumentation. The used surgical procedures for the **XS LATOR** were new to the surgeon and surgical staff; hence surgery time will become even less with experience.

Since the implant system does not use energy sources besides the initial mechanical energy of the pre-strained rod/springs, the temperature of the implants and the surrounding tissue will not rise above the limit of 45°C, although a minor temperature rise can occur due to energy dissipation in especially the NiTi rod during intense spinal motion.

The *in vivo* experiments showed that blood loss due to surgery is around 100 ml, which is far below the limit of 1000 ml. Following surgery, the pigs recovered fast and showed no signs of chronic pain or discomfort from the implant. The **XS LATOR** is thus not likely to generate chronic back-pain. Of course, from the *in vivo* experiments it is difficult to conclude whether a patient's life will be of superior quality post-operatively compared to pre-operatively. However, a small system that is not visible from outside the body and achieves shape correction while spinal flexibility is preserved and normal growth is allowed can be regarded as a major improvement over current fusion systems. This is to be considered a mental advantage for the patient.

We examined scoliosis induction since quadruped animals such as pigs generally do not develop idiopathic scoliosis. To investigate the difference between scoliosis correction and scoliosis induction and the effectiveness of the **XSTOR**, Meijer developed two (generic) Finite Element (FE) models of the adolescent (10-year-old) human trunk: a normal and a scoliotic spine (Figure 9.2).¹⁹ It was concluded that scoliosis induction in a healthy spine by application of a torque is different from scoliosis correction in a scoliotic spine. More specifically, the lateral motion coupled to axial torsion using the **XSTOR** is larger in correction than in induction. Additionally, Meijer found that, in an adolescent, the generated shape change in terms of a Cobb-angle is larger in correction than induction, given a specific applied force.

Obviously, the human spine is different from the porcine spine. Despite dissimilarities in shape and biomechanical properties, Wilke *et al.* and Busscher *et al.* concluded that the thoracolumbar porcine spine can be used as a representative model for investigation of spinal behaviour in humans.^{1,16} A young porcine spine experiences a growth spurt similar to an adolescent human spine. Since we implanted the 'inverse' **XSTOR** in a young porcine model, the results from our *in vivo* experiment (and Meijer) suggest that the **XSTOR** corrects torsion but also a significant part of the lateral bending and performs better in correction (of adolescent scoliosis) than in induction.

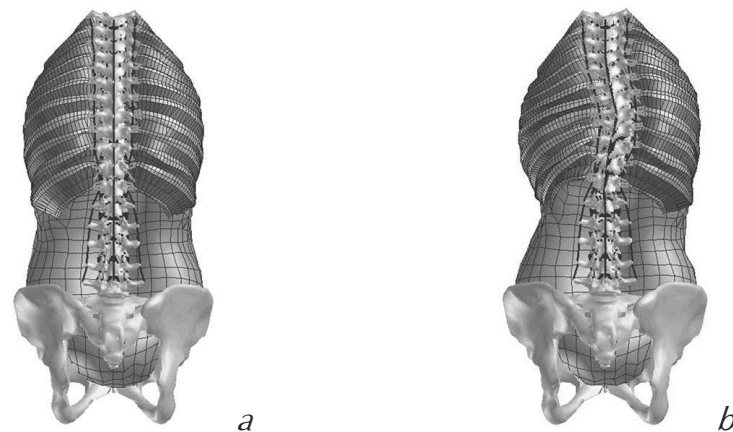


Figure 9.2: Modelling of scoliosis

A healthy (a) and a scoliotic (b) FE model created for studying the effect of an implant on the spinal shape. Pictures taken from: Meijer.¹⁹

<i>Severity (S)</i>		<i>Detection (D)</i>		<i>Occurrence (O)</i>	
1	No effect	1	Certain	1	None
2	Very minor; no action required	2	Almost certain	2	Unlikely
3	Medical attention recommended	3	High	3	Very low
4	Medical attention required	4	Moderately high	4	Low
5	Low priority surgery required	5	Moderate	5	Moderately low
6	Medium priority surgery required	6	Moderately low	6	Moderate
7	High priority surgery required	7	Low	7	Moderately high
8	Permanent loss of function	8	Very low	8	High
9	Permanent disability	9	Uncertain	9	Very high
10	Lethal injury	10	Undetectable	10	Inevitable

Table 9.3: Legend of FMEA grading

Descriptions of the scores on the scale of 0-10 for the three FMEA criteria.

In our *in vivo* study, we observed first signs of bone remodelling. After sacrificing the pigs, the vertebral bodies were found to be wedged and the spinous processes were found to be curved into the concavity of the spine. The Finite Element Analysis (FEA) only took into account wedging of intervertebral discs and remodelling of soft tissue. Bone remodelling was presumed not to occur in an early stadium of idiopathic adolescent scoliosis.²⁶ The validity of the assumption (Meijer) of complete soft tissue relaxation between the iteration of the long-term simulation is uncertain because the time scale in soft tissue adaptation is unknown and adaptation mechanics between healthy and scoliotic persons may be different. Therefore, the FEA presented by Meijer may not provide a realistic quantitative prediction of the biomechanical behaviour of the instrumented scoliotic spine,¹⁹ but it does provide a qualitative prediction.

9.3. FAILURE MODE EFFECT ANALYSIS (FMEA)

Although in the *in vivo* experiment, all twelve pigs instrumented with either an 'inverse' **XS TOR** or an 'inverse' **XS LAT** survived surgery and carried the implant without any neurological injuries, there are risks concerning the implantation of the **XS LATOR**. Using the results from the *in vivo* experiments, an impression of possible failures and their effects can be made. To assess the risks for the patient related to the surgical procedures and the post-operative functioning of the system, a Failure Mode Effect Analysis (FMEA) is performed. The FMEA is a generally used method for risk assessment and can be useful for quantifying and managing the risks and for the design of new strategies.

Various failures are graded on a scale of 0-10 using three criteria: Severity of failure (S), chance of detection (D) and the likelihood of occurrence (O). Table 9.3 gives a description of the scores for the three criteria.

The risk priority number (RPN) is calculated by multiplying the three scores ($S \cdot O \cdot D$). The RPN is then used to determine whether action regarding reduction of a part score is necessary.

9.3.a. Possible failures and their effects

The implantation procedure of the system comprises three stages. First, surgery is performed to attach the implant. To realise this, the implanted area is exposed. After anchoring of the implant, the wound must be closed. Second, a post-operative stage in which the implant is carried by the patient will last several months up to seven years. Third, after the implantation period, the system must be removed (explantation). In all three stages, system failures can occur. As part of the FMEA, Table 9.4 shows the failures and the potential causes that were identified during the process and the accompanying grades.

During surgery, various risks are introduced. Essential for the success of surgery is the pedicle screw insertion. Wrong screw insertion may cause severe injuries. For example, when a pedicle screw is inserted into the spinal canal damaging the spinal cord, the patient may be paralysed permanently. When the screw passes the anterior cortex of the vertebral body, the aorta may be penetrated which can be fatal to the patient. Screw misinsertion may also cause less severe but serious injuries to the patient such as nerve damage. In addition, screw misinsertion can cause a permanently damaged fixation of the implant. Fortunately, insertion of pedicle screws is nowadays established as a fixation method and the risks may be interpreted as low. Finally, damage to the posterior muscle tissue and to the periosteum must be taken into account since it will promote bone growth and fusion of the vertebrae.

After surgery, permanent force delivery on the spine, which is transferred by the anchor, is present. During the total implantation period, which may be several years, failures due to bone tissue damage may occur. These failures can be caused by screw pullout or rupture of transverse process, pedicle, or vertebral body. Another type of failure is originated in the implant itself. Because spinal motion is preserved by the system, the implant will endure large strains and accompanying local stresses. Implant failures such as rod breakage, spring breakage, and permanent deformation of springs may be the result. Such functional damage can increase the risk of spinal tissue damage.

Even when the implant is removed, damage to the spine can occur. During removal of bridges and pedicle screws, the vertebrae can be damaged. If excessive bone growth has taken place adjacent to the instrumentation, bone removal may be necessary. Moreover, removal of the high strength metal parts introduces additional risk because the resulting

voids will weaken the local vertebral structure. For example, the vertebral body can collapse after screw removal.

9.3.b. Necessary improvements

To effectively use the FMEA, recommendations regarding reduction of the determined risks must be made. First, current risk control mechanisms are identified. Current minimal invasive surgical procedures and the implementation of a flexible non-fusion system already offer a significant risk control. For example, preparation of the implanted area is performed by blunt dissection. Blunt dissection avoids muscle tissue damage and preserves the periosteum thereby controlling osteoinduction. Furthermore, using highly flexible implants and transferring relatively small forces to the implant, the loading of the anchors is kept low. After identification of these and other current controls, a list of recommended actions is made, which is presented in Table 9.5. To reduce the risks regarding pedicle screw insertion, image-guided surgery can be used. A prerequisite is of course that this expensive equipment must be available in the hospital. Solid screw fixation may be enhanced by omitting the screw thread tap manoeuvre prior to insertion. Using the tap will simplify the insertion but the potential for creation of a firm anchor will reduce.

In general, to control the quality of the product, it is advised to set up an extensive protocol that describes the various steps of the manufacturing processes. In addition, a protocol for the surgeon must be designed in which the minimal invasive blunt dissection procedure and the anchoring of the implant are reported.

In Table 9.4, two high scores in the RPN (risk priority number) column (144 and 210) can be observed. In the *in vivo* experiment, two sliding bushings and one bearing at the apex failed, which explains the relatively high scores. Steps must be taken to create an enhanced design; a change in bushing material and/or a slight increase in dimensions will decrease the risk of failure drastically.

	<i>Failure</i>	<i>Potential causes</i>	<i>Sev (S)</i>	<i>Det (D)</i>	<i>Occ (O)</i>	<i>RPN = S·D·O</i>
1	Damage spinal cord/nerves	Screw misplacement	9	1	1	9
2	Spring breakage	Fatigue failure	6	3	2	36
3	Detachment of U-part	Manufacturing failure	6	3	2	36
4	Puncture of aorta	Screw punctures aorta	10	1	4	40
5	Damage muscle tissue	Muscle tissue cut	2	3	8	48
6	Damage anterior tissue/artery	Awl misplacement	9	3	2	54
7	Infection	Insufficient sterilisation	3	4	5	60
8	Posterior artery cut	Use of sharp instrument	4	2	8	64
9	Plastic deformation of spring	High implant strain	2	8	4	64
10	Damage pedicle	High screw forces	6	4	3	72
12	Damage periosteum	Use of invasive tools	3	3	8	72
13	Screw pullout	Screw misinsertion	6	4	3	72
14	Vertebral body rupture	High screw forces	8	3	3	72
15	Bending moment too small	Manufacturing failure	2	7	6	84
16	Torsion moment too small	Manufacturing failure	2	7	6	84
17	Implant reaches max length	Implant too short	6	5	3	90
18	Transverse process rupture	Cable too tight	6	4	4	96
19	NiTi rod breakage	Fatigue failure	6	2	8	96
20	Failure of apex attachment	High forces	6	4	6	144
21	Failure of bushing	High local forces	5	7	6	210

Table 9.4: Risk grading

Various failures are graded on a scale of 0-10 using three criteria: Severity of failure (S), chance of detection (D) and the likelihood of occurrence (O). Risk priority number (RPN) is calculated by multiplying the three scores (S·O·D).

	<i>Failure</i>	<i>Potential effects</i>	<i>Current controls</i>	<i>Recommended actions</i>
1	Damage spinal cord/nerves	Paralysis	Frontal C-bow scan	Image-guided surgery
2	Spring breakage	Implant failure	Optimisation of material	Setup quality protocol
3	Detachment of U-part	Implant failure	Visible quality control	Setup welding protocol
4	Puncture of aorta	Severe internal bleeding	Short screws	Image-guided surgery
5	Damage muscle tissue	Pain and immobility	Blunt dissection	Do not use surgical blades
6	Damage anterior tissue/artery	Internal bleeding	Rim on awl	Instruction surgeon
7	Infection	Tissue degeneration	Follow protocol	Quality control
8	Posterior artery cut	Blood loss	Blunt dissection	Avoid sharp instruments
9	Plastic deformation of spring	Loss of correction	High flexibility	Increase flexibility
10	Damage pedicle	Implant failure	Flexible implant	Image-guided surgery
12	Damage periosteum	Osteoinduction	Blunt dissection	Do not use invasive tools
13	Screw pull-out	Implant failure	Pedicle probe/sounder	Do not use screw tap
14	Vertebral body rupture	Loss of spinal function	Flexible implant	None
15	Bending moment too small	Loss of correction	Detailed instructions	Setup quality protocol
16	Torsion moment too small	Loss of correction	Detailed instructions	Setup quality protocol
17	Implant reaches max length	Arrest of spinal growth	Margin of safety	Patient specific length
18	Transverse process rupture	Implant failure	Tensile stress control	None
19	NiTi rod breakage	Implant failure	Optimisation of material	Setup quality protocol
20	Failure of apex attachment	Implant failure	High flexibility	Increase strength
21	Failure of bushing	Decreased motion	Low friction materials	Increase bushing strength

Table 9.5: Risk control

The effects of the failures with current controls and recommended actions are listed in this table.

9.4. RECOMMENDATIONS

9.4.a. Preservation of bone structures

The heterotopic bone growth was limited by performing minimal invasive surgery. However, heterotopic ossification, which still occurred, may be limited further. The use of non-steroidal anti-inflammatory drugs is known to inhibit osteogenic activity and to limit spinal fusion.²⁷ Therefore, the use of non-steroidal anti-inflammatory drugs, such as ketorolac tromethamine, seems promising, which should be further studied. The ossification around the anchors and some other parts could obstruct explantation of the implant. It remains to be seen whether it is necessary to remove all parts of the implants. For example, removal of pedicle screws leaves a large hole in the pedicle. It may be wise to keep the screws in place. Nonetheless, it is essential to inactivate the implant, which could be achieved by partial explantation. Partial explantation consists of removing only the NiTi rod (**XSLAT**) and the springs/U-loops (**XSTOR**) or removing the same element including the bearing houses and the cross-bridges. Removal of bridges and bearing houses may include cutting of (heterotopic) bone structures, which will reactivate bone growth. We recommend keeping the periosteum intact as much as possible during explantation even if that implies keeping screws, bridges and bearing houses *in situ*.

9.4.b. Improvements on the design

Some minor improvements must be carried out to improve functional performance of the **XSLATOR** and prevent post-operative failures. The geometry of the bearing in the middle fixation element may be adjusted to prevent *in vivo* fixation failure. Furthermore, to prevent welding cracks causing the Ti6Al4V ring to detach from the NiTi rod, it is suggested to use identical materials (NiTi) for welding or to use any other type of connection.

In vivo performance of UHMWPE can be adversely affected by sterilisation procedures.²⁸ Most common procedures are steam sterilisation, ethylene oxide (EtO) sterilisation and gamma irradiation. In our *in vivo* experiment, we used steam sterilisation. Although the UHMWPE bushings survived steam sterilisation, it is recommended to avoid this method for all UHMWPE parts because thermal degradation can cause problems (*e.g.* functional failure) in long-term implantation. Sterilisation by gamma irradiation is recommended for UHMWPE parts.²⁸ Since steam sterilisation is the standard sterilisation procedure in hospitals in the Netherlands, the use of other materials may be considered. For example, carbon reinforced PEEK, which is a heat- and wear-resistant polymer, is a valid alternative that can be steam sterilised successfully (Figure 9.3).²⁹ Replacement of UHMWPE by PEEK will also limit the plastic deformations observed *in vivo*.

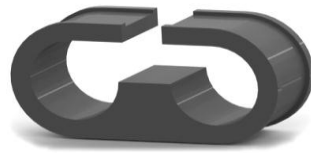


Figure 9.3: Improved bushing design

An improved design of the sliding bushing (manufactured from carbon reinforced PEEK) will prevent the fixation from slipping off the U-shaped rod, improve bearing strength and prevent thermal degradation due to steam sterilisation. Picture taken from: Wiggers.³⁰

In our *in vivo* experiment, we examined the benefits of assembling a significant part of the implants during surgery. For that reason, a mailbox-type bearing was manufactured, which enabled the U-loop to be slid into the bearing. The main goal for *in situ* assembly was to insert the functional part of the implant after complete fixation of the bridges and bearings. After fixation of the total system, a ring was attached using a simple procedure to the U-shaped loops that prevented the implant from disassembly. In practice however, the *in situ* assembly (combining the functional spring element with the bearing system) appeared unnecessary thus allowing further pre-assembly of the implant. Hence, the bearing system and end-ring may be modified to optimise for shape and functionality.

The concept of application of a relatively constant moment (during growth and shape correction) requires a low stiffness in bending and torsion. Besides a maintained post-operative bending moment, low stiffness is a prerequisite for maintaining spinal flexibility. It may therefore be recommended to further improve the design regarding bending and torsion stiffness. The use of more flexible materials or the application of altered geometry may be considered to decrease the stiffness in bending and torsion. Major shortcoming is the increase in dimension, which could accompany such design modifications.

9.4.c. Topics for future research

The next stage in the development of the implant system is to perform preparations for series production. For this, a production plan must be set up. Series production may require modifications to reduce manufacturing time, costs *etc.* The main difficulty for series production is the manufacturing of the U-parts since *e.g.* the required high-temperature deformation can adversely affect material properties. In a redesign, the U-parts were split into two parallel rods and an elbow joint. The elbow joint connects the two parallel rods of the implant (creating the U-shaped part). With this modification, the integrity of the mechanical behaviour is preserved (Figure 9.4).³⁰



Figure 9.4: Optimising manufacturing procedures

To optimise manufacturing of the U-shaped rods for series production, an elbow joint may be created to connect two parallel rods. The elbow joint can be shrink-fitted onto the two parallel rods. Picture taken from: Wiggers.³⁰

In our *in vivo* porcine model, we instrumented separate implants only, either the **XS LATOR** or the **XS TOR**. To investigate the combined effect *in vivo*, in future research the effect of combining the two implants should be determined. Such an experiment may consist of implanting a complete and enhanced (**XS LATOR**) system in a porcine model. In addition, long-term performance of the system (fatigue, wear) and its effects on the porcine spine (tissue, bone growth, and deformation) may be examined by implantation over a longer period, for example one year. The use of a different pig breed such as the Yucatan mini pig may then be considered because accommodation of the fast-growing Dutch Landrace pigs will get problematic due to their large increase in size and weight.

We performed minimal invasive surgery on the pigs. This minimal invasive surgery was successful but could be improved. Using the knowledge of experts on this issue, the procedures can be enhanced and optimized. In the proposed *in vivo* experiment, these optimised surgical procedures should be performed and the effects of the non-steroidal anti-inflammatory drugs on heterotopic ossification should be examined.

Fatigue behaviour of the implant is dependent on the alternating strains that occur *in vivo*. The incidence and magnitude of alternating strains is dependent on spinal motion during daily activities. However, the amount and frequency of spinal motion that occurs in patients is still unknown. Therefore, additional experiments should be performed to determine this relative vertebral motion. Such an experiment may consist of measuring spinal motion of adolescents using inertial motion trackers that are connected to the skin at the posterior spine. Each subject may be measured for at least a week to get representative data. The actual alternating strains that occur in the **XS LATOR** can be deduced from these motion capture experiments. These strains can be used to perform additional fatigue tests. Accurate prediction of fatigue behaviour can be accomplished by performing tests in a set-up in which the complete implant is subjected to repetitive strains representative of daily spinal motions.

Little is known about the passive *in vivo* stiffness of the numerous segments in the human trunk, which must be significantly higher than the measured *in vitro* stiffness of an isolated spine. Stiffness measurements of the spine segments can be helpful in understanding the biomechanical behaviour of the human spine in general. Moreover, a standardised and quick method for performing measurements on a specific patient can be useful also in the determination of the exact forces/moments to be applied in that patient for scoliosis correction. Currently, an apparatus is being designed to develop such an easy method for quick stiffness determination. As a result, accurate measurements of adolescent subjects will be performed and presented in a future study.

The Finite Element scoliotic and healthy models developed by Meijer can help in determination of the effect of simultaneous instrumentation of the two implants and in further optimising the performance of the **XS LATOR**. In clinical practise, a custom-made scoliotic model, representing the exact deformity of a specific patient can be used to simulate the effect of the **XS LATOR**. Using the results of the simulation, selection of the instrumented vertebral levels and the required forces and dimensions can be determined. As a result, the **XS LATOR** will achieve optimal results on shape correction.

9.5. CONCLUSIONS

The conclusions regarding the results from the *in vitro* and *in vivo* experiments, which were evaluated based on the requirements can be summarised as follows:

The **XS LATOR** is a highly flexible implant system; it is able to induce lateral bending and torsion in pigs relatively independently.

The use of relatively small bending and torsion moments enables a gradual deformation over a period of weeks.

The generated torque and bending moment are fairly constant during growth and significant shape change.

The two separate 'inverse' versions of the implants (**XS TOR** and **XS LAT**) mainly affect their intended directions.

Although in scoliosis correction the coupling effect of lateral bending and torsion is expected to be stronger (using the **XS TOR**), implantation of the **XS LATOR** suggests to provide accurate control of shape change in scoliosis correction.

Using minimal invasive surgery, damage of tissue surrounding the implants is limited and bone structure integrity is preserved.

The **XS LATOR** fulfils the technical requirements listed in Chapter 3.

Due to the low stiffness, the **XS LATOR** is able to adjust to any spinal motion that will occur after implantation.

The range of motion (ROM) of the spine after implantation with the **XS LATOR** is comparable to the original uninstrumented ROM of the spine.

Tissue response towards the implant is low. In terms of biocompatibility, the implant can be regarded as safe.

The risks for the patient due to implant failure and surgical procedures are considered low when small design improvements on the bearings are carried through.

Additional experiments must be performed to determine long-term performance reliability of the implant system.

9.6. REFERENCES

1. Busscher, I., Ploegmakers, J., Verkerke, G. & Veldhuizen, A. Comparative anatomical dimensions of the complete human and porcine spine. *European Spine Journal* **19**, 1104-1114 (2010).
2. Guille, J.T., D'Andrea, L.P. & Betz, R.R. Fusionless treatment of scoliosis. *Orthopedic Clinics of North America* **38**, 541-545 (2007).
3. Thompson, G.H., Akbarnia, B.A. & Campbell, R.M.J. Growing rod techniques in early-onset scoliosis. *Journal of Pediatric Orthopaedics* **27**, 354-361 (2007).
4. Samdani, A.F., *et al.* Bilateral use of the vertical expandable prosthetic titanium rib attached to the pelvis: a novel treatment for scoliosis in the growing spine. *J Neurosurg Spine* **10**, 287-292 (2009).
5. Maruyama, T. & Takeshita, K. Surgical treatment of scoliosis: a review of techniques currently applied. *Scoliosis* **3**, 6 (2008).
6. Costa, L., *et al.* Oxidation in orthopaedic UHMWPE sterilized by gamma-radiation and ethylene oxide. *Biomaterials* **19**, 659-668 (1998).
7. Shabalovskaya, S.A. Surface, corrosion and biocompatibility aspects of Nitinol as an implant material. *Bio-Medical Materials and Engineering* **12**, 69 (2002).
8. Matsuno, H., Yokoyama, A., Watari, F., Uo, M. & Kawasaki, T. Biocompatibility and osteogenesis of refractory metal implants, titanium, hafnium, niobium, tantalum and rhenium. *Biomaterials* **22**, 1253-1262 (2001).
9. Steinemann, S.G. Metal implants and surface reactions. *Injury* **27**, Supp 3, S/C16-S/C22 (1996).
10. ASTM Standard F2624 - 07 (2008). Standard test method for static, dynamic and wear assessment of extra-discal spinal motion preserving implants. ASTM International, West Conshohocken, PA, 2008, DOI: 10.1520/F2624-07, www.astm.org.
11. Toth, J.M., *et al.* Polyetheretherketone as a biomaterial for spinal applications. *Biomaterials* **27**, 324-334 (2006).

12. Sobhi, H., Matthews, M., Grandy, B., Masnovi, J. & Riga, A. Selecting polymers for medical devices based on thermal analytical methods. *Journal of Thermal Analysis and Calorimetry* **93**, 535-539 (2008).
13. Troccoli, C., E. Spinal surgery - new technologies. *Sector: Medical Devices & Procedures* (2004).
14. Busscher, I., *et al.* *In vitro* biomechanical characteristics of the spine: a comparison between human and porcine spinal segments. *Spine* **35**, E35-42 (2010).
15. Panjabi, M.M., Brand, R.A. & White, A.A. Mechanical properties of the human thoracic spine as shown by three-dimensional load-displacement curves. *J Bone Joint Surg Am* **58**, 642-652 (1976).
16. Wilke, H.-J., Geppert, J. & Kienle, A. Biomechanical *in vitro* evaluation of the complete porcine spine in comparison with data of the human spine. *European Spine Journal* **20**, 1859-1868 (2011).
17. Morlock, M.M., *et al.* Determination of the *in vivo* loading of the lumbar spine with a new approach directly at the workplace - first results for nurses. *Clinical Biomechanics* **15**, 549-558 (2000).
18. Hedman, T.P., Kostuik, J.P., Fernie, G.R. & Heller, W.G. Design of an intervertebral disc prosthesis. *Spine* **16**, S256-S260 (1991).
19. Meijer, G.J.M. Development of a non-fusion scoliosis correction device - numerical modelling of scoliosis correction. PhD-thesis, University of Twente, Enschede. (2011).
20. Wynarsky, G.T. & Schultz, A.B. Optimization of skeletal configuration: studies of scoliosis correction biomechanics. *J Biomech* **24**, 721-732 (1991).
21. Benabdallah, S.M.H. & Yelle, H. Static and quasi-dynamic coefficient of friction of three engineering thermoplastics: UHMWPE, PA 66, POM. *Journal of Materials Science* **26**, 2445-2450 (1991).
22. Wang, X., Mabrey, J.D. & Agrawal, C.M. An interspecies comparison of bone fracture properties. *Bio-Medical Materials and Engineering* **8**, 1-9 (1998).
23. Pearce, A.I., Richards, R.G., Milz, S., Schneider, E. & Pearce, S.G. Animal models for implant biomaterial research in bone: a review. *Eur Cell Mater* **13**, 1-10 (2007).
24. Ferretti, C., *et al.* Osteoinduction: translating preclinical promise into clinical reality. *British Journal of Oral and Maxillofacial Surgery* **48**, 536-539 (2010).
25. Biscevic, M., *et al.* The posterior corrective spondylodesis - method of choice of surgical scoliosis treatment. *Med Arh* **65**, 149-152 (2011).

26. Will, R.E., Stokes, I.A., Qiu, X., Walker, M.R. & Sanders, J.O. Cobb angle progression in adolescent scoliosis begins at the intervertebral disc. *Spine* **34**, 2782-2786 (2009).
27. Glassman, S.D., *et al.* The effect of postoperative nonsteroidal anti-inflammatory drug administration on spinal fusion. *Spine (Phila Pa 1976)* **23**, 834-838 (1998).
28. Affatato, S., *et al.* The performance of gamma- and EtO-sterilised UHMWPE acetabular cups tested under severe simulator conditions. Part 2: wear particle characteristics with isolation protocols. *Biomaterials* **24**, 4045-4055 (2003).
29. Kurtz, S.M. & Devine, J.N. PEEK biomaterials in trauma, orthopedic, and spinal implants. *Biomaterials* **28**, 4845-4869 (2007).
30. Wiggers, J. Industrialisation of a non-fusion scoliosis correction system. Master's thesis, University of Twente, Enschede. (2012).

SUMMARY

One of the tasks of the spine is to support the trunk, head and upper extremities. Flexibility is provided by means of accumulative segmental motion. Although the spine is a highly functional and stable construction, problems concerning stability occasionally occur. If, for example, for some reason spinal development during adolescence malfunctions, a deformity such as scoliosis may develop. Scoliosis is a deformity of the spine, characterised by a lateral curvature and an axial rotation. Treatment of scoliosis includes non-surgical and surgical interventions. Current surgical treatment of scoliosis is unsatisfactory because it embraces the permanent immobilisation of several vertebrae, which results in a fused spine that is unable to flex and to develop normally in immature patients. Therefore, an improved method is required.

This dissertation addresses the development of a new implant system that delivers a revolutionary surgical solution to a problem classified as 'adolescent idiopathic scoliosis' (AIS). This non-fusion correction system (**XS_{LATOR}**) comprises two (separate) implants. One implant (**XS_{TOR}**) is a torsion-generating element that applies a torque on the spine to correct the axial rotation of the vertebrae. The other implant (**XS_{LAT}**) is a lateral bending element that applies a bending moment to correct the lateral curvature. The implants can be used together in such a way that an optimal configuration for each patient can be implemented. The system will be implanted in the adolescent during the growth phase and removed when the spine is fully grown, which means that the implants must be functional for a period of ten years.

Unlike current fusion systems, the system is highly flexible thus fusion of the vertebrae will be avoided. Consequently, the imposed corrective moment and torque on the spine are small but remain present all the time and thus generate a gradual shape change as observed in orthodontic braces. Axial motion is possible due to U-loops at both ends of the devices. The U-loops can slide into plain bearings. With axial motion three aspects are covered: spinal growth, variations in spinal lengths of the patients and axial motion due to daily activities.

Both the **XS_{TOR}** and **XS_{LAT}** use three vertebrae for anchoring. One, two, or three anchors may be shared during fixation of the two implants. For fixation to the vertebrae we developed an anchor (**XS_{FIX}**) that is less destructive to spinal structures than conventional anchors. The **XS_{FIX}** is a posterior fixation system that does not use screws. Instead, it attaches posteriorly to both transverse processes of a vertebra to create a strong fixation. To test the strength of the **XS_{FIX}** we performed an experiment, in which the **XS_{FIX}** was compared with a commonly used pedicle screw anchor (PSA) system. It appeared that the lower spinal region (low thoracic and lumbar vertebrae) can best be instrumented with pedicle screws. For fixation of flexible spinal systems to the higher spinal region (high and mid thoracic vertebrae), the **XS_{FIX}** is preferred over the PSA.

To test the final design of the system, functional prototypes of 'inverse' implants were manufactured. These 'inverse' implants, which aimed for induction of scoliosis instead of correction, were implanted in twelve pigs after which the effect on spinal shape change and on spinal fusion was examined. Spinal growth and corresponding lengthening of the implants was observed in all animals. Although some cartilage degeneration occurred in the vertebral joints instrumented with pedicle screws, the vertebrae in the instrumented region appeared not to be fused. The results show that the system is capable of inducing significant deformities in two different directions. The use of relatively small bending and torsion moments enabled a gradual deformation over a period of weeks. The results suggest that splitting up the functionality of the implants in two parts will have advantages over the single action implants, in which surgery mainly focuses on the bending deformity.

The 'inverse' implants were also tested on their mechanical behaviour by determination of the forces and moments that act on the anchored vertebrae. These tests showed that the **XS_{TOR}** and the **XS_{LAT}** are able to generate a torque and a bending moment that remain (fairly) constant during spinal growth, when also a shape change due to the generated moment/torque is achieved. The stiffness of the **XS_{LATOR}** is only a small fraction of the stiffness of conventional spinal fusion system, which enables the system to adjust without obstructing spinal motion including growth. This preservation of spinal flexibility after implantation will help preventing fusion of the vertebrae. Of course, minimal invasive surgery must be performed to preserve the periosteum and prevent other tissue damage, which significantly contributes to the minimisation of ossification of the spine.

Fatigue tests of a pseudo-elastic NiTi bending spring, which is the functional element of the **XS_{LAT}**, showed the susceptibility to bending fatigue when a highly pre-bent spring is subjected to cyclic bending. The cyclic strains that will occur in the spring during daily bending could cause spring failure in long-term implantation. However, the amount of strain that will occur in the spring after implantation is unclear since the area of daily spinal motion is still unexplored. The *in vivo* experiments showed that all functional elements of the implants (bending and torsion springs) survived the implantation period, which was three months (maximally). Further investigation must be performed to show if and which modifications of the system must be carried through to create an implant that remains functional for ten years of implantation.

In conclusion, the **XS_{LATOR}** is able to create a spinal shape change in both torsion and lateral bending, to allow spinal motion and growth and to prevent vertebral fusion. We expect that the system behaves similarly in scoliosis correction. This means that a new way of treating scoliosis is possible, starting already during growth when scoliosis is less severe and ending after growth by removing the system. Further research must be performed to determine the fatigue limits of the **XS_{LATOR}**.

SAMENVATTING

Een van de taken van de wervelkolom is het ondersteunen van de romp, het hoofd en de armen. De relatieve beweging van de wervels zorgt voor de flexibiliteit. Normaal gesproken is de wervelkolom een zeer stabiel en functioneel geheel. Toch kan er soms een misvorming optreden, vooral tijdens een periode van snelle groei. Scoliose bijvoorbeeld, wat een zijwaartse verkromming is van de rug in combinatie met torsie, is een dergelijke vervorming. De resultaten van zowel chirurgische als niet-chirurgische behandelingen zijn op erg onbevredigend. Hoewel een chirurgische methode, wat inhoudt dat de wervels geïmmobiliseerd worden, wel kan corrigeren, zijn de nadelen groot. Het gefuseerde deel van de rug kan niet meer buigen en groei van de rug wordt belemmerd. Een nieuwe methode voor behandeling van scoliose is daarom wenselijk.

Dit proefschrift beschrijft de ontwikkeling van een nieuw implantatiesysteem dat een revolutionaire (chirurgische) oplossing biedt voor adolescentie idiopathische scoliose (scoliose bij tieners). Het systeem, de **XS_{LATOR}** genaamd, bestaat uit twee implantaten. Het eerste, de **XS_{TOR}**, genereert een torsiemoment en beoogt de torsie in de wervelkolom te corrigeren. Het tweede implantaat, de **XS_{LAT}**, genereert een buigmoment en beoogt daarmee de zijwaartse buiging te corrigeren. Optimale correctie kan worden bewerkstelligd door bij een patiënt beide implantaten tegelijkertijd op zodanige wijze te implanteren dat de juiste krachten/momenten op de juiste wervels aangrijpen. De implantaten dienen tijdens de groeiperiode aan de rugzijde geïmplanteerd te worden en pas verwijderd na de groei. Dit betekent dat het systeem tien jaar functioneel moet zijn.

De opgelegde correctiemomenten van de **XS_{LATOR}** zijn zeer klein, maar blijven aanwezig tijdens het bewegen van de rug. De hoge flexibiliteit van de functionele elementen moet ervoor zorgen dat fusie van de wervels wordt voorkomen. Net als bij de beugel in het gebit zorgen kleine krachten/momenten voor een geleidelijke vormverandering. Glijlagers zorgen ervoor dat de wervels in lengterichting ten opzichten van elkaar kunnen bewegen. Hiermee wordt groei van de rug toegelaten, en tevens een hoge flexibiliteit in buiging en torsie bereikt. Twee U-bochten zorgen ervoor dat het systeem kan verlengen terwijl de krachten en momenten aan de wervels overgedragen blijven worden.

Zowel de **XS_{TOR}** als de **XS_{LAT}** gebruikt drie wervels voor verankering. Een, twee of drie ankers kunnen gedeeld worden bij bevestiging van beide systemen. Een nieuw anker (**XS_{FIX}**) werd ontwikkeld, welke minder beschadigend is voor de rug dan huidige systemen. De **XS_{FIX}** gebruikt geen schroeven zoals vele andere systemen, maar kabels die om beide zijuitsteeksels van een wervel gebonden worden om zo een solide fixatie te verkrijgen. De **XS_{FIX}** werd getest door het systeem te vergelijken met een gangbare pedikelschroef-fixatie. Het bleek dat op de lage rugwervels (de onderste zeven) het beste de pedikelschroef-fixatie toegepast kan worden. Voor fixatie van een flexibel implantaat zoals de **XS_{LATOR}** aan de overige wervels kan het beste de **XS_{FIX}** worden gebruikt.

Voor proefdierexperimenten werden er 'inverse' implantaten gemaakt die een tegengestelde werking hebben, wat wil zeggen dat de implantaten trachten een scoliose creëren (in plaats van corrigeren). Deze experimenten wezen uit dat de 'inverse' implantaten de groei van de wervels niet belemmerde. Het bleek dat de wervels niet fuseerden, ondanks beschadigingen van kraakbeen in de wervelgewrichtjes. De resultaten laten tevens zien dat het systeem in staat is om wezenlijke vormverandering van de wervelkolom te bewerkstelligen in zowel buiging als torsie. Het gebruik van slechts kleine buig- en torsiemomenten zorgen voor een langzame vormverandering in een periode van een aantal weken. De resultaten suggereren dat het splitsen van de functies van het systeem door het toepassen van twee afzonderlijke implantaten (torsie en zijwaartse buiging) voordelig is ten opzichte van huidige systemen waarbij men zich slechts voornamelijk richt op zijwaartse buiging in scoliose.

De 'inverse' implantaten werden getest op mechanisch gedrag, wat wil zeggen de er werd gekeken naar de krachten en momenten die ze leveren tijdens implantatie. Een mechanische testopstelling simuleerde de rug van de varkens in verschillende standen. Daarbij werd groei van de rug gemodelleerd. De testen lieten zien dat de **XS_{TOR}** en de **XS_{LAT}** een redelijk constant torsiemoment en buigmoment genereren tijdens groei van het systeem terwijl een geleidelijke vormverandering plaatsvindt. De stijfheid van het gehele systeem (**XS_{LATOR}**) is extreem laag in vergelijking met de erg stijve huidige implantaten die fusie veroorzaken. Door behoud van flexibiliteit na implantatie kan fusie van de rug worden voorkomen. De toegepaste chirurgische ingreep moet daarbij wel minimaal invasief zijn, wat inhoudt dat de weefsels, in het bijzonder het botvlies van de wervels, zoveel mogelijk onbeschadigd blijven om botwoekering te beperken.

Vermoeiingstesten op een functioneel onderdeel van de **XS_{LAT}**, namelijk een extreem elastisch nikkel-titanium veer, wezen uit dat dit onderdeel gevoelig is voor vermoeiing wanneer het in grote mate voorgespannen is. De wisselende rekken die optreden in de veer tijdens het uitvoeren van bewegingen in het dagelijks leven, zouden voor een breuk van de veer kunnen zorgen. Echter, de hoeveelheid rek die op zal treden na de implantatie is onduidelijk. Tijdens het uitvoeren van de experimenten is bij geen enkel dier die een **XS_{LAT}** geïmplanteerd kreeg een breuk van de veer opgetreden (in een periode van maximaal 3 maanden). Verder onderzoek moet uitwijzen of (en welke) er wijzingen aan moeten worden doorgevoerd om het systeem tien jaar te laten functioneren.

Concluderend kan gesteld worden dat de **XS_{LATOR}** in staat is om een vormverandering te creëren in torsie en buiging. Het systeem laat natuurlijke bewegingen en groei toe en doet de rug derhalve niet fuseren. We verwachten dat het systeem zich op soortgelijke wijze gedraagt tijdens scoliosecorrectie. Dit betekent dat een nieuwe methode van scoliosecorrectie mogelijk is. Deze methode kan al tijdens de groei, wanneer scoliose nog mild is, worden gestart en beëindigd worden aan het einde van de groeiperiode. Verder onderzoek naar de vermoeiing van het systeem is nodig.

DANKWOORD

Aangezien het dankwoord normaalgesproken het best gelezen deel van een proefschrift is, kan de lezer dat vanzelfsprekend niet onthouden worden. Als eerste wil ik even melden dat ik het functioneren binnen het wekelijkse team (Bart, Edsko, Jasper, Gerdine en ik) als zeer prettig heb ervaren. De wekelijkse besprekingen waren zeer nuttig, vooral ook als stok achter de deur. De samenkomsten waren doorgaans erg gezellig, mede doordat niemand een stukje humor schuwde.

Om toch een min of meer gestructureerd geheel te houden wil de mensen in dit dankwoord in verschillende categorieën opdelen te weten: (a) collega's die direct bijgedragen hebben aan het tot stand komen van het proefschrift, (b) collega's die bijgedragen hebben aan het op prettige wijze werken aan het onderzoek/proefschrift en dus indirect een steentje hebben bijgedragen, (c) studenten die bijgedragen hebben aan het proefschrift, (d) bedrijven of instellingen die een belangrijke bijdrage hebben geleverd aan het ontwerp, productie of testen van de prototypes, (e) de proefdieren en (f) de familieleden die op een ander niveau hebben bijgedragen tot het tot stand komen van het proefschrift. De volgende mensen wil ik danken:

- (a) Als eerste mijn directe begeleider Edsko voor zijn (vrijwel) altijd wijze opmerkingen en scherpe blik op allerlei zaken. Van hem heb ik geleerd kritisch te kijken naar alle aspecten op het technisch vlak; mijn promotor Bart Verkerke voor het geven van de kans om te promoveren. Zijn structurele wekelijkse begeleiding en knopen-doorhak-ondersteuning hebben mij enorm geholpen goede vorderingen te maken in het project; Gerdine Meijer voor de interessante en leuke discussies, het zonder morren spelen van persoonlijke assistente en de gezelligheid op onze kamer. Niet onbelangrijk zijn daarbij geweest de lekkere appeltaarten en de altijd aanwezige dropbox; Geert Monnick voor zijn hulp in het assembleren van verschillende opstellingen (vermoeiingsmachine, mechanische testopstelling), het fabriceren van de benodigde chirurgische instrumenten, het polijsten van die vermoeiende staafjes en het regelen van allerhande zaken zoals bestellingen en opdrachten voor bedrijven; Jasper Homminga zijn begeleiding en het functioneren als assistent-promotor. Hoewel hij niet direct mijn begeleider was heb ik toch veel gehad aan zijn kijk op zaken vanuit een iets ander perspectief, om zodoende e.e.a. in een breder context te plaatsen; Iris Busscher voor haar hulp bij de eerste *in vivo* experimenten.
- (b) Alexander en Wouter voor het (domme) gelul in het lab tijdens de koffie (en de zendpiraat op de vrijdagmiddag); mijn nieuwe maat Jan (voor het begrip van mijn ongein en het verlichten van mijn werkbelasting tijdens de laatste fase; het BSS-BW voetbalteam (dat nogal in samenstelling wisselde), waarvan ik de namen maar niet noem; Mijn DETO 4/5 teamgenoten, Berto en Reinhart voor de noodzakelijke wekelijkse relativering, vooral tijdens het weekend.

- (c) Jochem Talsma, Erwin Platenkamp, Douwe van Manen, Jochem Wiggers; Vincent Cloostermans voor zijn bijdrage aan hoofdstuk 5; Douwe van Manen in het bijzonder voor zijn geweldige inzet bij het uitvoeren van de *in vivo* experimenten. Zijn bijdrage is erg groot geweest in het tot stand komen van hoofdstuk 8.
- (d) René Aquarius en Willem van de Wijdeven van het UMC St. Radboud Nijmegen voor de hulp bij de fixatie-experimenten; GML Instruments (onder leiding van Hans Plaggenmars en Albert Krikken) voor het altijd op tijd leveren van de implantaten; Johan Oonk van Technolas voor het telkens last-minute lassen van de implantaten; Gert Nijenbanning van Baat Medical en Marc Sanders van Biomet voor hun adviezen; Gerhard Rakhorst voor het uitvoeren van de operaties; de mensen van de Centrale Dienst Proefdieren en Radiologie van het UMC Groningen voor hun assistentie bij de *in vivo* experimenten. De nog niet eerder genoemde leden van de STW-gebruikerscommissie: Jaap van Dieën, Bart Koopman, Paul Groenenboom, Henry van der Valk, Rob Slootman, Bas van Riggelen, Dick Schipper, Theo van Kooten, Idsart Kingma, Albert van der Veen, Albert Veldhuizen, Sjoerd Bulstra en Frans van der Helm.
- (e) Mijn dikke roze vriendjes Purk & Snurk, Mini & Maxi, Lucky & Strike, Roze Rinus & P., Billie & Betsie, Bella & Donna, Harrie & Bo, Porgy & Bess wil ik bedanken voor het grootste offer dat mogelijk is.
- (f) Ma voor het oneindig groot vertrouwen in mij, de onvoorwaardelijke liefde en steun; pa voor het nooit-opgeven-karakter, en samen met Annette het o.a. altijd voorzien van mobiliteit en het tot beschikking stellen van de sauna; Vincent en Klarine voor hun grenzeloze onbaatzuchtigheid, gastvrijheid en gezelligheid; Len Wessels voor de vreugde in het leven van onze familie; Mart Wessels voor het redden van SuperLen; De 'wat een familie' Den Drijver voor de gezellige zondagmiddagen en -avonden. En natuurlijk als laatste mijn prachtige en lieve vrouw (zeg maar) Charon Wessels, die een zeer belangrijke bijdrage gegeven heeft aan mijn levensvreugde en me natuurlijk heeft gesteund tijdens het gehele traject.

Dit proefschrift werd gefinancierd door:



GML-INSTRUMENTS is producent van fijnmechanische instrumenten, gereedschappen en onderdelen, Onze opdrachtgevers bestaan uit ongeveer 60 verschillende bedrijven uit binnen- en buitenland, die in verschillende sectoren actief zijn. Met een klein team maken we een technische zeer hoogwaardig product. Voor ons staat de tevredenheid van klanten en personeel voorop.

www.gml-instruments.nl



DePuySynthes Spine, onderdeel van Johnson & Johnson, is toonaangevend in de ontwikkeling, productie en introductie van innovatieve producten in de wereld van de wervelkolomchirurgie. Bij de ontwikkeling van nieuwe producten zien wij het als onze verantwoordelijkheid om een concrete bijdrage te leveren aan de ontwikkeling en bevordering van nieuwe technieken die bijdragen aan het maatschappelijk welzijn. De verbetering van kwaliteit van leven staat hierbij centraal.

www.depuysynthes.com



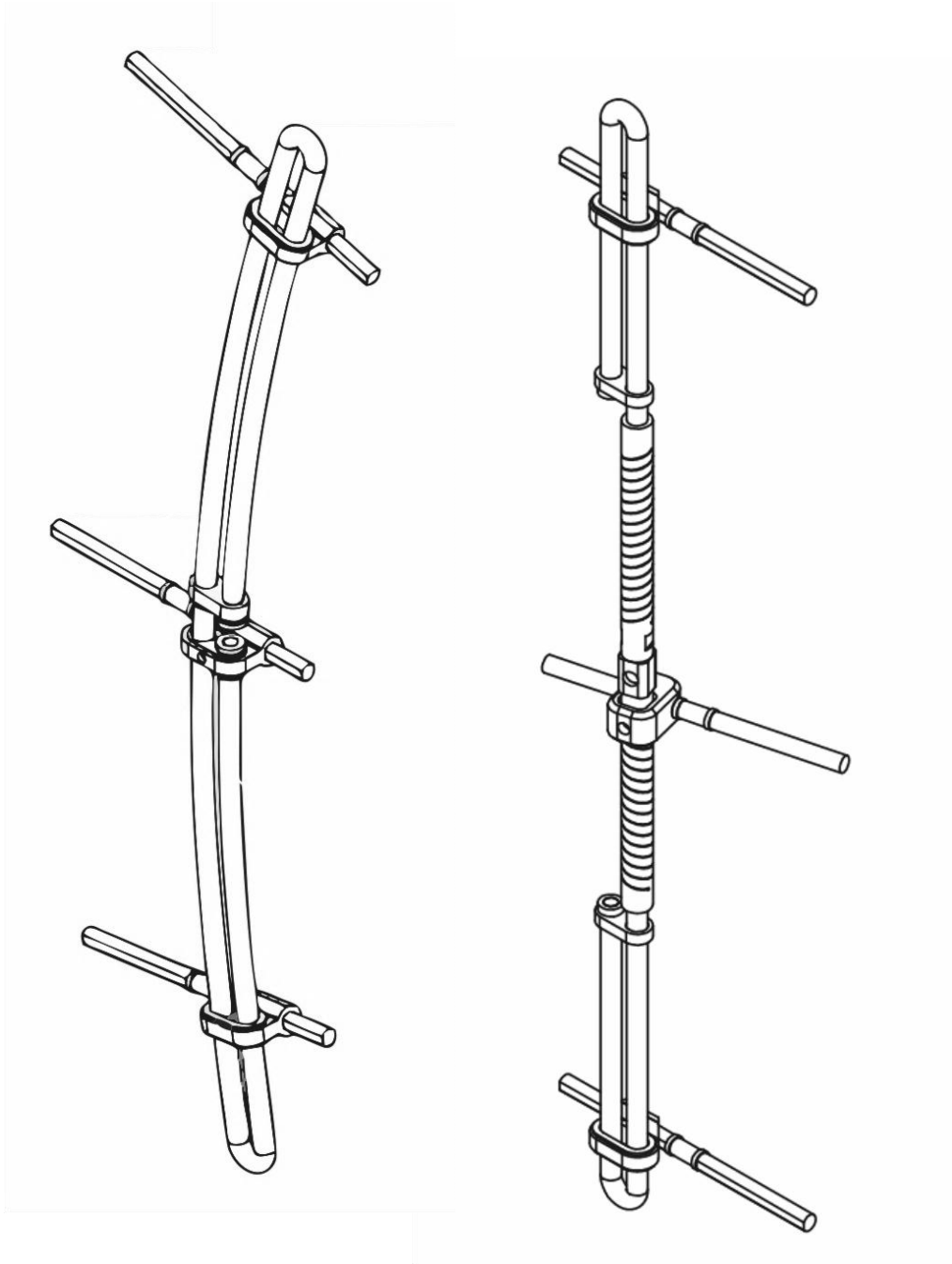
www.baatmedical.com



Burgemeester J.C. van den Bergplein 1a
7642 GR Wierden
Tel: 0546-571986

ewessels@knoware.nl

Appendix



APPENDIX

I. IMPLANTATION SYSTEM FOR TREATMENT OF A DEFECTIVE CURVATURE OF THE SPINAL COLUMN

The invention relates to an implantation system for treatment of a defective curvature of the spinal column.

Such a disorder of the spinal column is often referred to as “scoliosis”. A commonly used treatment of scoliosis is to perform an operation, wherein an implant is fixedly attached to at least the defective longitudinal part of the spine, mostly at the posterior side of the spine. Therein, the implant has at least one rod, having high bending and torsional stiffness. The shape of that rod closely resembles the desired (*i.e.* “healthy”) curvature of the defective part of the spine. The rod is provided with at least two anchoring elements, which are fixedly attached to the rod at distant locations in longitudinal direction of the rod. During the performing of the operation the defective part of the spine is instantaneously deformed as much as possible so as to match its desired curvature as much as possible. With the spine being in this corrected state, one of the two anchoring elements is fixedly attached to one vertebra of the defective spine, while the other anchoring element is fixedly attached to another vertebra of the defective spine. Thus, the implanted rod, having high stiffness, secures the corrected state of the spine.

This commonly used treatment goes hand in hand with the occurrence of fusion of adjacent vertebrae of the treated part of the spine. This fusion gradually occurs after the operation due to mutual immobility of said adjacent vertebrae, which is a consequence of the implanted high-stiffness rod that secures the treated part of the spine. For this commonly used treatment, surgeons consider such fusion as a desirable effect, since it stabilizes the imposed, corrected curvature of the spine. In addition, such fusion lightens the implant’s task and thereby prevents eventual failure of the implant, which usually is unable to long-lastingly withstand heavy loads. For these reasons, in performing this commonly used treatment, surgeons in fact usually apply additional measures aiming at further stimulating fusion and the speed thereof, such as the additional measure of roughening vertebrae surfaces.

However, this commonly used treatment has several drawbacks. One of the drawbacks is that the implanted device and/or the fused vertebrae impair the patient’s possibilities to perform various flexible movements of the spine. Further drawbacks for example relate to problems associated with growing spinal columns of children. In fact, the abovementioned implanted devices impair a natural healthy growth of the spine. For example, an implant being posteriorly fixed to a spine may lead to a spine that undesirably grows in a backwards bending fashion. Hence, in view of such growth-

related drawbacks, this commonly used treatment requires re-operations to be carried out, which is very undesirable for many evident reasons.

In view of the abovedescribed drawbacks, WO02/17803A2 and WO2010/030906A1 disclose alternative implants aiming at addressing such drawbacks related to reduced flexibility of the spine and related to growth of the spinal column. Such an alternative known implant not only has at least one vertebra-anchoring element, which is fixedly attached to a rod, but also at least one other vertebra-anchoring element, which is slidably connected to the same rod. Thanks to the slidability of the rod relative to the other vertebra-anchoring element, such an alternative implanted configuration, as compared to the abovedescribed commonly used implanted configurations, provides improved flexibility of the spine and reduces some of the abovementioned growth-related drawbacks. Amongst others, such an alternative implanted configuration, as compared to the abovedescribed commonly used implanted configurations, aims at avoiding fusion of vertebrae, instead of aiming at stimulating such fusion.

However, the alternative implants known from WO02/17803A2 and WO2010/030906A1 still have drawbacks, which are explained as follows.

In case the rod of such an alternative known implanted device has relatively high stiffness, it is disadvantageous that the flexibility of the spine still is poor, while fusion of vertebrae is not effectively prevented then.

If, on the other hand, the rod of such an alternative known implanted device would have relatively low stiffness, it is disadvantageous that the corrective force action that the rod applies to the spinal column for correcting the defective curvature of the spinal column, decreases with progressing growth of the spine. The reason for this decreasing corrective force action is that the corrective deformation of the spinal column achieved by a low-stiffness-rod (which of course is much lower than the instantaneous large corrective deformation achieved by a high-stiffness-rod) only gradually and slowly increases in the course of time when the patient is wearing the implant over the years. By such a gradual increase of the corrective deformation of the spinal column, the rod gradually becomes less tensioned and, accordingly, the corrective force action that the rod applies to the spinal column gradually decreases. In addition, as the spine grows during the years, the distance between the two abovementioned vertebra-anchoring elements (one of which is slidable relative to the rod), increases which has a further reducing influence on the corrective force action that the rod applies to the spinal column. And, on top of that, contrary to the fact that the corrective force action in fact is gradually decreasing over time, the higher loads that the patient's spine has to carry due to the patient's growing body and weight in fact require a gradual increase of the corrective force action delivered by the rod. Hence, the application of a low-stiffness-rod in such an alternative known implanted device with partly slidable rod still requires re-operations/adjustments to be carried out, which is very undesirable.

In light of the above, it is an object of the invention to provide at least an alternative solution according to which a defective curvature of the spinal column is treated, while maintaining as much as possible:

flexibility of the spine; and/or
a natural healthy growth of the spine; and/or
efficiency and effectivity of the corrective treatment over time, while avoiding re-operations and implant adjustments as much as possible.

For that purpose, the invention provides an implantation system for treatment of a defective curvature of the spinal column of a patient, the system comprising:

at least one element being elongated in a longitudinal direction;
at least one first bone fixation element being arranged for being fixedly attached to a first vertebra of said spinal column, the first bone fixation element being fixedly attached to said elongated element at a first location along said longitudinal direction of the elongated element;
at least one second bone fixation element being arranged for being fixedly attached to a second vertebra of said spinal column, said second vertebra being different from said first vertebra; and
guiding structure through which the second bone fixation element is slidably and contactingly connected to the elongated element for guiding the second bone fixation element relative to the elongated element in a sliding range along said longitudinal direction, said sliding range being distant from said first location;

wherein the elongated element has bending resilience and/or torsional resilience for resiliently applying in mounted condition of the implantation system, via said first and second bone fixation elements and via said first and second vertebrae, corrective bending and/or torsional force action to said spinal column for correcting said defective curvature;

wherein in at least part of said sliding range the transverse cross-sectional shape of said elongated element is different from that of a single rod having a circular transverse cross-sectional circumference; and

wherein said guiding structure is arranged in such manner that, in said mounted condition and under application of said corrective force action, in response to longitudinal growth of said spinal column, the responsive sliding of said second bone fixation element relative to said elongated element in said at least part of said sliding range away from the first location causes said corrective force action to be higher than if in said at least part of said sliding range the transverse cross-sectional shape of the elongated element would have been the same as that of said single rod having a circular transverse cross-sectional circumference.

Hence, the implantation system according to the invention not only has said first bone fixation element, which is fixedly attached to the elongated element, but also the second bone fixation element, which is slidably connected to that elongated element. In this respect, the implantation system according to the invention is similar to the abovedescribed implants known from WO02/17803A2 and WO2010/030906A1. Therefore, already for similar reasons as for these known implants, the implantation system according to the invention provides improved flexibility of the spine and reduces some of the growth-related drawbacks. Amongst others, the implantation system according to the invention aims at avoiding fusion of vertebrae.

In fact, these specific improvements may be better than for these known implants, since the implantation system according to the invention allows for resiliently applying in its mounted condition relatively low bending resilience and/or torsional resilience of the elongated element, which relatively low resiliences further improve the flexibility of the spine and further prevent fusion of vertebrae. The reasons that low resiliences may be applied in a system according to the invention, lie in the recited transverse cross-sectional shape of said elongated element in combination with the recited guiding structure. That is, for a system according to the invention in response to longitudinal growth of said spinal column, the responsive sliding of said second bone fixation element relative to said elongated element in said at least part of said sliding range away from the first location causes said corrective force action to be higher than possible for the abovedescribed implants known from WO02/17803A2 and WO2010/030906A1. Note that for the lastmentioned known implants the elongated element is a single rod having a circular transverse cross-sectional circumference and that such circularity together with the different guiding structure of these known implants unavoidably brings along loss of corrective force action during such sliding, as explained. Hence, as compared with and contrary to the implants known from WO02/17803A2 and WO2010/030906A1, by using low resiliences of the elongated element the implantation system according to the invention provides further improved flexibility of the spine, while at the same time preserving efficiency and effectivity of the corrective treatment over time, *i.e.* when the spinal column grows, thus avoiding undesirable re-operations and implant adjustments as much as possible.

It is remarked that according to the invention said loss of corrective force action during such sliding is counteracted not only when applying relatively low bending resilience and/or torsional resilience of the elongated element, but also when applying relatively high bending resilience and/or torsional resilience of the elongated element.

In summary, for a system according to the invention, the transverse cross-sectional shape of the elongated element in combination with the special arrangement of the guiding structure provides automatical adjustment of the corrective force action in dependence of growth of the spinal column. The system according to the invention allows for good

flexibility of the spine and for a natural healthy growth of the spine, while it avoids re-operations and implant adjustments.

In a preferable embodiment of the invention said guiding structure is realized in that the elongated element is shaped to comprise a resilient U-shaped portion, said U-shaped portion having two legs and an interconnecting part interconnecting said two legs, wherein said U-shaped portion with its interconnecting part is facing away from said first location, wherein one of said two legs is a free ending leg of the elongated element, said free ending leg having bending resilience, wherein said sliding range is extending along at least part of said U-shaped portion, and wherein said sliding and contacting connection is present between the second bone fixation element and at least said free ending leg of the U-shaped portion.

Thanks to said U-shaped portion, loss of corrective bending and/or torsional force action is counteracted over time, *i.e.* when the spinal column grows. That is, such loss of corrective force action can be reduced, said corrective force action can be maintained or said corrective force action can even be increased when the spinal column grows. Such a U-shaped portion not only provides reliability of the system, but also is easy to manufacture.

In relation to such a U-shaped portion, it is remarked that the invention may, more in general, be embodied in an implantation system for treatment of a defective curvature of the spinal column of a patient, the system comprising:

- at least one element being elongated in a longitudinal direction;
- at least one first bone fixation element being arranged for being fixedly attached to a first vertebra of said spinal column, the first bone fixation element being fixedly attached to said elongated element at a first location along said longitudinal direction of the elongated element;
- at least one second bone fixation element being arranged for being fixedly attached to a second vertebra of said spinal column, said second vertebra being different from said first vertebra; and
- guiding structure through which the second bone fixation element is slidably and contactingly connected to the elongated element for guiding the second bone fixation element relative to the elongated element in a sliding range along said longitudinal direction, said sliding range being distant from said first location;

wherein the elongated element has bending resilience and/or torsional resilience for resiliently applying in mounted condition of the implantation system, via said first and second bone fixation elements and via said first and second vertebrae, corrective bending and/or torsional force action to said spinal column for correcting said defective curvature;

characterized in that

said guiding structure is realized in that the elongated element is shaped to comprise a resilient U-shaped portion, said U-shaped portion having two legs and an interconnecting part interconnecting said two legs, wherein said U-shaped portion with its interconnecting part is facing away from said first location, wherein one of said two legs is a free ending leg of the elongated element, said free ending leg having bending resilience, wherein said sliding range is extending along at least part of said U-shaped portion, and wherein said sliding and contacting connection is present between the second bone fixation element and at least said free ending leg of the U-shaped portion.

In another preferable embodiment of the invention said guiding structure comprises helically shaped structure defining a helical path for said guiding the second bone fixation element relative to the elongated element in the sliding range.

Thanks to said helically shaped structure, loss of corrective torsional force action is counteracted over time, *i.e.* when the spinal column grows. That is, such loss of corrective force action can be reduced, said corrective force action can be maintained or said corrective force action can even be increased when the spinal column grows. Such a helically shaped structure not only provides reliability of the system, but also is easy to manufacture.

In relation to such a helically shaped structure, it is remarked that the invention may, more in general, be embodied in an implantation system for treatment of a defective curvature of the spinal column of a patient, the system comprising:

- at least one element being elongated in a longitudinal direction;
- at least one first bone fixation element being arranged for being fixedly attached to a first vertebra of said spinal column, the first bone fixation element being fixedly attached to said elongated element at a first location along said longitudinal direction of the elongated element;
- at least one second bone fixation element being arranged for being fixedly attached to a second vertebra of said spinal column, said second vertebra being different from said first vertebra; and
- guiding structure through which the second bone fixation element is slidably and contactingly connected to the elongated element for guiding the second bone fixation element relative to the elongated element in a sliding range along said longitudinal direction, said sliding range being distant from said first location;

wherein the elongated element has bending resilience and/or torsional resilience for resiliently applying in mounted condition of the implantation system, via said first and second bone fixation elements and via said first and second vertebrae, corrective bending and/or torsional force action to said spinal column for correcting said defective curvature;

characterized in that

said guiding structure comprises helically shaped structure defining a helical path for said guiding the second bone fixation element relative to the elongated element in the sliding range.

In principle, there are various ways of realizing such a helically shaped structure, for example by applying helical grooves and/or helical ribs to a portion of the elongated element in the sliding range and/or to a portion of the second bone fixation element.

In a further preferable embodiment of the invention said helically shaped structure is realized in that the elongated element is shaped to comprise a helically shaped portion, wherein said sliding range is extending along at least part of said helically shaped portion, and wherein said sliding and contacting connection is present between the second bone fixation element and said helically shaped portion in such manner that, when the second bone fixation element slides along said helically shaped portion in said longitudinal direction, the orientation of the second bone fixation element relative to said helically shaped element follows said helical path.

In all embodiments of an implantation system according to the invention, the implantation system may comprise at least two specimens of said at least one second bone fixation element, each of said two specimens being associated with the same elongated element, wherein said two specimens are mutually lying on opposite sides of said first location, one of said two specimens being associated with a first corresponding one of said second vertebra and with a first corresponding one of said sliding range, the other one of said two specimens being associated with a second corresponding one of said second vertebra and with a second corresponding one of said sliding range.

In all embodiments of an implantation system according to the invention, the implantation system may comprise a plurality of said at least one elongated element, each one of said plurality being associated with the same first bone fixation element and with the same second bone fixation element.

In all embodiments of an implantation system according to the invention, at least one of said first bone fixation element may comprise two first bone fixators, being mutually spaced in a direction transverse to said longitudinal direction, and a first bridging part, which fixedly attaches the two first bone fixators relative to one another, and which bridging part is fixedly attached to the elongated element at said first location, each of said two first bone fixators being arranged for being fixedly attached to one and the same vertebra.

In all embodiments of an implantation system according to the invention, at least one of said second bone fixation element may comprise two second bone fixators, being mutually spaced in a direction transverse to said longitudinal direction, and a second bridging part, which fixedly attaches the two second bone fixators relative to one

another, wherein said sliding and contacting connection is present between said second bridging part and the elongated element, each of said two second bone fixators being arranged for being fixedly attached to one and the same vertebra.

These and other aspects of the invention will be apparent from and elucidated with reference to the embodiments described hereinafter by way of non-limiting examples only and with reference to the schematic figures in the enclosed drawing.

Fig. 1 shows, in rear view, an example of a defective curvature of the spinal column of a patient.

Fig. 2 shows, in a perspective view, an example of an embodiment of an implantation system according to the invention.

Fig. 3 shows, in a perspective view, an example of another embodiment of an implantation system according to the invention.

Figs. 4A, 4B and 4C respectively show, in mutually identical perspective views, three different tensioned deformation states of an example of an embodiment of part of an elongated element of an implantation system according to the invention, said part extending at least in a sliding range as defined by the recited invention.

Figs. 5A, 5B and 5C respectively show, in mutually identical plan views, another three different tensioned deformation states of the part shown in Figs. 4A, 4B and 4C.

Figs. 6A, 6B, 6C and 6D respectively show, in mutually identical perspective views, four differently slided states of an example of another embodiment of part of an elongated element of an implantation system according to the invention, said part extending at least in a sliding range as defined by the recited invention.

Fig. 7 shows, in a perspective view, an example of an embodiment of a second bone fixation element of an implantation system according to the invention.

Fig. 8 shows, in a perspective view, an example of another embodiment of a second bone fixation element of an implantation system according to the invention.

Fig. 1 shows a spinal column 20, hereinafter also referred to as spine 20, having a number of vertebrae, of which three vertebrae have been identified with reference numerals, *i.e.* a first vertebra 21, a second vertebra 22 and another second vertebra 23. The spine 20 has a defective curvature (“scoliosis”), which is substantially extending between the two vertebrae 22 and 23. The vertebra 21 is substantially located at the “apex” of the defective curvature. The laterally protruding bone parts of the vertebrae are called “transverse processes”. Fig. 1 shows the transverse processes 24 and 25 of vertebra 23.

In the rear view of Fig. 1 the defective curvature of spine 20 is clearly visible as a substantial lateral defective deformation of the spine. However, it should be understood that in most cases of scoliosis lateral defective deformation goes hand in hand with substantial torsional defective deformation relative to the longitudinal direction of the spine. Since Fig. 1 is a rear view, such torsional deformation, although present in spine 20, is less clearly visible in Fig. 1.

Reference is now made to Fig. 2, which shows the system 1 as an example of an embodiment of an implantation system according to the invention. System 1 comprises an elongated element 2, a first bone fixation element 31, a second bone fixation element 32 and another second bone fixation element 33.

Each of these bone fixation elements 31, 32 and 33 is arranged for being fixedly attached to a vertebra of a spinal column. For example, element 31 may be fixedly attached to vertebra 21 of spine 20, element 32 may be fixedly attached to vertebra 22 of spine 20 and element 33 may be fixedly attached to vertebra 23 of spine 20. For that purpose, each of these elements 31, 32 and 33 comprises two bone fixators 41 and 42, being mutually spaced in a direction transverse to the longitudinal direction of element 2, and a bridging part 43, which fixedly attaches the two bone fixators 41 and 42 relative to one another.

The bridging part 43 of first bone fixation element 31 is fixedly attached to the elongated element 2 at first location 11 along the longitudinal direction of element 2. In the shown example, this is realized by means of the shown attachment element 44.

On one side of the first location 11 the element 2 comprises a first helical spring 3, while on the other side of the first location 11 the element 2 comprises a second helical spring 4. In the shown example, the helical pitch of the first helical spring 3 has an opposite direction relative to the helical pitch of the second helical spring 4. The springs 3 and 4 provide the element 2 at least with torsional resilience. It is remarked that the springs may also be designed so as to provide, by themselves, the element 2 with additional bending resilience in whatever degree.

In the example of Fig. 2, the element 2 comprises a first U-shaped portion 50 on a side of the first helical spring 3 facing away from the first location 11, while the element 2 comprises a second U-shaped portion 60 on a side of the second helical spring 4 facing away from the first location 11.

The second bone fixation element 32 comprises a connection element 45 which is fixedly attached to the bridging part 43 of element 32. The connection element 45 comprises a passageway 46 through which the legs of the U-shaped portion 50 are extending. Via this connection element 45, the second bone fixation element 32 is slidably and contactingly connected to the elongated element 2 for guiding the second

bone fixation element relative to the elongated element in sliding range 12 along the longitudinal direction of element 2.

Similarly, the other second bone fixation element 33 comprises a similar connection element 45 which is fixedly attached to the bridging part 43 of element 33. Here, it are the legs of the U-shaped portion 60 which are extending through the passageway 46 of this similar connection element 45. This way, also the other second bone fixation element 33 is slidably and contactingly connected to the elongated element 2, this time for guiding the other second bone fixation element 33 relative to the elongated element in sliding range 14 along the longitudinal direction of element 2.

For each of the bone fixation elements 31, 32 and 33, both bone fixators 41 and 42 are arranged for being fixedly attached to one and the same vertebra. In the shown example, the bone fixators 41 and 42 are pedicle screws, various kinds of which are known in the art. However, instead of pedicle screws, various other kinds of bone fixators are possible, such as, for example, lamina hooks and sublaminar wires. Since, as explained in the introduction above, the implantation system according to the invention aims at avoiding fusion of vertebrae, it is preferable to use bone fixators which avoid damaging the vertebrae and especially the joints between the vertebrae. Hence, in a preferable embodiment, the bone fixators may be in the form of straps 441 and 442 shown in the embodiment of Fig. 8, which shows a second bone fixation element 432 comprising the same bridging part 43 and the same connection element 45 as those of the second bone fixation element 32 of Fig. 2. Such straps 441 and 442 may be fitted around the transverse processes 24 and 25 of a vertebra (see Fig. 1) and prevent damage to the vertebrae.

It is noted, by the way, that Fig. 8 more clearly shows the connection element 45 of the second bone fixation element 32 and of the other second bone fixation element 33 of Fig. 2. Particularly, Fig. 8 more clearly shows the abovementioned passageway 46 through the connection element 45. From Fig. 8 it can be seen that the passageway 46 has a slot-like transverse cross-sectional shape. This slot-like shape allows the two legs of the U-shaped portion 50, or 60, both of which are extending through the passageway 46, to laterally move towards and away from one another when one or both of these legs are resiliently deforming. However, in some cases, it is not strictly necessary or desired to allow the two legs of such a U-shaped portion to thus move towards and away from one another. In such cases a connection element can be used that comprises two separate passageways, such as the connection element 345 of the second bone fixation element 332 shown in Fig. 7. In Fig. 7 it can be seen that the connection element 345 has two separate passageways 346, in each of which one such leg of such a U-shaped portion may be received. Note that, purely by way of example, the second bone fixation element 332 shown in Fig. 7, is provided with pedicle screws 41 and 42.

Reference is now made to Fig. 2 again. A mounted condition of the implantation system 1 may for example be obtained when the bone fixators 41 and 42 of the first bone fixation element 31 are fixedly attached to vertebra 21 of Fig. 1, and the bone fixators 41 and 42 of the second bone fixation element 32 are fixedly attached to vertebra 22 of Fig. 1, and the bone fixators 41 and 42 of the other second bone fixation element 33 are fixedly attached to vertebra 23 of Fig. 1. The system 1 can be brought in its mounted condition in such manner that, by means of suitable pre-tensioning of the helical springs 3 and 4, these helical springs 3 and 4 in the mounted condition are resiliently applying, via the elements 31, 32 and 33 and via the vertebrae 21, 22 and 23, corrective torsional force action to the spine 20 for correcting the defective torsional curvature of the spine 20. Double arrow 15 in Fig. 2 illustrates possible relative rotational movements, around the longitudinal direction of element 2, of the first bone fixation element 31 relative to the second bone fixation element 32, as well as of the first bone fixation element 31 relative to the other second bone fixation element 33. These relative rotational movements are possible in said mounted condition, as allowed by and under influence of the resiliency of the helical springs 3 and 4.

Now, with additional reference to Figs. 4A, 4B and 4C, it is elucidated what happens when the spine 20 is growing in the course of time, which is the case when the system 1 is implanted into a growing child. The lastmentioned figures show the U-shaped portion 50 of Fig. 2. U-shaped portion 50 has two legs, 51 and 52, and an interconnecting part 53 interconnecting said two legs, wherein said U-shaped portion 50 with its interconnecting part 53 is facing away from the first location 11. One of said two legs is a free ending leg 51 of the elongated element 2, said free ending leg having bending resilience. The other leg 52 is connected to the helical spring 3. The sliding range 12 is extending along at least part of U-shaped portion 50. During longitudinal growth of the spine 20, vertebra 22 moves farther away from vertebra 21. This means that, averagely speaking, the connection element 45 will move farther away from the first location 11 in the course of time, *i.e.* in the direction of interconnecting part 53 of U-shaped portion 50. This means that the torque being delivered by helical spring 3 and, via the U-shaped portion 50, being transmitted to the connection element 45, which torque is indicated by the arrows T in Figs. 4A, 4B and 4C, will, averagely speaking, be transmitted at locations in the sliding range 12 closer and closer to the interconnecting part 53 in the course of time. This is exemplified by the consecutive Figs. 4A, 4B and 4C which show consecutive stages, respectively, during growth of the spine 20. In Figs. 4A, 4B and 4C, for purpose of elucidation only, deformation states of the U-shaped portion 50 are shown under the assumption that the torque T transmitted is equal throughout the three Figs. 4A, 4B and 4C. Due to the nature of the U-shape, the torsional deformation of the U-shaped portion 50 is largest in Fig. 4A and smallest in Fig. 4C, as clearly seen in Figs. 4A, 4B and 4C. This illustrates that the torsional stiffness of U-shaped portion 50, averagely speaking, becomes higher and higher in the course of time during growth of the spine 20.

Hence, from Figs. 4A, 4B and 4C it is clear that in the mounted condition of Fig. 2's system 1, thanks to the U-shaped portion 50, under application of the corrective force action by the helical spring 3, in response to longitudinal growth of the spine 20, the responsive sliding of the second bone fixation element 32 relative to the elongated element 2 in the sliding range 12 away from the first location 11 causes said corrective force action to be higher than if in the sliding range the transverse cross-sectional shape of the elongated element 2 would have been the same as that of said single rod having a circular transverse cross-sectional circumference. Note, that in the shown example the U-shaped portion 50 has a transverse cross-sectional shape corresponding to two, mutually spaced circular transverse cross-sectional circumferences.

Evidently, the above explanation analogously applies to the U-shaped portion 60 and the helical spring 4 of system 1, since they are forming similar structure as U-shaped portion 50 and helical spring 3.

Reference is now made to Fig. 3, which shows the system 101 as an example of another embodiment of an implantation system according to the invention. System 101 comprises an elongated element 102, a first bone fixation element 131, a second bone fixation element 32 and another second bone fixation element 33. The elements 131, 32 and 33 of system 101, as well as their functions, are similar to the elements 31, 32 and 33, as well as their functions, respectively, of system 1 of Fig. 2. For simplicity, the bone fixators of the elements 131, 32 and 33 have not been shown in Fig. 3. The shown attachment element 144, by means of which the bridging part 43 of first bone fixation element 131 is fixedly attached to the elongated element 102, is similar to the attachment element 44 of Fig. 2.

Furthermore, the elongated element 102 of Fig. 3's system 101 comprises first and second U-shaped portions 150 and 160 similar to the first and second U-shaped portions 50 and 60, respectively, of Fig. 2's system 1, be it that the legs 151, 152 and 161, 162 of U-shaped portions 150 and 160 are relatively longer than the legs of U-shaped portions 50 and 60. The portions 150 and 160 are located relative to a first location 111, in a similar way as in Fig. 2 the portions 50 and 60 are located relative to the first location 11. In Fig. 3 the sliding ranges similar to the sliding ranges 12 and 14 have been indicated by reference numerals 112 and 114, respectively.

The major difference between the system 101 of Fig. 3 and the system 1 of Fig. 2 is, that the system 101 does not have helical springs, such as the helical springs 3 and 4 of system 1. Instead, the nonfree-ending leg 152 of U-shaped portion 150 is connected in-line with, in fact is integrally formed with, the nonfree-ending leg 162 of the other U-shaped portion 160, without any helical spring in-between. The integrally formed nonfree-ending legs 152 and 162 of U-shaped portions 150 and 160 together form a bending rod 170, which provides the element 102 at least with bending resilience. It is

remarked that the bending rod 170 may also be designed so as to provide, by itself, the element 102 with additional torsional resilience in whatever degree.

A mounted condition of the implantation system 101 may for example be obtained when the first bone fixation element 131 is fixedly attached to vertebra 21 of Fig. 1, and the second bone fixation element 32 is fixedly attached to vertebra 22 of Fig. 1, and the other second bone fixation element 33 is fixedly attached to vertebra 23 of Fig. 1. The system 101 can be brought in its mounted condition in such manner that, by means of suitable pre-tensioning of the bending rod 170, this bending rod 170 in the mounted condition is resiliently applying, via the elements 131, 32 and 33 and via the vertebrae 21, 22 and 23, corrective bending force action to the spine 20 for correcting the defective lateral curvature of the spine 20.

Now, with additional reference to Figs. 5A, 5B and 5C, it is elucidated what happens when the spine 20 is growing in the course of time, which is the case when the system 101 of Fig. 3 is implanted into a growing child. It is noted that, although we are now elucidating the U-shaped portion 150 (or 160) of system 101, Figs. 5A, 5B and 5C are showing the U-shaped portion 50 of system 1 again. This, however, does not make any difference for this elucidation, since the U-shaped portion 150 of system 101 is similar to the U-shaped portion 50 of system 1.

As already mentioned above, the sliding range 12 is extending along at least part of U-shaped portion 50. During longitudinal growth of the spine 20, vertebra 22 moves farther away from vertebra 21. This means that, averagely speaking, the connection element 45 will move farther away from the first location 11 in the course of time, *i.e.* in the direction of interconnecting part 53 of U-shaped portion 50. This means that the force being delivered by bending rod 170 and, via the U-shaped portion 50, being transmitted to the connection element 45, which force is indicated by the arrows F in Figs. 5A, 5B and 5C, will, averagely speaking, be transmitted at locations in the sliding range 12 closer and closer to the interconnecting part 53 in the course of time. This is exemplified by the consecutive Figs. 5A, 5B and 5C which show consecutive stages, respectively, during growth of the spine 20. In Figs. 5A, 5B and 5C, for purpose of elucidation only, deformation states of the U-shaped portion 50 are shown under the assumption that the force F transmitted is equal throughout the three Figs. 5A, 5B and 5C. Due to the nature of the U-shape, the lateral deformation of the U-shaped portion 50 is largest in Fig. 5A and smallest in Fig. 5C, as clearly seen in Figs. 5A, 5B and 5C. This illustrates that the bending stiffness of U-shaped portion 50, averagely speaking, becomes higher and higher in the course of time during growth of the spine 20.

Hence, from Figs. 5A, 5B and 5C it is clear that in the mounted condition of Fig. 3's system 101, thanks to the U-shaped portion 150, under application of the corrective force action by the bending rod 170, in response to longitudinal growth of the spine 20, the responsive sliding of the second bone fixation element 32 relative to the elongated

element 102 in the sliding range 112 away from the first location 111 causes said corrective force action to be higher than if in the sliding range the transverse cross-sectional shape of the elongated element 2 would have been the same as that of said single rod having a circular transverse cross-sectional circumference. Note, that in the shown example the U-shaped portion 150 has a transverse cross-sectional shape corresponding to two, mutually spaced circular transverse cross-sectional circumferences.

Evidently, the above explanation analogously applies to the U-shaped portion 160 in relation to bending rod 170 of system 101, since it is forming similar structure as U-shaped portion 150 in relation to bending rod 170.

Reference is now made to Figs. 6A, 6B, 6C and 6D, which show another embodiment of part of an elongated element 202 of an implantation system according to the invention. Said part may be used in Fig. 2's system 1 instead of U-shaped portion 50 in Fig. 2. Such an incorporation of said part in system 1 is considered here, which is the reason why, similar to Figs. 4A, 4B and 4C, Figs. 6A, 6B, 6C and 6D show part of the helical spring 3. Hence, instead of U-shaped portion 50, the elongated element, now identified with reference numeral 202, comprises a helically shaped element 250, hereinafter referred to as helical strip 250. Furthermore, instead of Fig. 2's connection element 45, the elongated element 202 co-operates with another connection element 245 of the concerning second bone fixation element 232, which connection element 245 is arranged for contactingly sliding along helical strip 250 in the indicated sliding range 212.

The helical strip 250 and connection element 245 function as helically shaped guiding structure defining a helical path for guiding the second bone fixation element 232 relative to the elongated element 202 in the sliding range 212. When the second bone fixation element 232 slides along the helical strip 250 in longitudinal direction of the elongated element 202, the orientation of the second bone fixation element 232 relative to the helical strip 250 follows said helical path.

It is now assumed that the system 1, at the time of its implantation relative to the spine 20, has been brought in its mounted condition in such manner that, by means of suitable pre-tensioning of the helical spring 3, this helical spring 3 in the mounted condition is resiliently applying, via the elements 31 and 232 and via the vertebrae 21 and 22, corrective torsional force action to the spine 20 for correcting the defective torsional curvature of the spine 20.

Now, with reference to Figs. 6A, 6B, 6C and 6D, it is elucidated what happens when the spine 20 is growing in the course of time, which is the case when the system 1 is implanted into a growing child. During longitudinal growth of the spine 20, vertebra 22 moves farther away from vertebra 21. This means that, averagely speaking, the connection element 245 will move farther away from the first location 11 in the course

of time, *i.e.* in the direction away from the helical spring 3. Figs. 6A, 6B, 6C and 6D show consecutive stages, respectively, during such growth of the spine 20. As explained, the orientation of the second bone fixation element 232 relative to the helical strip 250 follows a helical path then.

Hence, from Figs. 6A, 6B, 6C and 6D it is clear that, when a suitable direction of the helical pitch of the first helical strip 250 has been chosen in dependence of the direction in which the helical spring 3 is pre-tensioned, under application of the corrective force action by the helical spring 3, in response to longitudinal growth of the spine 20, the responsive sliding of the second bone fixation element 232 relative to the elongated element 202 in the sliding range 212 away from the helical spring 3 causes said corrective force action to be higher than if in the sliding range the transverse cross-sectional shape of the elongated element 202 would have been the same as that of said single rod having a circular transverse cross-sectional circumference.

In the foregoing specification, the invention has been described with reference to specific examples of embodiments of the invention. However, various modifications and changes may be made therein without departing from the broader scope of the invention as set forth in the appended claims.

For example, in the shown embodiments, a system according to the invention comprises only one first bone fixation element and two second bone fixation elements for an elongated element. Various alternative configurations are possible. For example, it is possible to apply for an elongated element only one second bone fixation element, instead of two. Also it is possible to apply for an elongated element two, three, four, or more first bone fixation elements and three, four, or more second bone fixation elements, as well as any possible combinations of such numbers of first and second bone fixation elements for an elongated element.

Furthermore, an implantation system according to the invention may comprise a plurality of elongated elements, each one of said plurality being associated with the same at least one first bone fixation element and with the same at least one second bone fixation element. An example of such a system is *e.g.* obtained when the elongated element 102 of Fig. 3 by means of the attachment element 144 and the two connection elements 45 of Fig. 3 is connected to the three bridging parts 43 shown in Fig. 2 in such manner that the elongated elements 2 and 102 are extending side by side relative to one another.

Also, it is possible to integrate within a single one of the at least one elongated element of a system according to the invention, the functions of both a bending rod and a torsional spring, thus efficiently and compactly deriving benefit regarding maintaining suitable levels of both corrective bending force action and corrective torsional force action during growth of a spine, by means of only a single U-shaped portion. This way,

benefit is derived from the combined effects described with reference to Figs. 4A, 4B and 4C, on the one hand, and with reference to Figs. 5A, 5B and 5C, on the other hand.

Furthermore, it is also possible to apply a U-shaped portion, whose legs are nonparallel relative to one another. For example, the legs of a U-shaped portion may extend in helical shapes, more or less analogous to the helical shape of the helical strip shown in Figs. 6A, 6B, 6C and 6D. This way benefit is derived from the combined effects described with reference to Figs. 4A, 4B and 4C and/or Figs. 5A, 5B and 5C, on the one hand, and with reference to Figs. 6A, 6B, 6C and 6D, on the other hand.

However, other modifications, variations and alternatives are also possible. The specifications and drawings are, accordingly, to be regarded in an illustrative rather than in a restrictive sense.

In the claims, any reference signs placed between parentheses shall not be construed as limiting the claim. The word 'comprising' does not exclude the presence of other features or steps than those listed in a claim. Furthermore, the words 'a' and 'an' shall not be construed as limited to 'only one', but instead are used to mean 'at least one', and do not exclude a plurality. The mere fact that certain measures are recited in mutually different claims does not indicate that a combination of these measures cannot be used to advantage.

Claims

1. Implantation system for treatment of a defective curvature of the spinal column (20) of a patient, the system (1; 101) comprising:

at least one element (2; 102) being elongated in a longitudinal direction;

at least one first bone fixation element (31; 131) being arranged for being fixedly attached to a first vertebra (21) of said spinal column, the first bone fixation element being fixedly attached to said elongated element at a first location (11; 111) along said longitudinal direction of the elongated element;

at least one second bone fixation element (32, 33; 232; 332; 432) being arranged for being fixedly attached to a second vertebra (22, 23) of said spinal column, said second vertebra being different from said first vertebra; and

guiding structure (45, 50; 45, 150; 245, 250) through which the second bone fixation element (32) is slidably and contactingly connected to the elongated element (2) for guiding the second bone fixation element relative to the elongated element in a sliding range (12, 14; 112, 114; 212) along said longitudinal direction, said sliding range being distant from said first location;

wherein the elongated element (2; 102) has bending resilience and/or torsional resilience for resiliently applying in mounted condition of the implantation system (1; 101), via said first and second bone fixation elements and via said first and second vertebrae, corrective bending and/or torsional force action to said spinal column (20) for correcting said defective curvature;

characterized

in that in at least part of said sliding range (12; 112; 212) the transverse cross-sectional shape of said elongated element (2; 102) is different from that of a single rod having a circular transverse cross-sectional circumference; and

in that said guiding structure (45, 50; 45, 150; 245, 250) is arranged in such manner that, in said mounted condition and under application of said corrective force action, in response to longitudinal growth of said spinal column (20), the responsive sliding of said second bone fixation element (32; 232) relative to said elongated element (2; 102; 202) in said at least part of said sliding range (12; 112; 212) away from the first location (11; 111) causes said corrective force action to be higher than if in said at least part of said sliding range the transverse cross-sectional shape of the elongated element (2; 102; 202) would have been the same as that of said single rod having a circular transverse cross-sectional circumference.

2. Implantation system according to claim 1, wherein said guiding structure (45, 50; 45, 150) is realized in that the elongated element is shaped to comprise a resilient U-shaped portion (50; 150), said U-shaped portion having two legs (51, 52) and an interconnecting part (53) interconnecting said two legs, wherein said U-shaped portion with its interconnecting part is facing away from said first location (11; 111), wherein one of said two legs is a free ending leg (51) of the elongated element, said free ending leg having bending resilience, wherein said sliding range (12) is extending along at least part of said U-shaped portion, and wherein said sliding and contacting connection is present between the second bone fixation element (32) and at least said free ending leg (51) of the U-shaped portion.

3. Implantation system according to claim 1 or 2, wherein said guiding structure (245, 250) comprises helically shaped structure (250) defining a helical path for said guiding the second bone fixation element (232) relative to the elongated element (202) in the sliding range (212).

4. Implantation system according to claim 3, wherein said helically shaped structure (250) is realized in that the elongated element is shaped to comprise a helically shaped portion (250), wherein said sliding range (212) is extending along at least part of said helically shaped portion, and wherein said sliding and contacting connection is present between the second bone fixation element (232) and said helically shaped portion in such manner that, when the second bone fixation element (232) slides along said helically shaped portion (250) in said longitudinal direction, the orientation of the second bone fixation element relative to said helically shaped element follows said helical path.

5. Implantation system according to any one of the preceding claims, comprising at least two specimens (32, 33) of said at least one second bone fixation element, each of said two specimens being associated with the same elongated element (2; 102), wherein said two specimens are mutually lying on opposite sides of said first location (11; 111), one of said two specimens (32) being associated with a first corresponding one of said second vertebra (22) and with a first corresponding one of said sliding range (12; 112), the other one of said two specimens (33) being associated with a second corresponding one of said second vertebra (23) and with a second corresponding one of said sliding range (14; 114).

6. Implantation system according to any one of the preceding claims, comprising a plurality of said at least one elongated element (2, 102), each one of said plurality being associated with the same first bone fixation element (31) and with the same second bone fixation element (32).

7. Implantation system according to any one of the preceding claims, wherein at least one of said first bone fixation element (31) comprises two first bone fixators (41, 42), being mutually spaced in a direction transverse to said longitudinal direction, and a first bridging part (43), which fixedly attaches the two first bone fixators relative to one another, and which bridging part is fixedly attached to the elongated element (2) at said first location (11), each of said two first bone fixators being arranged for being fixedly attached to one and the same vertebra (21).

8. Implantation system according to any one of the preceding claims, wherein at least one of said second bone fixation element (32, 33) comprises two second bone fixators (41, 42), being mutually spaced in a direction transverse to said longitudinal direction, and a second bridging part (43), which fixedly attaches the two second bone fixators relative to one another, and wherein said sliding and contacting connection is present between said second bridging part (43) and the elongated element (2), each of said two second bone fixators being arranged for being fixedly attached to one and the same vertebra (22, 23).

Abstract

An implantation system for treatment of a defective curvature of the spinal column comprises an elongated element (2), a first bone fixation element (31) being fixedly attached to said elongated element, a second bone fixation element (32, 33), and guiding structure (45, 50) through which the second bone fixation element is slidably and contactingly connected to the elongated element. The elongated element has bending resilience and/or torsional resilience for applying corrective force action to the spinal column. A special arrangement of the guiding structure (45, 50) provides automatical adjustment of the corrective force action in dependence of growth of the spinal column. The system allows for good flexibility of the spine and for a natural healthy growth of the spine, while it avoids re-operations and implant adjustments.

(Fig. 2 is to be depicted with Abstract)

Fig. 1

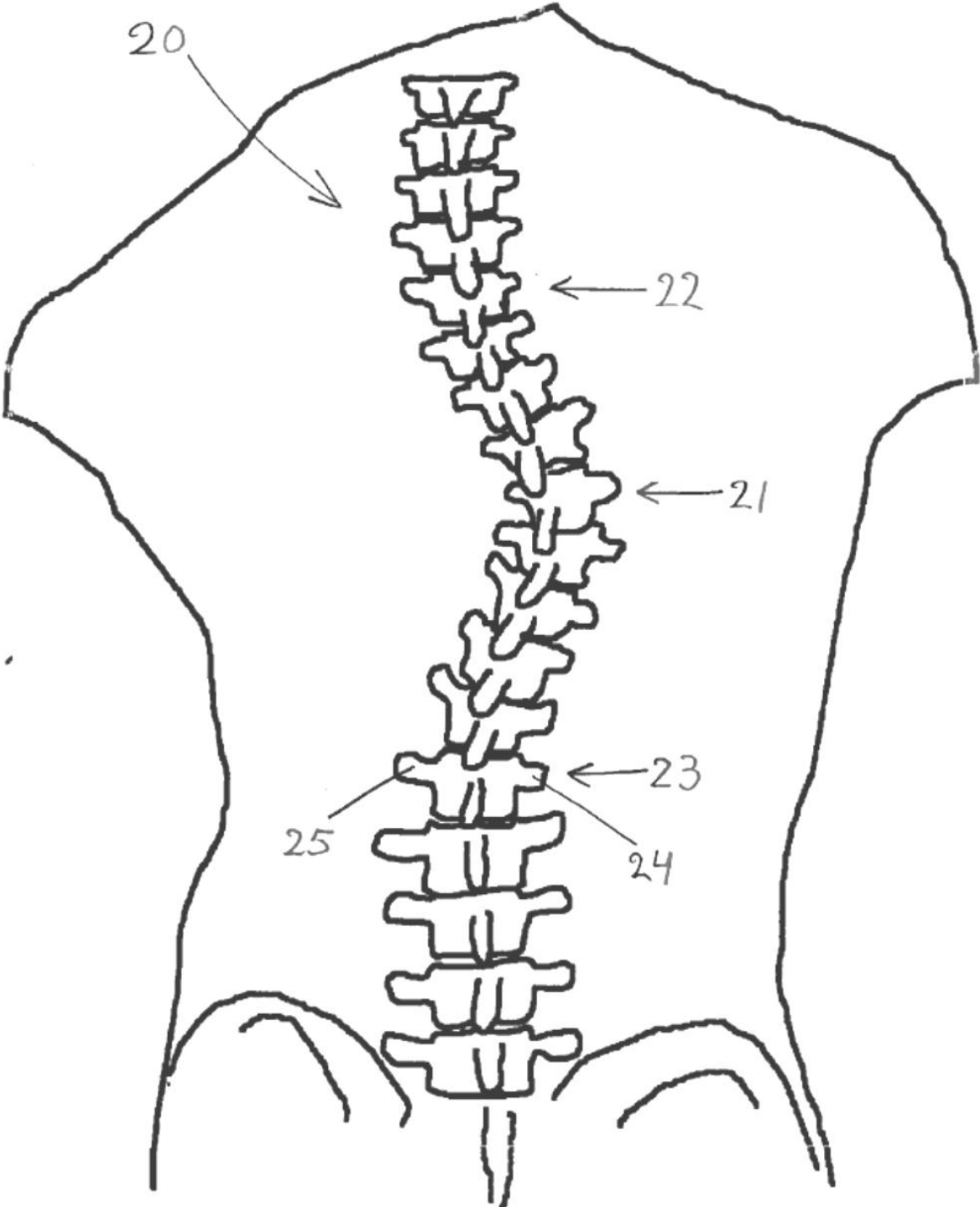


Fig. 2

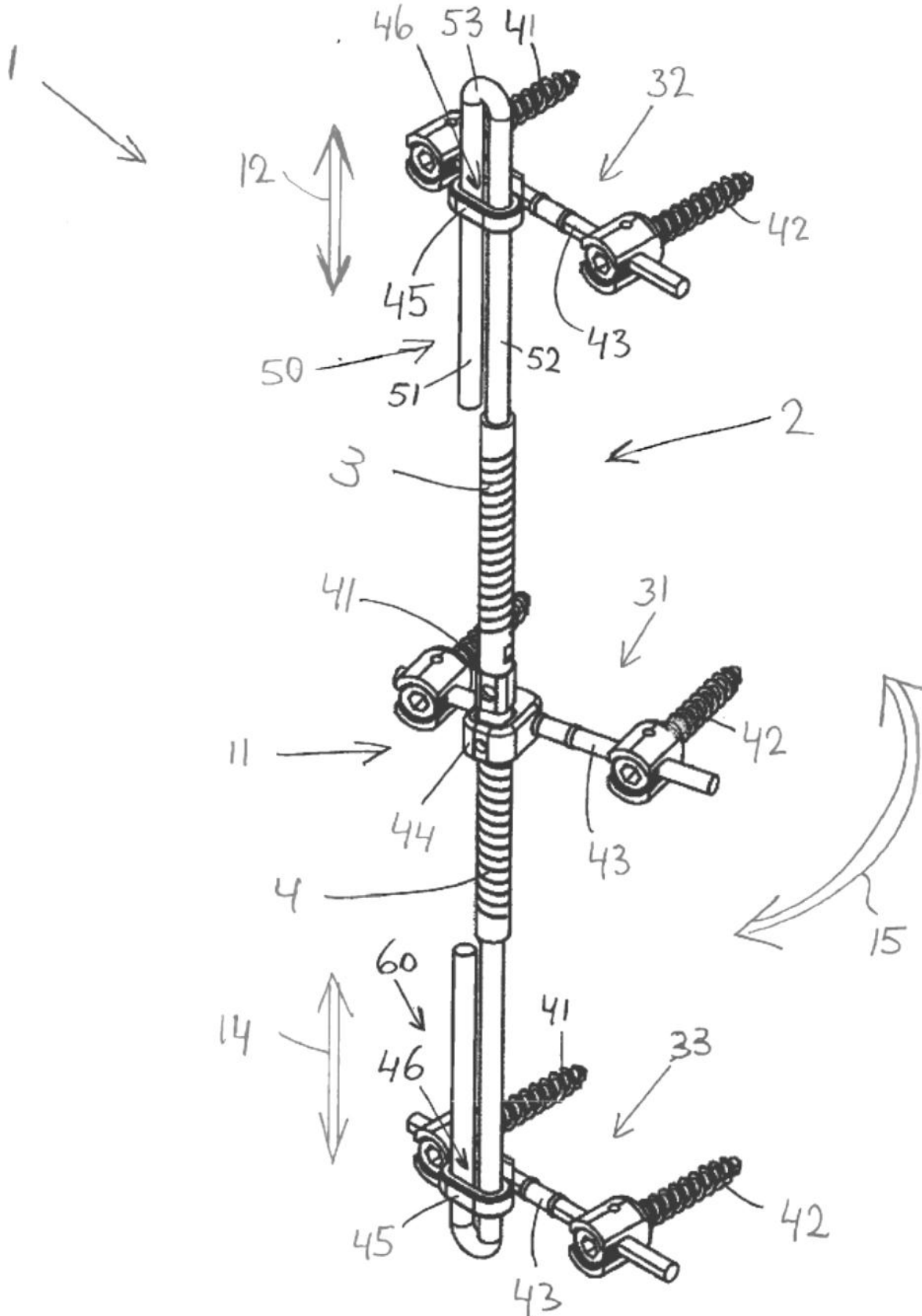


Fig.3

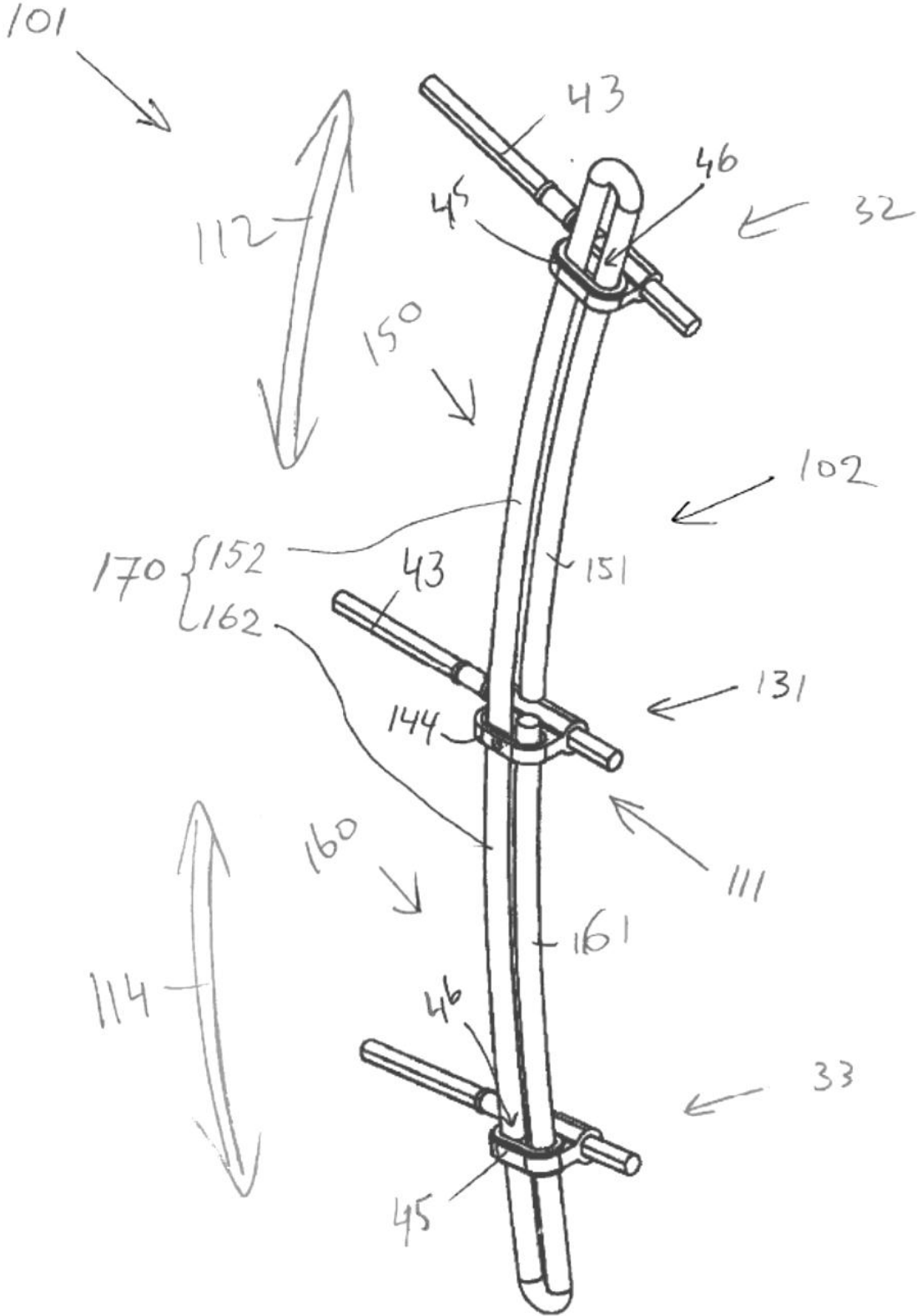


Fig. 4C

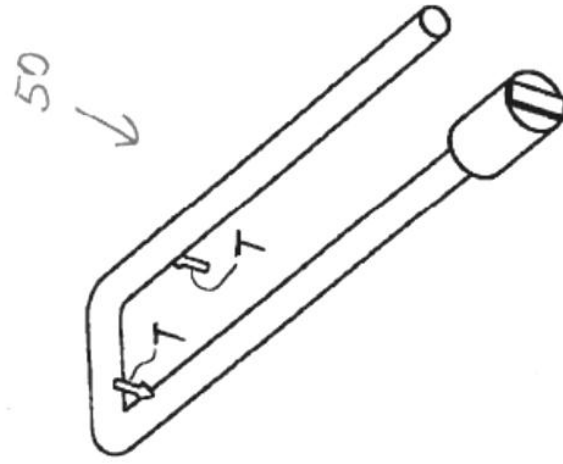


Fig. 4B

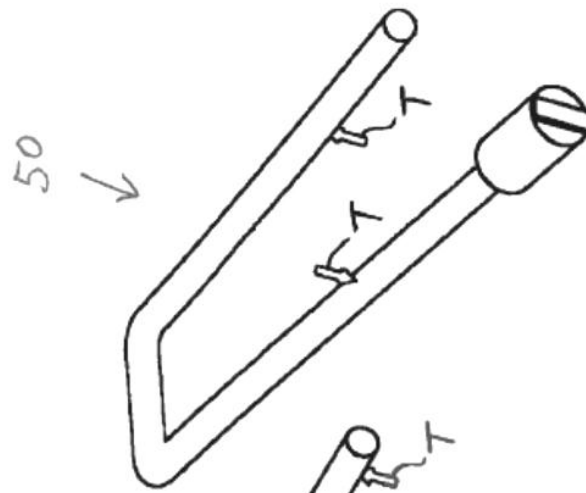


Fig. 4A

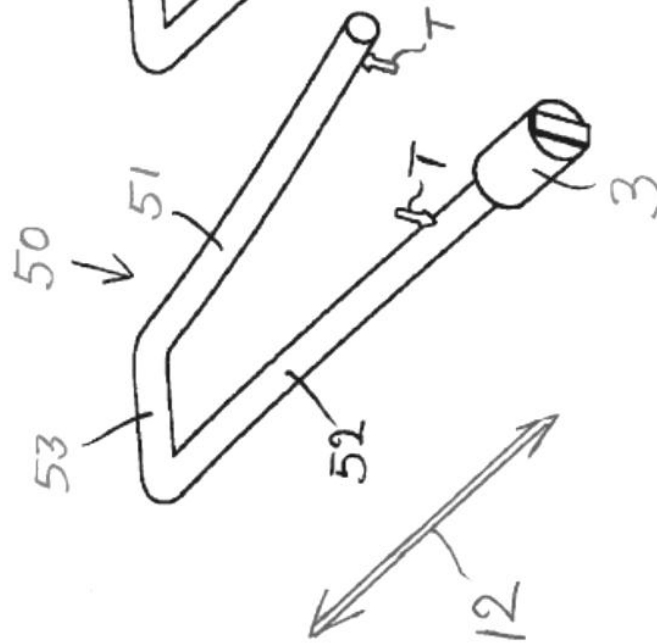


Fig. 5C

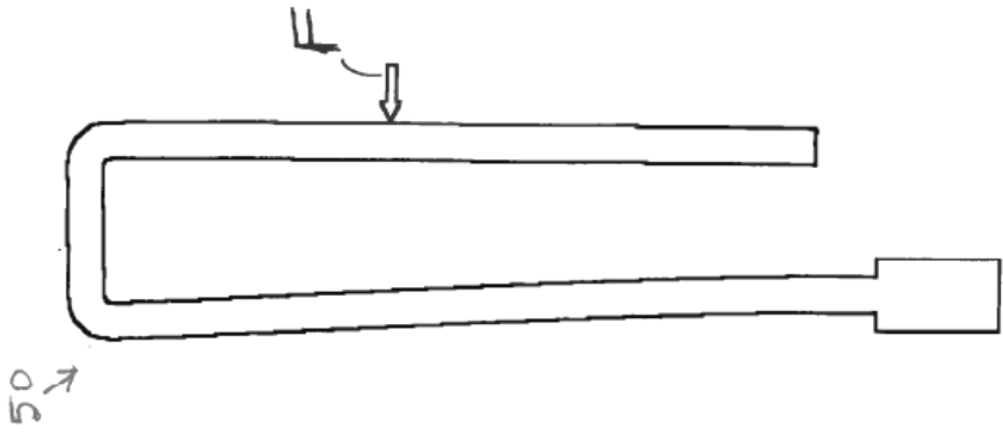


Fig. 5B

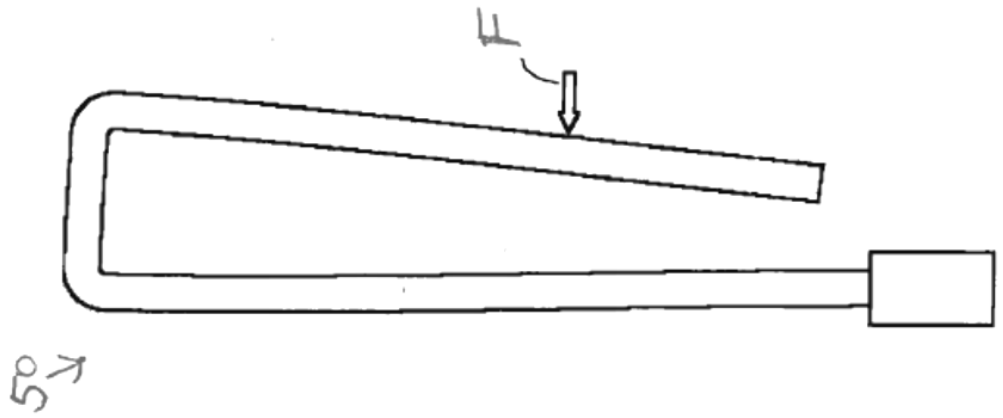
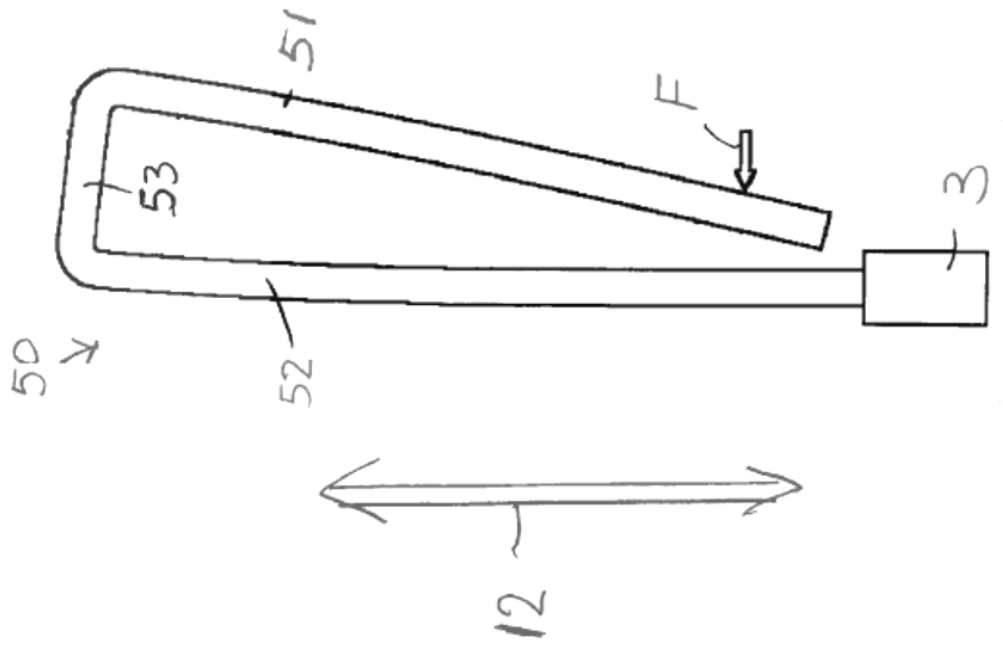
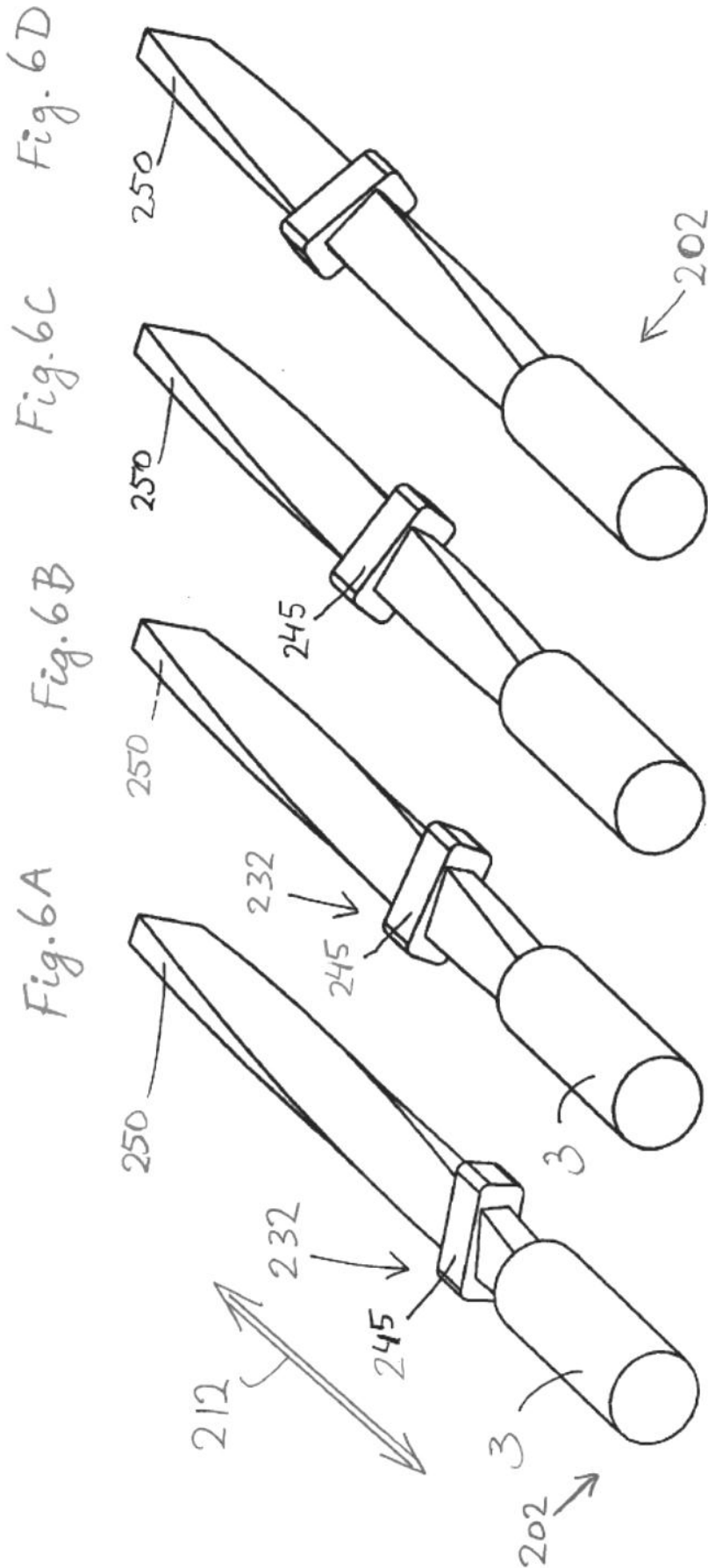
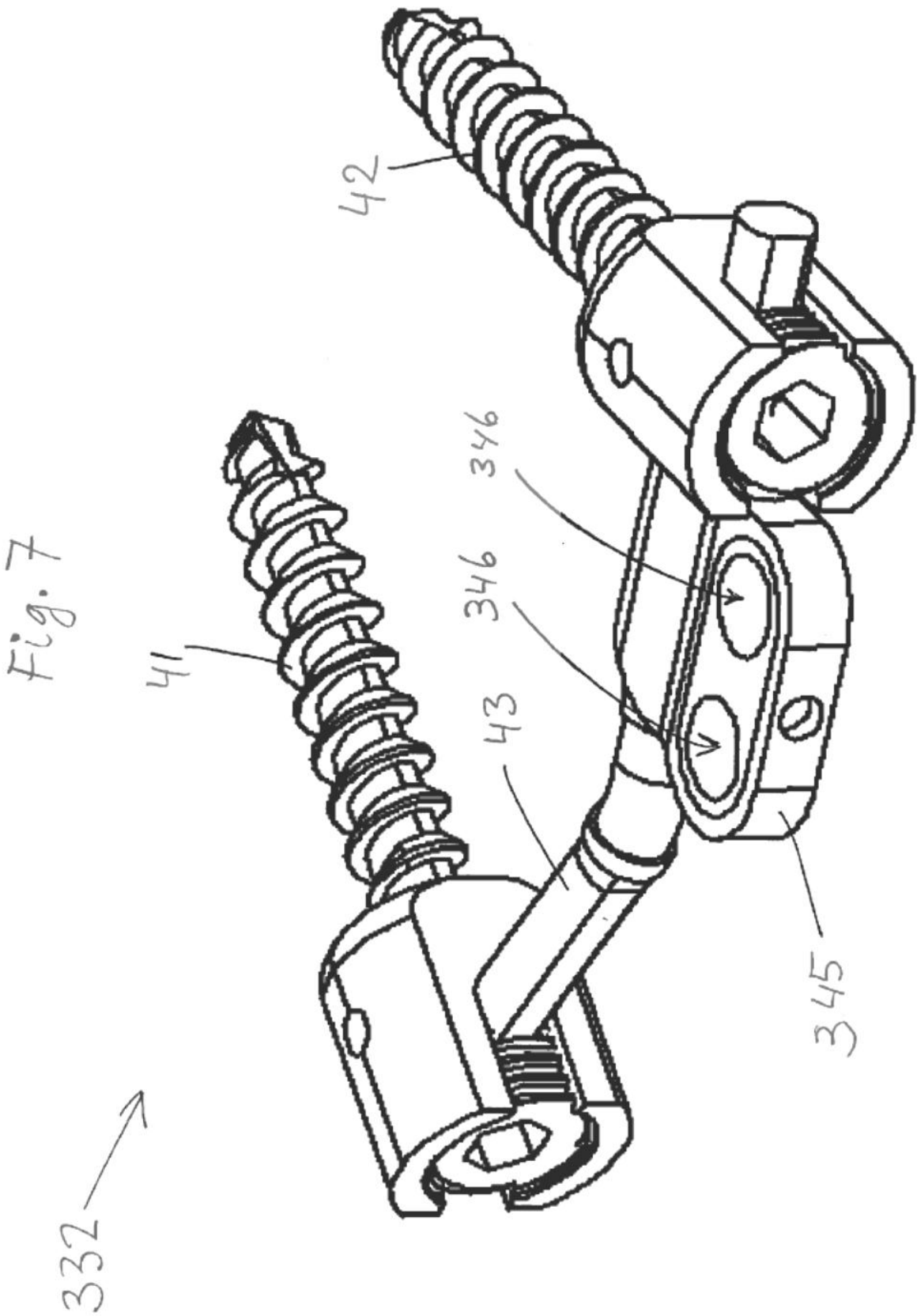
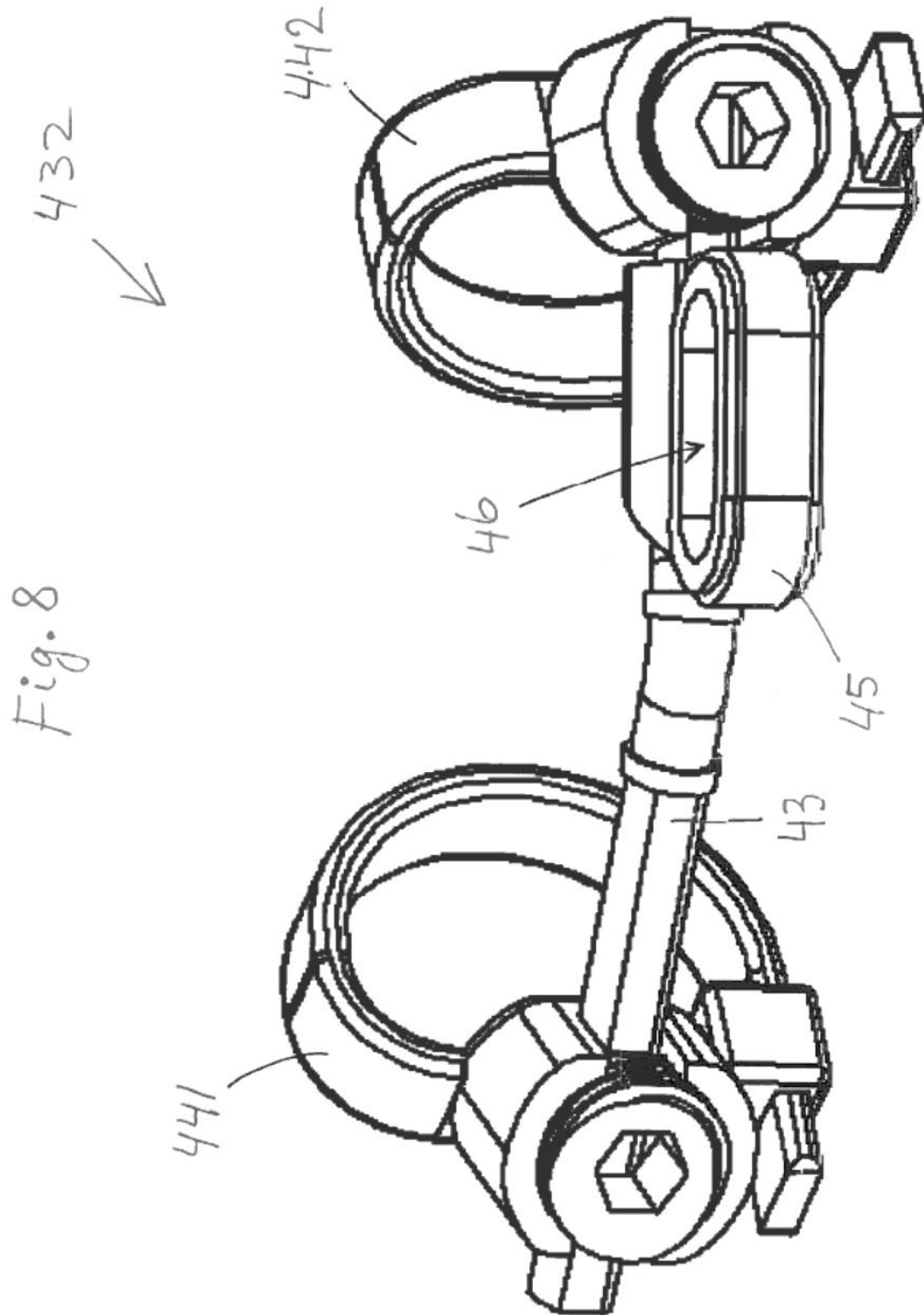


Fig. 5A









INDEX

A

Adolescent idiopathic scoliosis 9, 15
Alternating strain 138
Anchoring 22
Animal model 153
Annealing 133
Anterior 11
Anterior systems 22
Aorta 192
Apex 15, 215
Artificial vertebrae 116
Austenite 145
Axial rotation 40, 105, 116
Axial torsion 11

B

Bearing house 79
Bearing system 73
Bending moment 115
Bending spring 68
Biocompatibility 133
Blood loss 56, 189
Blunt dissection 173, 193
Bone fixation element 213
Bone graft 20
Bone growth 174
Bone remodelling 191
Braces 20
Bridge 98
Bridge bender 85
Bridge-angle measuring device 86
Bushing 115, 193, 196

C

Cable tie 99, 105
Cartilage 174
Caudal 11, 118, 153
Claims 224
Classification of scoliosis 16
Cobb-angle 15, 153, 161
Coil spring 79
Compact bone 12
Concave 10, 15
Confocal laser scanning microscopy 135
Correction strategies 20
Correction strategy 58
Correctional forces 55, 60
Cranial 11, 118, 153

Crankshafting 28, 155
Creep 42, 106
CT scan 161
Curvature 16, 17, 18, 19
Curve progression 155
Cyclic strain 133

D

Design process 67
Differential Scanning Calorimetry 134
Direct Vertebral Rotation 21

E

Elongated element 212
Energy source 67
Energy transformation 67
Extension 11, 13
Extensor muscles 13

F

Facet joint 13, 98, 107, 174
Failure mode effect analysis 191
Fatigue 129, 131
Fatigue crack growth 144
Fatigue crack propagation 145
Fatigue life 139
Fatigue limit 138
Finite Element Modelling 44, 46, 190
Fixation 71, 83, 92
Fixation strength 104, 105
Flexibility 124
Flexion 11
Flexor muscles 13
Force sensor 117
Four-point-bending 133
Fusion 20

G

Growth adaptation 70

H

Harrington procedure 21
Heat treatment 132, 134
Heterotopic ossification 188, 196
Hierarchic function model 61

I

Image-guided surgery 193
Implantation 89

<i>In vitro</i> experiment.....	113
<i>In vivo</i> animal model.....	156
<i>In vivo</i> experiment.....	89, 188, 191
Inclusions	143, 144
Inferior	11
Intervertebral disc.....	12
Intervertebral discs	11
Invention	208
iXS ANG	86
iXS BEN	85
iXS SET	86, 88
K	
Kyphosis	155, 171, 172
L	
Laser Beam Welding.....	85
Lateral	11
Lateral bending moment.....	121
Lateral flexion.....	11
Lateral force	99
Lengthening	120
Lenke Classification	16
Ligaments.....	12, 14
Long-term implantation	133
Luque trolley	26
M	
Mankin grading	170
Martensite.....	145
Materials	76
Medial	11
Memory metal	24, 81
Minimal invasive	45, 174, 198
Mini-pig.....	25
Morphologic chart.....	69
Most tilted vertebrae.....	84
N	
Neurological injury.....	191
Neutral zone.....	171
NiTi	44, 76, 82, 115, 117, 131, 133
Non-fusion.....	40
Non-fusion surgery.....	24, 156
Non-segmental spinal construct	119
O	
Oblique muscles	13
Orthobiom.....	25

Osteoinduction	45, 188
Osteoporosis	98
P	
Passivation	85
Patent application.....	84
Patient group	41
Pedicle screw insertion	192
Pedicle screws.....	22, 98
PEEK . 76, 81, 82, 106, 109, 157, 166, 167, 168, 182, 196, 197, 202	
Periosteum.....	174, 192, 193, 196
Phosphate buffered saline	131, 135
Physiotherapy	19
Plasma polishing	135, 145
Polishing.....	134
Poly-axial pedicle screws	22, 84
Porcine model.....	45, 89, 173
Porcine spine.....	45, 190
Posterior.....	11
Posterior systems.....	21
Pre-strain.....	136
Prototypes.....	89
Pseudo-elasticity	44
R	
Radiograph.....	161
Range of motion.....	77, 171, 199
Relaxation	42, 191
Requirements.....	52
Resilience	213
Risk assessment	191
Risk priority number	192
Rotational bending.....	133
Run-out strain	138
S	
Scoliosis.....	9, 155, 215
Scoliosis correction	67
Scoliosis induction.....	89, 190
Segmental spinal construct.....	21
Shape memory	44, 133
Shot peening	135, 144
Solutions	72
Spinal canal	12
Spinal column.....	208
Spinal configuration	116
Spinal cord	192
Spinal muscles.....	13
Spine	9, 10

Spine model	44	Transverse process.....	12, 84, 98, 106, 215
Spine surgery.....	20, 21, 56	Treatment of scoliosis.....	19
Spinous process.....	12	T-score	98
Spondylodesis	20, 21, 27	U	
Spongy bone.....	11	UHMWPE	76, 79, 115, 196
Staircase method	145	Uni-axial bending	133
Stakeholders.....	51	U-shaped portion.....	212, 213
Stapling.....	24	U-shaped rod	74, 75
Sterilisation	54, 89	V	
Stiffness.....	118, 119, 122	Vertebral body	11, 102, 192
Stress-induced phase transition.....	145	Vertebral column	10
Superior.....	11	Vertical Expandable Prosthetic Titanium Rib.....	24
Surface roughness.....	135, 144	Visco-elasticity	42
Surface treatment	131, 143	X	
Surgery time.....	56, 189	XS FIX	84, 98
Surgical instruments.....	85	XS LAT	81, 157
Surgical procedure	159	XS LATOR	77
Surgical treatment	20	XS TOR	79, 156
T		Y	
Ti6Al4V	76, 115, 196	Yucatan mini pig.....	198
Tissue response	200		
Torque	99, 101, 115		
Torque delivery	120		
Torque generator	86, 88		
Transformation temperature	134		
Transverse bridge.....	71, 156		

DEVELOPMENT OF A NON-FUSION SCOLIOSIS CORRECTION DEVICE

DESIGNING AND TESTING

Stellingen

behorend bij het proefschrift door
Martijn Wessels, 13 september 2012

1. Ten aanzien van scoliosecorrectie is de correctiekracht geleverd door een flexibel implantaat niet per definitie kleiner dan geleverd door een stijf implantaat, zelfs niet instantaan (dit proefschrift).
2. Het verschil tussen het kreukelen en het ontkreukelen van een papiertje is groter dan het verschil tussen scoliosecorrectie en –inductie (dit proefschrift).
3. Net als voor de revalidatie na een beroerte is de beste methode voor scoliosecorrectie minimale ondersteuning (dit proefschrift).
4. Een arts weet minder over je lichaam dan jezelf.
5. De ontwikkeling van de geneeskunde heeft er voor gezorgd dat er tegenwoordig veel meer mensen ziek zijn dan vroeger.
6. Als er iemand promoveert, zou er eigenlijk een degradatie tegenover moeten staan om het geheel te balanceren.
7. Talent voor specifieke sporten bestaat helemaal niet aangezien we als samenleving de spelregels zelf hebben bedacht.
8. Diegene die denkt dat de wartaal die Johan Cruijff bezigt, getuigt van bijzonder hoog intelligentieniveau, onderschat schromelijk zijn eigen denkvermogen.
9. Het onderscheid maken op grond van sekse, ras of godsdienst is geen kortzichtigheid maar juist een toonbeeld van ruimdenkendheid.
10. Het aanscherpen van de regels voor het inperken van criminaliteit en terrorisme heeft geen enkel nut aangezien criminelen en terroristen deze per definitie overtreden.